Introduction to Special Relativity, Quantum Mechanics and Nuclear Physics for Nuclear Engineers

Alex F Bielajew
The University of Michigan
Department of Nuclear Engineering and Radiological Sciences
2927 Cooley Building (North Campus)
2355 Bonisteel Boulevard
Ann Arbor, Michigan 48109-2104
U. S. A.
Tel: 734 764 6364
Fax: 734 763 4540
email: bielajew@umich.edu

December 15, 2014

Preface

This book arises from a series of hand-written notes I am continually revising in support of two courses I teach, each a three-credit (42 hour) junior-level course, *NERS311 and NERS 312: Elements of Nuclear Engineering and Radiological Sciences I and II* at the Department of Nuclear Engineering and Radiological Sciences at the University of Michigan.

More apt titles for these courses would be *NERS311: Modern Physics and Quantum Mechanics* and *NERS312: Nuclear Physics* because there is very little engineering in the course content. Rather, we shall dwell on the sciences that underpin Nuclear Engineering and Radiological Sciences, for it is essential that we understand, in some detail, the nature of the stuff we are engineering. Nuclear materials and the resultant radiation are really some of the most dangerous (and interesting) things in the world, and, in my view at least, understanding them, at least in some depth, is essential.

These two courses assume, and make great use of, the earlier background courses in mathematics and physics. So, if you get stuck on some mathematics or physics concept, please dive into your old notes and texts, or ask questions. These things may have seemed tired and dry when you learned them initially, but these courses will bring them to back to life, with some vigor, and a great deal of power. By their very nature, the consequences of Special Relativity and Quantum Mechanics are counterintuitive. Our understanding of very fast and/or very small objects is not reinforced by our everyday experiences. Consequently, the understanding of these phenomena falls to mathematical interpretation, that must be refined, to enable deeper understanding. Much like a blind person, whose other senses are sharpened to enable him or her to experience the world, so it is that mathematics becomes more important. Equations really do speak, if you listen the right way.

I would like to thank the students who took my first versions of there courses in the Fall of 2005, and Winter of 2006. Your feedback convinced me that I should undertake this writing. Your support was deeply appreciated. To you taking NERS 311 or 312 now, this is very much a work-in-progress. There will be spelling and grammatical errors, sloppy English, missing figures, the occasional bad equation, and, once in a while, a logical argument that does not make complete sense. If you find an error or can suggest an improvement, please bring it to me. I am most grateful for these. These notes may seem to be under constant revision. They are, and it is a natural part of their development. Please bear with this. On

the plus side, they're free!

About Krane's book, *Modern Physics*, Second edition

This is a decent text, good value for the money, but not perfect. If it were, these notes would not exist! I hope these notes bring some added value to the material. In several cases, I disagree with Krane's approach, and will offer a little more rigor. In a few cases, I'll disagree with Krane's interpretation of, in particular, Quantum Mechanics. This is not to say Krane's approach is wrong, because these topics are still being debated by theoretical physicists and natural philosophers. However, I will try to justify my view of things.

Two of the greatest things about Krane's book are the collection of Questions and Problems at the back of each Chapter. Good students should make use of these sections to the extent that your interest, energy and time permit. I will provide more encouragement throughout the text.

AFB, October 2, 2006

2008 update

In 2008, the 311 course was reduced to 3 credits from 4, at the expense of eliminating most of the Special Relativity material from the lectures. Most of that material is not essential to obtaining a thorough understanding of Quantum Mechanics and Nuclear Physics. What is essential, and what will continue to be taught are the relativistic kinematical relations, as we shall be learning about photons, that travel at the speed of light, and energetic electrons from β-decay, that have velocities close to the speed of light. I've elected to leave the Modern Physics material intact. It's good science culture, and perhaps an interested student or two will be motivated to study this topic deeper.

2009 update

Extensive revisions to most chapters have been undertaken. I'd like to thank Ms. Linda Park for her excellent and erudite proofreading of the technical and non-technical material. Linda, I am in awe of your attention-to-detail.

A brief note on chapter headings

Chapter and subchapter headings preceded by a dagger† do not exist in Krane's book, and are here for supplementary, prerequisite, or co-requisite study. They will be covered on a need-to basis. Chapter and subchapter headings preceded by an asterisk* are generally not covered in teaching the NERS 311/312 editions of the class.

AFB, July 16, 2009

Contents

Chapter 1

Introduction

1.1 About this book

This book arises from a series of hand-written notes I am continually revising in support of two courses I teach, each a three-credit (42 hour) junior-level course, *NERS311 and NERS 312: Elements of Nuclear Engineering and Radiological Sciences I and II* at the Department of Nuclear Engineering and Radiological Sciences at the University of Michigan.

More apt titles for these courses would be *NERS311: Modern Physics and Quantum Mechanics* and *NERS312: Nuclear Physics* because there is very little engineering in the course content. Rather, we shall dwell on the sciences that underpin Nuclear Engineering and Radiological Sciences, for it is essential that we understand, in some detail, the nature of the stuff we are engineering. Nuclear materials and the resultant radiation are really some of the most dangerous (and interesting) things in the world, and, in my view at least, understanding them, at least in some depth, is essential.

These two courses assume, and make great use of, the earlier background courses in mathematics and physics. So, if you get stuck on some mathematics or physics concept, please dive into your old notes and texts, or ask questions. These things may have seemed tired and dry when you learned them initially, but these courses will bring them to back to life, with some vigor, and a great deal of power. By their very nature, the consequences of Special Relativity and Quantum Mechanics are counterintuitive. Our understanding of very fast and/or very small objects is not reinforced by our everyday experiences. Consequently, the understanding of these phenomena falls to mathematical interpretation, that must be refined, to enable deeper understanding. Much like a blind person, whose other senses are sharpened to enable him or her to experience the world, so it is that mathematics becomes more important. Equations really do speak, if you listen the right way.

1.2 Modern Physics, Quantum Mechanics and Nuclear Physics

This book covers the essential components of Modern Physics, Quantum Mechanics and Nuclear Physics, suitable for Junior College-level engineers, and, perhaps, Engineering Physics majors and Physicists. Most of the applications that are discussed relate to the subject matter of Nuclear Engineering and the Radiological Sciences.

What is Modern Physics?

Modern Physics is, broadly speaking, inlcudes are the "new' Physics discovered starting at about 1900. Generally, one thinks of Relativity, both "Special" and "General", as well as Quantum Mechanics. In this course, to support the later topics, we study a few aspects of Special Relativity, and delve into Quantum Mechanics, and then Nuclear Physics.

In Special Relativity, we focus on particle and photon kinematics, photons that travel at the speed of light, c, and energetic particles, that may travel at velocities approaching c. There are numerous applications that require this knowledge, in Nuclear Engineering and Radiological Sciences. To name a few:

- Nuclear disintegrations from fission, radiate copious quantities of photons.

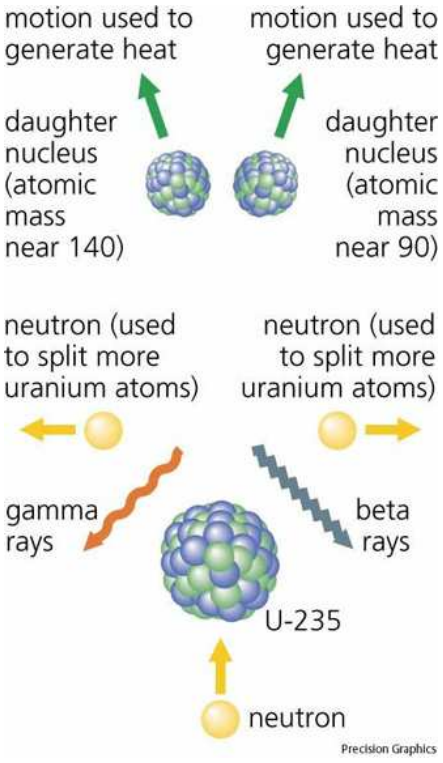

Figure 1.1: Radiation from nuclear fission

- Unstable isotopes often decay via photon emission, and energetic β decay.

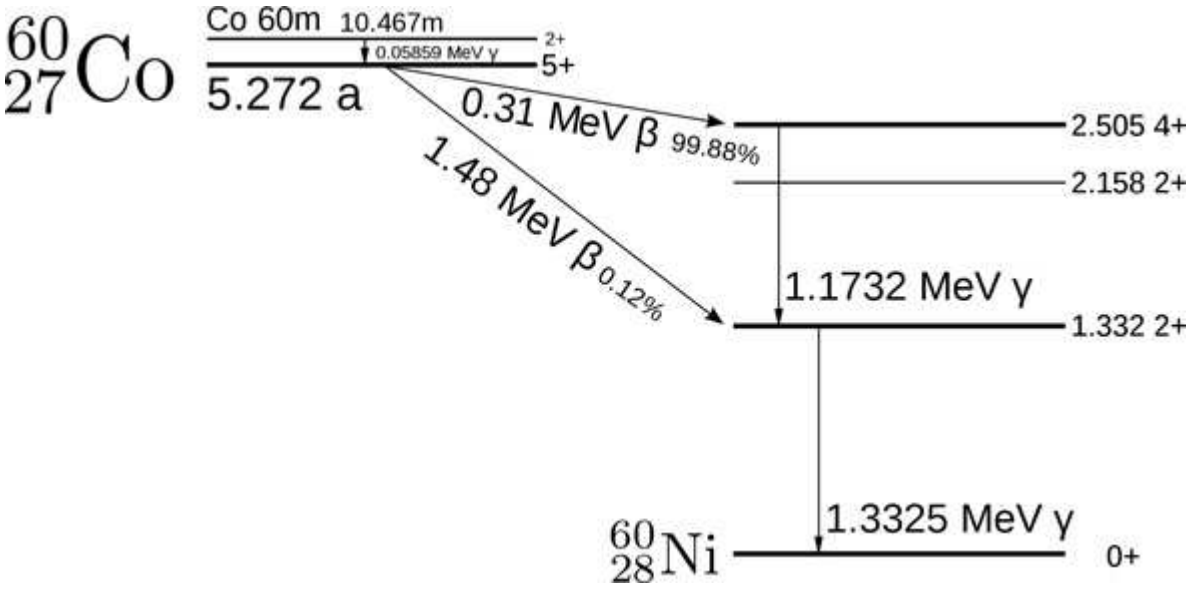

Figure 1.2: Decay Scheme of ^{60}Co

Indeed, ^{60}Co is one of the most commonly-used isotopes in the Medicine and Industry.

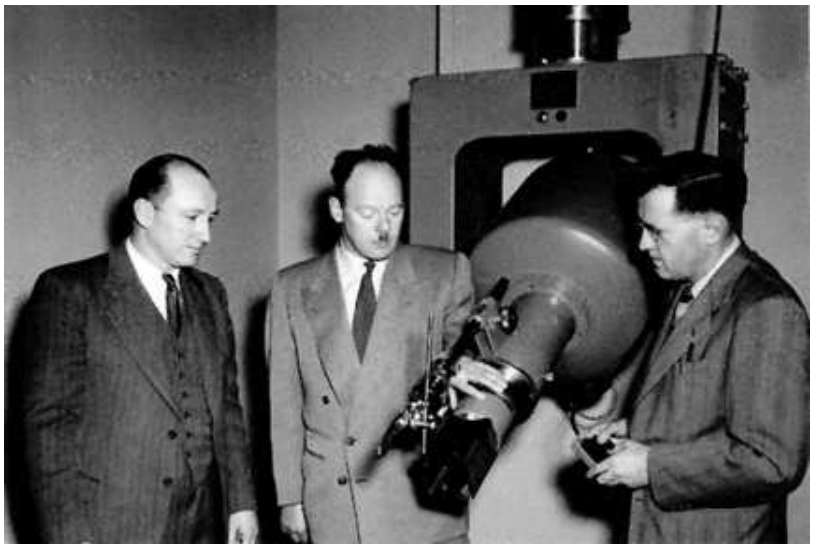

Figure 1.3: The first ^{60}Co machine, and two of its developers: R→L: Dr. Harold Johns, Univerity of Saskatchewan, the inventor, Mr. John MacKay, ACME Machine and Electroic Company, and "instrument maker who could make anything", who built it, and Dr. Sandy Watson, Director of the Saskatchewan Cancer Commission. (*ca.* 1950)

- Energetic electrons for medical treatments.

Figure 1.4: Gordon Isaacs, pictured here in 1957, receive the first electron-beam treatment for cancer of the retina. Gordon's right eye was lost to cancer but his left eye was spared.

- Energetic electrons for physics experiments.

Figure 1.5: The two-mile long Stanford Linear Accelerator

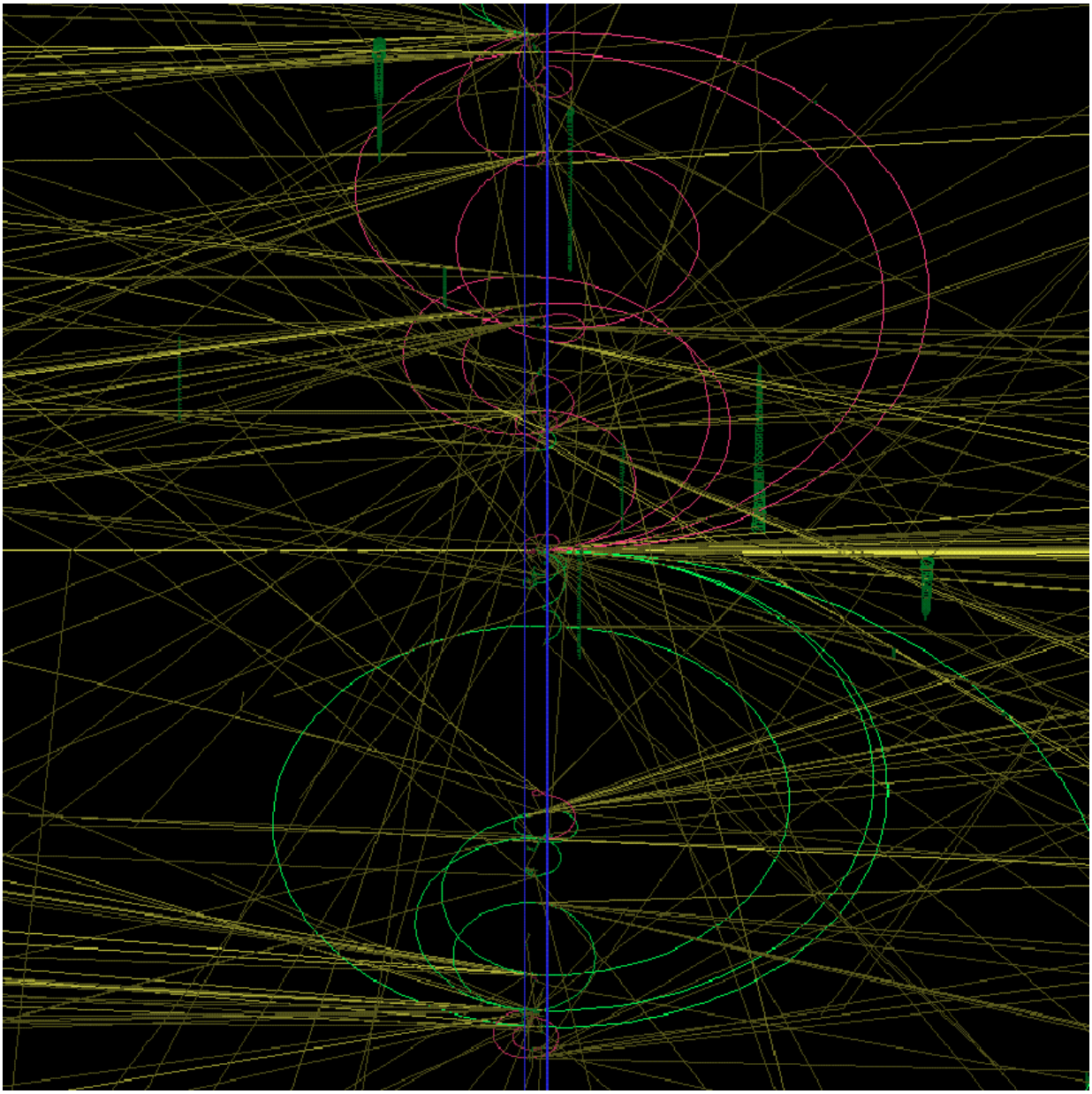

Figure 1.6: A Monte Carlo simulation of ten 1 GeV photons on a lead slab (in the center) encased in a bubble chamber. The color code is (yellow,green,red) for (photons, e^-, e^+). A magnetic field caused the electron tracks to spiral. The initiating photons are incident from the left (very narrow, yellow beam). $e^\pm$ pairs are created in the lead. These give off bremsstrahling photons, the narrow conical "spray" of photons to the right. Energetic $e^\pm$ spiral back, striking the lead slab again, causing more bremssrtahlung photons. Look for tight spirals of smaller energy electrons in the bubble chamber. These were set in mottion through the Compton interaction process.

- Electrons slowing down in materials emit bremsstrahlung photons. These photons are used to perform photon radiotherapy:

Figure 1.7: Medical linear accelrators (LINACs) accelerated eletrons to relativistic energies, and produce beams of photons through the bresstrahlung process. These are used for cancer radiotherapy treatment.

A more common name for bremsstahlung photons is "X-rays". X-rays are used for imaging the human body. This machine is a computed tomorograph (CT) scanner, sued to form 3-dimensional images of the inside of the body.

Figure 1.8: A CT scanner.

- Glow Blue! That's really Čerenkov radiation.
  See `http://en.wikipedia.org/wiki/Cherenkov_radiation`
  Čerenkov radiation, visible blue light, arises from fast electrons, close to the speed of light in vacuum, traveling faster than the speed of light in a dielectic medium with a refractive index greater than 1 (meaning the light travels slower than c). The electrons polarize the molecules of that medium, which then turn back rapidly to their ground state, emitting visible radiation. The lights waves then concentrate on wavefronts, much like sound waves in a sonic boom.

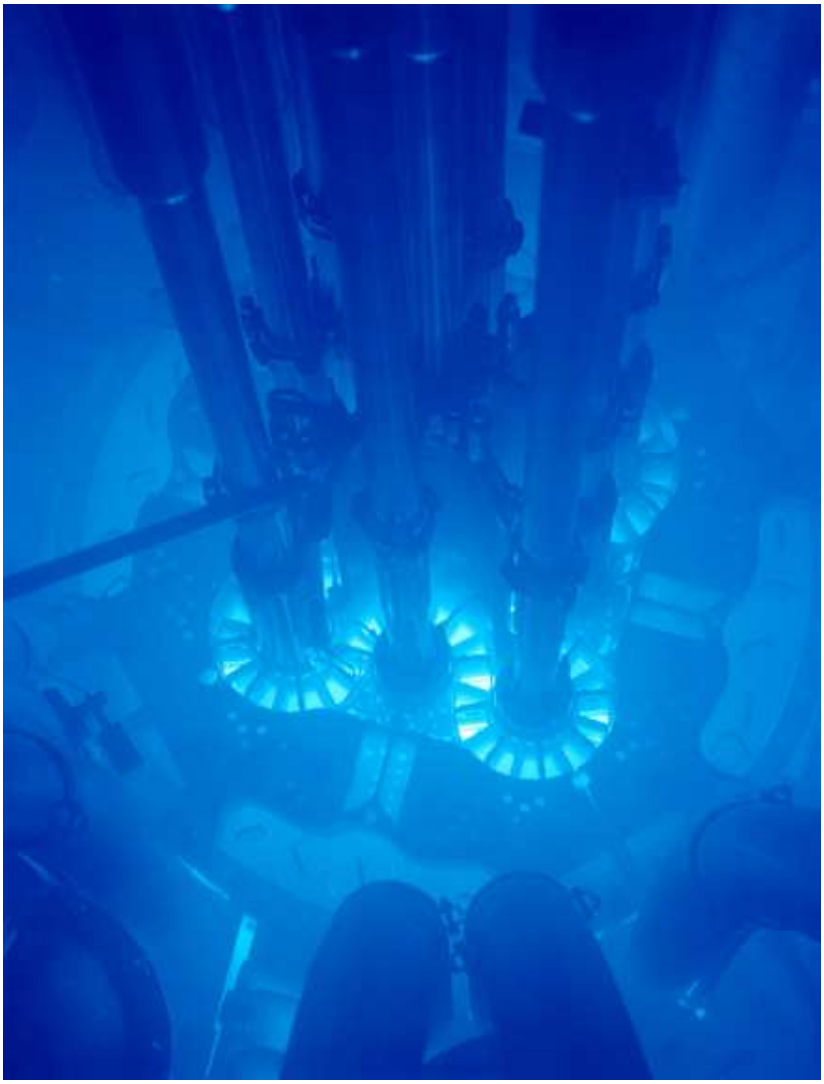

Figure 1.9: Čerenkov radiation, in the Advanced Test Reactor, part of the Idaho National Laboratory.

Pavel Alekseyevich Cherenkov (1904–1990) was the first to characterize this phenomenon completely, earning him the Nobel Prize in 1958.

Figure 1.10: Pavel Cherenkov

A brief note on chapter headings

Chapter and subchapter headings preceded by a dagger† exist for supplementary, prerequisite, or co-requisite study. They will be covered on a need-to basis. Chapter and subchapter headings preceded by an asterisk* are generally not covered in teaching the NERS 311/312 editions of the class, but are there for generality and completeness.

1.3 Some History

Around about the turn of the last century, at the dawn of the 1900s, physics was in a very smug and arrogant phase of its development. It was opined by some very famous physicists, that all the interesting physics had been discovered. *Classical Mechanics*[1] had been refined to such an advanced state, that it was thought that prediction of the future was tantamount to measuring enough inputs at some time, plugging these into the equations of motion, and letting the future unfold in a predictable fashion. This is quite depressing, eh? How

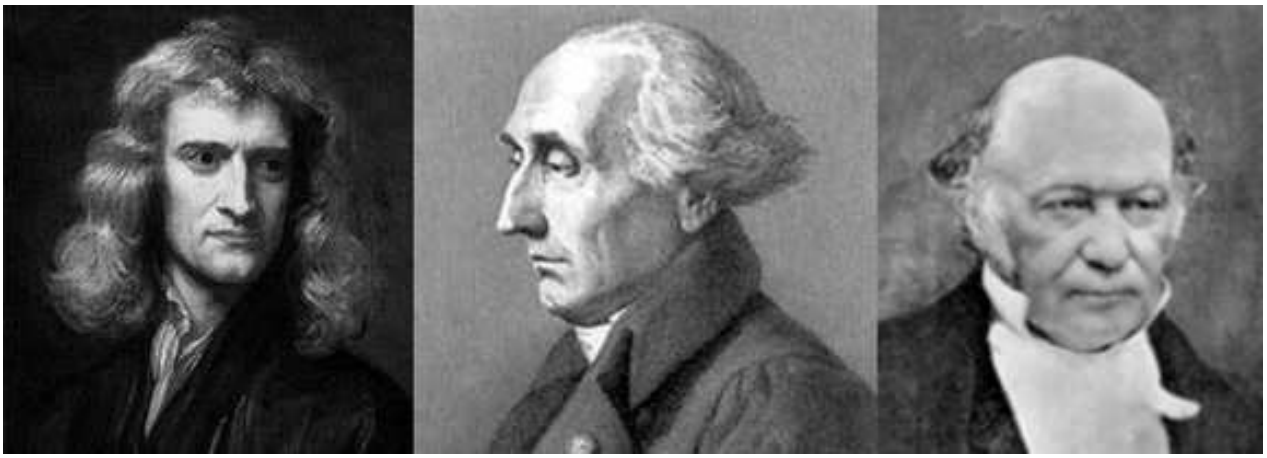

Figure 1.11: The three "giants" of Classical Mechanics(L→R): Isaac Newton (1642–1727), Joseph-Louis de Lagrange (1736–1813), and William Rowen Hamilton (1805-1865)

uninteresting life would be if all it was an enormous equation, with many variables, where, in principle, if never practically possible, the future is completely determined. In practical terms though, the motion of the planets, moons and suns are completely predictable, and every test (almost every test, to be completely honest) was proven beyond a doubt.

Compounding this arrogance was the unification of the phenomena of magnetism and electricity by Clerk Maxwell, in the theory of Classical Electrodynamics. Radio waves, electric

[1]Classical Mechanics is the study of the forces that act on particles with mass and objects, and the motions that result. At that time in history, it was thought to be the "Theory of Everything". See also: `http://en.wikipedia.org/wiki/Classical_mechanics`

motors, and all sorts of phenomena were completely explained. Electromagnetic waves were understood in terms of the theory of waves, with certain special laws, that govern their behavior. The development of Maxwell's equations was considered to be one of the greatest triumphs of the human intellect.

Figure 1.12: The four "giants" of Classical Electrodynamics (L→R): Michael Faraday (1791–1867), André-Marie Ampère (1775–1836), James Clerk Maxwell (1831–1879) and Carl Friedrich Gauss (1777-1855)

$$\begin{aligned}
\vec{\nabla}\cdot\vec{D} &= 4\pi\rho && \text{Gauss's Law of Electricity}\\
\vec{\nabla}\cdot\vec{B} &= 0 && \text{Gauss's Law of Magnetism}\\
\vec{\nabla}\times\vec{E} &= -\frac{1}{c}\frac{\partial\vec{B}}{t} && \text{Faraday's Law}\\
\vec{\nabla}\times\vec{H} &= \frac{4\pi}{c}\vec{J}+\frac{1}{c}\frac{\partial\vec{D}}{\partial t} && \text{Ampère-Maxwell Law}
\end{aligned}$$

Then, it all started to unravel, and it became very much more interesting.

Astronomers began to turn their increasingly powerful telescopes to view more and more distant galaxies, ones that were moving very, very fast with respect to the earth, close to the speed of light. It appeared that the Laws of Physics were different for these distant objects. Physicists have this compelling idea: that the Laws of Physics should be everywhere the same, no matter where in the universe one is, or how fast one is moving. This is called the Principle of Relativity. In Physics, the Principle of Relativity is a hypothesis, never proven wrong, that the Loaw of Physics are the same, no matter where in teh uUniverse one is. It is a prejudice, or an expectation of how the Universe ought to be organized, but one that has **never** steered us wrong, once we listened carefully to what Nature was really telling us. Careful analysis of Maxwell's Equations also revealed the same sort of discrepancy.

This was first realized by Lorenz, but the point was really driven home by Einstein's first paper on Special Relativity. Einstein recognized that the distant fast-moving galaxies and Maxwell's Equations did satisfy the Principle of Relativity, as long as you also insisted that the measured speed of light is the same for all observers, irrespective of how quickly they are moving with respect to a light source. This has the most interesting and counterintuitive consequences: like the length of an object measured by two different observers is different, or a clock seen by two different observers, moving with respect to each other, appears to run at different rates. These notions confuse us to this day, although they have been proven beyond doubt. If the speed of light were much slower, say, 200 km/h, this would be common, practical knowledge we would comprehend intuitively.

Consequently, the first thing we shall study is Special Relativity. The reason is, not only because it is interesting in and of itself, but, because we shall be studying particles and objects that move at a significant fraction of the speed of light, like β-particles in nuclear disintegration, and photons that do travel at the speed of light as a nucleus changes from state to state. We study "Special" Relativity, that restricts the observers to moving at constant velocity with respect to each other, in "inertial frames". This is a great simplification over the more complicated "General" Relativity, where forces may act upon the observers and objects. Special Relativity is complicated enough, as we shall see, and understanding it is sufficient for this course. General Relativity is a vast and wonderful subject that is discussed in specialist graduate courses in Physics Departments, to prepare future researchers for work in cosmology. The results of General Relativity are also exploited in science fiction. Black holes really do exist, there is a huge one at the center of our galaxy. Worm holes are possible too, but need very special conditions for their existence, as does time travel and moving instantaneously, beyond light speeds, to other areas of the galaxy. These latter phenomena have not been observed ... yet.

The other unraveling of our traditional understanding of Classical Physics, related to our investigations of energetic photons, and of electrons, as more powerful microscopes probed the fundamental particles of nature. Maxwell taught us that light is a wave, and the wave equations that describe the behavior of light and other electromagnetic waves, were well validated for a very vast range of phenomena. However, when the light became more energetic in certain ways, newly discovered phenomena, like the photoelectric effect, could only be explained, if high energy photons could be considered to be "particles"[2]. As a physical phenomenon, the acceptance of light as a collection of particles, does not seem to be very hard to accept. The counter to this was, however, that particles, like electrons, participated in phenomena (like fluorescence) in ways that could only be explained by considering all particles, and all objects, as waves[3]! This ushered in the new physics, Quantum Mechanics, that is able to describe the interference pattern that a single particle makes, going through

[2]This idea, put forward by Einstein in 1905, won him the Nobel Prize in 1921. Einstein proposed the Theory of Special Relativity in 1905 as well. 1905 was a great year for Albert!

[3]This was proposed by Louis de Broglie in 1925 in his Doctoral Thesis! He was rewarded with a Nobel Prize only 4 years later.

two places, at, more or less, the same time. This notion is so confounding, that it can befuddle even the deepest thinkers. Yet, it revolutionized physics in a fundamental way, and has been proven beyond the shadow of a doubt.

Thus, Quantum Mechanics, the physics that must be used to describe the really smallest things in the universe, was born, and verified by every experiment thrown at it for explanation. Classical Mechanics is still true, for heavier objects, but it is understood to be the "heavy" limit of Quantum Mechanics. The evidence for the veracity of Quantum Mechanics is the strongest for the lightest particles. So, we study Quantum Mechanics, and eventually end up, in the first course, with a tour de force example of the power of Quantum Mechanics, namely the decay scheme of the hydrogen atom, and hydrogenic atoms. We shall even explain, albeit only semi-quantitatively, all of chemistry!

Then, with the power and insights from Special Relativity and Quantum Mechanics, in the second term we tackle the most knotty problem of Nuclear Physics. Here the particles are thousands of times heavier than electrons, quantum and classical intuition are both essential in understanding these complicated objects.

Once we complete the second term's material on Nuclear Physics, you will have under your belts, a solid theoretical understanding of the background of Nuclear Engineering and the Radiological Sciences, that should serve you well in the upper division courses. I trust you will find it more than an exercise to get through the prerequisite material. The new knowledge, and intuition that arise as a result of its study, are essential skills for a modern scientist and engineer.

1.4 Review of Classical Physics

1.4.1 Mechanics

The kinetic energy (a scalar) of a mass of mass m moving with velocity $\vec{v}$ in some direction is:

$$K = \frac{1}{2}mv^2 \ . \tag{1.1}$$

Its momentum[4] (a vector), is:

$$\vec{p} = m\vec{v} \ . \tag{1.2}$$

(1.1) $\rightarrow$ (1.2) $\Rightarrow$:

[4]In this book I'll denote a vector with an arrow over it. Some authors prefer to use **bold font** for vectors.

$$\vec{p} \cdot \vec{p} = p^2 = m\vec{v} \cdot m\vec{v} = m^2 \vec{v} \cdot \vec{v} = m^2 v^2 \ . \tag{1.3}$$

(1.1) & (1.3)/(2m) $\Rightarrow$:

$$\frac{p^2}{2m} = \frac{m^2 v^2}{2m} = \frac{1}{2} m v^2 = K \ .$$

Thus, we have another way of writing the kinetic energy:

$$K = \frac{p^2}{2m} \ . \tag{1.4}$$

The kinetic energy change across a potential difference of 1 volt is:

$$\Delta K = 1eV \approx 1.602 \times 10^{-19} \text{ J} \tag{1.5}$$

for a singly charged particle (one unit of charge e).

Collision Kinematics

Consider the following collision:

Here, objects with mass m_1 and m_2 collide, exchange some mass (no mass is lost or gained in classical mechanics) to produce m_a and m_b, with velocities as shown. The symbol Q stands for the activation energy. If it is negative, the reaction is "endothermic", that is, energy is required to make the reaction proceed. This energy must be supplied by the kinetic energy of the incoming particles, before the reaction can proceed, and is not available to the resultant particles. If Q is positive, the reaction is 'exothermic", that is, energy is released after the reaction takes place, and is available to be taken up by the resultant particles as kinetic energy.

If we know $\vec{v_1}$, $\vec{v_2}$, m_1, m_2, m_a, m_b, and Q, and measure **two** of the components of $\vec{v_a}$ or $\vec{v_b}$, then the other components of $\vec{v_a}$ **and** $\vec{v_b}$ may be determined.

We do this by invoking the most powerful conservation laws in physics:

1. The conservation of energy,
2. the conservation of momentum (all components),
3. the conservation of mass (classical physics only).

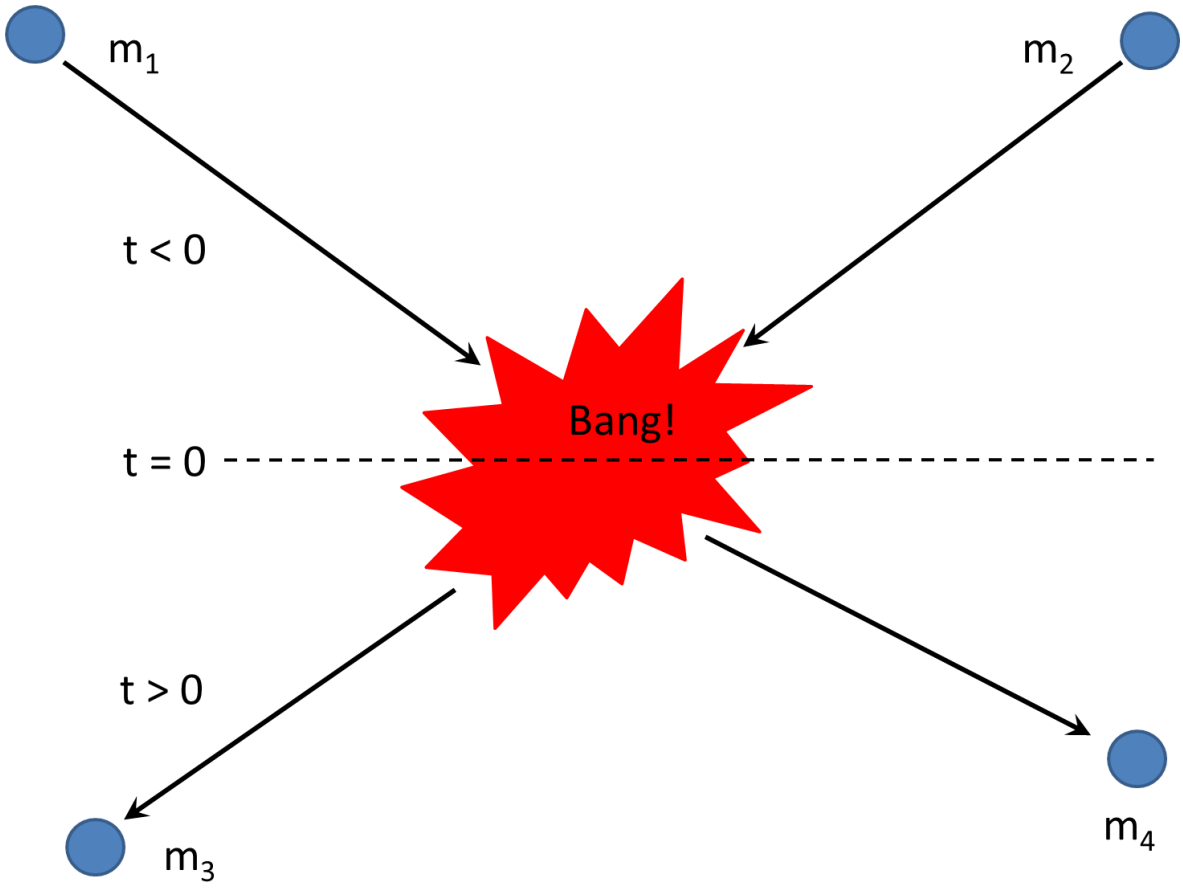

Figure 1.13: Collision between two particles

Conservation of Energy implies (Shorthand: CoE⇒)

$$\frac{1}{2}m_1(v_{1,x}^2+v_{1,y}^2+v_{1,z}^2)+\frac{1}{2}m_2(v_{2,x}^2+v_{2,y}^2+v_{2,z}^2)+Q=\frac{1}{2}m_a(v_{a,x}^2+v_{a,y}^2+v_{a,z}^2)+\frac{1}{2}m_b(v_{b,x}^2+v_{b,y}^2+v_{b,z}^2)\ . \tag{1.6}$$

Conservation of Momentum in the x-direction implies (Shorthand: CoM$_x$ ⇒):

$$m_1v_{1,x}+m_2v_{2,x}=m_av_{a,x}+m_bv_{b,x}\ . \tag{1.7}$$

Conservation of Momentum in the other 2 spatial coordinates implies:
CoM$_y$ ⇒:

$$m_1v_{1,y}+m_2v_{2,y}=m_av_{a,y}+m_bv_{b,y}\ . \tag{1.8}$$

CoM$_z$ ⇒:

$$m_1v_{1,z}+m_2v_{2,z}=m_av_{a,z}+m_bv_{b,z}\ . \tag{1.9}$$

Finally, Conservation of Mass implies (Shorthand: CoM⇒):

$$m_1+m_2=m_a+m_b\ . \tag{1.10}$$

Thus, these 5 equations, (1.6)–(1.10), have, in principle, 17 unknowns: m_1, $v_{1,x}$, $v_{1,y}$, $v_{1,z}$, m_2, $v_{2,x}$, $v_{2,y}$, $v_{2,z}$, m_a, $v_{a,x}$, $v_{a,y}$, $v_{a,z}$, m_b, $v_{b,x}$, $v_{b,y}$, $v_{b,z}$, and Q[5]. This means that, if we know (through measurement, perhaps) 13 of them, we may find the other 4 by manipulating the above equations. Or, if we know 12 of them, we may relate any kinematic variable to any other, through the process of elimination. It always works, without fail. Sometimes, it's just a little more difficult to extract the information arithmetically, but it is always possible.

In more condensed vector notation,

CoE⇒

$$\frac{m_1v_1^2}{2}+\frac{m_2v_2^2}{2}+Q=\frac{m_av_a^2}{2}+\frac{m_bv_b^2}{2}\ , \tag{1.11}$$

while Co$\vec{M}$ ⇒

$$m_1\vec{v}_1+m_2\vec{v}_2=m_a\vec{v}_a+m_b\vec{v}_b\ . \tag{1.12}$$

Solution Strategies

These kinematic equations, while they represent something clear, are fraught with mathematical pitfalls, partly because what they are describing, is full of physical richness. It helps

[5]Later on, when we discuss relativistic kinematics, we shall see that $Q=(m_1+m_2-m_a-m_b)c^2$, where c is the speed of light. The mass differences are usually so small that Conservation of Mass is employed without loss of accuracy in a non-relativistic analysis.

to know exactly what one is after, and proceed with care. Here is an example. Let's say that one wants to eliminate $\vec{v}_b$. Here is a procedure that eliminates it with a minimum of effort. First, isolate the terms with $\vec{v}_b$, or v_b^2 on the right hand side (RHS) of (1.12) and (1.11). Then,

$(1.12)^2$ - $2m_b\times$ (1.11) $\Rightarrow$

$$(m_1\vec{v}_1 + m_2\vec{v}_2 - m_a\vec{v}_a)^2 - m_b(m_1v_1^2 + m_2v_2^2 - m_av_a^2) - 2m_bQ = 0 \ , \tag{1.13}$$

and v_b has vanished.

An equivalent way of writing (1.13) is:

$$\vec{\xi}^2 - 2m_b(\kappa + Q) = 0 \ , \tag{1.14}$$

where $\vec{\xi} \equiv m_1\vec{v}_1 + m_2\vec{v}_2 - m_a\vec{v}_a$, and $\kappa \equiv (m_1v_1^2 + m_2v_2^2 - m_av_a^2)/2$. This alternative form will be useful to us later when we discuss relativistic collisions.

Similarly, if you want to eliminate other kinematic quantities, similar isolation and subtraction will work. The examples and problems will serve to illustrate this.

Illustration: 1D elastic collision, equal masses

Question: Imagine an object of mass m (the projectile), strikes another object (the target), that is identical in all respects. The struck object is initially at rest, the collision is elastic, and the whole event takes place in 1 dimension. (The velocity of any resultant object is colinear with the initial direction of motion.) The collision is elastic*, that is, $Q = 0$, and there is no exchange of mass, that is, there are two objects of mass m after the collisions as well. What happens after the collision?*

Answer: The details will be worked out in class, however, let us discuss the result. Those among us who have played billiards know the answer intuitively. However, the kinematics of billiard balls[6] is identical to that of sub-relativistic neutrons. After the collision, an object of mass m is going in the same direction as the projectile, and one object remains behind, at rest.

Discussion: A billiards player knows that the projectile (the cue ball) will strike the target ball, and, in the absence of any spin, come to a complete stop. The target ball, on the other hand, will acquire the speed and direction (assuming a straight-on hit) of the cue ball. Let us imagine, however, that we do not see or hear the collision occur, that the projectile and the target are the same color, and only observe the resultant trajectories. The mathematics does not reveal which object acquires the final momentum. Is it the target or projectile? The projectile could have simply passed through the target ball without setting it in motion.

[6]Anyone studying the behavior of particle collisions would be well served, by engaging in recreational billiards. You can quote me on that!

We can not tell. Conservation of energy and momentum does not concern itself with the details of the "collision". The conservation laws simple relate the initial and final conditions, at a level of abstraction and power beyond the dynamics of the collision. For all we know, the projectile and target could have exchanged some equal part of their masses. We'd have no way of knowing. Although we know this not to be the case for billiard balls, for neutrons we have no way of knowing.

Application: Newton's cradle

Explain how the Newton's Cradle works.
See `http://en.wikipedia.org/wiki/Newton%27s_cradle` for some interesting discussion and history.

Related problems

Problem: Imagine an object of mass m (the projectile), strikes another object (the target), that is identical in all respects. The struck object is initially at rest, the collision is inelastic, and both balls fuse together. What happens after the collision? What is the Q-value of this reaction?

This example will also be worked out in class.

2D elastic collision, equal masses

Problem: Show, when two balls collide elastically, with one of them being initially at rest, that the angle between the two resultant directions is always always $90°$*. How does this result include the result of the previously discussed 1D elastic scattering?*

Solution:

1. *Set up the CoE and Co*$\vec{M}$ *equations assuming "2" is at rest:*

$$\frac{1}{2}mv_1^2 = \frac{1}{2}mv_a^2 + \frac{1}{2}mv_b^2 \tag{1.15}$$

$$m\vec{v}_1 = m\vec{v}_a + m\vec{v}_b \tag{1.16}$$

2. *We require the angle between the resultant trajectories. The cosine of this angle is obtained by* $\vec{v}_a \cdot \vec{v}_b$*. To isolate this: (1.16)*^{2}*/(2m*^{2}*) - (1.15)/m* $\Rightarrow$

$$\vec{v}_a \cdot \vec{v}_b = 0 \ . \tag{1.17}$$

Interpretation: If v_a *and* v_b *are both non-zero, we see that the angle between the outgoing billiard balls is* $\pi/2$*, a right angle — the well-know result (at least to billiard players*[7]*). If*

[7]This analysis neglects the spin on the billiard balls, a very simplifying assumption. In billiards, the ability to control the spin and recoil trajectory of the cue ball, is what separates the "sharks" from the "marks".

either v_a or v_b is zero, (1.17) yields the result of the opening angle as "undefined". We can interpret this as $\pi/2$ in the limit as either the grazing blow, or the near-perfect direct shot. In both cases, one of the balls will have a trajectory with infinitesimally small velocity, at right angles to the speedier ball.

Zero-Momentum Frame

Sometimes, it is advantageous to work in an inertial frame where there is no net momentum. The velocity of this frame is determined as follows:

We seek a velocity $\vec{V}$ that, when subtracted from the velocities of the initial particles, has zero resultant momentum. Thus, appealing to the left hand side (LHS) of (1.11) we want:

$$m_1(\vec{v}_1 - \vec{V}) + m_2(\vec{v}_2 - \vec{V}) = 0 \ , \tag{1.18}$$

for which the solution is:

$$\vec{V} = \frac{m_1\vec{v}_1 + m_2\vec{v}_2}{m_1 + m_2} \ . \tag{1.19}$$

Perform the calculation extracting the kinematic relations, in this frame. That is, $\vec{v}_1 \to \vec{v}_1 - \vec{V}$, and so on. And then, once the desired result is obtained, transform the velocity vectors in the opposite direction.

2D elastic collision, equal masses

Problem: repeat this problem in the zero-momentum frame, transform back to the rest frame of the target particle, and show the same result.

Particle-at-Rest Frame

At other times, it is advantageous to work in a frame where one of the particles in the initial state is at rest (the stationary target), since in fact, this is usually the case. But, had we started from the situation described in (1.10) and (1.11) we may transform to a reference frame where the target (m_2, say) is at rest by subtracting $\vec{v}_2$ from all velocities in the problem, then rotating the new $\vec{v}_1$ into the z-direction, and the new $\vec{v}_a$ and $\vec{v}_b$ into the xz-plane, so it can be visualized on the blackboard, or paper. After the required kinematical quantities are obtained, reverse the rotations[8], and reverse the velocity transformation and you're done.

This situation (target-at-rest) is very important since it often represents the starting physical condition. Let us illustrate what happens to (1.13) in this circumstance. Setting $\vec{v}_2 = 0$ in (1.13) gives us:

[8]Rotations do not commute, so be careful of the order!

$$m_a^2 v_a^2 - 2m_1 m_a v_1 v_a \cos\theta_a + m_1^2 v_1^2 - m_b(m_1 v_1^2 - m_a v_a^2) - 2m_b Q = 0 \ , \qquad (1.20)$$

where θ_a is the angle of m_a with respect to (wrt) the z-axis, in spherical-polar coordinates. Or, more suggestively,

$$[m_a(m_a + m_b)]v_a^2 + [-2m_1 m_a v_1 \cos\theta_a]v_a + [m_1(m_1 - m_b)v_1^2 - 2m_b Q] = 0 \ . \qquad (1.21)$$

This can be regarded as a solution of θ_a in terms of v_a, or a quadratic formula of the form

$$Ax^2 + Bx + C = 0 \ ,$$

for which the solution of v_a in terms of θ_a is well known. (A, B, C are constants, and we seek the values of x for which the above is true.) We shall leave further exploration of this quadratic solution to the examples and problems. However, the quadratic equation has a rich variety of solutions. Sometimes, there are no solutions (kinematically restricted) or one or two solutions. We shall revisit this topic later in the course.

Illustration

Consider the following collision between two identical masses, travelling with equal but opposite velocities along the x-direction, that produce two masses, m_a and m_b. (Yes! The figure is missing!)

By applying the conservation laws we just discussed, we can show that the resultant velocities are:

$$v_b = \pm\sqrt{\frac{m_a}{m_b}}v \ ; \ v_a = \mp\sqrt{\frac{m_b}{m_a}}v \ ,$$

where the final velocities are oriented in directions opposite. (Demonstration to be given in class.)

This makes sense! There is no net momentum before the collision and so you expect the lighter particle to be moving faster and in the opposite direction to the heavier particle. It is also easy to verify that the initial and final kinetic energies are the same.

Potential, Kinetic, Total Energy, Angular Momentum

A particle (Let's think of this as a small object.) moving in one dimension can be subjected to a force $F(x)$ that causes it to move. Associated with this force is a potential, $U(x)$. External forces and potentials are related by:

Figure 1.14: An illustration of the use of conservation laws

$$F(x) = -\frac{\mathrm{d}U(x)}{\mathrm{d}x} \ . \tag{1.22}$$

In three dimensions, we have $F(\vec{x})$ and $U(\vec{x})$, that are similarly related:

$$F(\vec{x}) = -\vec{\nabla}U(\vec{x}) \ . \tag{1.23}$$

The total energy, E, of a particle subjected to an external force is, in one dimension, a constant:

$$E = K(x) + U(x) \ . \tag{1.24}$$

In three dimensions, a system of N particles has its total energy conserved as well, and may be written:

$$E = \sum_{i=1}^{N} [K(\vec{x_i}) + U(\vec{x_i})] \ . \tag{1.25}$$

Angular momentum $\vec{L}$ for a single particle is also conserved. It is expressed in terms of the cross product of the position and momentum as:

$$\vec{L} = \vec{x} \times \vec{p} \ . \tag{1.26}$$

In three dimensions, a system of N particles has its total angular momentum conserved as well, and may be written:

$$\vec{L} = \sum_{i=1}^{N} \vec{x_i} \times \vec{p_i} \ . \tag{1.27}$$

1.5 Units and Dimensions

1.6 Significant Figures

Physical things are measured two ways. There are integral quantities, *e.g.* 3 electrons, 4 photons, *etc.* It doesn't make sense to say "A tritium nucleus is made up of 1.0 protons and 2.0 neutrons.", because 1.0 and 2.0 are not integers, and there should be no ambiguity in the number of discrete particles. The correct statement would be, "A tritium nucleus is made up of 1 proton and 2 neutrons."

Other quantities are not discrete. There *is* ambiguity in the statement, "The α-particle has an energy of 5 MeV.", because there is no statement as to how good the "5" is. The best we can do, is to give to a precision, of that participant, with the least. That's not the best situation, but it is what we have to live with, without more information.

For example, consider:

$$r = a \blacksquare b \ ,$$

where $\blacksquare$ represents one of the operators, $\times$, $\div$, $+$, or $-$. Define a "precision operator", $\mathcal{P}()$, that returns the precision of its argument. For example, $\mathcal{P}(1.37) = \mathcal{P}(0.000137) = 3$. Then,

$$\mathcal{P}(r) = \min \mathcal{P}(a), \mathcal{P}(b) \ .$$

If you come across a statement like, "The α-particle has an energy of 5 MeV.", it is likely an error, because no educator wishes to be ambiguous. If he or she does, and it's on purpose,

then the question was designed to make you think. It is valid to say, "The α-particle has an energy of 5 MeV (exactly).", in which case, you are expected to treat the "5" as an exact real number, with infinite precision.

In some situations, you will be told, "The α-particle has an energy of 5.02±0.13 MeV.", in which case you will be expected to estimate what the error is, on the final quantity, if you use it in a computation. That is discussed later in this chapter.

1.7 Theory, Experiment, Law

1.8 †Basic Error Estimation

1.8.1 Accounting for Estimated Error for Independent Quantities

Suppose M is a measured quantity, the result of some calculation or experiment, that depends on two other quantities, a and b, that have their own estimated uncertainties σ_a and σ_b. Assuming that the relative errors in a and b are small (*i.e.* we propagate first-order errors only), and a and b are independent (the result of two independent measurements), then the estimated error in M, namely σ_M, is determined as follows:

$$\sigma_M = \sqrt{\left(\frac{\partial M(a,b)}{\partial a}\right)^2 \sigma_a^2 + \left(\frac{\partial M(a,b)}{\partial b}\right)^2 \sigma_b^2} \ , \tag{1.28}$$

and the fractional error is:

$$\frac{\sigma_M}{M} = \frac{1}{M(a,b)} \sqrt{\left(\frac{\partial M(a,b)}{\partial a}\right)^2 \sigma_a^2 + \left(\frac{\partial M(a,b)}{\partial b}\right)^2 \sigma_b^2} \ . \tag{1.29}$$

The extension to measurements that have three or more independent inputs, is straightforward.

Some examples:

1. Q: After a collision reaction involving two protons, the two protons have kinetic energies 2.8 ± 0.6 and 10.0 ± 1.0 MeV. What is the total combined resultant kinetic energy and its estimated error?

   A: The total energy is

   $$K = K_1 + K_2 \ .$$

Therefore, by the rule stated above,

$$\sigma_K = \sqrt{\sigma_{K_1}^2 + \sigma_{K_2}^2} \ .$$

Therefore,

$$K = 12.8 \pm 1.2 \text{ MeV} \ .$$

Food for thought: How should you state the result if the energy of the second proton was 10±1 MeV?

2. Q: *$M(a, b, c) = ab^2c^3$. What is the relative estimated error in M?*

   A: You can show that

$$\frac{\sigma_M}{M} = \sqrt{\left(\frac{\sigma_a}{a}\right)^2 + 4\left(\frac{\sigma_b}{b}\right)^2 + 9\left(\frac{\sigma_c}{c}\right)^2} \ .$$

   Note: Don't expect this very neat expression for all calculations of relative error. It is really a fortuitous result of the given form of M.

1.9 Questions

Answer those questions (on paper or in your head). If you can't find a good answer, re-read the relevant sections of Chapter 1. If you still can't find a good answer, ask a colleague, a TA, or a Prof. A question asked in class is worth 100 asked silently.

Some of these questions may appear on assignments or exams.

1.10 Problems

If you find some of these problems interesting, attempt them on paper. If you can't find a good answer, re-read the relevant sections of Chapter 1. If you still can't find a good answer, try working it out with a colleague, ask a TA, or a Prof.

Some of these problems may appear on assignments or exams.

1.11 Supplementary Problems

1. *After a collision reaction involving two individual protons and one neutron, the neutron has kinetic energy* 2.8±0.6 *MeV while the two protons each have kinetic energy* 10.0±1.0 *MeV. What is the total combined resultant kinetic energy and its estimated error?*

2. *Prove that a sliding (not rolling) billiard ball striking a stationary billiard ball (both with the same mass), scatters such that the angle between them is always $\pi/2$.*

3. *A stationary (at rest, no velocity) nucleus of mass M splits into two nuclei with unequal masses (m_1 and m_2) accompanied by the release of energy Q. (You may assume that $M = m_1 + m_2$.) The direction of motion of the lighter daughter particle is (θ, ϕ), in polar coordinates, measured from the z-axis. Find expressions for the kinetic energy, speed, momentum, and directions of the resultant nuclei.*

4. *The event described in problem 3 is seen by an observer moving along the z-axis in the negative direction with speed v_0. Find expressions for the kinetic energy, speed, momentum, and directions of the resultant nuclei, as seen by this observer.*

5. *Suppose that the initial nucleus in problem 3 was not at rest, but moving with kinetic energy K_0 in 16 positive x-direction. After the split, one of the daughter nuclei moves in the x-direction. Find expressions for the direction of the second nucleus, and the speeds of both. Solve this in 2 ways: a) By direct application of conservation laws in the frame where the original nucleus is moving with kinetic energy K_0. b) By applying the result of the previous problem (rest frame of the original nucleus) and then switching to a reference frame where the initial nucleus has kinetic energy K_0.*

6. *With reference to problem 5, now consider that $Q = 92.0 \pm 0.05$ MeV and $K_0 = 40.0 \pm 0.1$ MeV. Q and K_0 are assumed to be uncorrelated. The original nucleus has a mass of 8u (exact), while the masses of the daughter nuclei are 5u (exact) and 3u (exact). Obtain numerical results for both cases, but this time, estimate the expected error.*

Chapter 2

The Special Theory of Relativity

Read Chapter 2 of the hand-written notes

2.1 *Classical Relativity

Consider an observer, named O, who measures the position of an object in his coordinate system as $\vec{x} = (x, y, z)$, at time t. A second observer, named O', is in an inertial frame (no forces acting on the observer), but moving at linear velocity $\vec{u}$ with respect to O. This second observer measures the position of the object in his coordinate system to be $\vec{x}' = (x', y', z')$, at time t'. Now, we impose some constraints on our two observers to simplify the discussion. (It's not necessary to impose these constraints, it just makes the discussion much simpler.)

1. Both O and O' measure time in the same way, with a clock of *identical* design and function. Thus, any time interval between two events measured by O to be Δt is identical to the time interval $\Delta t'$ observed by O' for the same two events. In other words, the time difference between two events measured by both is the same. That is, $\Delta t = \Delta t'$.

2. At $t = 0$ and $t' = 0$, the coordinate systems of the two observers are perfectly aligned, with $\vec{x} = \vec{x}'$, or equivalently, $(x, y, z) = (x', y', z')$ at $t = 0$ and $t' = 0$. That is, the axes are all perfectly aligned, and the coordinate systems coincident.

3. Both O and O' measure distance (displacements) in the same way, with an instrument of *identical* design and function.

4. Both O and O' measure mass in the same way, with an instrument of *identical* design and function. The mass of the object seen by O and O' are identical.

Consequences:

1. Observer O sees observer O' moving with velocity $\vec{u}$, while observer O' sees observer O moving with velocity $-\vec{u}$.

2. Simultaneous events seen by observer O at time t are also seen by observer O' as simultaneous.

3. A displacement between two simultaneous events measured by O to be $\Delta\vec{x}$ is identical to the displacement $\Delta\vec{x}'$ observed by O' for the same two simultaneous events. This is illustrated in Figure 2.1.

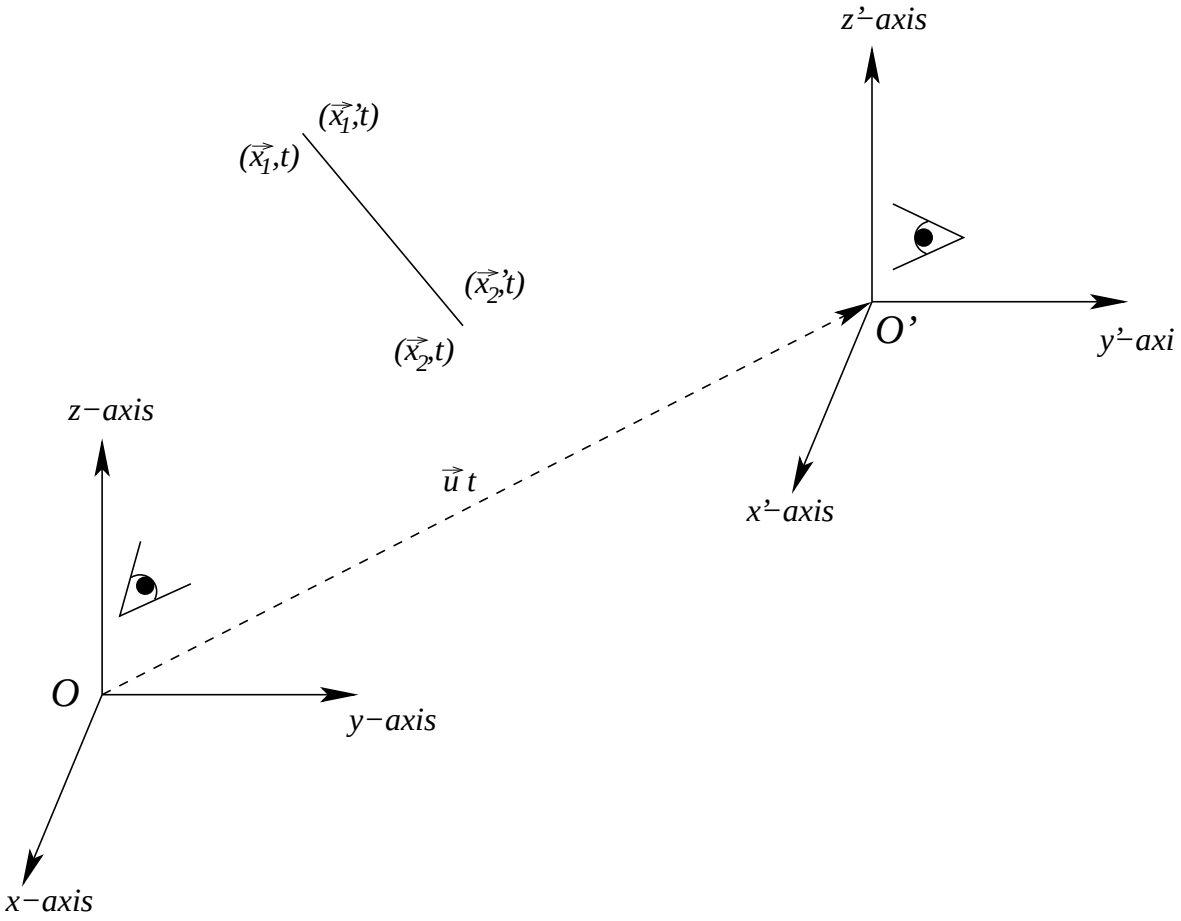

Figure 2.1: Galilean transformation of a displacement.

4. The coordinates of an event in one coordinate system may be related to the other by means of the *Galilean Transformation*:

$$\vec{x}'(t) = \vec{x}(t) - \vec{u}t$$

5. If $\vec{x}(t)$ represents the trajectory of a particle observed by observer O, then it is easily shown that the velocities are connected by:

$$\vec{v}'(t) = \vec{v}(t) - \vec{u} \ ,$$

since $\vec{u}$ is a vector that is constant in time. This shows that Newton's First Law of Motion holds in both frames. If $\vec{v}(t)$ is constant in time, then so is $\vec{v}'(t)$, and the motion (velocity) of the object persists in both frames unless acted on by another force.

6. The accelerations observed by the two observers, is easily shown to be constant,

$$\vec{a}'(t) = \vec{a}(t) \ .$$

Since $\vec{F} = ma$, the force on the object measured by both observers is the same, and Newton's Second Law of Motion applies equally in both frames.

If there are equal and opposing forces on the object in one frame, they are measured to be the same in the moving frame. Newton's Third Law of Motion is preserved.

Hence, the Classical Laws of Physics are the same in both frames.

2.2 *The Michelson-Morley Experiment

Oddly enough, the speed of light is not measured anymore, it has been assigned, via definition in 1983, that of an exact constant:

$$c = 299\ 792\ 458 \text{ m/s} \ .$$

You would only be wrong by about 0.1% if you said it was 3×10^8 m/s, and this approximation is often used in quick numerical calculations.

It is truly remarkable how slow the speed of light is! It takes light about $1/7^{\text{th}}$ of a second to circumnavigate the earth at the equator, and goes about a foot in a nanosecond.

So, if light really has a finite speed, and Galilean transformations are true, we should be able to measure how fast we are moving relative to it. That was the purpose of the Michelson-Morley experiment, the most famous failed experiment in physics[1].

Their experiment showed conclusively, that the speed of light is constant, no matter what direction the earth was moving. Albert Einstein's leap of imagination was to say that it is a fundamental property of light.

[1]That failed experiment got Albert Michelson a Nobel Prize in 1907.

*How the Michelson-Morley Experiment Works

Referring to the figure (it's missing!), let's imagine that the speed of the earth through the ether is u, directed from right to left, along the length $\overline{\mathrm{AC}}$. A pulse of radiation leaves S, the source, and travels upstream against the ether, and is split into two pulses by a "half-mirror" at A. One of the pulses goes along the length $\overline{\mathrm{AC}}$, gets reflected by a mirror at C, back again to the "half-mirror" at A and up to the detection apparatus, that is labeled by D. The half of the pulse that gets split off at A, goes along the length $\overline{\mathrm{AB}}$, gets reflected by the mirror at B, back again to the "half-mirror" at A and up to the detection apparatus at D.

The first pulse, once it leaves the splitter, takes total time

$$t_{||} = \frac{2\overline{\mathrm{AC}}}{c}\frac{1}{1-u^2/c^2} + \frac{\overline{\mathrm{AD}}}{c}\frac{1}{\sqrt{1-u^2/c^2}} \ , \tag{2.1}$$

to complete the journey. Here c is the speed of light (assuming the ether is at rest!).

Since we expect that $u \ll c$, we can do a series expansion of (2.1) in u^2/c^2 and find that, to lowest surviving order in u^2/c^2, that

$$t_{||} \approx \frac{2\overline{\mathrm{AC}}}{c}(1+u^2/c^2) + \frac{\overline{\mathrm{AD}}}{c}(1+\frac{u^2/c^2}{2}) \ , \tag{2.2}$$

which is an excellent approximation, when u is very small compared to c.

Using the same method, the second pulse takes time,

$$t_{\perp} = \frac{2\overline{\mathrm{AB}}}{c}\frac{1}{\sqrt{1-u^2/c^2}} + \frac{\overline{\mathrm{AD}}}{c}\frac{1}{\sqrt{1-u^2/c^2}} \ , \tag{2.3}$$

which, in the $u \ll c$ approximation is

$$t_{\perp} \approx \frac{2\overline{\mathrm{AB}}}{c}(1+\frac{u^2/c^2}{2}) + \frac{\overline{\mathrm{AD}}}{c}(1+\frac{u^2/c^2}{2}) \ . \tag{2.4}$$

The difference between them is

$$\Delta t_0 = t_{||} - t_{\perp} = 2\frac{\overline{\mathrm{AC}}-\overline{\mathrm{AB}}}{c} + \frac{\overline{\mathrm{AC}}}{c}\frac{2u^2}{c^2} - \frac{\overline{\mathrm{AB}}}{c}\frac{u^2}{c^2} \ . \tag{2.5}$$

That difference eliminates the contribution from $\overline{\mathrm{AD}}$. If $\overline{\mathrm{AC}}$ were exactly equal to $\overline{\mathrm{AB}}$, then the experiment would give a direct measurement of the speed of the earth through the ether. But that is impossible to do, because the difference would have to be immeasurably small.

So, they flipped the apparatus by $\pi/2$, so that S and D were in the same place, but B and C changed positions. This results in a time difference of,

$$\Delta t_{\pi/2} = t_{||} - t_{\perp} = 2\frac{\overline{\mathrm{AC}} - \overline{\mathrm{AB}}}{c} + \frac{\overline{\mathrm{AC}}}{c}\frac{u^2}{c^2} - \frac{\overline{\mathrm{AB}}}{c}\frac{2u^2}{c^2} \ , \tag{2.6}$$

and the difference between these two, is

$$\Delta t = \Delta t_0 - \Delta t_{\pi/2} = \frac{\overline{\mathrm{AC}} + \overline{\mathrm{AB}}}{2c}\frac{u^2}{c^2} \ , \tag{2.7}$$

thus ridding the experiment of the differences in distances between the half-mirror and the mirrors, and yielding a direct measure of the speed of the earth through the ether.

As the story unfolded, u was measured to be zero, no matter where the earth was in its yearly revolution around the sun, and the only conclusion that made sense was that light could propagate through a vacuum. That begged the question, "If there is no ether, then what can we say about the speed of light in different inertial frames?" That's exactly what Einstein had something to say about ...

2.3 *Einstein's Postulates

Einstein formulated his Special Theory of Relativity on two postulates, one of them a genuinely new idea:

1. The principle of relativity: *The laws of physics are the same in all inertial reference frames.*
2. Constant speed of light: *The speed of light has the same value in all inertial reference frames.*

The consequences of this idea are remarkable. All three of the constraints we applied to Galilean transformations: time, length and mass equivalence, must be undone. We will investigate these in the next section.

2.4 *The Lorentz Transformation

The Lorentz transformation relating two observers, O and O', where O' is moving along the positive x-axis with respect to O at speed u is:

$$\begin{aligned} x' &= \frac{x - ut}{\sqrt{1 - u^2/c^2}} \\ y' &= y \\ z' &= z \\ t' &= \frac{t - (u/c^2)x}{\sqrt{1 - u^2/c^2}} \ . \end{aligned} \tag{2.8}$$

I'd like to introduce a more compact notation. Factors like u/c and $\sqrt{1 - u^2/c^2}$ occur so frequently that the following convenient shorthand notation is often used:

$$\begin{aligned} \beta_u &= u/c \\ \gamma_u &= \frac{1}{\sqrt{1 - \beta^2}} \ . \end{aligned} \tag{2.9}$$

Frequently, when there is only one velocity in the discussion, the subscript u is dropped. β is the ratio of the velocity in question to the speed of light, while γ is related (as we shall see shortly) to the energy and momentum of a particle with mass.

The following property, a consequence of (2.8) is often employed to simplify expressions:

$$\gamma^2 - \beta^2\gamma^2 = 1 \ . \tag{2.10}$$

With this shorthand, the Lorentz transformation may be written:

$$\begin{aligned} x' &= \gamma(x - \beta ct) \\ y' &= y \\ z' &= z \\ ct' &= \gamma(ct - \beta x) \ . \end{aligned} \tag{2.11}$$

*Lorentz Transformation of Position and Time with Arbitrary Velocity

$O'(x', y', z', t') \to O(x, y, z, t)$, where the relative motion of O' with respect to O is along the positive $\vec{u}$-axis with speed u and direction $\hat{n}_u$:

$$\begin{aligned} ct' &= \gamma_u(ct - \vec{\beta}_u \cdot \vec{x}) \\ \vec{x}' &= \vec{x} - \gamma_u\vec{\beta}_u ct + (\gamma_u - 1)(\hat{n}_u \cdot \vec{x})\hat{n}_u \ . \end{aligned} \tag{2.12}$$

*Length Contraction

With the Lorentz transformation, we are now in a position to obtain the formulae for length contraction and time dilation more simply.

Suppose that O measures a space and temporal displacement with coordinates at (x_1, t_1) and (x_2, t_2). In O''s frame, these coordinates correspond to (x'_1, t'_1) and (x'_2, t'_2). Thus, $\Delta x' = x'_2 - x'_1$ and $\Delta x = x_2 - x_1$ are related by (2.11) and found to be:

$$\Delta x' = \gamma(\Delta x - u\Delta t) \ , \tag{2.13}$$

where $\Delta t = t_2 - t_1$. Now, both O and O' make *simultaneous* measurements of the length of an object aligned along the direction of motion. O' measures the "proper" length, since the object is at rest in his frame. (By definition, the "proper" length is the length of an object as measured in its rest frame. It is always measured to be shorter if in motion relative to the frame in which the measurement is made.) However, O measures a different length L, given from (2.13) as:

$$L_0 = \gamma L, \text{ or } L = L_0/\gamma \ . \tag{2.14}$$

Thus, O measures the object as being "shorter".

*Length Contraction with Arbitrary Velocity

$$\begin{aligned} \vec{L} &= \vec{L}_0 - (\gamma_u - 1)\hat{n}_u(\hat{n}_u \cdot \vec{L}_0)/\gamma_u \\ \hat{n}_u \cdot \vec{L} &= (\hat{n}_u \cdot \vec{L}_0)/\gamma_u \\ \hat{n}_u \times \vec{L} &= \hat{n}_u \times \vec{L}_0 \end{aligned} \tag{2.15}$$

*Time Dilation

Now, consider the same situation in terms of time. According to (2.13),

$$c\Delta t' = \gamma(c\Delta t - \beta\Delta x) \ . \tag{2.16}$$

From (2.13),

$$\Delta x' = \gamma(\Delta x - \beta c\Delta t) \ , \tag{2.17}$$

or,

From (2.13),

$$\Delta x = \frac{\Delta x'}{\gamma} + \beta c \Delta t \ . \tag{2.18}$$

(2.18) $\rightarrow$ (2.16) $\Rightarrow$

$$c\Delta t' = \gamma(c\Delta t - \beta[\Delta x'/\gamma + \beta c \Delta t]) \ . \tag{2.19}$$

Observer O''s clock is stationary, so that $\Delta x' = 0$ and he measures the "proper" time Δt_0. (By definition, the "proper" time is the time as measured in the rest frame of the clock taking the measurement. If the clock is in motion, a stationary observer, comparing a time interval with an identical clock in his time frame, observes the moving clock to run slower.) After a little rearrangement, we obtain:

$$\Delta t_0 = \Delta t/\gamma, \text{ or } \Delta t = \gamma \Delta t_0 \ . \tag{2.20}$$

That it, a moving clock is always observed to run at a slower rate than that measured in a frame where the clock is stationary.

*Velocity Transformation

Just as distance and time differences vary according to the frame of reference, so do the velocities, as measured by two observers in different frames. We'll start with (2.11), and differentiate both sides with respect to t'.

$$\begin{aligned} \frac{\mathrm{d}x'}{\mathrm{d}t'} &= \gamma_u \left(\frac{\mathrm{d}x}{\mathrm{d}t'} - u \frac{\mathrm{d}t}{\mathrm{d}t'} \right) \\ \frac{\mathrm{d}y'}{\mathrm{d}t'} &= \frac{\mathrm{d}y}{\mathrm{d}t'} \\ \frac{\mathrm{d}z'}{\mathrm{d}t'} &= \frac{\mathrm{d}z}{\mathrm{d}t'} \\ c &= \gamma_u (c \frac{\mathrm{d}t}{\mathrm{d}t'} - \beta_u \frac{\mathrm{d}x}{\mathrm{d}t'}) \ . \end{aligned} \tag{2.21}$$

Extracting 3 common factors results in:

$$\begin{aligned} v'_x &= \gamma_u \left(\frac{\mathrm{d}t}{\mathrm{d}t'}\right)(v_x - u) \\ v'_y &= \left(\frac{\mathrm{d}t}{\mathrm{d}t'}\right) v_y \\ v'_z &= \left(\frac{\mathrm{d}t}{\mathrm{d}t'}\right) v_z \\ \frac{\mathrm{d}t}{\mathrm{d}t'} &= \frac{1}{\gamma_u(1 - \beta_u v_x/c)} \ . \end{aligned} \tag{2.22}$$

Using the last of the above equations to replace for $\mathrm{d}t/\mathrm{d}t'$ in the previous 3, we obtain:

$$\begin{aligned} v'_x &= \frac{v_x - u}{1 - \beta_u v_x/c} \\ v'_y &= \frac{v_y}{\gamma_u(1 - \beta_u v_x/c)} \\ v'_z &= \frac{v_z}{\gamma_u(1 - \beta_u v_x/c)} \ . \end{aligned} \tag{2.23}$$

*Lorentz Transformation of Velocity with Arbitrary Direction

$\vec{v}'$ related to $\vec{v}$, where the relative motion of the inertial frame measuring $\vec{v}'$ with respect to the inertial frame measuring $\vec{v}$, is along the positive $\vec{u}$-axis with speed u:

$$\vec{v}' = \frac{\vec{v} - \vec{u}\gamma_u + (\gamma_u - 1)(\vec{u} \cdot \vec{v})\vec{u}/u^2}{\gamma_u(1 - \vec{u} \cdot \vec{v}/c^2)} \tag{2.24}$$

*Lorentz Transformation of Dilation Factor

$$\gamma_{v'} = \gamma_u \gamma_v (1 - \vec{u} \cdot \vec{v}/c^2) \tag{2.25}$$

*Lorentz Transformation of Velocity and Dilation Factor

$$\vec{v}'\gamma_{v'} = \gamma_v(\vec{v} - \vec{u}\gamma_u + (\gamma_u - 1)(\vec{u} \cdot \vec{v})\vec{u}/u^2) \tag{2.26}$$

Relativistic Energy and Momentum

The relativistic energy and momentum of an object with mass m and velocity $\vec{v}$:

$$\begin{aligned} E &= mc^2\gamma_v \\ \vec{p} &= m\gamma_v\vec{v} \\ (mc^2)^2 &= E^2 - (c\vec{p})^2 \end{aligned} \tag{2.27}$$

*Lorentz Transformation Energy and Momentum

The Lorentz transformation energy and momentum of an object with mass m and velocity $\vec{v}$ to an inertial frame that is moving along the positive x-axis with speed u:

$$\begin{aligned} E' &= \gamma_u(E - up_x) \\ \vec{p}'_x &= \gamma_u(p_x - uE/c^2) \\ \vec{p}'_y &= p_y \\ \vec{p}'_z &= p_z \end{aligned} \tag{2.28}$$

*Lorentz Transformation Energy and Momentum with Arbitrary Direction

The Lorentz transformation energy and momentum of an object with mass m and velocity $\vec{v}$ to an inertial frame that is moving along the positive $\vec{u}$-axis with speed u:

$$\begin{aligned} E' &= \gamma_u(E - \vec{u}\cdot\vec{p}) \\ \vec{p}' &= \vec{p} - \vec{u}\gamma_u E/c^2 + (\gamma_u - 1)(\vec{u}\cdot\vec{p})\vec{u}/u^2 \\ (mc^2)^2 &= E'^2 - (c\vec{p}')^2 \end{aligned} \tag{2.29}$$

*The Relativistic Doppler Effect

The relativistic Doppler effect, measured along the relative velocity vector between two objects, is given by:

$$\frac{\nu}{\nu_0} = \sqrt{\frac{1 \pm \beta}{1 \mp \beta}}\,, \tag{2.30}$$

where ν_0 is the frequency of the light source in the rest frame of the source. The top signs in the numerator and denominator of (2.30) signify that the source and observer are approaching each other, while the bottom signs signify that the source and observer are receding from each other. (Here, β is the relative speed of the source as seen by the observer.)

If the relative line of motion is different from the direction of observation, one can show that:

$$\frac{\nu}{\nu_0} = \gamma(1 - \hat{n} \cdot \vec{\beta}) \ , \tag{2.31}$$

where $\vec{\beta} = \vec{u}/c$, and $\hat{n}$ is a unit vector along the line from the observer to the source.

2.5 Relativistic Dynamics

In this section we concern ourselves, primarily, with two-body scattering of relativistic particles, including photons. We start with some review of kinematic variables.

Symbol	= Expression	Interpretation
v		speed of a particle with mass
c		speed of light, speed of massless particles
β, or β_v	v/c	speed (in units of c) of a particle with mass $0 \leq \beta < 1$
γ or γ_v	$(1-\beta^2)^{-1/2}$	"energy factor", "dilation factor", "contraction factor"
		γ is often used as a symbol to represent a photon
	mc^2	rest mass energy of a particle with mass
E	$mc^2\gamma$	total energy of a particle with mass (rest + kinetic energy)
E_γ		total (or kinetic) energy of a photon (or massless particle)
K	$mc^2(\gamma - 1)$	kinetic energy of a particle with mass
$\vec{p}$	$mc\vec{\beta}\gamma$, $m\vec{v}\gamma$	momentum of a particle with mass
$\vec{p}_\gamma$	E_γ/c	magnitude of momentum of a photon, or particle without mass
$(mc^2)^2$	$E^2 - (pc)^2$	fundamental relation linking m, E, and $\lvert\vec{p}\rvert^2$
1	$\gamma^2(1-\beta^2)$	useful property of γ and β

Table 2.1: Relativistic kinematic variables

Non-relativistic limit

When performing relativistic calculations, one technique for verifying your result is to determine the non-relativistic limit. Generally, this is done by making a Taylor expansion in β, (See Chapter 18.) and keep leading order expressions that express the non-relativistic limit. Factors of β should be replaced by cv, and the final result should resemble:

$$\lim_{\beta \to 0} (\text{Relativistic expression}) = (\text{Non} - \text{relativistic expression}) + O(1/c^n) \ , \tag{2.32}$$

where $n \geq 1$. Finally the non-relativistic limit is obtained by setting the $O(1/c^n)$ expressions to zero. Note that some expressions are intrinsically relativistic and not reducible to non-

relativistic limits. For example, rest mass energy, and photon kinematic variables are some that we have encountered to far.

For example, the kinetic energy of a particle of mass m, in the limit that $\beta \to 0$ is:

$$\lim_{\beta\to 0} K = \lim_{\beta\to 0} mc^2(\gamma - 1) = \frac{1}{2}mv^2 + O(1/c^2) \ , \tag{2.33}$$

while its momentum is

$$\lim_{\beta\to 0} mc\vec{\beta}\gamma = m\vec{v} + O(1/c^2) \ , \tag{2.34}$$

Relativistic Collision Kinematics

We now repeat the discussion of Section 1.4.1 but include the effect of relativistic speeds.

Consider the collision of two moving particles with masses m_1 and m_2, producing particles m_a and m_b following the collision. We conserve *total* energy and momentum, to obtain the following equations:

CoE⇒

$$m_1c^2\gamma_1 + m_2c^2\gamma_2 = m_ac^2\gamma_a + m_bc^2\gamma_b \ , \tag{2.35}$$

We note that Q is the zero-speed limit of (2.35) and is included automatically in the subsequent analysis.

Co$\vec{M}$ ⇒

$$m_1c\vec{\beta}_1\gamma_1 + m_2c\vec{\beta}_2\gamma_2 = m_ac\vec{\beta}_a\gamma_a + m_bc\vec{\beta}_b\gamma_b \ . \tag{2.36}$$

Solution Strategies

How we manipulate (2.35) and (2.36) depends on what information we know, and what information we wish to extract. We shall discuss the most common situation now, and leave some of the special cases to the examples and problems.

The most common situation involves the scattering of a known projectile from a known target, where initial masses and velocities are known, to a set of final particles whose masses are known, but only the lighter product particle leaves the collision area. (For example, a proton scattering from a stationary nucleus, with a transformed nucleus and a neutron in the final state.) Since the heavier product particle stays in the collision area, it is unobserved, hence its velocity is not measurable, and we strive to eliminate it. We proceed as follows.

Reorganize (2.35) and (2.36) as follows, to put the kinematics of the "b" particle on the right hand side (RHS) of the equations:

From the CoE equation:

$$m_1c^2\gamma_1 + m_2c^2\gamma_2 - m_ac^2\gamma_a = m_bc^2\gamma_b \ , \tag{2.37}$$

and the Co$\vec{M}$ equation:

$$m_1 c\vec{\beta_1}\gamma_1 + m_2 c\vec{\beta_2}\gamma_2 - m_a c\vec{\beta_a}\gamma_a = m_b c\vec{\beta_b}\gamma_b \ . \tag{2.38}$$

Dividing the square of (2.37) by c^4 and subtracting the square of (2.38) divided by c^2 gives us:

$(2.37)^2/c^4$ - $(2.38)^2/c^2 \Rightarrow$

$$(m_1\gamma_1 + m_2\gamma_2 - m_a\gamma_a)^2 - (m_1\vec{\beta_1}\gamma_1 + m_2\vec{\beta_2}\gamma_2 - m_a\vec{\beta_a}\gamma_a)^2 = m_b^2\gamma_b^2(1-\beta_b^2) \ . \tag{2.39}$$

The motivation for this arithmetical manipulation is now evident: no factors of c appear, and most importantly, we may exploit the $\beta\gamma$ relation, $\gamma^2(1-\beta^2)$ to great effect. Doing so results in:

$$m_1^2+m_2^2-m_a^2-m_b^2+2m_1m_2\gamma_1\gamma_2(1-\vec{\beta_1}\cdot\vec{\beta_2}) = 2m_1m_a\gamma_1\gamma_a(1-\vec{\beta_1}\cdot\vec{\beta_a})+2m_2m_a\gamma_2\gamma_a(1-\vec{\beta_2}\cdot\vec{\beta_a}) \ . \tag{2.40}$$

We see that we have isolated the only unknown quantity, $\vec{\beta_a}$, and by inference γ_a on the RHS of (2.40). We may further reduce this equation by noting that the mass term on the LHS may be rewritten as follows:

$$m_1^2 + m_2^2 - m_a^2 - m_b^2 = (m_1 + m_2 - m_a - m_b)(m_1 + m_2 + m_a + m_b) = (\Delta M)M \ , \tag{2.41}$$

where $M = M_i + M_f = m_1 + m_2 - m_a - m_b$ is the sum of the masses of the initial and final particles, while $\Delta M = M_i - M_f = m_1 + m_2 - m_a - m_b$ is the difference of the sum of the initial masses and the sum of the final masses of the particles participating in the reaction. We also note that ΔMc^2 is the reaction Q-value discussed previously. Note how it appears naturally in the analysis, while it has to be "tacked on" in an *ad hoc* fashion in the non-relativistic analysis.

So, finally we write:

$$(\Delta M)M+2m_1m_2\gamma_1\gamma_2(1-\vec{\beta_1}\cdot\vec{\beta_2}) = 2m_1m_a\gamma_1\gamma_a(1-\vec{\beta_1}\cdot\vec{\beta_a})+2m_2m_a\gamma_2\gamma_a(1-\vec{\beta_2}\cdot\vec{\beta_a}). \tag{2.42}$$

Having derived a relativistic result, we should check that it gives the correct non-relativistic limit. To do this, we note that we can rewrite

(2.39) as:

$$\vec{P}^2 - 2m_b(K+Q) = (Q+K)^2/c^2 \ , \tag{2.43}$$

where

$$\vec{P} \equiv m_1 c\vec{\beta}_1\gamma_1 + m_2 c\vec{\beta}_2\gamma_2 - m_a c\vec{\beta}_a\gamma_a \ ,$$

and

$$K \equiv m_1c^2(\gamma_1 - 1) + m_2c^2(\gamma_2 - 1) - m_ac^2(\gamma_a - 1) \ .$$

(2.43) is fully relativistic. Obtaining the non-relativistic form is tantamount to replacing $\vec{P}$ and K with their non-relativistic counterparts (given below (1.14) and setting the $1/c^2$ on the RHS of (2.43) to zero. This agrees with the non-relativistic form given in (1.14), and we have verified the non-relativistic limit of our relativistic expression. It is not absolutely foolproof, however, verifying non-relativistic limits is a very important verification tool.

2D relativistic elastic collision, equal masses

Problem: Find the opening angle of the resultant particles, when a relativistic particle of mass m, collides with an equal mass, at rest. Show explicitly the transition to the well-known non-relativistic limit?

Solution:

1. *Set up the CoE and Co$\vec{M}$ equations assuming "2" is at rest:*

$$mc^2\gamma_0 + mc^2 = mc^2\gamma_1 + mc^2\gamma_2 \quad (2.44)$$
$$mc\vec{\beta}_0\gamma_0 = mc\vec{\beta}_1\gamma_1 + mc\vec{\beta}_2\gamma_2 \quad (2.45)$$

2. *We require the angle between the resultant trajectories. The cosine of this angle is obtained by $\vec{\beta}_1 \cdot \vec{\beta}_2$. To isolate this: (2.44)^2/$(mc^2)^2$ - (2.45)^2/$(mc)^2$ $\Rightarrow$*

$$\gamma_1\gamma_2\vec{\beta}_1 \cdot \vec{\beta}_2 = \gamma_1\gamma_2 - \gamma_0 \ .$$

If we let Θ represent the opening angle of the outgoing particles, we may manipulate the above (Show this!) equation to be:

$$\cos\Theta = \sqrt{\frac{K_1K_2}{(K_1 + 2mc^2)(K_2 + 2mc^2)}} \ , \quad (2.46)$$

explicitly showing the dependence on the outgoing kinetic energies.

This relationship is plotted in Figure 2.2 for a logarithmic spacing of K_1/K_0 between 0.01 and 1000.

Taking $c \to \infty$ yields the expected result, that the opening angle is $\pi/2$, in a non-relativistic analysis. This is tantamount to saying that $K_a << mc^2$ and $K_b << mc^2$.

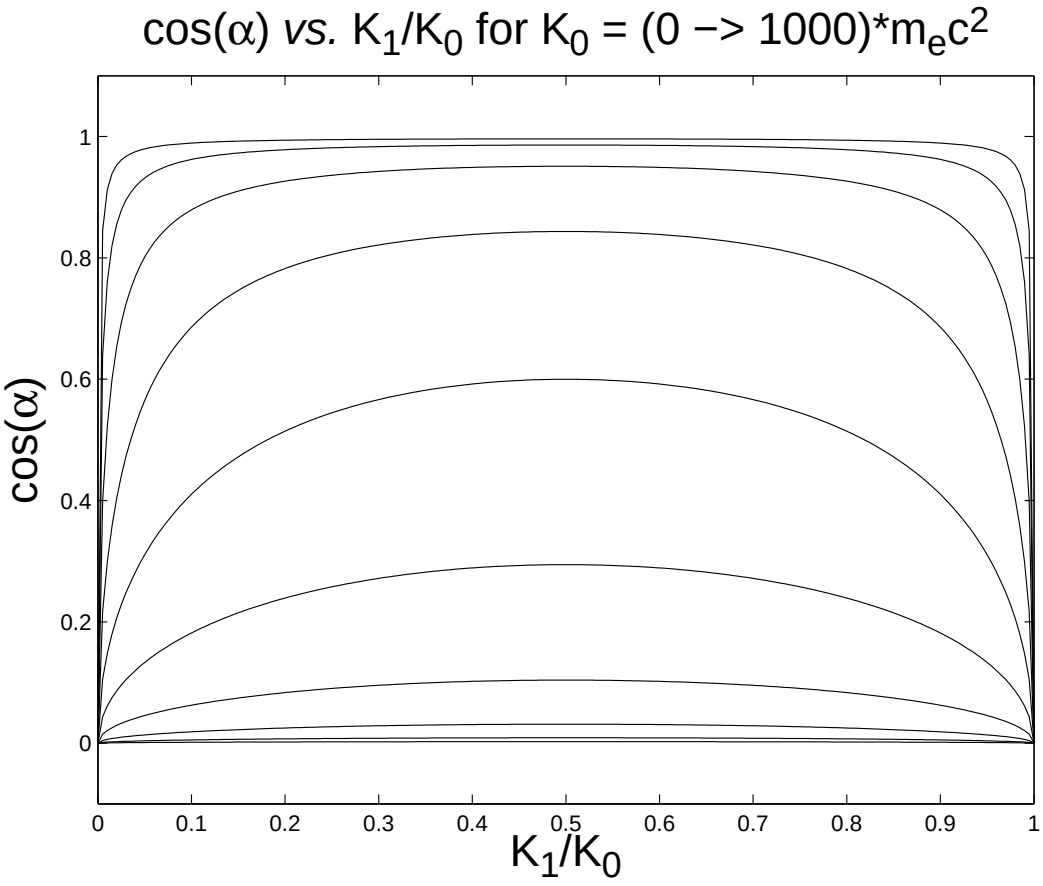

Figure 2.2: $\cos\theta$ *vs.* K_1/K_0

However, (2.46) contains even more information. It says that if either outgoing particle is non-relativistic, that is, $K_1 << mc^2$ *or* $K_2 << mc^2$*, the opening angle tends to* $\pi/2$*. Finally, if either outgoing particle is at rest, the opening angle is* $\pi/2$*, exactly as in the non-relativistic case, and also true for the relativistic case. It is a consequence of the conservation of energy and momentum in both non-relativistic and relativistic formalisms.*

Interpretation: In the case that both outgoing particles are relativistic, (2.46) demonstrates that the opening angle is less than $\pi/2$*. Since* $K_1 = K_0 - K_2$*, it also follows that there must be a particular sharing of the initial kinetic energy,* K_0*, with that of the outgoing particles, that minimizes the opening angle. Since (2.46) is symmetric under the interchange* $1 \leftrightarrow 2$*, the sharing of kinetic energy can not be asymmetric. Therefore the only symmetric way of sharing the energy is to give each outgoing particle half. You can prove this mathematically*[2]*,*

[2]The mathematician within me is prone to say that a mathematical proof is always more general and powerful than a physical one. Historically, though, it is well known that physicists, even theoretical ones,

but making the argument this way is more fun. Therefore at the midpoint, $K_1 = K_2 = K_0/2$, and the minimum opening angle can be shown to be given by:

$$\cos\alpha_{\rm min} = \frac{K_0}{K_0 + 4mc^2} \ . \tag{2.47}$$

This relationship is plotted in Figure 2.3 for a logarithmic spacing of K_1/K_0 between 0.01 and 1000.

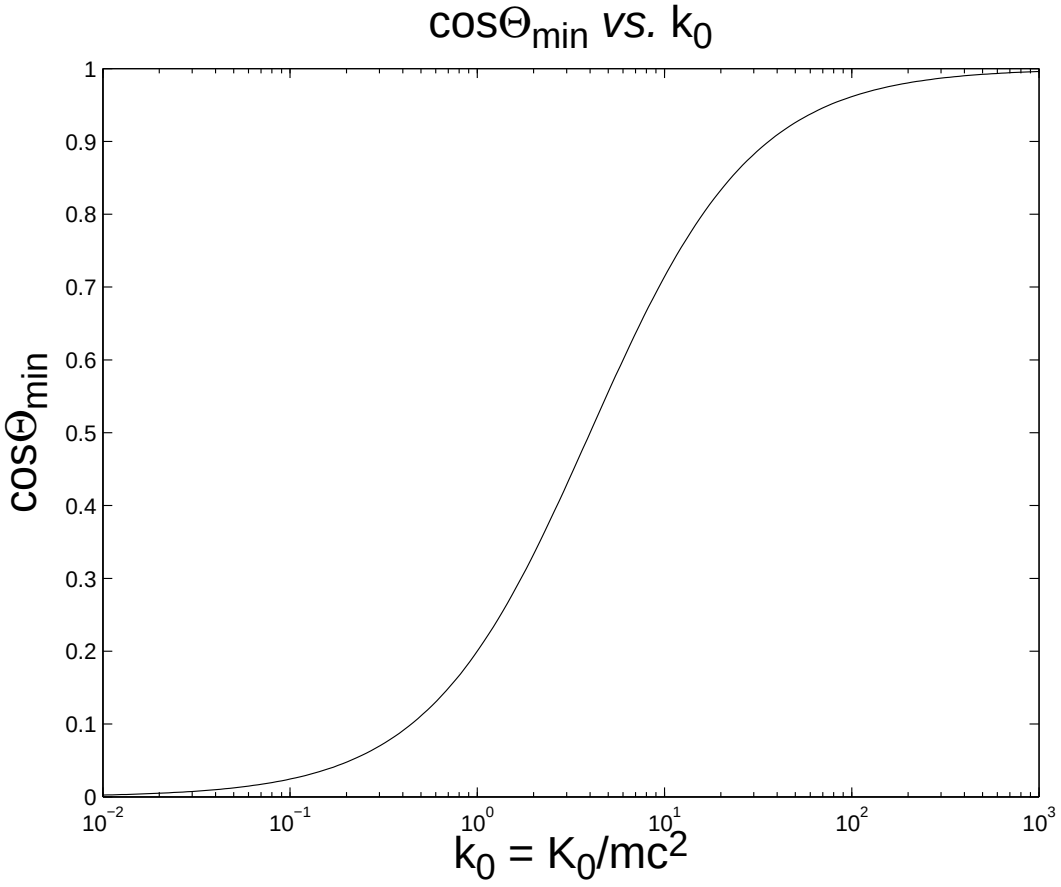

Figure 2.3: $\cos\theta_{\rm min}$ *vs.* K_1/K_0

We note from (2.47) that the expected non-relativistic limit is obtained again. However, as the incoming kinetic energy is extended upwards into the relativistic range, the energy

are better socially-adjusted than mathematicians. Then again, mathematicians ... (I digress). Here's the proof. Consider a function, $f(x)$, that is symmetric about the origin. (Any different point of symmetry may be used, but it can be translated back to the origin.) It follows that the function's first derivative is antisymmetric, and must pass through the origin. Hence, the origin is the location of an extremum of $f(x)$. *Q.E.D.*

is increasingly carried into the forward direction. This is the principle upon which particle ray-guns operate. It is also responsible for spectacular accidents when charged high energy particle beams are mistakenly steered into beam pipes and magnets.

Zero-Momentum Frame

We can also perform ant calculation in the zero-momentum frame. in these set of notes, we don't exploit the zero-momentum frame extensively, since the laboratory frame makes more sense for nuclear engineering and radiological applications (fixed targets, β- and γ-decay). High-energy physics exploit the zero-momentum frame extensively, since particle-antiparticle colliders operate in the zero-momentum frame. We shall exploit it, however, for two important illustrations:

1. Particle/antiparticle creation with mass

Consider a collision of two photons, going in exact opposite directions, each with energy E_0. E_0 is arranged so that after the collision, a particle and antiparticle, each with mass m, is at rest. Thus, by CoE, $E_0 = 2mc^2$.

Now consider that a different observer, moving along the direction of one of the photons, observes the event. In his frame of motion, the pair of particles is moving in the direction opposite to him. In his frame of motion, his expressions for CoE and Co$\vec{M}$ are:

$$2mc^2\gamma = E_+ + E_- \tag{2.48}$$
$$2mc\beta\gamma = (E_+ + E_-)/c \ , \tag{2.49}$$

where β is the observer's velocity with respect to the zero-momentum frame, E_+ is the higher energy photon he observes, with E_- is the lesser energy photon in his frame. By manipulating the equations in the now familiar way, we may relate the energy of the photon in the moving frame, relative to the rest frame. The result is:

$$E_\pm = E_0\sqrt{\frac{1 \pm \beta}{1 \mp \beta}} \ , \tag{2.50}$$

where we consistently use only the upper or lower signs in the expressions involving $\pm$ or $\mp$.

Thus, we have derived the Doppler effect stated in (2.30), whereby motion toward a photon increases its energy, and motion away decreases its energy.

2. Particle/antiparticle decay into photons

Here we consider a particle with mass m, β_0, γ_0 on a collision course with its antiparticle, moving in the exact opposite direction. They annihilate, producing two photons, each with

energy E_0, moving in exact opposite directions, along the original direction of motion. An observer, moving with parameters β and γ, along the original direction of motion, observes the same annihilation, and his CoE and Co$\vec{M}$ equations take the forms:

$$\begin{aligned} mc^2\gamma_+ + mc^2\gamma_- &= E_+ + E_- \quad (2.51) \\ mc\gamma_+ + mc\gamma_- &= (E_+ + E_-)/c \ . \quad (2.52) \end{aligned}$$

Here, the "+" refers to the more energetic particle and photon in the frame of the observer. The arithmetic is a little more involved than in the previous example, but, after some work, we can conclude that:

$$\gamma_\pm = \gamma_0\gamma(1 \pm \beta\beta_0) \ , \quad (2.53)$$

which expresses a "Doppler shift", but for particles with mass.

Applying (2.53), imagine that the observer is traveling at exactly β_0, putting one of the charged particles in the rest frame. The higher energy electron will have a "γ-shift" of approximately $2\gamma_0^2$. For example, the Stanford Linear Accelerator produces electrons and electrons with energies of about 50 GeV, a γ-shift of about 10^5. The collision of these particles in the zero-momentum frame, is equivalent to a fixed target γ-shift of 2×10^5. It is no wonder that particle-antiparticle colliders are such an important research tool.

Sticky collisions/exploding masses

Finally, we end this section with a discussion on inelastic collisions.

In the last chapter, we inferred the Q-value of a sticky collision. Let's reformulate the problem in a relativistic framework. Imagine that a particle of mass m_0, with speed v_0, strikes an identical particle at rest, and they fuse. You can not balance the CoE and Co$\vec{M}$ equations if the masses are allowed to remain unchanged. One finds, in this case that the fused mass is

$$m = 2m_0\sqrt{\frac{1+\gamma_0}{2}} \ .$$

The increase in mass is due to the increase in internal energy of the mass m.

Similarly, if a mass m explodes into two equal masses, m_0, you may show that

$$m = 2m\gamma_0 \ .$$

In other words, internal energy is converted into kinetic energy of the resultant particles.

2.6 Questions

Answer these questions (on paper or in your head). If you can't find a good answer, re-read the relevant sections of Chapter 2. If you still can't find a good answer, ask a colleague, a TA, or a Prof.

Some of these questions may appear on assignments or exams.

2.7 Problems

If you find some of these problems interesting, attempt them on paper. If you can't find a good answer, re-read the relevant sections of Chapter 2. If you still can't find a good answer, try working it out with a colleague, ask a TA, or a Prof.

Some of these problems may appear on assignments or exams.

Chapter 3

The Particlelike Properties of Electromagnetic Radiation

Reach Chapter 3 of the and-written notes. Most of this chapter is just a stub.

3.1 Review of Electromagnetic Waves

3.2 The Photoelectric Effect

Planck's Constant

$$\begin{aligned} h &= 6.626\ 069\ 96(33) \times 10^{-34}\ \mathrm{J \cdot s} \\ &= 4.135\ 667\ 33(10) \times 10^{-15}\ \mathrm{eV \cdot s} \\ \hbar &= h/2\pi \\ &= 1.054\ 571\ 628(53) \times 10^{-34}\ \mathrm{J \cdot s} \\ &= 6.582\ 118\ 99(16) \times 10^{-16}\ \mathrm{eV \cdot s} \end{aligned} \tag{3.1}$$

Energy of a Photon

$$\begin{aligned} E &= h\nu \\ &= \hbar\omega \end{aligned} \tag{3.2}$$

Momentum of a Photon

$$\begin{aligned} c\vec{p} &= h\nu\hat{n} \\ &= \hbar\vec{k} \\ &= hc\hat{n}/\lambda \\ &= \hbar c\hat{n}/\cancel{\lambda} \end{aligned} \tag{3.3}$$

where $\hat{n}$ is a unit vector in the direction of the photon.

3.3 Blackbody Radiation

3.4 The Compton Effect

Compton's Formula

for the difference in primary, E, and scattered photon energy, E' related to the scattering angle, θ, of the scattered photon, with respect to the incoming photon's direction, when scattered from an electron with mass m_e in the rest frame of the electron.

$$\frac{1}{E'} - \frac{1}{E} = \frac{1}{m_e c^2}(1 - \cos\theta) \ . \tag{3.4}$$

3.5 Other Photon Processes

3.6 What is a Photon?

Chapter 4

The Wavelike Properties of Particles

Read Chapter 4 of the hand-written notes.

4.1 De Broglie's Hypothesis

De Broglie's Wavelength

The wavelength of any particle, with or without mass, is related to the magnitude of its momentum. p, by the relation:

$$\lambda = \frac{h}{p} \, . \tag{4.1}$$

Energy of a Particle in Terms of its Frequency

$$\begin{aligned} E &= h\nu \\ &= \hbar\omega \end{aligned} \tag{4.2}$$

Momentum of a Particle in Terms of its Wavenumber

$$\begin{aligned} c\vec{p} &= h\nu\hat{n} \\ &= \hbar\vec{k} \\ &= \hbar c\hat{n}/\lambda \end{aligned} \tag{4.3}$$

where $\hat{n}$ is a unit vector in the direction of the particle.

4.2 Uncertainty Relationships for Classical Waves

4.3 Heisenberg Uncertainty Relationships

Heisenberg's Uncertainty Relationships

$$\begin{aligned} \Delta p_x \Delta x &\geq \hbar/2 \\ \Delta p_y \Delta y &\geq \hbar/2 \\ \Delta p_z \Delta z &\geq \hbar/2 \\ \Delta E \Delta t &\geq \hbar/2 \end{aligned} \tag{4.4}$$

4.4 Wave Packets

The general form for a wavepacket moving along the x-axis is given by:

$$f(x,t) = \frac{1}{\sqrt{2\pi}} \int_{-\infty}^{\infty} \mathrm{d}k\, A(k)\, e^{i[kx-\omega(k)t]} \ , \tag{4.5}$$

where $A(k)$ represents the "strength" of the contribution of wave number k to the formation of the packet. In complete generality, the frequency ω can be a function of the wavenumber, so we write its dependence on k explicitly as $\omega(k)$.

The expression (4.5) is a "Fourier" transform. If we know the wavenumber spectrum, $A(k)$, we can form its wavepacket, $f(x,t)$. Conversely, if we know the shape of the wavepacket at $t = 0$, we can determine the wavenumber spectrum by using the inverse property of Fourier transforms. and computing:

$$A(k) = \frac{1}{\sqrt{2\pi}} \int_{-\infty}^{\infty} \mathrm{d}x\, f(x,0)\, e^{-ikx} \ . \tag{4.6}$$

If we set $t = 0$ in (4.5) and substitute for $A(k)$ from (4.6), we get, after some rearranging:

$$f(x,0) = \int_{-\infty}^{\infty} \mathrm{d}x'\, f(x',0) \left(\frac{1}{2\pi}\right) \int_{-\infty}^{\infty} \mathrm{d}k\, e^{ik(x-x')} \ . \tag{4.7}$$

We must get the same function back, so this identifies one form of the Dirac "δ-function" commonly seen when doing Fourier transforms, namely:

$$\delta(x-x') = \frac{1}{2\pi} \int_{-\infty}^{\infty} \mathrm{d}k\, e^{ik(x-x')} \ . \tag{4.8}$$

There are many forms of Dirac's δ-function. It has the peculiar property that:

$$f(x) = \int_{x_1}^{x_2} \mathrm{d}x' \, \delta(x' - x) f(x') \ , \tag{4.9}$$

as long as $x_1 < x < x_2$, and zero otherwise.

Another form of the δ-function commonly seen in Fourier transform analysis is

$$\delta(k - k') = \frac{1}{2\pi} \int_{-\infty}^{\infty} \mathrm{d}x \, e^{i(k-k')x} \ . \tag{4.10}$$

Uncertainty Relationship

It can be shown from the general properties of Fourier transforms that:

$$\Delta x \Delta k \geq \frac{1}{2} \ . \tag{4.11}$$

(Note to self: Proof to follow at some later date.)

Multiplying by $\hbar$ gives Heisenberg's uncertainty relationship:

$$\Delta x \Delta p \geq \frac{\hbar}{2} \ . \tag{4.12}$$

Group Velocity

Consider now, (4.5), and imagine that the frequencies are strongly centered on some principle frequency k_0, and that it is weakly dispersive, so that we may write in a Taylor expansion:

$$\omega(k) = \omega(k_0) + \left(\frac{\mathrm{d}\omega}{\mathrm{d}k} \right)_{k=k_0} (k - k_0) \cdots \ , \tag{4.13}$$

and substitute this back into (4.5) and obtain:

$$f(x,t) \approx \frac{1}{\sqrt{2\pi}} \int_{-\infty}^{\infty} \mathrm{d}k \, A(k) \, e^{i[kx - \omega_0 t - v_\mathrm{g}(k-k_0)t]} \ , \tag{4.14}$$

where $\omega_0 = \omega(k_0)$ and $v_\mathrm{g} = \left(\frac{\mathrm{d}\omega}{\mathrm{d}k}\right)_{k=k_0}$. The above can be rearranged to give:

$$f(x,t) \approx \frac{e^{i(k_0 v_\mathrm{g} - \omega_0)t}}{\sqrt{2\pi}} \int_{-\infty}^{\infty} \mathrm{d}k \, A(k) \, e^{ik(x - v_\mathrm{g} t)} \ , \tag{4.15}$$

or,

$$f(x,t) \approx f(x - v_{\rm g}t, 0)e^{i(k_0 v_{\rm g} - \omega_0)t} \ , \tag{4.16}$$

which, apart from the overall phase term in the exponential, looks like the original shape of $f(x,t)$ at $t = 0$ moving with velocity $v_{\rm g}$. This is the "group" velocity for a general, weakly dispersive wavepacket.

Does it make sense? If we identify the energy of a wave as $E = \hbar\omega$ and the magnitude of its momentum as $p = \hbar k$, we can identify the group velocity as

$$v_{\rm g} = \frac{{\rm d}\omega}{{\rm d}k} = \frac{\hbar {\rm d}\omega}{\hbar {\rm d}k} = \frac{{\rm d}E}{{\rm d}p} \ . \tag{4.17}$$

The group velocity of a photon ($E = cp$) is c, for a non-relativistic particle with mass m [$E = p^2/(2m)$] it is p/m (or what we have called v), and for a relativistic particle with mass m [$E^2 - (cp)^2 = (mc^2)^2$] it is pc^2/E, also what we have been calling v. So, it does make sense!

4.5 Probability and Randomness

4.6 The Probability Amplitude

Chapter 5

The Schrödinger Equation in 1D

Before introducing the Schrödinger equation, justifying it, solving it, and delving into 1D applications and solutions, let us start with the Newtonian physics of a single particle with mass m, under the influence of some potential, and build upon that, to justify the Schrödinger equation.

Classical 1D motion in a potential

The energy balance equation, in this case, is:

$$E(t) = \frac{1}{2}m\dot{x}^2 + V(x,t) \ , \tag{5.1}$$

where the total energy, $E(t)$, is shared between the kinetic energy of the particle[1], $K = \frac{1}{2}m\dot{x}^2$, and its potential, $V(x,t)$ at the point x in space, at time t. This equation describes the position, momentum, and total energy, of a particle at position x, in space, at time t.

If the potential is independent of time, that is, $V(x,t) = V(x)$, then the total energy, $E(t)$, is a constant in time, E_0. Explicitly,

$$E_0 = \frac{1}{2}m\dot{x}^2 + V(x) \ . \tag{5.2}$$

Consequently, a first derivative of (5.2) with respect to t gives:

$$\dot{x}[m\ddot{x} - F(x)] \ = 0, \tag{5.3}$$

for which, mathematically speaking, there are two solutions:

[1]The dot notation indicates a derivative with respect to time. For example, $\dot{x} = v$, $\ddot{x} = \dot{v} = a$

$$\dot{x} = 0 \ , \tag{5.4}$$

and

$$m\ddot{x} - F(x) \ = 0, \tag{5.5}$$

also known as Newton's Second Law of Motion, where $F(x) = -\mathrm{d}V(x)/\mathrm{d}x$.

The first solution, $\dot{x} = 0$, is the static solution, *i.e.* no motion at all. This equation is fundamental to the area of Statics[2].

The second solution, gives rise to Kinematics[3]. (5.5) may, in principle, be solved exactly, albeit, maybe only using computers. It is a second-order differential equation, requiring two boundary conditions to be specified, the position and/or momentum of the particle at two locations in time and space. The large body of knowledge encompassed by Classical Mechanics is based on this equation.

We shall do just one example, as a segue into Quantum Mechanics.

The Harmonic Oscillator

The harmonic oscillator, in Classical Mechanics, refers to the potential,

$$V(x) = \frac{1}{2}kx^2; \quad \text{with} \quad F(x) = -kx; \quad \text{and} \quad m\ddot{x} + kx \ = 0 \ . \tag{5.6}$$

In (5.6), k is the "spring" constant. A pysical realisation

5.1 Justifying the Schrödinger Equation

The 1-dimensional time-dependent Schrödinger equation] is the governing equation for determining the wavefunction, $\psi(x,t)$ of a single non-relativistic particle with mass m. It's most general form, including time and an arbitrary potential $V(x,t)$, is:

$$\frac{-\hbar^2}{2m}\frac{\partial^2\psi(x,t)}{\partial x^2} + V(x,t)\psi(x,t) = i\hbar\frac{\partial\psi(x,t)}{\partial t} \ . \tag{5.7}$$

[2]Quoting from: `http://en.wikipedia.org/wiki/Statics`: *Statics is the branch of mechanics that is concerned with the analysis of loads (force and torque, or "moment") on physical systems in static equilibrium, that is, in a state where the relative positions of subsystems do not vary over time, or where components and structures are at a constant velocity. When in static equilibrium, the system is either at rest, or its center of mass moves at constant velocity.*

[3]Quoting from: `http://en.wikipedia.org/wiki/Kinematics`: *Kinematics is the branch of classical mechanics that describes the motion of points, bodies (objects) and systems of bodies (groups of objects) without consideration of the causes of motion.*

5.2 The Schrödinger Recipe

5.3 Probability Densities and Normalization

A Schrödinger wavefunction and it's first derivatives are continuous everywhere, and normalized by integrating over all space as follows:

$$\int_{-\infty}^{\infty} \mathrm{d}x \, [\psi(x,t)]^* \psi(x,t) = 1 \ . \tag{5.8}$$

The probability density is defined as follows:

$$p(x,t) = \psi^*(x,t)\psi(x,t) \ . \tag{5.9}$$

The expectation value of a function or operator F of x, and/or t is calculated as follows:

$$\langle F \rangle = \int \mathrm{d}x \, \psi^*(x,t) F(x,t) \psi(x,t) \ . \tag{5.10}$$

When F is an operator, it is understood that it operates on the wavefunction to the right.

The probability current is defined as follows:

$$S(x,t) = \frac{-\hbar}{m} \, \mathrm{Im} \left\{ \psi(x,t) \left[\frac{\partial \psi^*(x,t)}{\partial x} \right] \right\} \ . \tag{5.11}$$

The continuity relation governs the flow of probability:

$$\frac{\partial p(x,t)}{\partial t} + \frac{\partial S(x,t)}{\partial x} = 0 \ . \tag{5.12}$$

Important expectation values:

$$\begin{aligned}
\langle p \rangle &= -i\hbar \left\langle \frac{\partial}{\partial x} \right\rangle \\
\langle p^2 \rangle &= -\hbar^2 \left\langle \frac{\partial^2}{\partial x^2} \right\rangle \\
\langle T \rangle &= \frac{-\hbar^2}{2m} \left\langle \frac{\partial^2}{\partial x^2} \right\rangle \\
\langle E \rangle &= i\hbar \left\langle \frac{\partial}{\partial t} \right\rangle \\
\Delta x &= \sqrt{\langle x^2 \rangle - \langle x \rangle^2} \\
\Delta p_x &= \sqrt{\langle p_x^2 \rangle - \langle p_x \rangle^2}
\end{aligned} \tag{5.13}$$

The time-independent 1-dimensional Schrödinger equation is the governing equation for determining the wavefunction, $u(x,t)\exp(-iEt/\hbar)$ of a single non-relativistic monoenergetic particle with mass m, when the potential is independent of time. It's most general form, including an arbitrary time-independent potential $V(x)$, is:

$$\frac{-\hbar^2}{2m}u''(x) + V(x)u(x) = Eu(x) \ , \tag{5.14}$$

where $u'(x) = \mathrm{d}u(x)/\mathrm{d}x$, and $u''(x) = \mathrm{d}^2u(x)/\mathrm{d}x^2$.

Some common abbreviations (the Dirac bra-ket notation)

$$\begin{aligned} |n\rangle &= \psi_n(x) \\ \langle m| &= \psi_m^*(x) \\ \langle m|n\rangle &= \int_{-\infty}^{\infty} \mathrm{d}x\, \psi_m^*(x)\psi_n(x) \\ \langle m|f(x)|n\rangle &= \int_{-\infty}^{\infty} \mathrm{d}x\, \psi_m^*(x)f(x)\psi_n(x) \end{aligned} \tag{5.15}$$

5.4 Applications of Scattering in 1D

Note to self: Discussion of "free particles". Discussion of the difference between scattering problems and bound-state problems.

5.4.1 Time-Independent Scattering Applications

Barrier, Step and Trough Potentials (One-Boundary Problems)

Name	Characteristics of potential	Boundary conditions
Barrier	$V(x) = V_0\theta(x)$, $E_0 < V_0 < \infty$	$u_{\mathrm{I}}(0) = u_{\mathrm{II}}(0)$, $u'_{\mathrm{I}}(0) = u'_{\mathrm{II}}(0)$
Step	$V(x) = V_0\theta(x)$, $0 < V_0 < E_0$	$u_{\mathrm{I}}(0) = u_{\mathrm{II}}(0)$, $u'_{\mathrm{I}}(0) = u'_{\mathrm{II}}(0)$
Trough	$-\infty < V_0 < 0$, $E_0 > 0$	$u_{\mathrm{I}}(0) = u_{\mathrm{II}}(0)$, $u'_{\mathrm{I}}(0) = u'_{\mathrm{II}}(0)$

Table 5.1: Some characteristics of barrier, step, and trough potentials we have encountered in the course.

Solution strategy:

1. From (**??**), the form of the one-dimensional time independent Schrödinger equation is

$$\frac{-\hbar^2}{2m}u''(x) + V(x)u(x) = Eu(x) \ . \tag{5.16}$$

When the potential is a constant, this may be rewritten as:

$$u''(x) \pm k^2 u(x) = 0 \ , \tag{5.17}$$

where

$$k^2 = \frac{2m|E - V_0|}{\hbar^2} \ .$$

The plus sign is taken in regions where $E > V_0$, and the negative sign in regions where $E < V_0$.

2. Solve (**??**) to obtain two candidate solutions, $u_{\rm I}(x)$ and $u_{\rm II}(x)$. You must have two solutions for each region, since (**??**) is a second order differential equation.

3. In regions where $E > V_0$, the candidate solutions are of the form $e^{\pm ikx}$. The plus sign in the exponential is for a wave traveling to the right, and the negative sign for a wave traveling to the left. You can incorporate this interpretation into the boundary condition to eliminate one of them in certain regions. (Example, no wave traveling to the left in region II.)

4. In regions where $E < V_0$, the candidate solutions are of the form $e^{\pm kx}$. The plus sign in the exponential is for a wave traveling to the right, and the negative sign for a wave traveling to the left. You can incorporate this interpretation into the boundary condition to eliminate one of them in certain regions. (Example, wave must diminish at $|x|$ increases.)

5. If the potential is not infinite in magnitude, apply the boundary condition that the wavefunctions and their slopes must be continuous at the boundaries.

6. If the potential is infinite in magnitude, apply the boundary condition that the wavefunctions must go to zero, where the magnitude of the potential is infinite. The slope need not go to zero.

7. Assume that the incoming wave is normalized, and obtain the amplitudes of all other waves with respect to that.

8. Calculate the probability current, S_0, for the incoming wave from (**??**). Similarly, calculate the probability currents for the reflected, S_r, and transmitted, S_t, waves.

9. Calculate the reflection and transmission coefficients, $R = |S_r/S_0|$, $T = |S_t/S_0|$.

Solution for the one-boundary problems:

Characteristic	Barrier	Step	Trough
wavefunctions, region I	$Ae^{ik_0x} + Be^{-ik_0x}$	$Ae^{ik_0x} + Be^{-ik_0x}$	$Ae^{ik_0x} + Be^{-ik_0x}$
wavefunctions, region II	Ce^{-Kx} $K = \sqrt{2m(V_0 - E_0)}/\hbar$	Ce^{ikx} $k = \sqrt{2m(E_0 - V_0)}/\hbar$	Ce^{ikx} $k = \sqrt{2m(E_0 - V_0)}/\hbar$
R	1	$(k_0 - k)^2/(k_0 + k)^2$	$(k_0 - k)^2/(k_0 + k)^2$
T	0	$4k_0k/(k_0 + k)^2$	$4k_0k/(k_0 + k)^2$

Table 5.2: The solution to the three one-boundary potentials

Two-Boundary Barriers, Steps and Wells

These are the three important solvable problems with two boundaries and three regions. The solution strategy is similar to the one-boundary case.

Name	Characteristics of the potential	Boundary conditions
Barrier	$V(x) = +\|V_0\|\theta(x)\theta(L - x)$, $0 < E_0 < V_0$	$u_{\rm I}(0) = u_{\rm II}(0)$,$u'_{\rm I}(0) = u'_{\rm II}(0)$,$u_{\rm II}(0) = u_{\rm III}(0)$,$u'_{\rm II}(0) = u'_{\rm III}(0)$
Step	$V(x) = +\|V_0\|\theta(x)\theta(L - x)$, $V_0 < E_0 < \infty$	$u_{\rm I}(0) = u_{\rm II}(0)$,$u'_{\rm I}(0) = u'_{\rm II}(0)$,$u_{\rm II}(0) = u_{\rm III}(0)$,$u'_{\rm II}(0) = u'_{\rm III}(0)$
Well	$V(x) = -\|V_0\|\theta(x)\theta(L - x)$, $E_0 > 0$	$u_{\rm I}(0) = u_{\rm II}(0)$,$u'_{\rm I}(0) = u'_{\rm II}(0)$,$u_{\rm II}(0) = u_{\rm III}(0)$,$u'_{\rm II}(0) = u'_{\rm III}(0)$

Table 5.3: Some characteristics of barrier, step, and trough potentials we have encountered in the course.

5.5 Applications of Time-Independent Bound States

Here we summarize the results for the important 1-D potentials.

Name	Nickname	Characteristics of potential	Boundary conditions
Box potential	Box	$V = 0$ for $0 \le x \le L$ and ∞ elsewhere	$u(0) = 0$, $u(L) = 0$
Symmetric box potential	Symbox	$V = 0$ for $-D \le x \le D$ and ∞ elsewhere	$u(-D) = 0$, $u(D) = 0$
Harmonic potential	Spring	$V = \frac{1}{2}kx^2$ for $-\infty \le x \le \infty$ $(k > 0)$	$\lim_{x\to\pm\infty} u(x) \to 0$

Table 5.4: Some characteristics of the three binding potentials we have encountered in the course so far.

Characteristic	Box	Symbox	Spring
energy levels	$\frac{\hbar^2\pi^2n^2}{2mL^2}$ $n = 1, 2, 3 \cdots \infty$	$\frac{\hbar^2\pi^2(n+1)^2}{8MD^2}$ $n = 0, 1, 2 \cdots \infty$	$\hbar\omega_0(n + 1/2)$, $\omega_0 = \sqrt{k/m}$ $n = 0, 1, 2 \cdots \infty$
eigenfunctions	$\sqrt{\frac{2}{L}} \sin \frac{n\pi x}{L}$	$\sqrt{\frac{1}{D}} \cos \frac{(n+1)\pi x}{2D}$ (n even) $\sqrt{\frac{1}{D}} \sin \frac{(n+1)\pi x}{2D}$ (n odd)	$\sqrt{\frac{\alpha}{2^n n!\sqrt{\pi}}} \exp[-\frac{1}{2}(\alpha x)^2] H_n(\alpha x)$ $\alpha = \left(\frac{\hbar^2}{mk}\right)^{(1/4)} = \sqrt{\frac{\hbar}{m\omega_0}}$ $H_0(z) = 1$; $H_1(z) = 2z$ $H_n(z) = 2zH_{n-1}(z) - 2(n-1)H_{n-2}(z)$

Table 5.5: The solution to the three potentials

5.6 Transitions

5.7 †Time-Dependent Perturbations

5.7.1 Fermi's Golden Rule #2

Fermi's Golden Rule #2 is one of the central equations in radiation physics, as it is employed to obtain decay rates and cross sections. Thus, a clear derivation is called for.

Consider the Schrödinger equation for a single particle in a static binding potential:

$$\mathcal{H}_0\Psi(x,t) = \frac{i}{\hbar}\Psi(x,t) \ , \tag{5.18}$$

where

$$\begin{aligned} \mathcal{H}_0 &= \mathcal{T} + V(x) \ , \\ \mathcal{T} &= -\frac{\hbar^2}{2m}\frac{\mathrm{d}^2}{\mathrm{d}x^2} \ . \end{aligned} \tag{5.19}$$

We know that such a potential has a set of orthonormal eigenstates:

$$|j\rangle = \Psi_j(x,t) = u_j(x)e^{-E_jt/\hbar} \ , \tag{5.20}$$

with eigenenergies, E_j. These eigenstates are orthonormal, that is,

$$\langle i|j\rangle = \delta_{ij} \ . \tag{5.21}$$

We know that the E_j's are constants, and fixed. By Heisenberg's Uncertainly Principle, we also know that all eigenstates are stable, as there is no mechanism for decay. In Nature, we know that excited states eventually decay to the ground state, and the purpose of this derivation is to obtain an expression for that decay rate.

We start by assuming that there is a perturbation potential that is time dependent, $V_{\rm p}(x,t)$.

Now we solve:

$$(\mathcal{H}_0 + V_{\rm p})\Psi = \frac{i}{\hbar}\frac{\partial \Psi}{\partial t} \ , \tag{5.22}$$

where Ψ is the general solution to the entire problem, with both static and perturbation potentials included.

To start, we write $\Psi(x,t)$ as a superposition of the eigenstates of the $\mathcal{H}_0$ operator, that is:

$$\Psi(x,t) = \sum_j a_j(t)\Psi_j(x,t) \ . \tag{5.23}$$

Taking the partial derivative (13.31) with respect to t gives: (Henceforth, for brevity, obvious functional dependencies on space and time will usually be suppressed.)

$$\frac{\partial \Psi}{\partial t} = \sum_j \left(\dot{a}_j - i\frac{E_j}{\hbar}\right)\Psi_j \ . \tag{5.24}$$

(13.32) + (13.31) $\longrightarrow$ (13.30) $\Rightarrow$

$$\sum_j a_j(\mathcal{H}_0 - E_j)\Psi_j + \sum_j (a_j V_{\rm p} - i\hbar\dot{a}_j)\Psi_j = 0 \ . \tag{5.25}$$

The first summation is zero, because each Ψ_j is a eigenfunction of the unperturbed $\mathcal{H}_0$ with eigenenergy E_j. Thus,

$$\sum_j (a_j V_{\rm p} - i\hbar\dot{a}_j)\Psi_j = 0 \ , \tag{5.26}$$

or,

$$\sum_j (a_j V_{\rm p} - i\hbar\dot{a}_j)|j\rangle = 0 \ . \tag{5.27}$$

Let $|f\rangle$ be the state that the excited states $|j\rangle$ transitions to. You can think of $|f\rangle$ as the ground state, or at least a lower excited state.

$\langle f| \bigotimes$ (13.35) $\Rightarrow$

$$\sum_j (a_j \langle f|V_{\rm p}|j\rangle e^{i(E_j-E_f)/\hbar} - i\hbar \dot{a}_j)\delta_{jf} = 0 \ . \tag{5.28}$$

Using the shorthand notation $V_{jf} \equiv \langle f|V_{\rm p}|j\rangle$ and $\omega_{jf} \equiv (E_j - E_f)/\hbar$, we have:

$$i\hbar \dot{a}_f = \sum_j a_j V_{jf} e^{i(E_j-E_f)/\hbar} \ . \tag{5.29}$$

(13.37) represents, at least in principle, an exact solution to the problem. All one needs to do is to set an initial condition, say, $a_n(0) = 1$ (the excited state) and then all the other a's, potentially an infinite number if them (!) to zero, and then let the solution evolve. Note that every single eigenstate can be involved in the eventual de-excitation of $|n\rangle$. This approach is more amenable to numerical solution. So, to proceed with the analysis, we make the

Small perturbation approximation

In this approximation, we only have two states, the initial excited and final states, $|i\rangle$ and $|f\rangle$. None of the other states are assumed to be involved. In the spirit of this approximation, we treat the a's on the right hand side of (13.37) as constants. (This is how the system would evolve for small t for any perturbation, large or small.)

Hence, we set $a_i(t) = 1 \ \forall \ t$, $a_f(0) = 0$, we allow these to change with time, and all the other a's are set to zero for all time. This allows us to integrate the equation, resulting in:

$$a_f = V_{if} \frac{1 - e^{i\omega_{if}}}{\hbar\omega_{if}} \ . \tag{5.30}$$

Now, we evaluate the occupation probability of the state to which the transition is made,

$$P = |a_f|^2 = |V_{if}|^2 \frac{(1 - e^{i\omega_{if}})(1 - e^{-i\omega_{if}})}{(\hbar\omega_{if})^2} \ . \tag{5.31}$$

Using some trigonometric identities, this can be recast into the following form:

$$P = |a_f|^2 = \frac{|V_{if}|^2}{\hbar^2} \frac{\sin^2(\omega_{if}t/2)}{(\omega_{if}/2)^2} \ . \tag{5.32}$$

The derivation of (13.40) assumed that the energy of the initial state $|i\rangle$ is precisely known. However, we know from the Heisenberg's Uncertainly Principle, $\Delta E \Delta t \geq \hbar/2$, that the energy of an excited state can not be known precisely, but distributed in some way. So, assume that the energy of the excited state is distributed according to some distribution $\rho(\omega)$. We must integrate over all of these to obtain the occupation probability:

$$P = \int_{-\infty}^{\infty} \mathrm{d}\omega \, \frac{|V_{if}|^2}{\hbar^2} \rho(\omega) \frac{\sin^2((\omega_{if} - \omega)t/2)}{((\omega_{if} - \omega)/2)^2} \ . \tag{5.33}$$

The

$$\frac{\sin^2((\omega_{if} - \omega)t/2)}{((\omega_{if} - \omega)/2)^2}$$

term in the above equation acts as a delta function for large t, narrowing as t increases. We eventually want to consider the decay of the excited state to the final state, so we take the large t limit to obtain, after a change of variables:

$$P = \frac{|V_{if}|^2}{\hbar^2} \rho(\omega_{if}) 2t \int_{-\infty}^{\infty} \mathrm{d}x \, \frac{\sin^2 x}{x^2} \ . \tag{5.34}$$

The integral evaluates numerically to π, thus

$$P = \frac{2\pi}{\hbar^2} |V_{if}|^2 \rho(\omega_{if}) t \ . \tag{5.35}$$

We can also rewrite $\rho(\omega_{if})$ in terms of E_{if}. Since $E_{if} = \hbar\omega_{if}$,

$$P = \frac{2\pi}{\hbar} |V_{if}|^2 \rho(E_{if}) t \ . \tag{5.36}$$

Finally, the rate of decay, $\lambda = \mathrm{d}P/\mathrm{d}t$. Hence,

---

$$\lambda = \frac{2\pi}{\hbar} |V_{if}|^2 \rho(E_{if}) \ , \tag{5.37}$$

---

and we have derived Fermi's Golden Rule #2.

A few comments are in order.

The "blurring" function $\rho(E_{if})$ is sometimes referred to as the "density of final states". We had to introduce it, in a somewhat *ad hoc* fashion to recognize that excited states are, indeed, "blurred". However, it is fascinating to note, that this blurring is directly connected to the existence of final states for the system to accept the decay. For example, a typical nuclear decay involves the release of a γ. Unless this γ has a quantum state to occupy it, there can be no quantum mechanical transition. Hence, our interpretation of the 'blurring" of excited states depends on our ability to measure its decay. If there is no decay mode, then this

density of states function drops to zero, the decay does not occur, and hence, the energy of the excited state is precise! (But not measurable!)

What is the nature of this "blurring"?

5.7.2 The Lorentz Distribution

If an excited state can decay, we may write its wavefunction in the following form:

$$\Psi(x,t) = u(x)e^{iE_i t/\hbar}\frac{e^{-t/(2\tau)}}{\sqrt{\tau}} \ , \tag{5.38}$$

where τ is its mean life. This interpretation follows directly from the probability density of the excited state:

$$|\Psi(x,t)|^2 = |u(x)|^2\frac{e^{-t/\tau}}{\tau} \ , \tag{5.39}$$

giving the well-known exponential decay law, properly normalized over the domain $0 \leq t < \infty$. Here we are adopting the normalization convention that

$$\int_0^\infty \mathrm{d}t\, |\Psi(x,t)|^2 = |u(x)|^2 \ .$$

Just as the dynamic variables k and x are related by Fourier transforms in the operational sense, this is true as well for ω and t. Hence the above distribution in time, namely $e^{-t/\tau}$, is converted to a distribution in frequency by its Fourier transform, namely,

$$\Psi_i(x,\omega) = u_i(x)\frac{1}{\sqrt{2\pi\tau}}\int_0^\infty \mathrm{d}t\, e^{i(\omega_i-\omega)t}e^{-t/(2\tau)} \ , \tag{5.40}$$

where $\omega_i = E_i$ and $\omega = E$.

After performing the integral

$$\Psi_i(x,\omega) = u_i(x)\frac{1}{\sqrt{2\pi\tau}}\frac{1}{i(\omega_i-\omega)+1/(2\tau)} \ . \tag{5.41}$$

Therefore,

$$|\Psi_i(x,\omega)|^2 = |u_i(x)|^2\frac{1}{2\pi\tau}\left(\frac{1}{(\omega_i-\omega)^2+(1/(2\tau))^2}\right) \ . \tag{5.42}$$

In terms of E rather than ω,

$$|\Psi_i(x,E)|^2 = |u_i(x)|^2 \frac{\Gamma}{2\pi}\left(\frac{1}{(E_i-E)^2+(\Gamma/2)^2}\right) \ , \tag{5.43}$$

where $\Gamma \equiv \hbar/\tau$.

Thus we have found the form of the Lorentz distribution:

$$|\Psi_i(x,E)|^2 = |u_i(x)|^2 \frac{\Gamma}{2\pi}\left(\frac{1}{(E_i-E)^2+(\Gamma/2)^2}\right) \ . \tag{5.44}$$

One may easily verify that:

$$\int_{-\infty}^{\infty} \mathrm{d}E\, |\Psi_i(x,E)|^2 = |u(x)|^2 \ . \tag{5.45}$$

Chapter 6

The Rutherford-Bohr Model of the Atom

Read Chapter 6 of thje on-line notes.

6.1 Basic Properties of Atoms

6.2 The Thomson Model

6.3 The Rutherford Nuclear Atom

6.4 Line Spectra

6.5 The Bohr Model

6.6 The Franck-Hertz Experiment

6.7 The Correspondence Principle

6.8 Deficiencies of the Bohr Model

Chapter 7

The Hydrogen Atom

Before discussing the H-atom solutions to the Schrödinger equation, however, we start with a general discussion of the dynamic of 2-body systems in both Classical and Quantum Mechanics.

7.0.1 Central force, two-body systems in Classical Mechanics

Consider two non-notating bodies, m_1, and m_2 in the presence of a potential, $V(\vec{x})$. The total energy of this system is:

$$E = \frac{1}{2}m_1|\dot{\vec{x}}_1|^2 + \frac{1}{2}m_2|\dot{\vec{x}}_2|^2 + V(\vec{x}_1, \vec{x}_2) \ , \tag{7.1}$$

that shows the contributions of the kinetic energies of each body and the potential, that acts on each body at their point in space.

Now consider the special case that each body exerts an equal and opposite force on the other, and that the potential, in the absence of any additional external force, takes the form, $V(\vec{x}_1, \vec{x}_2) = V(|\vec{x}_1 - \vec{x}_2|)$. This is a special, but important subset of general two-body forces, called the *central* force[1].

Nature abounds with two-body central forces, *viz.* the gravitational force, and the electrostatic force, to cite two important examples.

The existence of a central force permits us to recast (7.1) in a much simpler fashion. If we make the following change of variables:

[1]Not all two-body forces are central. Most importantly for us, the strong forces between two nucleons contains a large spin-dependent non-central component.

$$\begin{aligned} \vec{r} &= \vec{x}_1 - \vec{x}_2 \\ \vec{R} &= \frac{m_1\vec{x}_1 + m_2\vec{x}_2}{m_1 + m_2} \ , \end{aligned} \tag{7.2}$$

we will find that (7.1) becomes:

$$E = \frac{1}{2}M|\dot{\vec{R}}|^2 + \frac{1}{2}\mu|\dot{\vec{r}}|^2 + V(r) \ , \tag{7.3}$$

where

$$\begin{aligned} M &= m_1 + m_2 \\ \mu &= \frac{m_1 m_2}{m_1 + m_2} \ . \end{aligned} \tag{7.4}$$

We see that the energy divides into two components, the kinetic energy of the aggregate, at the center-of-mass coordinate $\vec{R}$, and a dynamic component of the relative component $\vec{r}$, but with a reduced mass, μ.. There is no force on the aggregate, and thus its kinetic energy is a constant, that we shall call K_M. Thus,

$$E_\mu \equiv E - E_M = \frac{1}{2}\mu|\dot{\vec{r}}|^2 + V(r) \ . \tag{7.5}$$

7.0.2 Central force, two-body systems in Quantum Mechanics

7.1 The Schrödinger Equation in 3D

The 3-dimensional Schrödinger equation is the governing equation for determining the wavefunction, $\psi(\vec{x},t))$ of a single non-relativistic particle with mass m. It's most general form, including time and an arbitrary potential $V(\vec{x},t)$, is:

$$i\hbar\frac{\partial\psi(\vec{x},t)}{\partial t} = \frac{-\hbar^2}{2m}\nabla^2\psi(\vec{x},t) + V(\vec{x},t)\psi(\vec{x},t)) \ . \tag{7.6}$$

A Schrödinger wavefunction and it's first derivatives are continuous everywhere, and normalized by integrating over all space as follows:

$$\int \mathrm{d}\vec{x}\,[\psi(\vec{x},t)]^*\psi(\vec{x},t) = 1 \ . \tag{7.7}$$

The probability density is defined as follows:

$$p(\vec{x},t) = \psi^*(\vec{x},t)\psi(\vec{x},t) \ . \tag{7.8}$$

The expectation value of a function or operator F of $\vec{x}$, and/or t is calculated as follows:

$$\langle F \rangle = \int \mathrm{d}\vec{x}\, \psi^*(\vec{x},t) F(\vec{x},t) \psi(\vec{x},t) \ . \tag{7.9}$$

When F is an operator it is understood that it operates on the wavefunction to the right.

The probability current (*aka* vector current) is defined as follows:

$$\vec{S}(\vec{x},t) = \frac{-\hbar}{m} \mathrm{Im}\{\psi(\vec{x},t)[\vec{\nabla}\psi^*(\vec{x},t)]\} \tag{7.10}$$

The continuity relation governs the flow of probability:

$$\frac{\partial p(\vec{x},t)}{\partial t} + \vec{\nabla} \cdot \vec{S}(\vec{x},t) = 0 \ . \tag{7.11}$$

Important expectation values

$$\begin{aligned}
\langle \vec{x} \rangle &= \langle x\hat{x} + y\hat{y} + z\hat{z} \rangle \\
\langle \vec{x} \cdot \vec{x} \rangle &= \langle x^2 + y^2 + z^2 \rangle \\
\langle \vec{p} \rangle &= -i\hbar \langle \vec{\nabla} \rangle \\
\langle \vec{p} \cdot \vec{p} \rangle &= -\hbar^2 \langle \vec{\nabla} \cdot \vec{\nabla} \rangle \\
\langle T \rangle &= \frac{-\hbar^2}{2m} \langle \nabla^2 \rangle \\
\langle E \rangle &= i\hbar \left\langle \frac{\partial}{\partial t} \right\rangle \\
\Delta x &= \sqrt{\langle x^2 \rangle - \langle x \rangle^2} \\
\Delta p_x &= \sqrt{\langle p_x^2 \rangle - \langle p_x \rangle^2}
\end{aligned} \tag{7.12}$$

The time independent 3-dimensional Schrödinger equation is the governing equation for determining the wavefunction, $u(\vec{x},t)) \exp(-iEt/\hbar)$ of a single monoenergetic non-relativistic particle with mass m, when the potential is independent of time. It's most general form, including an arbitrary time-independent potential $V(\vec{x})$, is:

$$\frac{-\hbar^2}{2m} \nabla^2 u(\vec{x}) + V(\vec{x}) u(\vec{x}) = E u(\vec{x}) \tag{7.13}$$

7.2 The Hydrogenic Atom Wave Functions

7.3 Radial Probability Densities

7.4 Angular Momentum and Probability Densities

7.5 Intrinsic Spin

7.6 Energy Level and Spectroscopic Notation

7.7 The Zeeman Effect

7.8 Fine Structure

Chapter 8

Many-Electron Atoms

Read Chapter 8 of the hand-written notes.

8.1 The Pauli Exclusion Principle

8.2 Electronic States in Many-Electron Atoms

8.3 The Periodic Table

8.4 Properties of the Elements

8.5 X-Rays

8.6 Optical Spectra

8.7 Addition of Angular Momenta

8.8 Lasers

8

Chapter 9

Review of Classical Physics Relevant to Nuclear Physics

Chapter 10

Nuclear Properties

Note to students and other readers: This Chapter is intended to supplement Chapter 3 of Krane's excellent book, "Introductory Nuclear Physics". Kindly read the relevant sections in Krane's book first. This reading is supplementary to that, and the subsection ordering will mirror that of Krane's, at least until further notice.

A nucleus, discovered by Ernest Rutherford in 1911, is made up of nucleons, a collective name encompassing both neutrons (n) and protons (p).

Name	**symbol**	**mass (MeV/c^2**	**charge**	**lifetime**	**magnetic moment**
neutron	n	939.565378(21)	0 e	881.5(15) s	-1.91304272(45) μ_{N}
proton	p	938.272046(21)	1 e	stable	2.792847356(23) μ_{N}

The neutron was theorized by Rutherford in 1920, and discovered by James Chadwick in 1932, while the proton was theorized by William Prout in 1815, and was discovered by Rutherford between 1917 and 1919m and named by him, in 1920.

Neutrons and protons are subject to all the four forces in nature, (strong, electromagnetic, weak, and gravity), but the strong force that binds nucleons is an intermediate-range force that extends for a range of about the nucleon diameter (about 1 fm) and then dies off very quickly, in the form of a decaying exponential. The force that keeps the nucleons in a nucleus from collapsing, is a short-range repulsive force that begins to get very large and repulsive for separations less than a nucleon radius, about $\frac{1}{2}$ fm. See Fig. 10.1 (yet to be created).

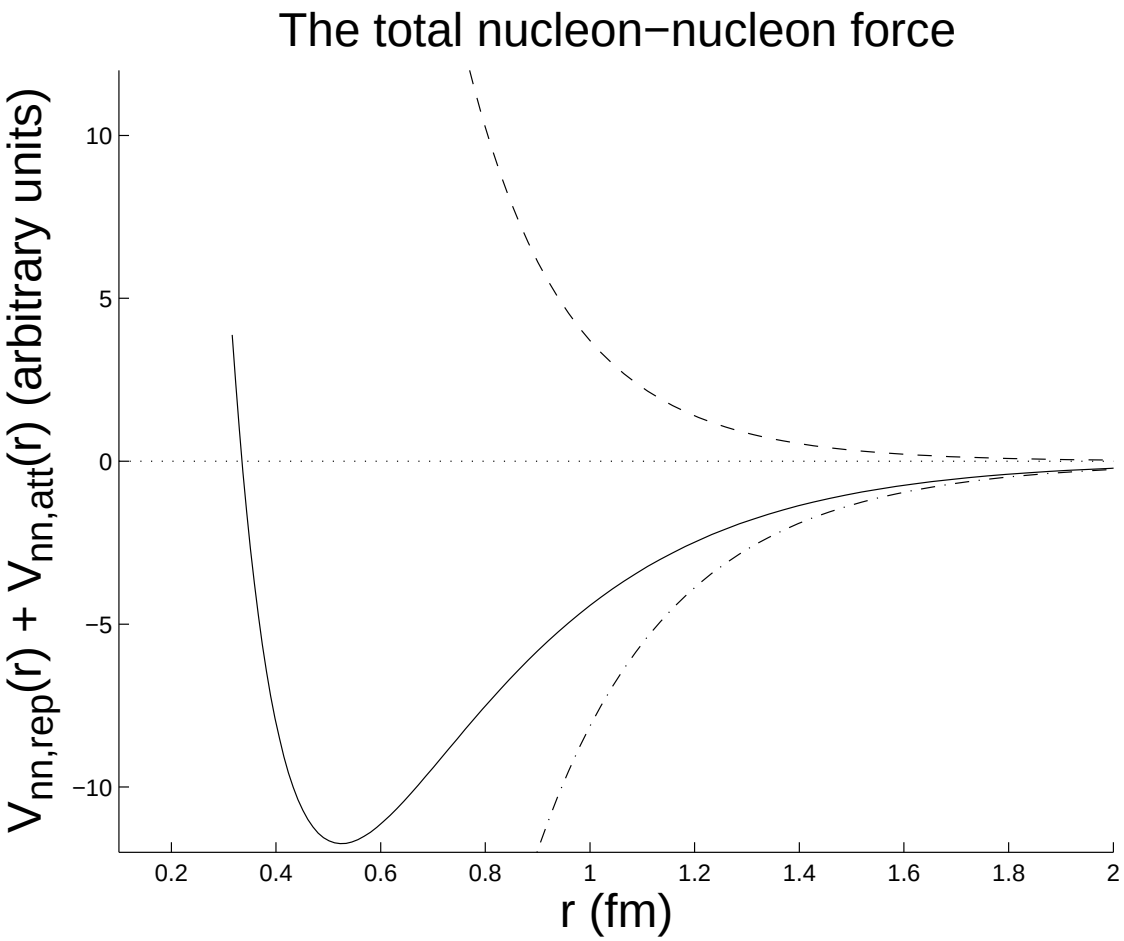

a

Figure 10.1: A sketch of the nucleon-nucleon potential.

The n-n, n-p, and p-p nuclear forces are all almost identical. (There are some important differences.) Of course, there is an additional p-p Coulombic repulsive potential, but that is separate from the nuclear force.

Owing to these nuclear forces between individual nucleons, a nucleus is tightly bound. The consequence is, from the attractive/repulsive form of the nuclear force, that the nucleons are in very close proximity. One can almost imagine a nucleus being made up of incompressible nucleonic spheres, sticking to one other, with a "contact" potential, like ping-pong balls smeared with petroleum jelly. A further consequence of the nuclear force is that nucleons in the nuclear core move, in what seems to be, a constant potential formed by the attraction of its nearby neighbors, only those that are in contact with it. A nucleon at the surface of a nucleus has fewer neighbors, and thus, is less tightly bound.

Nucleons are spin-$\frac{1}{2}$ particles (*i.e.* fermions). Hence the Pauli Exclusion Principle applies. That is, no two identical nucleons may possess the same set of quantum numbers. Consequently, we can "build" a nucleus, much as we built up an atom (in NERS311), by placing individual electrons into different quantum "orbitals", with orbitals being filled according to energy hierarchy, with a maximum of two electrons (spin up and spin down) to an orbital. Nucleons are formed in much the same way, except that all the force is provided by the other constituent nucleons, and there are two different "flavors" of nucleon, the neutron and the proton.

So, it seems that we could build a nucleus of almost any size, were it not for two physical facts that prevent this. The Pauli Exclusion Principle prevents the di-nucleon from being bound. Thus, uniform neutron matter does not exist in nature, except in neutron stars, where gravity, a long-range force, provides the additional binding energy to enable neutron matter to be formed. Thus, to build nuclei, we need to add in approximately an equal proportion of protons. However, this also breaks down because of Coulomb repulsion, for A (the total number of nucleons) greater than about 200 or so.

Moderate to large size nuclei also have more neutrons in the mix, thereby pushing the protons farther apart. It is all a matter of balance, between the Pauli Exclusion Principle and the Coulomb repulsion. And, that balance is remarkably delicate. The di-neutron is *not* bound, but *just* not bound. The deuteron *is* bound, but only *just* so. The alpha particle is tightly bound, but there are no stable $A = 5$ nuclei. ^{5}He $(2p + 3n)$ has a half-life of only 7.9×10^{-22} seconds, while ^{5}Li $(3p + 2n)$ has a half-life of only $\approx 3 \times 10^{-22}$ seconds. Those lifetimes are so short, that the unbalanced nucleon can only make a few orbits of the nucleus before it breaks away. Nature is delicately balanced, indeed.

Since we have argued that nuclei are held together by a "contact" potential, it follows that nuclei would tend to be spherical in "shape", and hence[1] it is reasonable to make mention of ...

[1] Admittedly, these are classical concepts. However, classical concepts tend to be very useful when discussing nuclei as these objects seem to straddle both the classical and quantum descriptions of its nature, with one foot set solidly in both.

10.1 The Nuclear Radius

Like the atom, the radius of a quantum object is not a precisely defined quantity; it depends on how that characteristic is measured. We can, with the proper tools, ask some very interesting things about the nucleus. Let us assume that the charge-independence of the nucleus means that the proton charge density and the neutron charge density are the same. Thus, a measure of the proton charge distribution yields direct knowledge of the neutron charge distribution. (In actual fact, the proton charge density distribution is forced to greater radius by Coulomb repulsion, but this effect is almost negligible.)

How may we measure the proton charge distribution?

In Nuclear and Particle Physics, the answer to this question usually takes some form of "Bang things together and see what happens!" In this case, we'll use electrons as the projectile and the nucleus as the target. The *scattering amplitude* is given by a proportionality (describing the constants necessary to convert the $\propto$ to an $=$ would be an unnecessary distraction):

$$F(\vec{k}_i, \vec{k}_f) \propto \langle e^{i\vec{k}_f\cdot\vec{x}}|V(\vec{x})|e^{i\vec{k}_i\cdot\vec{x}}\rangle \ , \tag{10.1}$$

where $e^{i\vec{k}_i\cdot\vec{x}}$ is the initial unscattered electron wavefunction, $e^{i\vec{k}_f\cdot\vec{x}}$ is the final scattered electron wavefunction, and $\vec{k}_i/\vec{k}_f$ are the initial/final wavenumbers.

Evaluating ...

$$\begin{aligned} F(\vec{k}_i, \vec{k}_f) &\propto \int \mathrm{d}\vec{x}\ e^{-i\vec{k}_f\cdot\vec{x}}V(\vec{x})e^{i\vec{k}_i\cdot\vec{x}} \\ &\propto \int \mathrm{d}\vec{x}\ V(\vec{x})e^{i(\vec{k}_i-\vec{k}_f)\cdot\vec{x}} \\ &\propto \int \mathrm{d}\vec{x}\ V(\vec{x})e^{i\vec{q}\cdot\vec{x}} \ , \end{aligned}$$

where $\vec{q} \equiv \vec{k}_i - \vec{k}_f$ is called the *momentum transfer*.

Thus, we see that scattering amplitude is proportional to the 3D Fourier Transform of the potential.

$$F(\vec{k}_i, \vec{k}_f) \equiv F(\vec{q}) \propto \int \mathrm{d}\vec{x}\ V(\vec{x})e^{i\vec{q}\cdot\vec{x}} \ , \tag{10.2}$$

For the present case, we apply the scattering amplitude to the case where the incident electron scatters from a much heavier nucleus that provides a scattering potential of the form:

$$V(\vec{x}) = -\frac{Ze^2}{4\pi\epsilon_0}\int \mathrm{d}\vec{x}' \ \frac{\rho_p(\vec{x}')}{|\vec{x}-\vec{x}'|} \ , \tag{10.3}$$

where $\rho_p(\vec{x}')$ is the number density of protons in the nucleus, normalized so that:

$$\int \mathrm{d}\vec{x}' \ \rho_p(\vec{x}') \equiv 1 \ . \tag{10.4}$$

That is, the potential at $\vec{x}$ arises from the electrostatic attraction of the elemental charges in $\mathrm{d}\vec{x}$, integrated over all space. In order to probe the shape of the charge distribution, the reduced wavelength of the electron, $\lambda/2\pi$, must be less than the radius of the nucleus. Evaluating ...

$$\frac{\lambda}{2\pi} = \frac{\hbar}{p_e} = \frac{\hbar c}{p_e c} \approx \frac{\hbar c}{E_e} = \frac{197 \ [\mathrm{MeV.fm}]}{E_e} < R_N \ ,$$

where R_N is the radius of the nucleus. The above is a relativistic approximation. (That is why the $\approx$ appears; $p_e c \approx E_e$.) The calculation is justified, however, since the inequality implies that the energy of the electron-projectile must be many 10s or 100s of MeV for the condition to hold. As we raise the electron energy even more, and it approaches 1 GeV or more, we can even begin to detect the individual charges of the constituent particles of the protons (and neutrons), the constituent quarks.

Proceeding with the calculation, taking the potential in (10.3) and putting it in (10.2), results in:

$$F(\vec{q}) \propto \left(-\frac{Ze^2}{4\pi\epsilon_0}\right)\int \mathrm{d}\vec{x} \ \int \mathrm{d}\vec{x}' \ \frac{\rho_p(\vec{x}')}{|\vec{x}-\vec{x}'|} e^{i\vec{q}\cdot\vec{x}} \ . \tag{10.5}$$

We choose the constant of proportionality in $F(\vec{q})$, to require that $F(0) \equiv 1$. The motivation for this choice is that, when $\vec{q} = 0$, the charge distribution is known to have no effect on the projectile. If a potential has no effect on the projectile, then we can rewrite (10.5) as

$$F(0) = 1 \propto \left(-\frac{Ze^2}{4\pi\epsilon_0}\right)\int \mathrm{d}\vec{x} \ \int \mathrm{d}\vec{x}' \ \frac{\rho_p(\vec{x}')}{|\vec{x}-\vec{x}'|} \ , \tag{10.6}$$

thereby determining the constant of proportionality. The details of this calculation will be left to enthusiastic students to discover for themselves. The final result is:

$$F(\vec{q}) = \int \mathrm{d}\vec{x} \ \rho_p(\vec{x}) e^{i\vec{q}\cdot\vec{x}} \ . \tag{10.7}$$

Thus, we have determined, at least for charge distributions scattering other charges, that the scattering amplitude is the Fourier Transform of the charge distribution.

This realization is one of the most important discoveries of nuclear structure physics: namely, that a measurement of the scattering of electrons (or other charged particles) from charge distributions, yields a direct measure of the shape of that charge distribution. One merely has to invert the Fourier Transform.

We also note, from (10.4) that $F(0) = 1$.

10.1.1 Application to spherical charge distributions

Most nuclei are spherical in shape, so it behooves us to examine closely, the special case of spherical charge distributions. In this case, $\rho_p(\vec{x}) = \rho_p(r)$, and we write (10.7) more explicitly in spherical polar coordinates:

$$F(\vec{q}) = \int_0^{2\pi} \mathrm{d}\phi \int_0^{\infty} r^2 \mathrm{d}r \ \rho_p(r) \int_0^{\pi} \sin\theta \mathrm{d}\theta \ e^{iqr\cos\theta} \ . \tag{10.8}$$

The only "trick" we have used is to align our coordinate system so that $\vec{q} = q\hat{z}$. This is permissible since the charge distribution is spherically symmetric and there is no preferred direction. Hence, we choose a direction that makes the arithmetic easy. The remaining integrals are elementary, and one can easily show that:

$$F(q) = \frac{4\pi}{q} \int_0^{\infty} r \mathrm{d}r \ \rho_p(r) \sin qr \ . \tag{10.9}$$

Figure 10.2: From “Introductory Nuclear Physics”, by Kenneth Krane

Figure 10.3: From “Introductory Nuclear Physics”, by Kenneth Krane

Figure 10.4: From “Introductory Nuclear Physics”, by Kenneth Krane

Conclusions from the data shown?

1. The central density, is (roughly) constant, almost independent of atomic number, and has a value about $0.13/\text{fm}^3$. This is very close to the density nuclear in the infinite radius approximation,
$$\rho_0 = 3/(4\pi R_0^3) \ .$$

2. The "skin depth", s, is (roughly) constant as well, almost independent of atomic number, with a value of about 2.9 fm, typically. The skin depth is usually defined as the difference in radii of the nuclear densities at 90% and 10% of maximum value.

3. Measurements suggest a best fit to the radius of nuclei:
$$R_N = R_0 A^{1/3} \quad ; \quad R_0 \approx 1.22 \text{ [fm]}, 1.20 \longrightarrow 1.25 \text{ is common.} \tag{10.10}$$
however, values from 1.20$\longrightarrow$1.25 are commonly found

   A convenient parametric form of the nuclear density was proposed by Woods and Saxon (*ca.* 1954).
$$\rho_N(r) = \frac{\rho_0}{1 + \exp\left(\frac{r - R_N}{t}\right)}$$
   where t is a surface thickness parameter, related to s, by $s = 4t\log(3)$.

An example of this distribution is shown in Figure 10.5

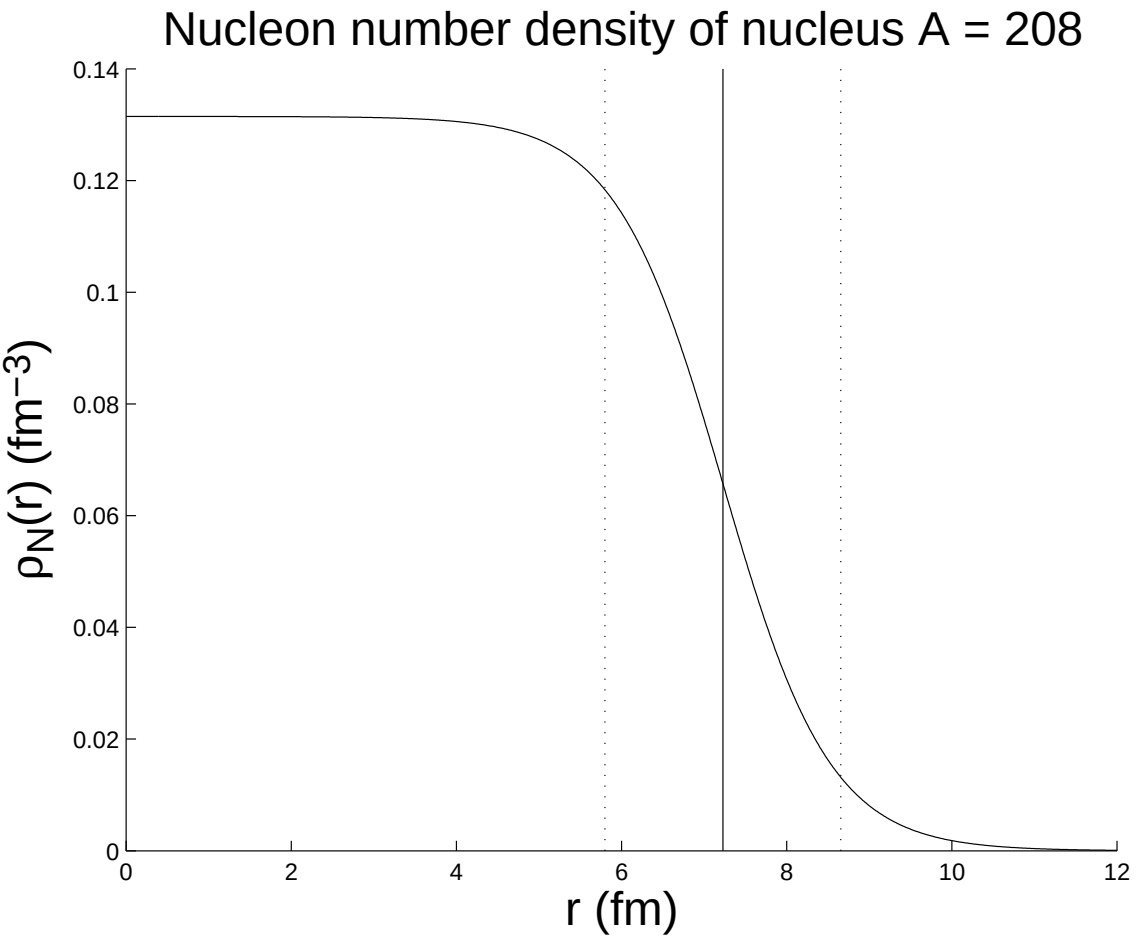

Figure 10.5: The Woods-Saxon model of the nucleon number density. In this figure, $A = 208$, $R_0 = 1.22$ (fm), and $t = 0.65$ (fm). The skin depth is shown, delimited by vertical dotted lines.

Let's work out a specific, but important realization of a charge distribution, namely, a uniform proton distribution, up to some radius R_N, the radius of the nucleus.

Example: Uniform nucleon charge density

In this case, the normalized proton density takes the form:

$$\rho_p(r) = \frac{3}{4\pi R_N^3}\Theta(R - r) \ . \tag{10.11}$$

Thus, combining (10.9) and (10.11), gives, after some reorganization:

$$F(q) = \frac{3}{(qR_N)^3}\int_0^{(qR_N)} \mathrm{d}z \ z \sin z \ , \tag{10.12}$$

which is easily evaluated to be,

$$F(q) = \frac{3[\sin(qR_N) - qR_N\cos(qR_N)]}{(qR_N)^3} \ , \tag{10.13}$$

for which $F(0) = 1$, as expected.

Technical side note:
The following `Mathematica` code was useful in deriving the above relations.

```
(* Here Z == q*R_N: *)

(3/Z^3)*Integrate[z Sin[z], {z,0,Z}]

Series[3*(Sin[Z] - Z*Cos[Z])/Z^3,{Z,0,2}]
```

Graphical output of (10.13) is given in Figure 10.6. We note, in particular, the zero minima when $\tan(qR_N) = qR_N$. The shape of the lobes is determined by the nuclear shape, while the minima are characteristic of the sharp edge. Measurements do not have such deep minima, since the nuclear edge is blurred, and the projectile energies are not exact, but slightly distributed, and the detectors have imperfect resolution. However, the measurements do, unambiguously, reveal important details of the nuclear shape.

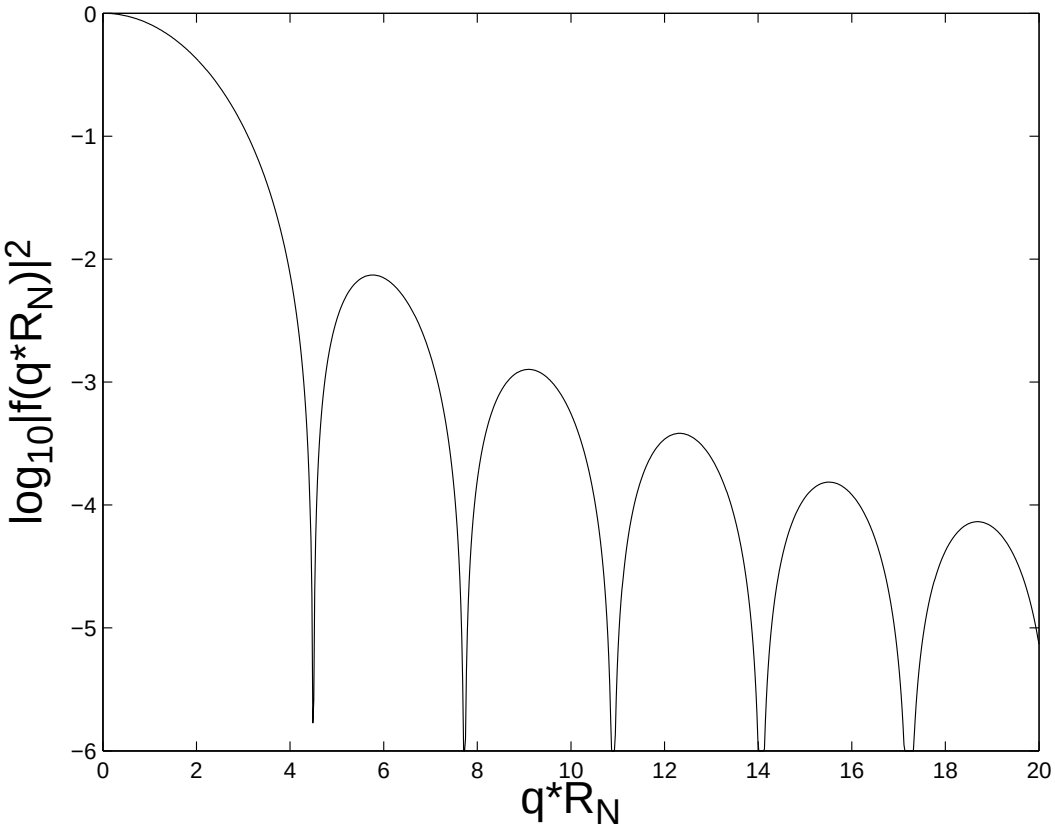

Figure 10.6: Graphical output corresponding to (10.13).

Technical side note:
The following `Matlab` code was useful in producing the above graph.

```
N = 1000; fMin = 1e-6; zMax = 20; % Graph data
z = linspace(0,zMax,N); f = 3*(sin(z) - z.*cos(z))./z.^3;
f(1) = 1; % Overcome the singularity at 0
f2 = f.*f;
for i = 1:N
   f2(i) = max(fMin,f2(i));
end
plot(z,log10(f2),'-k')
xlabel('\fontsize{20}q*R_N')
ylabel('\fontsize{20}log_{10}|f(q*R_N)|^2')
```

10.1.2 Nuclear shape data from electron scattering experiments

---

Technical side note:
The mathematical details can be found in the supplemental notes.

Most of the mathematical detail is given in the supplementary notes to this lecture. Those notes obtain the following, very significant result.

What is measured in a scattering experiment is the relative intensity of deflected projectiles (e), scattered into different angles, by the nucleus (N). This is also known as the scattering cross section, differential in scattering angle. The result is that:

$$\frac{\mathrm{d}\sigma_{eN}}{\mathrm{d}\Omega} = \frac{\mathrm{d}\sigma_{eN}^{\mathrm{Ruth}}}{\mathrm{d}\Omega}|F(q)|^2 \ , \tag{10.14}$$

where $\mathrm{d}\sigma_{eN}^{\mathrm{Ruth}}/\mathrm{d}\Omega$ is the classical Rutherford cross section discussed in NERS311 (but re-derived in the supplemental notes to include relativistic kinematics, and $F(q)$ is the scattering amplitude we have been discussing so far. $|F(q)|^2$ is the scattering amplitude, modulus squared. (It can, in general, be complex.)

Hence, we have a direct experimental determination of the form factor, as a ratio of measurement data (the measured cross section), and a theoretical function, the Rutherford cross section.

$$|F(q)|^2 = \left(\frac{\mathrm{d}\sigma_{eN}^{\mathrm{meas}}}{\mathrm{d}\Omega}\right) \Bigg/ \left(\frac{\mathrm{d}\sigma_{eN}^{\mathrm{Ruth}}}{\mathrm{d}\Omega}\right) \ . \tag{10.15}$$

All that remains is to take the square root, and invert the Fourier Transform, to get $\rho(r)$. This is always done via a relatively simple numerical process.

Although the form factor $|F(q)|^2$ is given in terms of q, we may cast it into more recognizable kinematic quantities as follows. Recall,

$$q = \sqrt{q^2} = \sqrt{|\vec{k}_i - \vec{k}_f|^2} = \sqrt{2k^2(1-\cos\theta)} \ , \tag{10.16}$$

the final step above being obtained since this is an elastic scattering process, where $k = |\vec{k}_i| = |\vec{k}_f|$ and $\vec{k}_i \cdot \vec{k}_f = k^2 \cos\theta$.

Thus, electron scattering experiments yield exquisitely detailed data on the shape of nuclei. Figure 3.11 in Krane depicts some very detailed data that shows the departure from the classical Rutherford scattering cross section, as the projectile's energy, α-particles in this case, is increased. The classical interpretation is that the projectile is penetrating the nucleus. The Quantum Mechanical picture is that the projectile's wave function has a wave number small enough to start resolving the finite size of the nucleus. We now examine another way that experiments can yield information about the nuclear shape.

10.1.3 Nuclear size from spectroscopy measurements

Nuclear and atomic spectroscopy, the technique of measuring the energies of nuclear and atomic transitions, is one of the most precise measurements in nuclear science. If that is the case, then spectroscopy ought to be able to measure differences in transition energies that arise from the finite nuclear size.

Assume, for the sake of argument, that the nucleus is a sphere of radius R_N. An ideal probe of the effect of a finite-sized nucleus *vs.* a point-nucleus (as in the Schrödinger atomic model), would be a $1s$ atomic state, since, of all the atomic electron wavefunctions, the $1s$ state has the most probability density in the vicinity of the nucleus.

The shift of energy of the $1s$ can be estimated as follows:

$$\Delta E_{1s} = \langle \psi_{1s} | V_\circ(r) - V_\cdot(r) | \psi_{1s} \rangle \ , \tag{10.17}$$

where the ψ_{1s} is the $1s$ wavefunction for the point-like nucleus, $V_\circ(r)$ is the Coulomb potential for the finite nucleus, and $V_\cdot(r)$ is the point-like Coulomb potential. This way of estimating energy shifts comes formally from "1st-order perturbation theory", where it is assumed that the difference in potential has only a small effect on the wavefunctions. For a uniform sphere of charge, we know from Classical Electrostatics, that $V_\circ(r) = V_\cdot(r)$ for $r \geq R_N$.

$$\begin{aligned} V_\circ(r \leq R_N) &= -\frac{Ze^2}{4\pi\epsilon_0 R_N}\left[\frac{3}{2} - \frac{1}{2}\left(\frac{r}{R_N}\right)^2\right] \\ V_\circ(r \geq R_N) &\equiv V_\cdot(r) = -\frac{Ze^2}{4\pi\epsilon_0 r} \end{aligned} \tag{10.18}$$

We evaluate this by combining (10.18) with (10.17) and using the hydrogenic wavefunctions given in NERS311 and also in Krane II (Tables 2.2 and 2.5), and obtain:

$$\Delta E_{1s} = \frac{Ze^2}{4\pi\epsilon_0 R_N}\frac{4Z^3}{a_0^3}\int_0^{R_N} \mathrm{d}r r^2 e^{-2Zr/a_0}\left[\frac{R_N}{r} - \frac{3}{2} + \frac{1}{2}\left(\frac{r}{R_N}\right)^2\right] \ . \tag{10.19}$$

In unitless quantities, we may rewrite the above as:

$$\Delta E_{1s} = Z^2\alpha^2(m_e c^2)\left(\frac{2ZR_N}{a_0}\right)^2 \int_0^1 \mathrm{d}z e^{-(2ZR_N/a_0)z}\left[z - \frac{3}{2}z^2 + \frac{z^4}{2}\right] \ . \tag{10.20}$$

Across all the elements, the dimensionless parameter $(2ZR_N/a_0)$ spans the range $2\times10^{-5} \longrightarrow\approx 10^{-2}$. Hence, the contribution to the exponential, in the integral, is inconsequential. The remaining integral is a pure number and evaluates to 1/10. Thus, we may write:

$$\Delta E_{1s} \approx \frac{1}{10} Z^2\alpha^2(m_e c^2)\left(\frac{2ZR_N}{a_0}\right)^2 \ . \tag{10.21}$$

This correction is about 1 eV for $Z = 100$ and much smaller for lighter nuclei.

Nuclear size determination from an isotope shift measurement

Let us imagine how we are to determine the nuclear size, by measuring the energy of the photon that is given off, from a $2p \rightarrow 1s$ transition.

The Schrödinger equation predicts that the energy of the photon will be given by:

$$(E_{2p\rightarrow 1s})_\circ = (E_{2p\rightarrow 1s})_\cdot + \langle\psi_{2p}|V_\circ(r) - V_\cdot(r)|\psi_{2p}\rangle - \langle\psi_{1s}|V_\circ(r) - V_\cdot(r)|\psi_{1s}\rangle \ , \tag{10.22}$$

or,

$$(\Delta E_{2p\rightarrow 1s})_\circ = \langle\psi_{2p}|V_\circ(r) - V_\cdot(r)|\psi_{2p}\rangle - \langle\psi_{1s}|V_\circ(r) - V_\cdot(r)|\psi_{1s}\rangle \ , \tag{10.23}$$

expressing the change in the energy of the photon, due to the effect of finite nuclear size.

The latter term, $\langle\psi_{1s}|V_\circ(r) - V_\cdot(r)|\psi_{1s}\rangle$, has been calculated in (10.21). We now consider the former term, $\langle\psi_{2p}|V_\circ(r) - V_\cdot(r)|\psi_{2p}\rangle$. Figure 10.7 shows the $1s$ and $2p$ hydrogenic radial probabilities for the $1s$ and $2p$ states, each divided by their respective maxima. (This corresponds to having divided the $2p$ function by a factor of about 89.) The vertical line near the origin is the radius of an $A = 208$ nucleus, assuming $R_N = 1.22A^{1/3}$. That radius has been multiplied by a factor of 10 for display purposes. The actual value is $ZR_N/a_0 = 0.0112$, assuming further, that $Z = 82$.

As can be seen from this figure, the overlap of the $2p$ state is many orders of magnitude smaller than that of the $1s$ state. Hence, the term $\langle\psi_{2p}|V_\circ(r) - V_\cdot(r)|\psi_{2p}\rangle$ may be safely ignored in (10.23). Therefore, we can conclude, from (10.21), that the photon's energy is reduced by,

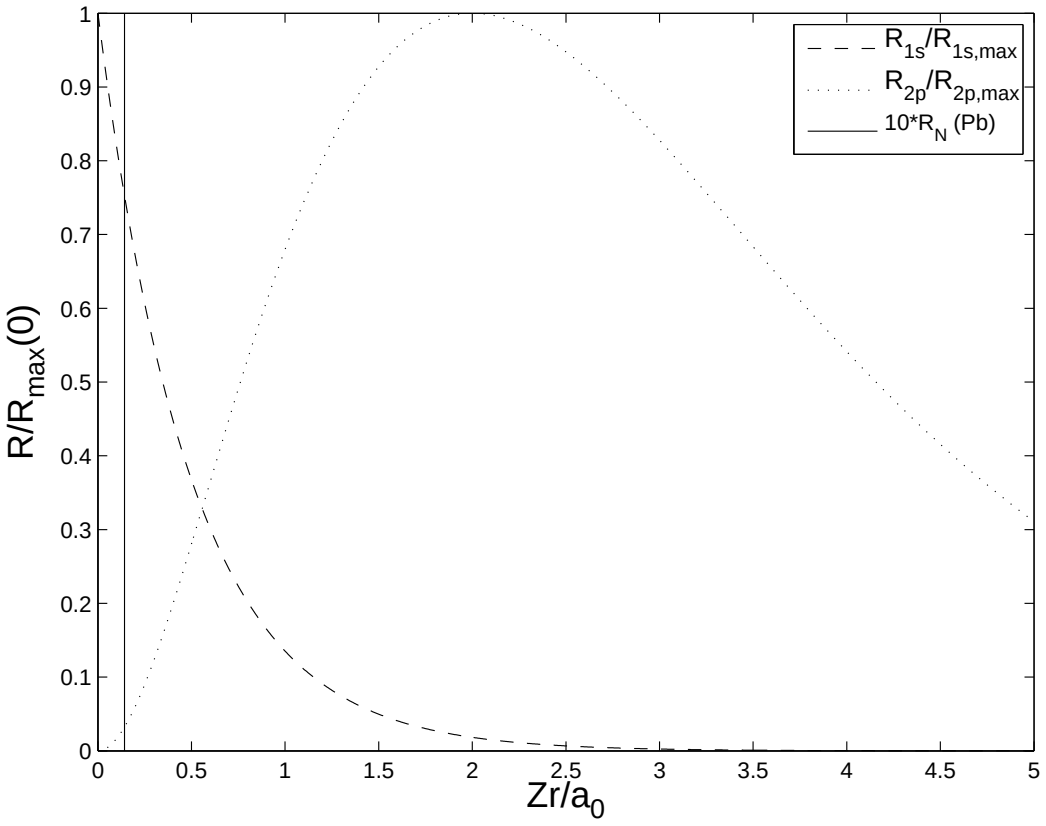

Figure 10.7: Overlap of $1s$ and $2p$ electronic orbitals with the nuclear radius. The nuclear radius depicted is for $A = 208$ and has been scaled upward by 10 for display purposes.

$$\Delta E_{2p\to 1s} \approx -\frac{1}{10} Z^2 \alpha^2 (m_e c^2) A^{2/3} \left(\frac{2ZR_0}{a_0}\right)^2 , \tag{10.24}$$

for a uniformly charged nucleus with radius $R_N = R_0 A^{1/3}$.

However, we have yet to make the connection to a measurement, because the measurement of a photon's energy from a realistically shaped nucleus can not be compared with that of an identical atom with a point nucleus. That does not exist in nature. Instead, consider the following: the transition energy for two isotopes of the same element, A and A'. The difference in this transition energy may be determined experimentally, and we obtain:

$$\Delta E_{2p\to 1s}(A) - \Delta E_{2p\to 1s}(A') = \frac{1}{10} Z^2 \alpha^2 (m_e c^2) \left(\frac{2ZR_0}{a_0}\right)^2 (A'^{2/3} - A^{2/3}) . \tag{10.25}$$

The measured quantity is called the K X-ray *isotope shift*. The following few pages show measurements of isotope shifts, for K X-Rays and optical photon isotope shifts.

Figure 10.8: Fig 3.6 from Krane, K X-ray shifts for Hg.

Figure 10.9: Fig 3.7 from Krane, optical shifts for Hg.

A better probe of nuclear shape can be done by forming muonic atoms, formed from muons (usually from cosmic rays), that replace an inner K-shell electron, and has significant overlap of its wavefunction with the nucleus.

Figure 10.10: Fig 3.8 from Krane, K X-ray shifts for muonic Fe.

All these data are consistent with a nuclear size with a radius, $R_N = R_0 A^{/3}$, and a value for $R_0 \approx 1.2$ fm.

Charge radius from Coulomb energy in mirror nuclei

A mirror-pair of nuclei are two nuclei that have the same atomic mass, but the number of protons in one, is the number of neutrons in the other, and the number of protons and neutrons in one of the nuclei differs by only 1. So, if Z is the atomic number of the higher atomic number mirror nucleus, it has $Z-1$ neutrons. Its mirror pair has $Z-1$ protons and Z neutrons. The atomic mass of both is $2Z-1$. Examples of mirror pairs are: ^{3}H/^{3}He, and ^{39}Ca/^{39}K.

These mirror-pairs are excellent laboratories for investigating nuclear radius since the nuclear component of the binding energy of these nuclei ought to be the same, if the strong force does not distinguish between nucleons. The only remaining difference is the Coulomb self-energy. For a charge distribution with Z protons, the Coulomb self-energy is:

$$E_{\rm C} = \frac{1}{2}\frac{Z^2 e^2}{4\pi\epsilon_0}\int {\rm d}\vec{x}_1 \rho_p(\vec{x}_1)\int {\rm d}\vec{x}_2 \rho_p(\vec{x}_2)\frac{1}{|\vec{x}_1-\vec{x}_2|}\ . \tag{10.26}$$

The factor of 1/2 in front of (10.26) accounts for the double counting of repulsion that takes place when one integrates over the nucleus twice, as implied in (10.26).

For a uniform, spherical charge distribution of the form,

$$\rho_p(\vec{x}) = \frac{3}{4\pi R_N^3}\Theta(R_N - r)\ . \tag{10.27}$$

Figure 10.11: Fig 3.9 from Krane, composite K X-ray shift data.

As shown below:

$$E_{\rm C} = \frac{3}{5}\frac{Z^2e^2}{4\pi\epsilon_0 R_N} \ . \tag{10.28}$$

For a uniform, spherical charge distribution, given by (10.27):

$$\begin{aligned} E_{\rm C} &= \frac{1}{2}\frac{Z^2e^2}{4\pi\epsilon_0}\left(\frac{3}{4\pi R_N^3}\right)^2 \int_{|\vec{x}_1|\le R_N} {\rm d}\vec{x}_1 \int_{|\vec{x}_2|\le R_N} {\rm d}\vec{x}_2 \frac{1}{|\vec{x}_1-\vec{x}_2|} \\ &= \frac{1}{2}\frac{Z^2e^2}{4\pi\epsilon_0 R_N}\left(\frac{3}{4\pi}\right)^2 \int_{|\vec{u}_1|\le 1} {\rm d}\vec{u}_1 \int_{|\vec{u}_2|\le 1} {\rm d}\vec{u}_2 \frac{1}{|\vec{u}_1-\vec{u}_2|} \\ &= \frac{1}{2}\frac{Z^2e^2}{4\pi\epsilon_0 R_N} I \ , \end{aligned} \tag{10.29}$$

where

$$I = \left(\frac{3}{4\pi}\right)^2 \int_{|\vec{u}_1|\le 1} {\rm d}\vec{u}_1 \int_{|\vec{u}_2|\le 1} {\rm d}\vec{u}_2 \frac{1}{|\vec{u}_1-\vec{u}_2|} \ . \tag{10.30}$$

From (10.30), one sees that I has the interpretation as a pure number representing the average of $|\vec{u}_1-\vec{u}_2|^{-1}$, for two vectors, $\vec{u}_1$ and $\vec{u}_2$, integrated uniformly over the interior of a unit sphere. So, now it just remains, to calculate I. We'll work this out explicitly because the calculation is quite delicate. Features of this derivation are seen in several areas of Nuclear and Radiological Science.

Expanding the 3-dimensional integrals in (10.30) results in:

$$I = \left(\frac{3}{4\pi}\right)^2 \int_0^{2\pi} {\rm d}\phi_1 \int_0^{\pi} {\rm d}\theta_1 \sin\theta_1 \int_0^1 {\rm d}u_1 u_1^2 \int_0^{2\pi} {\rm d}\phi_2 \int_0^{\pi} {\rm d}\theta_2 \sin\theta_2 \int_0^1 {\rm d}u_2 u_2^2 \frac{1}{|\vec{u}_1-\vec{u}_2|} \ .$$

The following expression results from having done both azimuthal integrals, once having aligned the z-axis of the coordinate system with $\vec{u}_1$, when performing the 3 inner integrals. Then with the transformation $\cos\theta_1 \to \mu_1$ and $\cos\theta_2 \to \mu_2$, we obtain:

$$
\begin{aligned}
I &= \left(\frac{9}{2}\right)\int_0^1 \mathrm{d}u_1 u_1^2 \int_0^1 \mathrm{d}u_2 u_2^2 \int_{-1}^1 \mathrm{d}\mu_2 \frac{1}{\sqrt{u_1^2+u_2^2-2u_1u_2\mu_2}} \\
&= \left(\frac{9}{2}\right)\int_0^1 \mathrm{d}u_1 u_1 \int_0^1 \mathrm{d}u_2 u_2[(u_1+u_2)-|u_1-u_2|] \\
&= 9\int_0^1 \mathrm{d}u_1 u_1 \left[\int_0^{u_1} \mathrm{d}u_2 u_2^2 + u_1\int_{u_1}^1 \mathrm{d}u_2 u_2\right] \\
&= 9\int_0^1 \mathrm{d}u_1 \left[\frac{u_1^2}{2}-\frac{u_1^4}{6}\right] \\
&= 9\left[\frac{1}{6}-\frac{1}{30}\right] \\
&= \frac{6}{5}\,. \qquad (10.31)
\end{aligned}
$$

A common error in performing the above integral results from ignoring the absolute value in the 2$^{\text{nd}}$ step. Recall that $\sqrt{a^2} = |a|$, not a.

Finally, combining (10.29) and (10.31) gives us the final result expressed in (10.28).

The Coulomb energy differences are measured through β-decay endpoint energies (more on this later in the course), which yield very good information on the nuclear radius. The difference in Coulomb energies is given by:

$$
\begin{aligned}
\Delta E_{\mathrm{C}} &= \frac{3}{5}\frac{e^2}{4\pi\epsilon_0 R_N}[Z^2-(Z-1)^2] \\
&= \frac{3}{5}\frac{e^2}{4\pi\epsilon_0 R_N}(2Z-1) \\
&= \frac{3}{5}\frac{e^2}{4\pi\epsilon_0 R_0}A^{2/3}\,, \qquad (10.32)
\end{aligned}
$$

where, in the last step, we let $R_N = R_0 A^{1/3}$. (Recall, $A = 2Z-1$ for mirror nuclei.)

Figure 10.12: Fig 3.10 from Krane, Coulomb energy differences.

10.2 Mass and Abundance of Nuclei

Note to students: Read 3.2 in Krane on your own. You are responsible for this material, but it will not be covered in class.

10.3 Nuclear Binding Energy

In this section , we discuss several ways that the binding energy of the nucleus is tabulated in nuclear data tables. Nuclear binding energy is always related to the atomic mass, an experimentally derived quantity, one that is obtained with great precision through spectroscopy measurements, at least for nuclei that are stable enough. We start by discussing the binding energy of an atom, and then draw the analogy with the binding energy of the nucleus.

The rest mass energy of a neutral atom, $m_{_A}c^2$, and the rest mass energy of its nucleus, $m_{_N}c^2$, are related by:

$$m_{_A}c^2 = m_{_N}c^2 + Zm_ec^2 - B_e(Z,A) \ , \tag{10.33}$$

where $B_e(Z,A)$ is the *electronic* binding, the sum of the binding energies of all the electrons in the atomic cloud. The total electronic binding energy can be as large as 1 MeV in the heavier atoms in the periodic table. However, this energy is swamped by factors of 10^5–10^6 by the rest mass energy of the nucleus, approximately $A\times 1000$ MeV. Hence, the contribution of the electronic binding is often ignored, particularly when mass *differences* are discussed, as the electronic binding component largely cancels out. We shall keep this in mind, however.

One may estimate the total electronic binding as done in the following example.

Technical aside: Estimating the electronic binding in Pb:
Lead has the following electronic configuration:
$1s^2 2s^2 2p^6 3s^2 3p^6 3d^{10} 4s^2 4p^6 4d^{10} 5s^2 5p^6 4f^{14} 5d^{10} 6s^2 6p^2$,
or, occupancies of 2, 8, 18, 32, 18, 4 in the $n = 1, 2, 3, 4, 5, 6$ atomic shells. Thus,

$$B_e(82,208) \approx (82)^2(13.6 \text{ eV})\left(2 + \frac{8}{2^2} + \frac{18}{3^2} + \frac{32}{4^2} + \frac{18}{5^2} + \frac{4}{6^2}\right) = 0.8076 \text{ MeV} \ .$$

This is certainly an overestimate, since electron repulsion in the atomic shells has not been accounted for. However, the above calculation gives us some idea of the magnitude of the total electronic binding. (A more refined calculation gives 0.2074 MeV, indicating that the overestimate is as much as a factor of 4.) So, for the time being, we shall ignore the total electronic binding but keep it in mind, should the need arise.

By analogy, and more apropos for our purposes, we state the formula for the *nuclear binding energy*, $B_N(Z,A)$, for atom X, with atomic mass $m(^AX)$:

$$B_N(Z,A) = \left\{Zm_p + Nm_n - \left[m(^AX) - Zm_e\right]\right\}c^2 \ . \tag{10.34}$$

Since

$$m_p + m_e \approx m(^1H) \ ,$$

we may rewrite (10.34) as

$$B_N(Z,A) = [Zm(^1H) + Nm_n - m(^AX)]c^2 \ . \tag{10.35}$$

We emphasize, however, that electron binding energy is being ignored, henceforth[2].

Thus, we have obtained the binding energy of the nucleus in terms of the atomic mass of its neutral atom, $m(^AX)$. Conventionally, atomic masses are quoted in terms of the *atomic mass unit*, u. The conversion factor is $uc^2 = 931.494028(23)$ MeV.

Occasionally, it is the nuclear binding energy that is tabulated (it may be listed as *mass defect* or *mass excess*), in which case that data may be used to infer the atomic mass. A word of warning, however. Don't assume that the uses of *mass defect* or *mass excess* are consistent in the literature. One must always consult with the detailed descriptions of the data tables, to see the exact definition employed in that document.

Separation energies

Other measured data of interest that shine some light on the binding energy, as well as the nuclear structure of a given nucleus, is the neutron separation energy, S_n. That is the energy required to liberate a neutron from the nucleus, overcoming the strong attractive force. From the binding energy expressed in (10.35), we see that S_n takes the form:

$$\begin{aligned} S_n &= B_N\left({}^A_Z X_N\right) - B_N\left({}^{A-1}_{\ Z} X_{N-1}\right) \\ &= \left[m\left({}^{A-1}_{\ Z} X_{N-1}\right) - m\left({}^A_Z X_N\right) + m_n\right] c^2 \ . \end{aligned} \tag{10.36}$$

The proton separation energy is a similar quantity, except that it also accounts for the repulsion by the other protons in the nucleus.

$$\begin{aligned} S_p &= B_N\left({}^A_Z X_N\right) - B_N\left({}^{A-1}_{Z-1} X_N\right) \\ &= \left[m\left({}^{A-1}_{Z-1} X_N\right) - m\left({}^A_Z X_N\right) + m\left({}^1H\right)\right] c^2 \ . \end{aligned} \tag{10.37}$$

[2]To adapt these equations to account for electronic binding, (10.34) would take the form:

$$B_N(Z,A) = [Z(m_p + m_e) + Nm_{_N} - m(^AX)]c^2 - B_e(Z,A) \ .$$

Thus we see from (10.35), that measurement of atomic mass yields direct information on the binding energy. We also see from (10.36) and (10.37), that measurements of neutron and proton separation energies yield direct information on the difference in nuclear binding energy between two nuclei that differ in A by one neutron or proton.

There are 82 stable[3] elements. $^{209}_{83}$Bi, the most stable isotope of Bi, has a measured half-life of $(19 \pm 2) \times 10^{18}$ years (α-decay). Those 82 stable elements have 256 stable isotopes. Tin[4] has 10 stable isotopes ranging from ^{112}Sn–^{126}Sn. These stable isotopes, plus the more than 1000 unstable but usable nuclei (from the standpoint of living long enough to provide a direct measurement of mass), can have their binding energy characterized by a universal fitting function, the semiempirical formula for $B(Z, A) \equiv B_N(Z, A)$, a five-parameter empirical fit to the 1000+ set of data points. (The subscript N is dropped to distinguish B as the formula derived from data fitting.

Semiempirical Mass Formula – Binding Energy per Nucleon

The formula for $B(Z, A)$ is given conventionally as:

$$B(Z,A) = a_{\rm V} A - a_{\rm S} A^{2/3} - a_{\rm C} Z(Z-1) A^{-1/3} - a_{\rm sym} \frac{(A-2Z)^2}{A} + a_{\rm p} \frac{(-1)^Z [1 + (-1)^A]}{2} A^{-3/4} \ . \tag{10.38}$$

The numerical values of the fitting constants and the meaning of each term are given in the following table:

a_i	[MeV]	Description	Source
$a_{\rm V}$	15.5	Volume attraction	Liquid Drop Model
$a_{\rm S}$	16.8	Surface repulsion	Liquid Drop Model
$a_{\rm C}$	0.72	Coulomb repulsion	Liquid Drop Model + Electrostatics
$a_{\rm sym}$	23	n/p symmetry	Shell model
$a_{\rm p}$	34	n/n, p/p pairing	Shell model

Table 10.1: Fitting parameters for the nuclear binding energy

The explanation of each term follows:

[3]Let us use, as a working definition, that "stability" means "no measurable decay rate".

[4]Tin's remarkable properties arise from the fact that it has a "magic" number of protons (50). This "magic" number represents a major closed proton shell, in the "shell model" of the nucleus, that we shall study soon. Tin's remarkable properties don't stop there! Tin has 28 known additional unstable isotopes, ranging from ^{99}Sn–^{137}Sn! It even has a "doubly-magic" isotope, ^{100}Sn, with a half-life of about 1 s, discovered in 1994. Tin is the superstar of the "Chart of the Nuclides". And you thought tin was just for canning soup!

Volume attraction: This term represents the attraction of a core nucleon to its surrounding neighbors. The nuclear force is short-medium range, therefore, beyond the immediate neighbors, there is no further attraction. Thus we expect this term to be attractive, and proportional to the number of nucleons. Add one nucleon to the core, and the binding energy goes up by the same amount, regardless of what A is. Another way to see this is: the "bulk term" is proportional to the volume of material, thus it is proportional to R_N^3, or A, since $R_N \propto A^{1/3}$. This comes from considering the nucleus to be formed of an incompressible fluid of mutually-attracting nucleons, *i.e.* the Liquid Drop Model of the nucleus.

Surface attraction: The volume term overestimates the attraction, because the nucleons at the surface lack some of the neighbors that attract the core nucleons. Since the surface is proportional to R_N^2, this term is proportional to $A^{2/3}$, and is repulsive.

Coulomb repulsion: The Coulomb repulsion is estimated from (10.28). This term is proportional to $1/R_N$, or $A^{-1/3}$. The Z^2 is replaced by $Z(Z-1)$ since a proton does not repulse itself. As discussed previously, this term is derived from Electrostatics, but within the Liquid Drop Model, in which the electrostatic charge is considered to be spread continuously through the drop.

n/p symmetry: The Nuclear Shell Model predicts that nuclei like to form with equal numbers of protons and neutrons. This is reflected by the per nucleon factor of $[(A-2Z)/A]^2$. This "repulsion" minimizes (vanishes) when $Z = N$. This is a "Fermi pressure" term, meaning that the nucleus wants to maximize the difference of particle types in the nucleus.

n/n, p/p pairing: The Nuclear Shell Model also predicts that nuclei prefer when protons or neutrons are paired up in $n-n$, $p-p$ pairs. This factor is attractive, for an even-even nucleus (both Z and N are even), repulsive for an odd-odd nucleus, and zero otherwise. The $A^{-3/4}$ term is not easy to explain, and different factors are seen in the literature. This term comes from the spin-spin interaction. Like magnets (which is sort of, what nucleons are), want to anti-align their magnetic poles.

For a graphical representation of B/A, see figure 3.17 in Krane.

Using the expression (10.38) and adapting (10.35), we obtain the *semiempirical mass formula:*

$$m(^A X) = Z m(^1 H) + N m_n - B(Z,A)/c^2 \ , \tag{10.39}$$

that one may use to estimate $m(^A X)$ from measured values of the binding energy, or vice-versa.

Application to β-decay

β-decay occurs when a proton or a neutron in a nucleus converts to the other form of nucleon, $n \to p$, or $p \to n$. (An unbound neutron will also β-decay.) This process preserves

A. Therefore, one may characterize β-decay as an isobaric (*i.e.* same A) transition. For fixed A, (10.39) represents a parabola in Z, with the minimum occurring at (Note: There is a small error in Krane's formula below.):

$$Z_{\min} = \frac{[m_n - m(^1\mathrm{H})]c^2 + a_{\mathrm{C}} A^{-1/3} + 4a_{\mathrm{sym}}}{2a_{\mathrm{C}} A^{-1/3} + 8a_{\mathrm{sym}} A^{-1}} \ . \tag{10.40}$$

We have to use some caution when using this formula. When A is odd, there is no ambiguity. However, when the decaying nucleus is odd-odd, the transition picks up an additional loss in mass of $2a_{\mathrm{p}} A^{-3/4}$, because an odd-odd nucleus becomes an even-even one. Similarly, when an even-even nucleus decays to an odd-odd nucleus, it picks up a gain of $2a_{\mathrm{p}} A^{-3/4}$ in mass, that must be more than compensated for, by the energetics of the β-decay.

Figure 3.18 in Krane illustrates this for two different decays chains.

(10.40) can very nearly be approximated by:

$$Z_{\min} \approx \frac{A}{2} \frac{1}{1 + (1/4)(a_{\mathrm{C}}/a_{\mathrm{sym}})A^{2/3}} \ . \tag{10.41}$$

This shows clearly the tendency for $Z \approx N$ for lighter nuclei. For heavier nuclei, $A \approx 0.41$.

Binding Energy per Nucleon

The binding energy per nucleon data is shown in Krane's Figure 3.16 and the parametric fit shown in Krane's Figure 3.17. There are interesting things to note. $B(Z, A)/A$ ...

- peaks at about $A = 56$ (Fe). Iron and nickel (the iron core of the earth) are natural endpoints of the fusion process.
- is about 8 MeV $\pm$ 10 % for $A > 10$.

10.4 Angular Momentum and Parity

The total angular momentum of a nucleus is formed from the sum of the individual constituents angular momentum, $\vec{l}$, and spin, $\vec{s}$, angular momentum. The symbol given to the nuclear angular momentum is I. Thus,

$$\vec{I} = \sum_{i=1}^{A} (\vec{l_i} + \vec{s_i}) \ . \tag{10.42}$$

These angular momenta add in the Quantum Mechanical sense. That is:

$$\begin{aligned} \langle \vec{I}^2 \rangle &= \hbar^2 I(I+1) \\ I &= 0, \frac{1}{2}, 1, \frac{3}{2} \cdots \\ \langle I_z \rangle &= \hbar m_{_I} \\ m_{_I} &: -I \leq m_{_I} \leq I \\ \Delta m_{_I} &: \text{integral} \end{aligned} \tag{10.43}$$

Since neutron and proton spins are half-integral, and orbital angular momentum is integral, it follows that I is half-integral for odd-A nuclei, and integral for even-A nuclei.

Recall that parity is associated with a quantum number of ± 1, that is associated with the inversion of space. That is, if Π is the parity operator, acting on the composite nuclear wave function, $\Psi(\vec{x}; A, Z)$,

$$\Pi\Psi(\vec{x}; A, Z) = \pm\Psi(-\vec{x}; A, Z) \ . \tag{10.44}$$

The plus sign is associated with "even parity" and the minus sign with "odd parity".

Total spin and parity are measurable, and a nucleus is said to be in an I^π configuration. For example, ^{235}U has $I^\pi = \frac{7}{2}^-$, while ^{238}U has $I^\pi = 0^+$.

10.5 Nuclear Magnetic and Electric Moments

10.5.1 Magnetic Dipole Moments of Nucleons

We have learned from atomic physics, that the magnetic fields generated by moving charges, has a small but measurable effect on the energy levels of bound electrons in an atom. For example, the apparent motion of the nucleus about the electron (in the frame where the electron is at rest), leads to "fine structure" changes in atomic spectra. This arises because the nucleus can be thought of as a closed current loop, generating its own magnetic field, and that magnetic field exerts a torque on the spinning electron. Although the electron is a "point particle", that point charge is spinning, generating its own magnetic field. We know that two magnets exert torques on each other, attempting to anti-align the magnetic poles.

The nucleus itself, is made up of protons and neutrons that have intrinsic spin as well, generating their own "spin" magnetic fields, in addition to the orbital one. That provides an additional torque on the electron spins, resulting in the "hyperfine structure" of atomic energy levels.

"Superhyperfine structure" results from additional torques on the electron resulting from neighboring atoms in condensed materials, yet another set of forces on the electron.

These energy differences are small, but, nonetheless important, for interpreting atomic spectra. However, we are now concerned with nucleons, in a tightly-bound nucleus, all in close proximity to each other, all moving with velocities of about $0.001 \rightarrow 0.1$c. This is a radical departure from the leisurely orbit of an electron about a nucleus. This is a "mosh pit" of thrashing, slamming nucleons. The forces between them are considerable, and play a vital role in the determination of nuclear structure.

The orbital angular momentum can be characterized in classical electrodynamics in terms of a magnetic moment, $\vec{\mu}$:

$$\vec{\mu} = \frac{1}{2} \int \mathrm{d}\vec{x}\ \vec{x} \times J(\vec{x}) \ , \tag{10.45}$$

where $J(\vec{x})$ is the *current density*. For the purpose of determining the orbital angular momentum's contribution to the magnetic moment, the nucleons can be considered to be point-like particles. For point-like particles,

$$\mu = |\vec{\mu}| = g_l l \mu_N \ , \tag{10.46}$$

where l is the orbital angular momentum quantum number, g_l is the *g-factor or gyromagnetic ratio* ($g_l = 1$ for protons, $g_l = 0$ for neutrons, since the neutrons are neutral), and the nuclear magnetron, μ_N is:

$$\mu_N = \frac{e\hbar}{2m_p} \ , \tag{10.47}$$

defined in terms of the single charge of the proton, e, and its mass, m_p. Its current measured value is $\mu_N = 5.05078324(13) \times 10^{-27}$ J/T.

Intrinsic spins of the nucleons also result in magnetic moments. These are given by:

$$\mu = g_s s \mu_N \ , \tag{10.48}$$

where the *spin g factors* are known to be, for the electron, proton, neutron and muon:

Type	g_s (measured)	g_s (theory)
e	-2.002319043622(15)	agree!
p	5.585694713(90)	?
n	-3.82608545(46)	?
μ	-2.0023318414(12)	2.0023318361(10)

A simple(!) application of Dirac's *Relativistic Quantum Mechanics* and *Quantum Electrodynamics* (*aka* QED) leads to the prediction, $g_s = 2$ for the electron. The extra part comes from the *zitterbewegung* of the electron[5]. The fantastic agreement of g_s for the electron, between measurement and theory, 12 decimal places, is considered to be the most remarkable achievement of theoretical physics, and makes QED the most verified theory in existence.

I'm not aware of any theory for the determination of the nucleon g-factors. However, the measured values allow us to reach an important conclusion: The proton must be something very different from a point charge (else its g_s would be close to 2), and the neutron must be made up of internal charged constituents (else its g_s would be 0). These observations laid the groundwork for further investigation that ultimately led to the discovery (albeit indirectly), that neutrons and protons are made up of quarks. (Free quarks have never been observed.) This led to the development of *Quantum Chromodynamics* (*aka* QCD), that describes the the strong force in fundamental, theoretical terms. The unification of QCD, QED, and the weak force (responsible for β-decay) is called *The Standard Model* of particle physics.

Measurement and Theory differ, however, for the muon's g_s. It has been suggested that there is physics beyond The Standard Model that accounts for this.

Measurements of magnetic moments of nuclei abound in the literature. These magnetic moments are composites of intrinsic spin as well as the orbital component of the protons. Nuclear models provide estimates of these moments, and measured moments yield important information on nuclear structure. Table 3.2 in Krane provides some examples. Further exploration awaits our later discussions on nuclear models.

10.5.2 Quadrupole Moments of Nuclei

The electric quadrupole moment is derived from the following considerations.

The electrostatic potential of the nucleus is given by:

$$V(\vec{x}) = \frac{Ze}{4\pi\epsilon_0} \int \mathrm{d}\vec{x}' \; \frac{\rho_p(\vec{x}')}{|\vec{x} - \vec{x}'|} \; . \tag{10.49}$$

Now, imagine that we are probing the nucleus from a considerable distance, so far away from it, that we can only just discern the merest details of its shape. Given that $\rho_p(\vec{x}')$ is highly localized in the vicinity of the nucleus and our probe is far removed from it, we may expand (10.49) in a Taylor expansion in $|\vec{x}'|/|\vec{x}|$. Thus we obtain:

[5] According to Wikipedia, the term *zitterbewegung* is derived from German, meaning "trembling motion". According to Zack Ford (NERS312-W10 student), the word is derived from "cittern movements", a "cittern" (or "citter") being an old (Renaissance-era) instrument very similar to a guitar. I like Zack's definition better.

$$V(\vec{x}) = \frac{Ze}{4\pi\epsilon_0}\left[\frac{1}{|\vec{x}|}\int \mathrm{d}\vec{x}'\ \rho_p(\vec{x}') + \frac{\vec{x}}{|\vec{x}|^3}\cdot\int \mathrm{d}\vec{x}'\ \vec{x}'\rho_p(\vec{x}') + \frac{1}{2|\vec{x}|^5}\int \mathrm{d}\vec{x}'\ \left(3(\vec{x}\cdot\vec{x}')^2 - |\vec{x}|^2|\vec{x}'|^2\right)\rho_p(\vec{x}')\cdots\right] . \tag{10.50}$$

This simplifies to:

$$V(\vec{x}) = \frac{Ze}{4\pi\epsilon_0}\left[\frac{1}{|\vec{x}|} + \frac{Q}{2|\vec{x}|^3}\cdots\right] , \tag{10.51}$$

where

$$Q = \int \mathrm{d}\vec{x}\ \left(3z^2 - r^2\right)\rho_p(\vec{x}) . \tag{10.52}$$

We have used $\int \mathrm{d}\vec{x}\ \rho_p(\vec{x}) \equiv 1$ for the first integral in (10.50). This is simply a statement of our conventional normalization of $\rho_p(\vec{x})$. We also used $\int \mathrm{d}\vec{x}\ \vec{x}\rho_p(\vec{x}) \equiv 0$ in the second integral in (10.50). This is made possible by choosing the "center of charge" as the origin of the coordinate system for the integral. Finally, the third integral resulting in (10.52), arises from the conventional choice, when there is no preferred direction in a problem, and set the direction of $\vec{x}'$ to align with the z'-axis, for mathematical convenience.

Technical note: *The second integral can be made to vanish through the choice of a center of charge. This definition is made possible because the charge is of one sign. Generally, when charges of both signs are involved in an electrostatic configuration, and their respective centers of charge are different, the result is a non-vanishing term known as the electric dipole moment. In this case, the dipole moment is given by:*

$$\vec{d} = \int \mathrm{d}\vec{x}\ \vec{x}\rho(\vec{x}) .$$

Finally, when it is not possible to choose the z-axis to be defined by the direction of $\vec{x}$, but instead, by other considerations, the quadrupole becomes a tensor, with the form:

$$Q_{ij} = \int \mathrm{d}\vec{x}\ \left(3x_i x_j - |\vec{x}|^2\right)\rho_p(\vec{x}) .$$

The quantum mechanics analog to (10.52) is:

$$Q = \int \mathrm{d}\vec{x}\ \psi_N^*(\vec{x})(3z^2 - r^2)\psi_N(\vec{x}) , \tag{10.53}$$

where $\psi_N(\vec{x})$ is the composite nuclear wave function. The electric quadrupole moment of the nucleus is also a physical quantity that can be measured, and predicted by nuclear model theories. See Krane's Table 3.3.

Closed book "pop quiz" problems

Review: Basic math Need some questions here.

Review: Basic kinematics For a particle of mass m with velocity $\vec{v}$, what is its i) momentum, ii) total energy, iii) kinetic energy in both non-relativistic and relativistic formalisms.

Review: Basic kinematics For a massless particle with momentum $\vec{p}$, what is its i) total energy, ii) kinetic energy.

Review: Conservation laws, and two-body kinematics State the Conservation of Energy and the Conservation of Momentum equations for a 2-body interaction involving two masses, m_1 and m_2 with initial velocities $\vec{v}_1$ and $\vec{v}_2$. Perform this in both non-relativistic and relativistic formalisms.

Review: Electrostatics Need several questions here

Review: Error analysis Need several questions here

Compton interaction: description In words, describe "The Compton interaction".

Compton interaction: kinematics derivation Derive the relationship between the scattered γ energy and its scattering angle in the Compton interaction.

Schrödinger equation: basics What is the time dependent Schrödinger equation in 1D? 3D? What is the time independent Schrödinger equation in 1D? 3D? What is the main application of solutions to the time independent Schrödinger equation?

Schrödinger equation: basics Describe and state the expressions (1D and 3D) for the i) probability density, and ii) the probability current density.

Heisenberg Uncertainty Principle What is the Heisenberg Uncertainty Principle and what does it mean?

Pauli Exclusion Principle What is the Pauli Exclusion Principle and what does it mean?

The scattering amplitude for electron-nucleus scattering was given. Including the normalization factor, it is given by:

$$F(\vec{q}) = \frac{q^2}{4\pi} \int \mathrm{d}\vec{x} \int \mathrm{d}\vec{x}' \, \frac{\rho_p(\vec{x}')}{|\vec{x} - \vec{x}'|} e^{i\vec{q}\cdot\vec{x}} \ , \quad \text{where} \quad \int \mathrm{d}\vec{x}' \, \rho_p(\vec{x}') \equiv 1 \ .$$

1. Through re-arrangement and symmetry, show that:

$$F(\vec{q}) = \int \mathrm{d}\vec{x} \rho_p(\vec{x}') e^{i\vec{q}\cdot\vec{x}'} \left(\frac{q^2}{4\pi}\right) \int \mathrm{d}\vec{x} \, \frac{e^{i\vec{q}\cdot\vec{x}}}{|\vec{x}|} \ .$$

2. Then, show that Show:

$$F(\vec{q}) = \int \mathrm{d}\vec{x}' \ \rho_p(\vec{x}') e^{i\vec{q}\cdot\vec{x}'} \ .$$

Nuclear form factor One calculation that is used in the determination of the shape of the nucleus is:

$$\langle \vec{k_f} | \rho_p(\vec{x}) | \vec{k_i} \rangle$$

1. What is the integral implied by the above expression?
2. Evaluate this integral in the approximation that the proton charge density distribution is spherically symmetric, that is, $\rho_p(\vec{x}) = \rho_p(r)$. Express your result in terms of q, where $q = |\vec{k_i} - \vec{k_f}|$.

1.

$$\langle \vec{k_f} | \rho_p(\vec{x}) | \vec{k_i} \rangle = \int_{\vec{x}\in\mathbb{R}^3} \mathrm{d}\vec{x}\, e^{-i\vec{k_f}\cdot\vec{x}} \rho_p(\vec{x}) e^{i\vec{k_i}\cdot\vec{x}}$$

Note: "$\vec{x} \in \mathbb{R}$" is standard math shorthand for, "(x, y, z) each span all the real numbers"

2. If $\rho_p(\vec{x}) = \rho_p(r)$, and $q = |\vec{k_i} - \vec{k_f}|$, then $\langle \vec{k_f} | \rho_p(\vec{x}) | \vec{k_i} \rangle =$

$$\begin{aligned}
&\int_{\vec{x}\in\mathbb{R}^3} \mathrm{d}\vec{x}\, \rho_p(r) e^{i\vec{q}\cdot\vec{x}} \\
&\qquad = \int_0^{2\pi} \mathrm{d}\phi \int_0^{\pi} \sin\theta \mathrm{d}\theta \int_0^{\infty} r^2 \mathrm{d}r \rho_p(\vec{x}) e^{iqr\cos\theta} \\
&\qquad = 2\pi \int_{-1}^{1} \mathrm{d}\mu \int_0^{\infty} r^2 \mathrm{d}r\ \rho_p(r) e^{iqr\mu} \\
&\qquad = \frac{2\pi}{q} \int_0^{\infty} r \mathrm{d}r\, \rho_p(r) \sin qr
\end{aligned}$$

Answer this precocious child An 11-year old asks you: *"I learned in school about the nucleus and how the electrons go around around it and make atoms. But, I also know that unlike charges attract and like charges repel, so I understand why the electrons like to be close to the nucleus. But, I'm still confused...*
Why doesn't an atom collapse?
If a nucleus is made up of positive charge, why doesn't it fly apart?
The electron is made up of negative charge. Why doesn't IT fly apart?
What makes positive charge? What makes negative charge?"

You have probably seen the earth's moon, and know from your classes or readings, that it revolves around the earth. It does not crash into the earth, for the same reason that the negatively charged electrons do not collapse in on the positively charged nucleus. The electron is in motion, but there is a force keeping it there, called " centripetal

force", arising from the motion of the electron, that keeps it there. Maybe, when you were very young, one of your parents swung you around in a circle. Your body wanted to fly off, but your parent's arms kept you there. When my kids were young, I used to do this at the beach, in knee-deep water. I'd swing them in circles, and then let them go, and they'd fly off. Happily, most of them survived!

A nucleus is made up of protons, positively charged, and neutrons, that have no electric charge. For example, there is a single proton at the center of a hydrogen atom. There are two protons and two neutrons at the center of a helium atom. The protons and neutrons are attracted to each other by a "strong force", that is much stronger (about 100 times stronger) than the repulsive force due to the positive charge.

As far as we know, the electron is a fundamental, "point-like" particle. It does not fly apart, because there is nothing to tear apart!

All particles in nature are either positive, negative, or neutral. However, the protons and neutrons in a nucleus are not point-particles. Instead they are made up of other point-like (or so we think) particles called quarks, of which there are different kinds, either positive or negative (no neutral ones). These quarks are held together by the strong force too, and so, protons and neutrons are stable.

White lies, and other things to think about

- Look up, on Wikipedia (the Source of All Knowledge [SOAK], "centrifugal" and centripetal"

- Why do we only see one face of the moon. SOAK: "Libration"

- If you're going to experiment with a smaller sibling, spin them by holding their legs, not their arms.

Shoulders can separate a lot easier then legs. (It's sad that I know this.) SOAK: "Separated shoulder".

- Look up on SOAK: "Strong nuclear force", "quark"

- "String theory" is an effort to understand the point-like particles, in terms of something even more

fundamental: "string". You guessed it! SOAK: "string theory".

Closed book "exam" problems

1. **Nuclear Form Factor**

   The nuclear form factor, $F(\vec{q})$, is defined as follows:

   $$F(\vec{q}) = \int \mathrm{d}\vec{x}\, \rho_p(\vec{x}) e^{i\vec{q}\cdot\vec{x}} \ .$$

   If $\rho_p(\vec{x})$ is the proton density, normalized so that:

   $$\int \mathrm{d}\vec{x}\, \rho_p(\vec{x}) \equiv 1 \ ,$$

   show:

   (a)
   $$F(0) = 1$$

   (b)
   $$F(\vec{q}) = F(q) = \frac{4\pi}{q} \int r\mathrm{d}r\, \rho_p(r) \sin(qr) \ ,$$

   for spherically symmetric nuclei ($\rho_p(\vec{x}) = \rho_p(r)$).

   (c) Given that:

   $$\rho_p(\vec{x}) = N\Theta(R_N - r) \ ,$$

   where R_N is the radius of the nucleus, find an expression for the normalization constant, N above, in terms of R_N.

   (d) For the proton distribution implied by (c), show:

   $$F(q) = \frac{3}{(qR_N)^3}[\sin(qR_N) - qR_N \cos(qR_N)] \ .$$

   Hint: $\int \mathrm{d}x\, x \sin x = \sin x - x\cos x$.

   (e) From the expression for $F(q)$ in part (d) above, show that,

   $$\lim_{q\to 0} F(q) = 1 \ ,$$

   using either a Taylor expansion, or l'Hôpital's Rule.

2. **Nuclear Coulomb Repulsion Energy**

(a) The potential felt by a proton due to a charge distribution made up of the $Z-1$ other protons in the nucleus, is given by

$$V(\vec{x}) = \frac{(Z-1)e^2}{4\pi\epsilon_0} \int \mathrm{d}\vec{x}' \, \frac{\rho_p(\vec{x}')}{|\vec{x}-\vec{x}'|} \ ,$$

where

$$\int \mathrm{d}\vec{x}' \, \rho(\vec{x}') \equiv 1 \ .$$

With the assumption that the protons are uniformly distributed through the nucleus up to radius R_N, that is, $\rho(\vec{x}') = \rho_0$, for $0 \leq |\vec{x}'| \leq R_N$, show,

$$V(r) = \frac{(Z-1)e^2}{4\pi\epsilon_0 R_N} \left[\frac{3}{2} - \frac{1}{2} \left(\frac{r}{R_N} \right)^2 \right] \ .$$

From this expression, what can you tell about the force on a proton inside the nucleus?

(b) The Coulomb self-energy of a charge distribution is given by

$$E_c = \frac{e}{4\pi\epsilon_0} \left(\frac{1}{2} \right) \int \mathrm{d}\vec{x} \int \mathrm{d}\vec{x}' \, \frac{\rho(\vec{x})\rho(\vec{x}')}{|\vec{x}-\vec{x}'|} \ ,$$

where

$$Ze = \int \mathrm{d}\vec{x}' \, \rho(\vec{x}') \ .$$

Justify the factor of (1/2) in the above expression?

(c) Starting with the result of part a) or part b) of this problem, show, for a uniform charge distribution $\rho(\vec{x}') = \rho_0$, for $0 \leq |\vec{x}'| \leq R_N$, that,

$$E_c = \frac{3}{5} \frac{Z(Z-1)e^2}{4\pi\epsilon_0} \frac{1}{R_N} \ .$$

3. **Nuclear Binding Energy**

The semi-empirical formula for the total binding energy of the nucleus is:

$$B(Z,A) = a_{\mathrm{v}} A - a_{\mathrm{s}} A^{2/3} - a_{\mathrm{c}} Z(Z-1) A^{-1/3} - a_{\mathrm{sym}} \frac{(A-2Z)^2}{A} + p(N,Z) a_{\mathrm{p}} A^{-3/4} \ ,$$

where $p(N,Z)$ is 1 for even-N/even-Z, -1 for odd-N/odd-Z, and zero otherwise.

(a) Identify the physical meaning of the 5 terms in $B(A,Z)$. Explain which terms would go up, or go down with the addition of one additional neutron or one additional proton.

(b) With A fixed, $B(Z, A)$ is a quadratic expression in Z. Find its minimum, and discuss.

(c) Show that $p_{\mathrm{N,Z}}$ can be written:

$$p(Z, N) = \frac{1}{2}[(-1)^Z + (-1)^N] \ ,$$

or equivalently,

$$p(Z, A) = \frac{1}{2}(-1)^Z[(-1)^A + 1] \ .$$

(d) The neutron separation energy is defined by:

$$S_{\mathrm{n}} = B(Z, A) - B(Z, A - 1) \ ,$$

and the proton separation energy is defined by:

$$S_{\mathrm{p}} = B(Z, A) - B(Z - 1, A - 1) \ .$$

Using the large A approximation, namely:

$$(A - 1)^n \approx A^n - nA^{n-1} \ ,$$

develop approximate expressions for S_{n} and S_{p}.

4. **Quadrupole Moment**

The quadrupole moment, Q, in the liquid drop model of the nucleus is defined by:

$$Q = \int \mathrm{d}\vec{x}\rho_p(\vec{x})(3z^2 - r^2) \ ,$$

where $\rho_p(\vec{x})$ is the charge density per unit volume, normalized in the following way:

$$\int \mathrm{d}\vec{x}\rho_(\vec{x}) \equiv 1 \ .$$

We consider an ellipsoidal nucleus with a sharp nuclear edge, with its surface being given by:

$$\frac{x^2 + y^2}{a^2} + \frac{z^2}{b^2} = 1 \ ,$$

where the larger of a or b is the semimajor axis, and the smaller of the two, the semiminor axis.

(a) Sketch the shape of this nucleus, for both the prolate and oblate cases.

(b) Show that the volume of this nucleus is $V = (4\pi/3)a^2b$.

(c) Find an expression for Q, that involves only Z, a, and b.

(d) Discuss the cases $a > b$, $a < b$, $a = b$. Even if you have not found an expression for Q, you should be able to discuss this effectively, given its integral form above, and say something about the sign of Q depending on the relative size of a and b.

5. **Nuclear Structure and Binding Energy**

(a) **Theoretical foundations**

i. What is the liquid drop model of the nucleus?

ii. What is the shell model of the nucleus?

iii. How is Classical Electrostatics employed in describing the structure of the nucleus? Cite two examples.

(b) **Binding energy of the nucleus**

The semi-empirical formula for the total binding energy of the nucleus is:

$$B(Z,A) = a_{\rm V}A - a_{\rm S}A^{2/3} - a_{\rm C}Z(Z-1)A^{-1/3} - a_{\rm sym}\frac{(A-2Z)^2}{A} + a_{\rm p}\frac{(-1)^Z[1+(-1)^A]}{2}A^{-3/4}\,.$$

i. In the table below...

A. In the 3rd column, identify the nuclear model that gives rise to this term. The answer is started for you, in the 2nd row. Complete the remaining rows.

B. In the 4th column, identify how this term arises (qualitative explanation) from the nuclear model identified in the 3rd column. The answer is started for you, in the 2nd row. Complete the remaining rows.

C. In the 5th$^{\rm th}$ column, indicate with a "yes", "no", or "maybe", if this term would cause $B(Z,A)$ to go up with the addition of one more proton. If the answer is "maybe", explain.

D. In the 6th$^{\rm th}$ column, indicate with a "yes", "no", or "maybe", if this term would cause $B(Z,A)$ to go up with the addition of one more neutron. If the answer is "maybe", explain.

ii. Justify the exact dependence on Z and A for the $a_{\rm V}$, $a_{\rm S}$ and $a_{\rm C}$ terms. Qualitatively explain the dependence on Z and A for the $a_{\rm sym}$ term.

a_i	[MeV]	Theoretical origin	Description	$+p$?	$+n$?
a_{V}...	15.5	The theoretical model that suggests the term starting with a_{V} is the _____ model of the nucleus.	The term involving a_{V} comes from the idea that...		
a_{S}...	16.8				
a_{C}...	0.72				
a_{sym}...	23				
a_{p}...	34				

iii. With A fixed, $B(Z, A)$ is a quadratic expression in Z. Find its extremum, and discuss the relationship between the quadratic expression and β-decay.

6. **The Modeling of Protons in the Nucleus**

One approach to accounting for the effect of the electric charge of the protons, on the structure of the nucleus, is to combine the classical ideas of electrostatics with the liquid drop model of the nucleus. The approach starts with a calculation of the electrostatic potential of the nucleus, $V_{\mathrm{es}}(\vec{x})$, due to a distribution of protons, $\rho_p(\vec{x}')$.

$$V_{\mathrm{es}}(\vec{x}) = \frac{Ze}{4\pi\epsilon_0} \int \mathrm{d}\vec{x}' \; \frac{\rho_p(\vec{x}')}{|\vec{x} - \vec{x}'|} \quad ; \quad \int \mathrm{d}\,\vec{x}' \rho_p(\vec{x}') \equiv 1 \; .$$

$\vec{x}$ is a vector that can be positioned anywhere. $\vec{x}'$, the vector over which we integrate, is positioned only within the confines of the nucleus. The origin of the coordinate system for $\vec{x}'$, is located at the *center of charge*. In the following, $\hat{n}$ is a unit vector pointing in the direction of $\vec{x}$.

(a) Show, for $|\vec{x}| >> |\vec{x}'|$, that;

$$\begin{aligned} V_{\rm es}(\vec{x}) &= \frac{Ze}{4\pi\epsilon_0|\vec{x}|}\left[1+\frac{\hat{n}\cdot\vec{P}}{|\vec{x}|}+\frac{Q}{2|\vec{x}|^2}+\mathcal{O}\left(\frac{1}{|\vec{x}'|^3}\right)\right] \quad \text{where} \\ \vec{P} &\equiv \hat{n}\cdot\int \mathrm{d}\vec{x}'\ \vec{x}'\rho_p(\vec{x}') \\ Q &\equiv \int \mathrm{d}\vec{x}'\ \left[3(\hat{n}\cdot\vec{x}')^2-|\vec{x}'|^2\right]\rho_p(\vec{x}')\ . \end{aligned}$$

(b) Whether or not you derived the above expression, interpret the meaning of the 3 terms, $(1, \vec{P}, Q)$ in

$$\left[1+\frac{\hat{n}\cdot\vec{P}}{|\vec{x}|}+\frac{Q}{2|\vec{x}|^2}\right]\ .$$

(c) Why does $\vec{P}=0$ for the nucleus.

(d) If $\hat{n}$ is aligned with $\hat{z}$, show that:

$$Q=\int \mathrm{d}\vec{x}\ \rho_p(\vec{x})(3z^2-r^2)\ .$$

(e) Show that $Q=0$ if $\rho_p(\vec{x})$ is spherically symmetric, but otherwise arbitrary. That is, show:

$$Q=\int \mathrm{d}\vec{x}\ \rho_p(r)(3z^2-r^2)=0\ .$$

(f) The connection between the nuclear wavefunction, $\psi_N(\vec{x})$ and the proton density, in the liquid drop model of the nucleus is given by:

$$|\psi_N(\vec{x})|^2=\rho_p(\vec{x})\ .$$

Justify this assumption.

(g) If the nucleus is a uniformly charged ellipsoid of the form:

$$\frac{x^2+y^2}{a^2}+\frac{z^2}{b^2}=1\ ,$$

Show that

$$Q=\frac{2}{5}(b^2-a^2)\ .$$

Assignment-type problems

1. If all the matter on earth collapsed to a sphere with the same density as the interior of a nucleus, what would the radius of the earth be? Cite all sources of data you used.

2. **The effect of the nuclear edge on** $F(\vec{q})$

   (a) Find $F(\vec{q})$ for a uniformly charged sphere. For a uniform sphere, $\rho_{\rm p}(r) = \rho_0\Theta(R-r)$, where R is the radius of the nucleus.[6]

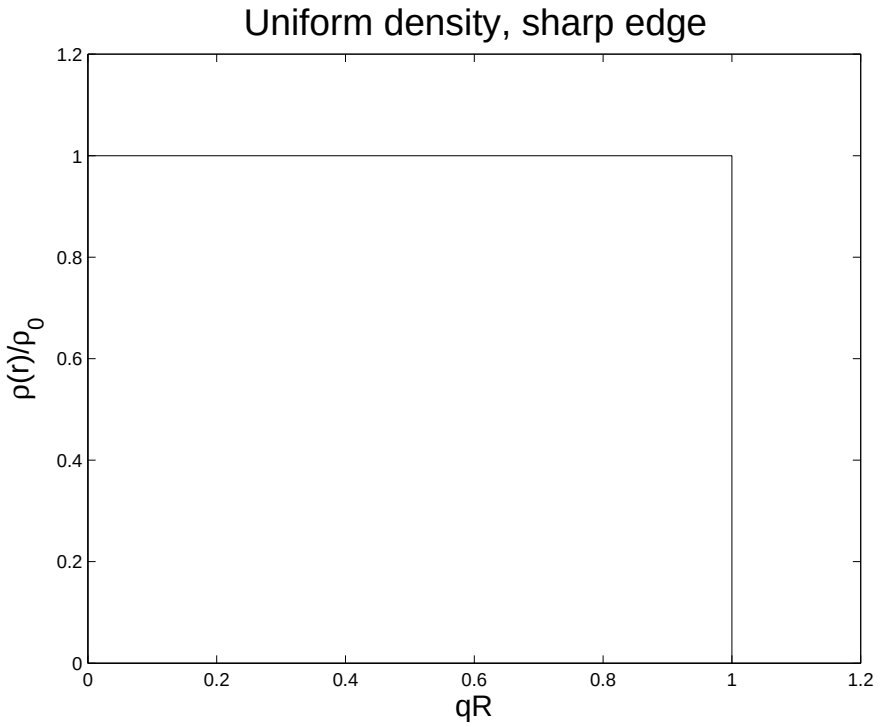

   Plot[7] $\log(|F(\vec{q})|^2)$ *vs.* qR.

[6]Mathematical note:

$$\begin{aligned}\Theta(z) &= 1\ ;\ z>0\\ &= 0\ ;\ z<0\end{aligned}$$

[7]Technical note: $|F(\vec{q})|)^2$ can be zero, so its logarithm would be $-\infty$, causing the plots to look strange. We need the logarithm to see the full structure of $|F(\vec{q})|^2$. So, in order to make the plots look reasonable, you will probably have to adjust the scale on the y-axis in an appropriate fashion.

(b) Do the same as in (a) but include a linear edge in the model of the nucleus. That is,

$$\begin{aligned}\rho_{\rm p}(r) &= \rho_0\Theta([R-t/2]-r) \\ &= \rho_0[1/2-(r-R)/t]\ ;\ R-t/2\le r\le R+t/2\ ,\end{aligned}$$

where t is the nuclear "skin depth", and, mathematically, can take any value between 0 and $2R$. Note that $\rho_{\rm p}(R-t/2)=\rho_0$ and $\rho_{\rm p}(R+t/2)=0$. Note also, that when $t=0$, the nuclear shape is the same as in part (a).

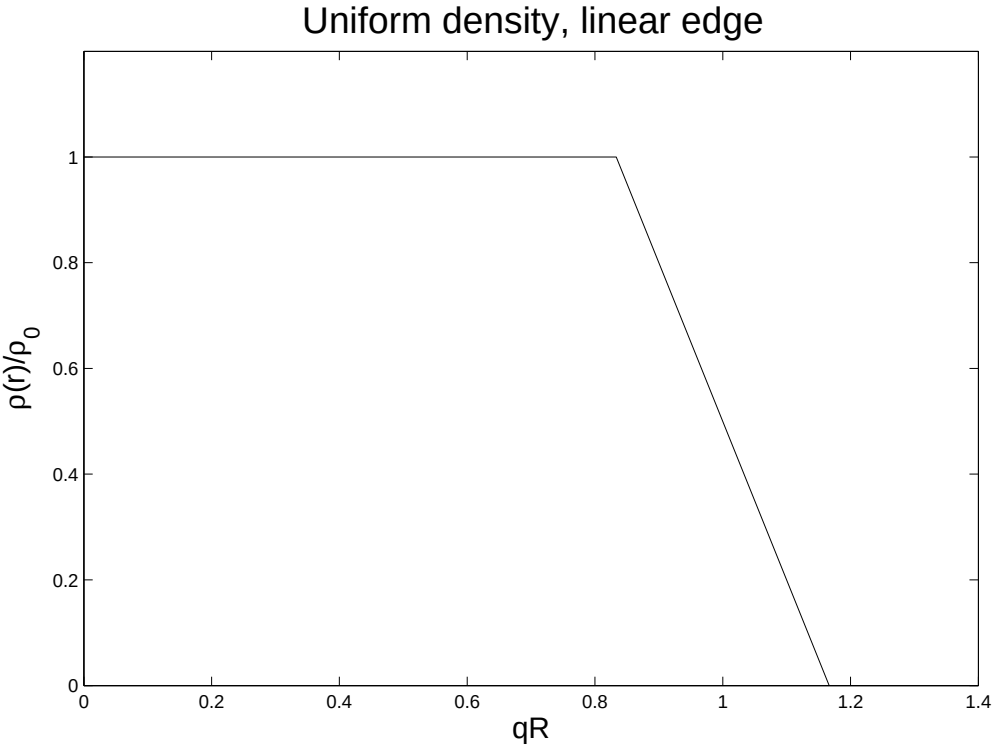

Plot $\log(|F(\vec{q})|^2)$ *vs.* qR as in part (a) showing several values of t over the entire domain of t, $0\le t\le 2R$. Compare with the result of part (a).

(c) Compare and discuss your results. Does the elimination of the sharp edge eliminate the sharp minima in $\log(|F(\vec{q})|^2)$? What else could be contributing to the reduction of the sharpness of these minima?

(d) Do the same as in (b) and (c) but include a cubic edge in the model of the nucleus. That is,

$$\begin{aligned}\rho_{\rm p}(r) &= \rho_0\Theta([R-t/2]-r) \\ &= \rho_0(A+Br+Cr^2+Dr^3)\ ;\ R-t/2\le r\le R+t/2\ .\end{aligned}$$

Arrange the four constants A, B, C, D such that:

$$\begin{aligned}\rho_{\rm p}(R-t/2) &= \rho_0 \\ \rho'_{\rm p}(R-t/2) &= 0 \\ \rho_{\rm p}(R+t/2) &= 0 \\ \rho'_{\rm p}(R+t/2) &= 0\end{aligned}$$

.

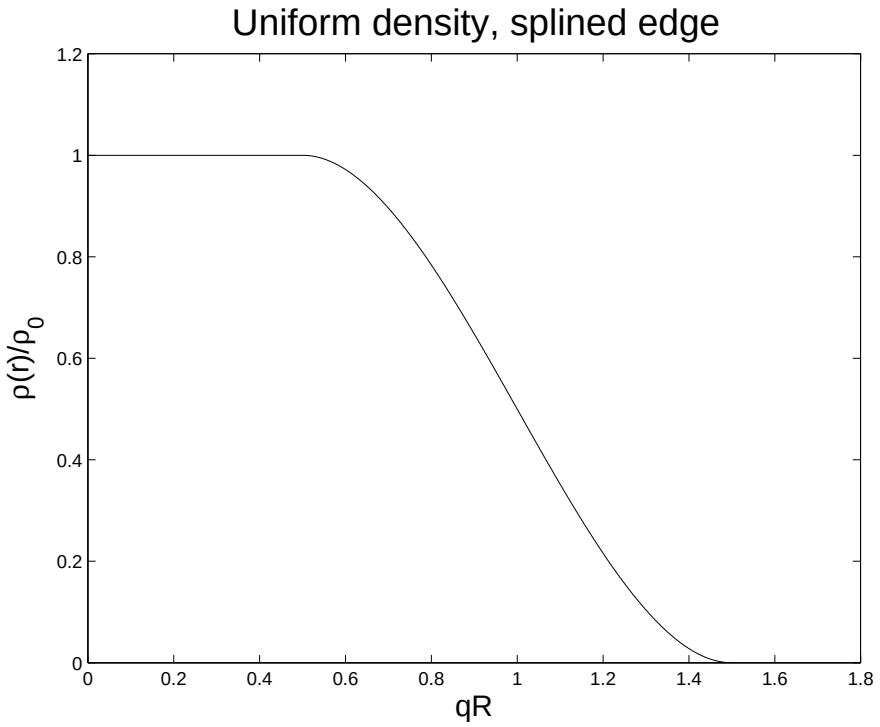

Plot $\log(|F(\vec{q})|^2)$ *vs.* qR as in part (b) showing several values of t over the entire domain of t, $0 \le t \le 2R$. Compare with the result of parts (a) and (b).

3. **Perturbation of atomic energy levels**

   (a) Read carefully and understand the text on pages 49–55 in Krane on this topic. Krane makes the assertion that ΔE_{2p} can be ignored for atomic electron transitions. Verify this assertion by repeating the calculation for ΔE_{2p} and obtain a relationship for $\Delta E_{2p}/\Delta E_{1s}$ for atomic electrons and muons. Evaluate numerically for ^{12}C and ^{208}Pb.

   (b) The results in (a), for muons, is suspect, because the muon's wavefunctions have significant overlap with the physical location of the nucleus, and the shape of the edge of the nucleus may play a significant role. Repeat the analysis of part (a), but introduce a skin depth using one of the models in Question 2) or some other model of your choosing. What do you conclude?

4. Show:

$$\frac{6}{5} = \left(\frac{3}{4\pi}\right)^2 \int_{|\vec{u}|\leq 1} \mathrm{d}\vec{u} \int_{|\vec{u}'|\leq 1} \mathrm{d}\vec{u}' \left(\frac{1}{|\vec{u}-\vec{u}'|}\right) \ ,$$

   which is used to find the energy of assembly of the protons in a nucleus.

   Then, consider:

$$I(n) = \left(\frac{3}{4\pi}\right)^2 \int_{|\vec{u}|\leq 1} \mathrm{d}\vec{u} \int_{|\vec{u}'|\leq 1} \mathrm{d}\vec{u}' \left(\frac{1}{|\vec{u}-\vec{u}'|^n}\right) \ ,$$

   where $n \geq 0$, and is an integer. From this, make conclusions as to the fundamental forces in nature, and their forms as applied to classical and quantum physics.

5. We have seen that the calculation of the scattering rate due to electron scattering from a bare nucleus approaches the Rutherford scattering law in the limit of small q. Discuss the onset of the departure of this change, via the nuclear form factor, as q gets larger. Adopt a more realistic model for the distribution of charge in the nucleus and see if you can match the data for the experiments shown in Figures 3.1 and 3.2 in Krane.

6. For low q, the electrons impinging on a nucleus have the positive charge of the nucleus screened by the orbital electrons. Develop an approximate model for the screening of the nuclei by the orbital electrons and demonstrate the effect on the Rutherford scattering law. Show that the forward scattering amplitude is finite and calculate its numerical value using sensible numbers for the parameters of your model.

7. The numerical data of the average shift given in Figure 3.8 of Krane can be matched very closely by introducing a realistic positive charge distribution in the nucleus. Introduce such a model and demonstrate that you obtain the correct numerical answer.

8. Calculate the muonic K X-ray shift for Fe using one of the following nuclear shapes:

$$\begin{aligned}\frac{\rho(r)}{\rho_0} &= 1 \text{ for } r \leq R - t_{\rm min}/2 \\ &= \frac{R + t_{\rm min}/2 - r)}{t_{\rm min}} \text{ for } R - t_{\rm min}/2 \leq r \leq R + t_{\rm min}/2 \\ &= 0 \text{ for } r \geq R + t_{\rm min}/2\end{aligned}$$

or, the Fermi distribution,

$$\frac{\rho(r)}{\rho_0} = \frac{1}{1 + \exp[(r - R)/a]} \ .$$

Compare with data. You may use $R = R_0 A^{1/3}$ with any value between 1.20 and 1.25 fm to got the K X-rays in the right place. Use $t_{\rm min} = 2.3$ fm, and make sure to interpret a in the right way with respect to $t_{\rm min}$, if you use the Fermi distribution.

Chapter 11

The Force Between Nucleons

Note to students and other readers: This Chapter is intended to supplement Chapter 4 of Krane's excellent book, "Introductory Nuclear Physics". Kindly read the relevant sections in Krane's book first. This reading is supplementary to that, and the subsection ordering will mirror that of Krane's, at least until further notice.

Imagine trying to understand chemistry before knowing Quantum Mechanics...

The understanding of the physical world was accomplished through many observations, measurements, and then trying to abstract them in a *phenomenological theory*, a "theory" that develops empirical relationships that "fit" the data, but do not explain why nature should behave this way. For example, Chemistry had organized the periodic table of the elements long before Quantum Mechanics was discovered.

Then, the Schrödinger equationwas discovered. Now we had a well-defined theory on which to base the basic understanding of atomic structure. With a solid fundamental theory, we now have a well-defined systematic approach:

- Solve the Schrödinger equationfor the H atom, treating p, e^- as fundamental point-charge particles, a good approximation since the electron wavefunctions overlap minimally with the very small, but finite-sized proton.
- Build up more complex atoms using the rules of Quantum Mechanics. Everything is treated theoretically, as a perturbation, since the Coulomb force is relatively weak. This is expressed by the smallness of the fine-structure constant:

$$\alpha = \frac{e^2}{4\pi\epsilon_0\hbar c} = 7.297\,352\,5376(50) \times 10^{-3} = \frac{1}{137.035\,999\,679(94)} \tag{11.1}$$

- The interaction between atoms is studied theoretically by *Molecular Theory*. Molecular Theory treats the force between atoms as a *derivative force*, a remnant of the more basic

Coulomb force that binds the atom. *Covalent bonds*, *ionic bonds*, *hydrogen bonds*, *Van der Wall forces* are quasi-theoretic, quasi-phenomenological derivatives of the desire of Quantum Mechanics to close shells by sharing electrons (*covalent bonding*, stealing electrons (*ionic bonds*, simple electrostatic attraction (*hydrogen bonds*), or dipole-dipole and higher multipole arrangements (*generalized Van der Wall forces*).

It is tempting to attempt the same procedure in nuclear physics. In this case, the simplest bound system is the deuteron. In atomic physics, the H-atom was the ideal theoretical laboratory for our studies. In nuclear physics, the simplest bound system is the deuteron, a neutron and a proton bound by the strong force. However, some physical reality imposes severe restrictions on the development of an analysis as elegant as in atomic or molecular physics:

- n and p are tightly bound, practically "in contact" with each other. In other words, their wavefunctions overlap strongly.
- n and p are not point-like particles. They have internal structure. Because their wavefunctions overlap so strongly, the internal structure of one, has an important effect on the other.
- The forces binding the nucleons is *strong*. The *strong-coupling constants* are of the order unity, whereas the fine-structure constant (for Coulomb forces) is small, about 1/137. Hence, perturbation methods, so successful for atomic and molecular theory, are almost completely ineffective.

The internal structure of a nucleon

The proton is comprised of 2 "up" (u) quarks, and one "down (d) quark, in shorthand, $p(uud)$. The neutron is $n(ddu)$. Here is a table of the known properties of n, p, u, d.

	mass [MeV]/c^2	charge (e)	total angular momentum ($\hbar$)
p	938.272013(23)	+1	1/2
n	939.565560(81)	0	1/2
u	1.5–3.3	+2/3	1/2
d	3.5–6.0	−1/3	1/2

The above table explains the observed charge of the n and p. One can also argue that the spins of the similar quarks in each nucleon "anti-align" (Invoke the Pauli Exclusion Principle.) to result in an overall spin-1/2 for the n and p. However, the mass discrepancy is phenomenal! It is explained as follows:

Quarks are so tightly bound to one another; so tightly bound, in fact, that if one injects enough energy to liberate a quark, the energy is used up in creating quark-antiquark pairs that bind, and prevent the observation of a "free quark". The "exchange particle" that binds the quarks is called the *gluon*. (The exchange particle for the Coulomb force is the photon.) Most of the mass of the nucleons come from the "cloud" of gluons that are present in the frenetic environment that is the inside of a nucleon. Recall that a nucleus was likened to a "mosh pit", in the previous chapter. The mayhem inside a nucleon defies description or analogy.

Since quarks are very tightly bound, covalent or ionic bonds between nucleons do not exist. All the forces are derivative forces, analogs to dipole-dipole (and higher multipolarity) interactions.

The "derivative" nucleon-nucleon force

This "derivative" nucleon-nucleon force is also called the *Meson Exchange Model*. The exchange particle, in this case, is thought of as being two mesons. A "vector" meson, mass $m_{\rm V}$, so named because it has spin-1, provides the short-ranged repulsive force that keep nucleons from collapsing together. A "scalar" spin-0 meson, mass $m_{\rm S}$, provides the slightly longer ranged attractive force. Both mesons are 100's of MeV, but $m_{\rm S} < m_{\rm V}$, with the result that a potential well is formed. This is apparent in the form of the potential given in (11.2), as well as in the sketch in Fig. 11.1.

$$V_{nn} = \frac{\hbar c}{r}\left\{\alpha_{\rm V}\exp[-(m_{\rm V}c/\hbar)r] - \alpha_{\rm S}\exp[-(m_{\rm S}c/\hbar)r]\right\} \tag{11.2}$$

The vector and scalar coupling constants, $\alpha_{\rm V}$ and $\alpha_{\rm S}$ are order unity. Note the similarity of this potential with the attractive or repulsive Coulomb potential, that may be written:

$$V_{\rm C} = \pm\frac{\hbar c\alpha}{r}\ ,$$

where α is the fine-structure constant expressed in (11.1). We immediately draw the conclusion that it is the mass of the exchange particle which determines the range of the force. The photon is massless, hence the Coulomb force is long.

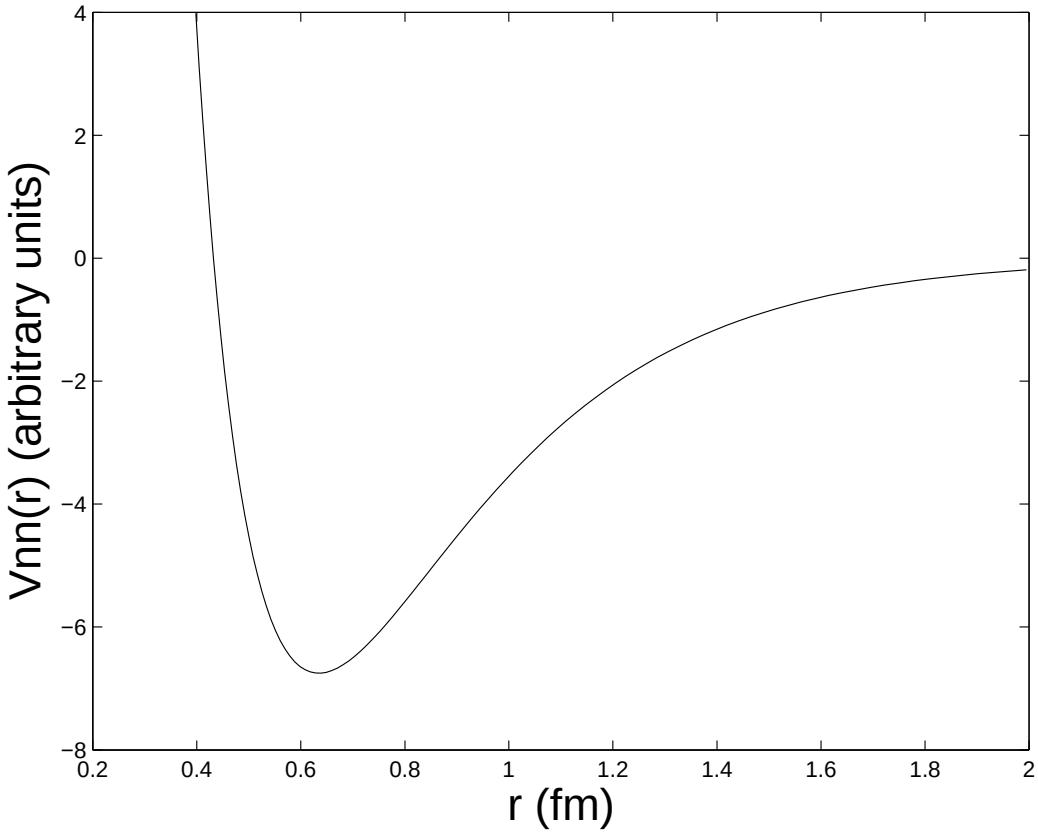

Figure 11.1: A sketch of the central part $V_{nn}(r)$ of the nucleon-nucleon potential.

A few noteworthy mentions for the strong force:

- The particles that feel the strong force are called "hadrons". Hadrons are bound states of quarks. The hadrons divide into 2 different types:
  - "Baryons" are 3-quark combinations, *e.g.* $p(uud)$, $n(ddu)$ ...
  - "Mesons" are combinations of two quarks, a quark-antiquark pair. *e.g.* the π-mesons, $\pi^+(u\overline{d})$, $\pi^-(d\overline{u})$, and the $\pi^0([d\overline{d}+u\overline{u}]/\sqrt{2})$ mesons, being the most "common". Note that the μ particle has been called the μ-meson. However, this usage has been deprecated since the discovery of quarks. The μ is a *lepton*, in the same class as electrons and neutrinos.
- The nuclear force is "almost" independent of nucleon "flavor", that is, V_{nn}, V_{np}, V_{pp} are almost the same. The p-p system also has a separate Coulomb repulsive force.
- The nuclear force depends strongly on the alignment of nucleon spins.
- As a consequence of the above, the nucleon-nucleon force is non-central, that is, $V(\vec{x}) \neq V_{nn}(r)$. The impact of this is that the orbital angular momentum is not a conserved quantity, although the total angular momentum, $\vec{I} = \vec{L} + \vec{S}$ **is** conserved.
- Including the non-central and Coulomb components, the complete nucleon-nucleon potential may be written:

$$V_N(\vec{x}) = V_{nn}(r) + V_{\rm C}(r) + V_{\rm so}(\vec{x}) + V_{\rm ss}(\vec{x}) \ , \tag{11.3}$$

  where $V_{nn}(r)$ is the central part of the strong force, $V_{\rm C}(r)$ is the Coulomb repulsive potential that is switched on if both nucleons are protons, $V_{\rm so}(\vec{x})$ is the "spin-orbit" part that involves the coupling of $\vec{l}$'s and $\vec{s}$'s, and $V_{\rm ss}(\vec{x})$ is the "spin-spin" part that involves the coupling of intrinsic spins.

11.1 The Deuteron

The deuteron, ^{2}H, also known as D, is made up of one neutron and one proton. It is relatively weakly bound (2.22452(20) MeV), but stable, and has a relative 0.015% natural isotopic abundance. Properties of the isotopes of hydrogen are given below:

^AX	abundance or $t_{1/2}$	I^π
^{1}H	0.99985%	$\frac{1}{2}^+$
^{2}H, or D	0.00015%	1^+
^{3}H, or T	12.3 y (β^--decay)	$\frac{1}{2}^+$

The deuteron is the only bound dinucleon. It can be easily understood that the diproton would be rendered unstable by Coulomb repulsion. Dineutrons do not exist in nature, not even as a short-lived unstable state. This is most likely due to the Pauli Exclusion Principle applied at the quark level — 3 up quarks and 3 down quarks (all the quarks in a deuteron) are more likely to bind than 4 downs and 2 ups (the quark content of a dineutron). The spin-1 nature of the deuteron is explained by the spin-spin interaction of the neutron and proton. Their magnetic moments have opposite signs to one another, hence the alignment of spins tends to antialign the magnetic dipoles, a more energetically stable configuration.

Cultural aside:
Deuterium is a form of water. It is extracted from natural water using electrolysis or centrifugal techniques, producing DOH or D_2O, also called "heavy water". Although heavy water is very similar to H_2O, there are small differences, and these can impact biological systems. It is estimated that drinking nothing but heavy water for 10–14 days is lethal. Reactor-grade heavy water costs about $600–$700 per kilogram!

The deuteron is the most ideal "laboratory" to study the nucleon-nucleon force. There are no bound states of the deuteron.

Binding energy of the deuteron

Using the mass-binding energy relation, (10.35), that is

$$B_N(Z,A) = [Zm(^1H) + Nm_n - m(^AX)]c^2 \ ,$$

we can evaluate the binding energy of the deuteron,

$$B_N(1,2) = [m(^1H) + m_n - m(D)]c^2 \ .$$

Krane gives 2.2463(4) MeV. Modern data gives the binding energy as 0.002388169(9) u, or 2.224565(9) MeV. The binding energy inferred from H(n,γ)D scattering experiments is 2.224569(2) MeV, and from D(γ,n)H experiments, 2.224(2) MeV. (Neutron spectroscopy is much less accurate than γ-spectroscopy.)

Why does the deuteron have only one bound state?

In NERS311 we discussed the s-state solutions to the 3D-Schrödinger equation. We discovered that, unlike the 1D-square well, which always has a bound state no matter the depth

of the well, the 3D requires the potential depth to to satisfy the following:

$$|V_0| > \frac{\pi^2\hbar^2}{8MR^2} \ .$$

In this case, M is the reduced mass, and R is the radius of the deuteron.

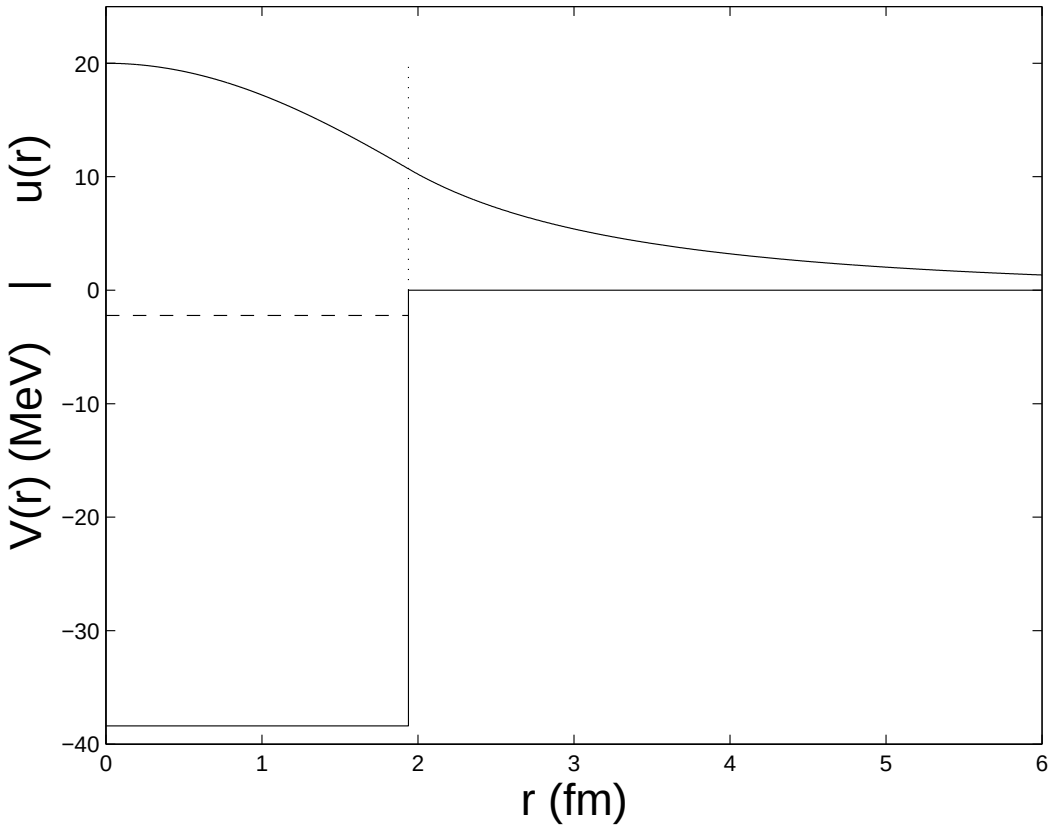

Figure 11.2: square-well potential model for the deuteron. The single bound level is shown at $E = -2.224$ MeV. The loose binding of the deuteron is indicated by the long exponential tail outside of the radius of the deuteron.

The spin and parity of the deuteron

The observed I^π of the deuteron is 1^+. We recall that the total spin is given by $\vec{I} = \vec{s}_n + \vec{s}_p + \vec{l}$. Therefore, with $I = 1$, applying the quantum mechanical rules for adding spins, we can only have 4 possible ways obtaining $I = 1$, namely:

S	l	I	π	?
$\uparrow\uparrow$	0	1	+1	yes
$\uparrow\uparrow$	1	1	-1	no
$\downarrow\uparrow$	1	1	-1	no
$\uparrow\uparrow$	2	1	+1	yes

We can rule out the $l = 1$ states due to the parity relation, $\pi = (-1)^l$. Without further knowledge, we can not rule out the $l = 2$ state. We can use experiments to determine which l-state contributes.

This can be done in two ways:

The magnetic dipole of the deuteron

If $l = 0$, only S can contribute to the magnetic moment. Following the discussion in Chapter 10, the magnetic moment would be given by:

$$\mu_{\rm D} = \frac{\mu_N}{2}(g_{sn} + g_{sp}) \ . \tag{11.4}$$

Using the data $g_{sn} = -3.82608545(46)$ and $g_{sp} = 5.585694713(90)$, we evaluate $(g_{sn} + g_{sp}) = 1.75960926(10)$, while experiment gives 1.714876(2), a difference of 0.044733(2). The difference is small but significant, indicating that the deuteron can not be a pure s state!

Since part of the nucleon-nucleon potential is non-central, bound states that do not have a unique $\langle\vec{l}\rangle$ are permissible. Hence if we consider that the deuteron is a mixture of s and d states, we can write:

$$\psi_{\rm D} = a_s\psi_s + a_d\psi_d \ , \tag{11.5}$$

where $|a_s|^2 + |a_d|^2 = 1$. Taking expectation values:

$$\mu = |a_s|^2\mu(l = 0) + |a_d|^2\mu(l = 2) \ , \tag{11.6}$$

with $\mu(l = 0)$ as given in (11.4) and $\mu(l = 2) = (3 - g_{sn} - g_{sp})\mu_N/4$ leads us to conclude[1] that the deuteron is 96% s and 4% d. It is a small correction but it is an interesting one, and a clear example of the non-conservation of orbital angular momentum when non-central forces and spins are involved.

[1]This calculation of $\mu(l = 2)$ would take several hours to explain. For more information see:
`www.physics.thetangentbundle.net/wiki/Quantum_mechanics/magnetic_moment_of_the_deuteron`

The quadrupole moment of the deuteron

Another demonstration that isolates the d component of the deuteron wave function, is the measurement of the quadrupole moment. An s state is spherical, and hence its quadrupole moment (Q) vanishes. The Q of the deuteron is measured to be $Q = 0.00288(2)$ b. A "b" is a "barn". A barn is defined as 10^{28} m^2, about the cross sectional area of a typical heavy nucleus. This unit of measure is a favorite among nuclear physicists.

Using (11.5) in the definition of the quadrupole moment given by (10.52), that is,

$$Q = \int \mathrm{d}\vec{x}\ \psi_N^*(\vec{x})(3z^2 - r^2)\psi_N(\vec{x})\ ,$$

results in

$$Q = \frac{\sqrt{2}}{10} a_s^* a_d \langle R_s|r^2|R_d\rangle - \frac{1}{20}|a_d|^2\langle R_d|r^2|R_d\rangle\ , \tag{11.7}$$

where R_s and R_d are the radial components of the deuteron's s and d wavefunctions. For consistency, a_s appears in (11.7) as its complex conjugate. However, the a_s and a_d constants may be chose to be real for the application, and thus we can replace $a_s^* = a_s$ and $|a_d|^2 = a_d^2$.The deuteron's radial wavefunctions are unknown and unmeasured. However, reasonable theoretical approximations to these can be formulated[2], and yield results consistent with the 96%/4% s/d mixture concluded from the deuteron's magnetic moment measurements.

11.2 Nucleon-nucleon scattering

This material will not be covered in NERS312. The section heading is included here as a "stub" to keep the subsection numbering in Krane and these notes aligned.

11.3 Proton-proton and neutron-neutron interactions

Ditto the italicized stuff above.

The NERS Department played an important role in the development of neutron spectroscopy and scattering. Please visit:

`http://www.ur.umich.edu/0708/Sep24_07/obits.shtml`

[2]Extra credit to any student who comes up with a decent approximation to the deuteron's wavefunctions, and calculates consistent results!

That link is an obituary of Professor John King, who was a pioneer in this area. His contributions to this research are outlined there.

11.4 Properties of the nuclear force

Described in the beginning of this chapter

11.5 The exchange force model

Also described elsewhere throughout this chapter

Closed book "pop quiz" problems

1.

2.

3.

4.

Chapter 12

Nuclear Models

Note to students and other readers: This Chapter is intended to supplement Chapter 5 of Krane's excellent book, "Introductory Nuclear Physics". Kindly read the relevant sections in Krane's book first. This reading is supplementary to that, and the subsection ordering will mirror that of Krane's, at least until further notice.

Many of the ideas and methods we learned in studying atoms and their quantum behavior, carry over to nuclear physics. However, in some important ways, they are quite different:

1. We don't really know what the nucleon-nucleon potential is, but we do know that it has a central, $V(r)$, and non-central part, $V(\vec{x})$. That is the first complication.

2. The force on one nucleon not only depends on the position of the other nucleons, but also on the distances between the other nucleons! These are called *many-body* forces. That is the second complication.

Let us illustrate this in Figure 12.1, where we show the internal forces governing a ^{3}He nucleus.

Figure 12.1: Theoretical sketch of a ^{3}He nucleus. *This sketch has not been created yet, so feel free to draw it in!*

The potential on the proton at $\vec{x}_1$ is given by:

$$V_{nn}(\vec{x}_2 - \vec{x}_1) + V_{nn}(\vec{x}_3 - \vec{x}_1) + V_{\rm C}(|\vec{x}_2 - \vec{x}_1|) + V_3(\vec{x}_1 - \vec{x}_2, \vec{x}_1 - \vec{x}_3, \vec{x}_2 - \vec{x}_3) \ , \qquad (12.1)$$

where:

Potential term	Explanation
$V_{nn}(\vec{x}_2 - \vec{x}_1)$	2-body strong nuclear force between p at $\vec{x}_1$ and p at $\vec{x}_2$
$V_{nn}(\vec{x}_3 - \vec{x}_1)$	2-body strong nuclear force between p at $\vec{x}_1$ and n at $\vec{x}_3$
$V_{\rm C}(\|\vec{x}_2 - \vec{x}_1\|)$	2-body Coulomb force between p at $\vec{x}_1$ and p at $\vec{x}_2$
$V_3(\cdots)$	3-body force strong nuclear force (more explanation below)

The 2-body forces above follow from our discussion of the strong and Coulomb 2-body forces. However, the 3-body term is a fundamentally different thing. You can think of V_3 as a "polarization" term—the presence of several influences, how 2 acts on 1 in the presence of 3, how 3 acts on 1 in the presence of 2, and how this is also affected by the distance between 2 and 3. It may seem complicated, but it is familiar. People act this way! Person 1 may interact with person 2 in a different way if person 3 is present! These many-body forces are hard to get a grip on, in nuclear physics and in human social interaction. Nuclear theory is basically a phenomenological one based on measurement, and 3-body forces or higher order forces are hard to measure.

Polarization effects are common in atomic physics as well.

Figure 12.2, shows how an electron passing by, in the vicinity of two neutral atoms, polarizes the proximal atom, as well as more distance atoms.

Returning to nuclear physics, despite the complication of many-body forces, we shall persist with the development of simple models for nuclei. These models organize the way we think about nuclei, based upon some intuitive guesses. Should one of these guesses have predictive power, that is, it predicts some behavior we can measure, we have learned something—not the entire picture, but at least some aspect of it. With no fundamental theory, this form of guesswork, phenomenology, is the best we can do.

Figure 12.2: A depiction of polarization for an electron in condensed matter. *This sketch has not been created yet, so feel free to draw it in!*

12.1 The Shell Model

Atomic systems show a very pronounced shell structure. See Figures 12.3 and 12.4.

Figure 12.3: For now, substitute the top figure from Figure 5.1 in Krane's book, p. 118. This figure shows shell-induced regularities of the atomic radii of the elements.

Figure 12.4: For now, substitute the bottom figure from Figure 5.1 in Krane's book, p. 118. This figure shows shell-induced regularities of the ionization energies of the elements.

Nuclei, as well, show a "shell-like" structure, as seen in Figure 12.5.

Figure 12.5: For now, substitute Figure 5.2 in Krane's book, p. 119. This figure shows shell-induced regularities of the $2p$ separation energies for sequences of isotones same N, and $2n$ separation energies for sequences of isotopes.

The peaks of the separation energies (hardest to separate) occur when the Z or N correspond to major closed shells. The "magic" numbers, the closed major shells, occur at Z or N: 2, 8, 20, 28, 50, 82, & 126.

The stable magic nuclei

Isotopes	Explanation	Natural abundance (%)
$^{3}_{2}\mathrm{He}_{1}$	magic Z	1.38×10^{-4}
$^{4}_{2}\mathrm{He}_{2}$	doubly magic	99.99986
$^{15}_{7}\mathrm{N}_{8}$	magic N	0.366
$^{16}_{8}\mathrm{O}_{8}$	doubly magic	99.76
$^{40}_{20}\mathrm{Ca}_{20}$	doubly magic	96.94
$^{42-48}_{20}\mathrm{Ca}_{20}$	magic Z	
$^{50}_{22}\mathrm{Ti}_{28}$	magic N	5.2
$^{52}_{24}\mathrm{Cr}_{28}$	magic N	83.79
$^{54}_{26}\mathrm{Fe}_{28}$	magic N	5.8
^{86}Kr, ^{87}Rb, ^{88}Sr, ^{89}Y, ^{90}Zr, ^{92}Mo	magic $N = 50$	
⋮	⋮	⋮
$^{208}_{82}\mathrm{Pb}_{126}$	doubly magic	52.3
$^{209}_{83}\mathrm{Bi}_{126}$	magic N	100, $t_{1/2} = 19 \pm 2 \times 10^{18}$ y

The Shell-Model idea

A nucleus is composed of a "core" that produces a potential that determines the properties of the "valence" nucleons. These properties determine the behavior of the nucleus much in the same way that the valance electrons in an atom determine its chemical properties.

The excitation levels of nuclei appears to be chaotic and inscrutable. However, there is order to the mess! Figure 12.6 shows the energy levels predicted by the shell model using ever-increasing sophistication in the model of the "core" potential. The harmonic oscillator potential as well as the infinite well potential predict the first few magic numbers. However, one must also include details of the profile of the nuclear skin, as well as introduce a spin-orbit coupling term, before the shells fall into place. In the next section we discuss the various components of the modern nuclear potential.

Details of the modern nuclear potential

A valence nucleon (p or n) feels the following central strong force from the core:

$$V_n(r) = \frac{-V_0}{1 + \exp\left(\frac{r - R_N}{t}\right)} \tag{12.2}$$

It is no coincidence that the form of this potential closely resembles the shape of the nucleus as determined by electron scattering experiments. The presence of the nucleons in the core, provides the force, and thus, the force is derived directly from the shape of the core.

Figure 12.6: The shell model energy levels. See Figures 5.4 (p. 121) and 5.6 p. 123 in Krane.

In addition to the "bulk" attraction in (12.2), there is a symmetry term when there is an imbalance of neutrons and protons. This symmetry term is given by:

$$V_{\rm S} = \frac{a_{\rm sym}}{A(A+1)}\left[\pm 2(N-Z)A + A - (N-Z)^2\right] \ , \tag{12.3}$$

with the plus sign is for a valence neutron and the negative sign for a valence proton. The form of this potential can be derived from the parametric fit to the total binding energy of a nucleus given by (10.38).

The parameters of the potential described above, are conventionally given as:

Parameter	Value	Interpretation
V_0	57 MeV	Potential depth of the core
R_N	$1.25A^{1/3}$	Nuclear radius
t	0.65 fm	Related to the nuclear skin depth
$a_{\rm sym}$	16.8 MeV	Symmetry energy
a_{so}	1 fm	Spin-orbit coupling (discussed below)

If the valence nucleon is a proton, an addition central Coulomb repulsion must be applied:

$$V_{\rm C}(r) = \frac{Ze^2}{4\pi\epsilon_0}\int {\rm d}\vec{x}'\rho_p(r')\frac{1}{|\vec{x}-\vec{x}'|} = \frac{Ze^2}{4\pi\epsilon_0}\frac{2\pi}{r}\int {\rm d}r' r'\rho_p(r')\left[(r+r') - |r-r'|\right] \ . \tag{12.4}$$

Recall that the proton density is normalized to unity by

$$1 \equiv \int \mathrm{d}\vec{x}' \rho_p(r') = 4\pi \int \mathrm{d}r' r'^2 \rho_p(r') \ .$$

Simple approximations to (12.4) treat the charge distribution as a uniform sphere with radius R_N. That is:

$$\rho_p(r) \approx \frac{3}{4\pi R_N^3} \Theta(R - r) \ .$$

However, a more sophisticated approach would be to use the nuclear shape suggested by (12.2), that is:

$$\rho_p(r) = \frac{\rho_0}{1 + \exp\left(\frac{r - R_N}{t}\right)} \ ,$$

determining ρ_0 from the normalization condition above.

The spin-orbit potential

The spin-orbit potential has the form:

$$V_{so}(\vec{x}) = -\frac{a_{so}^2}{r} \frac{\mathrm{d}V_n(r)}{\mathrm{d}r} \langle \vec{l} \cdot \vec{s} \rangle \ . \tag{12.5}$$

The radial derivative in the above equation is only meant to be applied where the nuclear density is changing rapidly.

Evaluating the spin-orbit term

Recall, $\vec{j} = \vec{l} + \vec{s}$. Hence, $\vec{j}^2 = \vec{l}^2 + 2\vec{l} \cdot \vec{s} + \vec{s}^2$. Thus, $\vec{l} \cdot \vec{s} = (1/2)(\vec{j}^2 - \vec{l}^2 - \vec{s}^2)$, and $\langle \vec{l} \cdot \vec{s} \rangle = (1/2)[j(j+1) - l(l+1) - s(s+1)]$.

The valence nucleon has spin-1/2. To determine the splitting of a given l into $j = l \pm \frac{1}{2}$ levels, we calculate, therefore:

$$\begin{aligned}
\langle \vec{l} \cdot \vec{s} \rangle_{j=l+\frac{1}{2}} &= [(l+1/2)(l+3/2) - l(l+1) - 3/4]/2 \\
&= l/2 \\
\langle \vec{l} \cdot \vec{s} \rangle_{j=l-\frac{1}{2}} &= [(l-1/2)(l+1/2) - l(l+1) - 3/4]/2 \\
&= -(l+1)/2 \\
\langle \vec{l} \cdot \vec{s} \rangle_{j=l+\frac{1}{2}} - \langle \vec{l} \cdot \vec{s} \rangle_{j=l-\frac{1}{2}} &= (2l+1)/2 \qquad (12.6)
\end{aligned}$$

$V_{so}(r)$ is negative, and so, the higher $j = l + \frac{1}{2}$ (orbit and spin angular momenta are aligned) is more tightly bound.

The shape of this potential is shown, for a valence neutron in Figure 12.7, and for a valence proton in Figure 12.8. For this demonstration, the core nucleus was ^{208}Pb. The l in the figures, to highlight the spin-orbit coupling, was chosen to be $l = 10$.

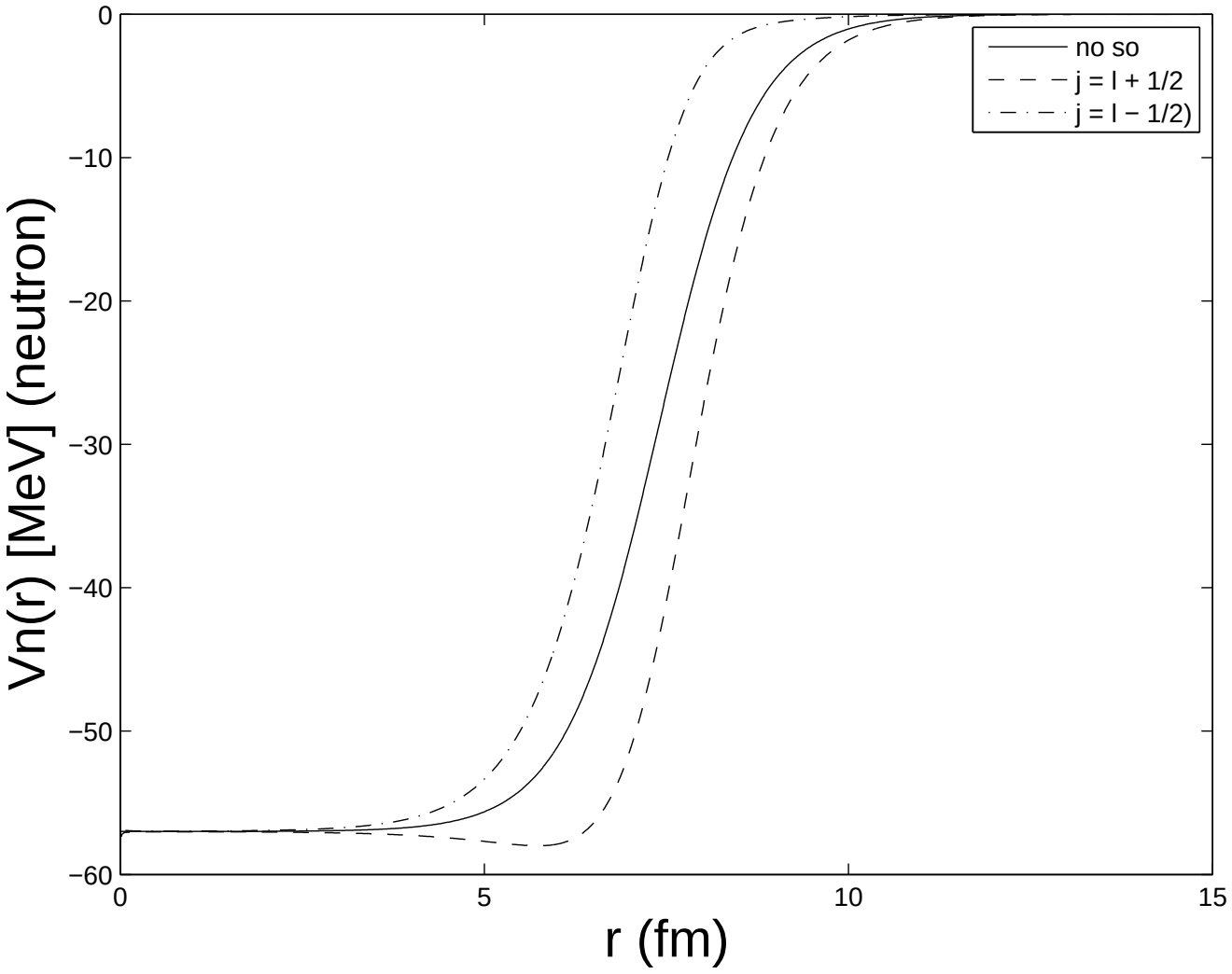

Figure 12.7: The potential of a ^{208}Pb nucleus as seen by a single valence neutron.

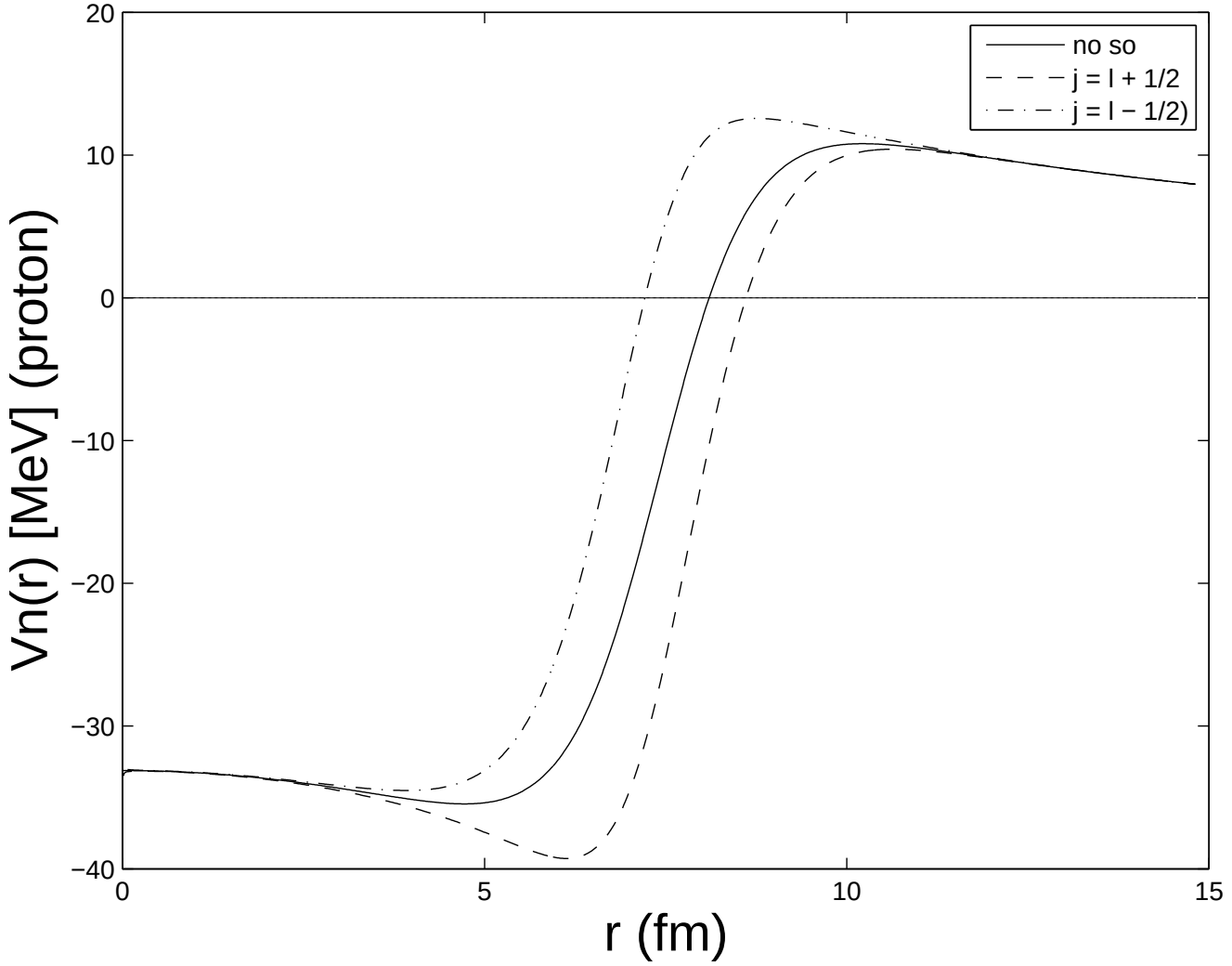

Figure 12.8: The potential of a ^{208}Pb nucleus as seen by a single valence proton. Note the effect of the Coulomb potential on the the potential near the origin (parabolic shape there), as well as the presence of the Coulomb barrier.

Determining the ground state I^π in the shell model

The spin and parity assignment may be determined by considering the nuclear potential described so far, plus one additional idea, the "Extreme Independent Particle Model" (EIPM). The EIPM is an addendum to the shell model idea, and it is expressed as follows. *All the characteristics of a given nucleus are determined by the unpaired valence nucleons. All pairs of like nucleons cancel one another's spins and parities.*

Applying EIPM for the example of two closely related nuclei is demonstrated in Figure 12.9.

Figure 12.9: A demonstration of the spin and parity assignment for ^{15}O and ^{17}O. $I^\pi(^{15}\mathrm{O}) = \frac{1}{2}^-$, while $I^\pi(^{17}\mathrm{O}) = \frac{5}{2}^+$. *This sketch has not been created yet, so feel free to draw it in!*

Another demonstration of the success of the EIPM model is to consider the isotopes of O.

Isotope of O	I^π, measured	I^π, EIPM prediction	decay mode	$t_{1/2}$/abundance
^{12}O	0^+ (est)	0^+	$2p$	$\approx 10^{-21}$ s
^{13}O	$\frac{3}{2}^-$	$\frac{3}{2}^-$	β^+, p	8.6 ms
^{14}O	0^+	0^+	γ, β^+	70.60 s
^{15}O	$\frac{1}{2}^-$	$\frac{1}{2}^-$	ε, β^+	2.037 m
^{16}O	0^+	0^+		99.757%
^{17}O	$\frac{5}{2}^+$	$\frac{5}{2}^+$		0.038%
^{18}O	0^+	0^+		0.205%
^{19}O	$\frac{5}{2}^+$	$\frac{5}{2}^+$	β^-, γ	26.9 s
^{20}O	0^+	0^+	β^-, γ	13.5 s
^{21}O	?	$\frac{5}{2}^+$	β^-, γ	3.4 s
^{22}O	0^+ (est)	0^+	β^-, γ	2.2 s
^{23}O	?	$\frac{1}{2}^+$	β^-, n	0.08 s
^{24}O	0^+ (est)	0^+	β^-, γ, n	65 ms

Other successes ...

Isotope	I^π
$^{13}_{5}\mathrm{Be}_8$	$\frac{3}{2}^-$
$^{14}_{6}\mathrm{C}_8$	0^+
$^{15}_{7}\mathrm{N}_8$	$\frac{1}{2}^-$
$^{16}_{8}\mathrm{O}_8$	0^+
$^{17}_{8}\mathrm{F}_8$	$\frac{5}{2}^+$
$^{18}_{10}\mathrm{Ne}_8$	0^+

EIPM prediction of the magnetic moment of the nucleus

The shell model, and its EIPM interpretation, can be tested by measuring and calculating the magnetic moment of a nucleus. Thus, the last unpaired nucleon determines the magnetic moment of the entire nucleus. Recall from Chapter 10, the definition of magnetic moment, μ, of a nucleus:

$$\mu = \mu_{\mathrm{N}}(g_l l_z + g_s s_z) \ , \tag{12.7}$$

where

Symbol	Meaning	Value
$\mu_{\rm N}$	Nuclear magnetron	$5.05078324(13) \times 10^{-27}$ J/T
g_l	Orbital gyromagnetic ratio	0 (neutron), 1 (proton)
g_s	Spin gyromagnetic ratio	$-3.82608545(46)$ (neutron) 5.585694713(90) (proton)
l_z	Maximum value of m_l	$j_z = \max(m_l)$
s_z	Maximum value of m_s	$s_z = \max(m_s) = 1/2$

However, neither $\vec{l}$ nor $\vec{s}$ is precisely defined for nuclei (recall the Deuteron) due to the strong spin-orbit coupling. Consequently, l_z and s_z can not be known precisely. However, total angular momentum, $\vec{j}$ and its maximum z-projection, j_z are precisely defined, and thus measurable.

Since $j_z = l_z + s_z$, we may rewrite (12.7) as:

$$\mu = \mu_{\rm N}(g_l j_z + (g_s - g_l)s_z) \ . \tag{12.8}$$

Computing the expectation value (*i.e.* the measured value) of μ gives:

$$\langle\mu\rangle = \mu_{\rm N}(g_l j + (g_s - g_l)\langle s_z\rangle) \ . \tag{12.9}$$

Since $\vec{j}$ is the only measurable vector in the nucleus, we can determine $\langle s_z\rangle$ from its projection along $\vec{j}$.

Thus, using projection vector language:

$$\begin{aligned}
\vec{s}_j &= \vec{j}\frac{(\vec{s}\cdot\vec{j})}{\vec{j}\cdot\vec{j}} \ , \\
s_z = \hat{z}\cdot\vec{s}_j &= j_z\frac{\vec{s}\cdot\vec{j}}{\vec{j}\cdot\vec{j}} \ , \\
\langle s_z\rangle &= j\frac{\langle\vec{s}\cdot\vec{j}\rangle}{j(j+1)} \ , \\
\langle s_z\rangle &= \frac{\langle\vec{s}\cdot\vec{j}\rangle}{(j+1)} \ , \\
\langle s_z\rangle &= \frac{\langle\vec{j}\cdot\vec{j}\rangle - \langle\vec{l}\cdot\vec{l}\rangle + \langle\vec{s}\cdot\vec{s}\rangle}{2(j+1)} \ , \\
\langle s_z\rangle &= \frac{j(j+1) - l(l+1) + s(s+1)}{2(j+1)} \ , \\
\langle s_z\rangle_{j=l+1/2} &= 1/2 \ , \\
\langle s_z\rangle_{j=l-1/2} &= -\frac{j}{2(j+1)} \ .
\end{aligned} \tag{12.10}$$

Substituting the results of (12.10) into (12.9) gives:

$$\begin{aligned} \langle\mu\rangle_{j=l+1/2} &= \mu_{\rm N}\left[g_l(j-\tfrac{1}{2})+\tfrac{1}{2}g_s\right] \\ \langle\mu\rangle_{j=l-1/2} &= \mu_{\rm N}\left[g_l\frac{j(j+\frac{3}{2})}{(j+1)}-\frac{g_s}{2}\frac{j}{(j+1)}\right] \end{aligned} \tag{12.11}$$

Comparisons of measurements with theory are given in Figure 12.10, for odd-neutron and odd-proton nuclei. These nuclei are expected to give the best agreement with the EIPM. The theoretical lines are know as Schmidt lines, honoring the first person who developed the theory. Generally, the trends in the data are followed by the Schmidt lines, though the measured data is significantly lower. The reason for this is probably a "polarization effect", where the intrinsic spin of the odd nucleon is shielded by the other nucleons in the nucleus as well as the virtual exchange mesons. This is very similar to a charged particle entering a condensed medium and polarizing the surrounding atoms, thereby reducing the effect of its charge. This can be interpreted as a reduction in charge by the surrounding medium. (The typical size of this reduction is only about 1–2%. However, in a nucleus, the forces are much stronger, and hence, so is the polarization. The typical reduction factor applied to the nucleons are g_s (in nucleus) $\approx 0.6 g_s$ (free).

Figure 12.10: *See Krane's Figure 5.9, p. 127*

Shell model and EIPM prediction of the quadrupole moment of the nucleus

Recall the definition of the quadrupole moment of a nucleus, given in (10.53) namely:

$$Q = \int {\rm d}\vec{x}\ \psi_N^*(\vec{x})(3z^2-r^2)\psi_N(\vec{x})\ .$$

A quantum-mechanical calculation of the quadrupole moment for a single odd proton, by itself in a subshell, is given by:

$$\langle Q_{\rm sp}\rangle = -\frac{2j-1}{2(j+1)}\langle r^2\rangle \ . \tag{12.12}$$

When a subshell contains more than one particle, all the particles in that subshell can, in principle, contribute to the quadrupole moment. The consequence of this is that the quadrupole moment is given by:

$$\langle Q\rangle = \langle Q_{\rm sp}\rangle \left[1 - 2\frac{n-1}{2j-1}\right] \ , \tag{12.13}$$

where n is the occupancy of that level. We can rewrite (12.13) in to related ways:

$$\begin{aligned} \langle Q\rangle(n) &= \langle Q_{\rm sp}\rangle \left[\frac{2(j-n)+1}{2j-1}\right] \ , \\ \langle Q\rangle(n_0) &= \langle Q_{\rm sp}\rangle \left[\frac{-2(j-n_0)-1}{2j-1}\right] \ , \end{aligned} \tag{12.14}$$

where $n_0 = 2j+1-n$ is the number of "holes" in the subshell. Thus we see that (12.14) predicts $\langle Q\rangle(n_0 = n) = -\langle Q\rangle(n)$. The interpretation is that "holes" have the same magnitude quadrupole moment as if there were the equivalent number of particles in the shell, but with a difference in sign. Krane's Table 5.1 (p. 129) bears this out, despite the generally poor agreement in the absolute value of the quadrupole moment as predicted by theory.

Even more astonishing is the measured quadrupole moment for single neutron, single-neutron hole data. There is no theory for this! Neutrons are not charged, and therefore, if Q were determined by the "last unpaired nucleon in" idea, Q would be zero for these states. It might be lesser in magnitude, but it is definitely not zero!

There is much more going on than the EIPM or shell models can predict. These are collective effects, whereby the odd neutron perturb the shape of the nuclear core, resulting in a measurable quadrupole moment. EIPM and the shell model can not address this physics. It is also known that the shell model prediction of quadrupole moments fails catastrophically for $60 < Z < 80$, $Z > 90$ $90 < N < 120$ and $N > 140$, where the measured moments are an order of magnitude greater. This is due to collective effects, either multiple particle behavior or a collective effect involving the entire core. We shall investigate these in due course.

Shell model predictions of excited states

If the EIPM were true, we could measure the shell model energy levels by observing the decays of excited states. Recall the shell model energy diagram, and let us focus on the lighter nuclei.

Figure 12.11: The low-lying states in the shell model

Let us see if we can predict and compare the excited states of two related light nuclei: ${}^{17}_{8}\mathrm{O}_9 = [{}^{16}_{8}\mathrm{O}_8] + 1n$, and ${}^{19}_{9}\mathrm{F}_8 = [{}^{16}_{8}\mathrm{O}_8] + 1p$.

Figure 12.12: The low-lying excited states of ${}^{17}_{8}\mathrm{O}_9$ and ${}^{19}_{9}\mathrm{F}_8$. Krane's Figure 5.11, p. 131

The first excited state of ${}^{17}_{8}\mathrm{O}_9$ and ${}^{19}_{9}\mathrm{F}_8$ has $I^\pi = 1/2^+$. This is explained by the EIPM interpretation. The "last in" unpaired nucleon at the $1d_{5/2}$ level is promoted to the $2s_{1/2}$ level, vacating the $1d$ shell. The second excited state with $I^\pi = 1/2^-$ does not follow the EIPM model. Instead, it appears that a core nucleon is raised from the $1p_{1/2}$ level to the $1d_{5/2}$ level, joining another nucleon there and canceling spins. The $I^\pi = 1/2^-$ is determined by the unpaired nucleon left behind. Nor do the third and fourth excited states follow the EIPM prescription. The third and fourth excited states seem to be formed by a core nucleon raised from the $1p_{1/2}$ level to the $2s_{1/2}$ level, leaving three unpaired nucleons. Since I is formed from the coupling of j's of $1/2$, $1/2$ and $5/2$, we expect $3/2 \leq I \leq 7/2$. $3/2$ is the lowest followed by $5/2$. Not shown, but expected to appear higher up would be the $7/2$. The parity is negative, because parity is multiplicative. Symbolically, $(-1)^p \times (-1)^d \times (-1)^s = -1$. Finally, the fifth excited state does follow the EIPM prescription, raising the "last in" unbound nucleon to $d_{3/2}$ resulting in an $I^\pi = 3/2^+$.

Hints of collective structure

Krane's discussion on this topic is quite good.

Figure 12.13: The low-lying excited states of ${}^{41}_{20}\mathrm{Ca}_{21}$, ${}^{41}_{21}\mathrm{Sc}_{20}$, ${}^{43}_{20}\mathrm{Ca}_{23}$, ${}^{43}_{21}\mathrm{Sc}_{22}$, ${}^{43}_{22}\mathrm{Ti}_{21}$. Krane's figure 5.12, p. 132

Verification of the shell model

Krane has a very interesting discussion on a demonstration of the validity of the shell model by investigating the behavior of s states in heavy nuclei. In this demonstration, the difference in the proton charge distribution (measured by electrons), is compared for ${}^{205}_{81}\mathrm{Tl}_{124}$ and ${}^{206}_{82}\mathrm{Pb}_{124}$.

$$\rho_{\mathrm{p}}^{{}^{205}_{81}\mathrm{Tl}_{124}}(r) - \rho_{\mathrm{p}}^{{}^{206}_{82}\mathrm{Pb}_{124}}(r)$$

${}^{206}\mathrm{Pb}$ has a magic number of protons and 124 neutrons while ${}^{205}\mathrm{Tl}$ has the same number of neutrons and 1 less proton. That proton is in an $s_{1/2}$ orbital. So, the measurement of the charge density is a direct investigation of the effect of an unpaired proton coursing though the tight nuclear core, whilst on its s-state meanderings.

12.2 Even-Z, even-N Nuclei and Collective Structure

All even/even nuclei are $I^\pi = 0^+$, a clear demonstration of the effect of the pairing force.

All even/even nuclei have an anomalously small 1st excited state at 2^+ that can not be explained by the shell model (EIPM or not). Read Krane pp. 134–138.

Consult Krane's Figure 5.15a, and observe that, except near closed shells, there is a smooth downward trend in $E(2^+)$, the binding energy of the lowest 2^+ states. Regions $150 < A < 190$ and $A > 220$ seem very small and consistent.

Quadrupole moment systematics

Q_2 is small for $A < 150$. Q_2 is large and negative for $150 < A < 190$ suggesting an *oblate* deformation

Consult Krane's Figure 5.16b: The regions between $150 < A < 190$ and $A > 220$ are markedly different. Now, consult Krane's Figure 5.15b that shows the ratio of $E(4^+)/E(2^+)$. One also notes something "special about the regions:$150 < A < 190$ and $A > 220$.

All this evidence suggests a form of "collective behavior" that is described by the *Liquid Drop Model* (LDM) of the nucleus.

12.2.1 The Liquid Drop Model of the Nucleus

In the the Liquid Drop Model is familiar to us from the semi-empirical mass formula (SEMF). When we justified the first few terms in the SEMF, we argued that the bulk term and the surface term were characteristics of a cohesive, attractive mass of nucleons, all in contact with each other, all in motion, much like that of a fluid, like water. Adding a nucleon liberates a certain amount of energy, identical for each added nucleon. The gives rise to the bulk term. The bulk binding is offset somewhat by the deficit of attraction of a nucleon at or near the surface. That nucleon has fewer neighbors to provide full attraction. Even the Coulomb repulsion term can be considered to be a consequence of this model, adding in the extra physics of electrostatic repulsion. Now we consider that this "liquid drop" may have collective (many or all nucleons participating) excited states, in the quantum mechanical sense[1].

These excitations are known to have two distinct forms:

- Vibrational excitations, about a spherical or ellipsoidal shape. All nucleons participate in this behavior. (This is also known as photon excitation.)
- Rotational excitation, associated with rotations of the entire nucleus, or possibly only the valence nucleons participating, with perhaps some "drag" on a non-rotating spherical core. (This is also known as roton excitation.)

Nuclear Vibrations (Phonons)

Here we characterize the nuclear radius as have a temporal variation in polar angles in the form:

$$R(\theta, \phi, t) = R_{\text{avg}} + \sum_{\lambda=1}^{\Lambda} \sum_{\mu=-\lambda}^{\lambda} \alpha_{\lambda\mu}(t) Y_{\lambda\mu}(\theta, \phi) \ , \tag{12.15}$$

[1]A classical liquid drop could be excited as well, but those energies would appears not to be quantized. (Actually, they are, but the quantum numbers are so large that the excitations appear to fall on a continuum.

Here, $R_{\rm avg}$ is the "average" radius of the nucleus, and $\alpha_{\lambda\mu}(t)$ are temporal deformation parameters. Reflection symmetry requires that $\alpha_{\lambda,-\mu}(t) = \alpha_{\lambda\mu}(t)$. Equation (12.15) describes the surface in terms of sums total angular momentum components $\vec{\lambda}\hbar$ and their z-components, $\mu\hbar$. The upper bound on λ is some upper bound Λ. Beyond that, presumably, the nucleus can not longer be bound, and flies apart. If we insist that the nucleus is an incompressible fluid, we have the further constraints:

$$\begin{aligned} V_N &= \frac{4\pi}{3} R_{\rm avg}^3 \\ 0 &= \sum_{\lambda=1}^{\Lambda} |\alpha_{\lambda,0}(t)|^2 + 2\sum_{\lambda=1}^{\Lambda}\sum_{\mu=1}^{\lambda} |\alpha_{\lambda\mu}(t)|^2 \end{aligned} \tag{12.16}$$

The λ deformations are shown in Figure 12.14 for $\lambda = 1, 2, 3$.

Figure 12.14: In this figure, nuclear surface deformations are shown for $\lambda = 1, 2, 3$

Dipole phonon excitation

The $\lambda = 1$ formation is a *dipole* excitation. Nuclear deformation dipole states are not observed in nature, because a dipole excitation is tantamount to a oscillation of the center of mass.

Quadrupole phonon excitation

The $\lambda = 2$ excitation is called a *quadrupole excitation* or a *quadrupole phonon excitation*, the latter being more common. Since $\pi = (-1)^\lambda$, the parity of the quadrupole phonon excitation is always positive, and it's $I^\pi = 2^+$.

Octopole phonon excitation

The $\lambda = 3$ excitation is called an *octopole excitation* or a *octopole phonon excitation*, the latter being more common. Since $\pi = (-1)^\lambda$, the parity of the octopole phonon excitation is always negative, and it's $I^\pi = 3^-$.

Two-quadrupole phonon excitation

Now is gets interesting! These quadrupole spins add in the quantum mechanical way. Let us enumerate all the apparently possible combinations of $|\mu_1\rangle$ and $|\mu_2\rangle$ for a two photon excitation:

$\mu = \mu_1 + \mu_2$	Combinations	d	$\mu_{\lambda=4}$	$\mu_{\lambda=3}$	$\mu_{\lambda=2}$	$\mu_{\lambda=1}$	$\mu_{\lambda=0}$
4	$\|2\rangle\|2\rangle$	1	y				
3	$\|2\rangle\|1\rangle, \|1\rangle\|2\rangle$	2	y	y			
2	$\|2\rangle\|0\rangle, \|1\rangle\|1\rangle, \|0\rangle\|2\rangle$	3	y	y	y		
1	$\|2\rangle\|\text{-}1\rangle, \|1\rangle\|0\rangle, \|0\rangle\|1\rangle, \|\text{-}1\rangle\|2\rangle$	4	y	y	y	y	
0	$\|2\rangle\|\text{-}2\rangle, \|1\rangle\|\text{-}1\rangle, \|0\rangle\|0\rangle, \|\text{-}1\rangle\|1\rangle, \|\text{-}2\rangle\|2\rangle$	5	y	y	y	y	y
-1	$\|1\rangle\|\text{-}2\rangle, \|0\rangle\|\text{-}1\rangle, \|\text{-}1\rangle\|0\rangle, \|\text{-}2\rangle\|1\rangle$	4	y	y	y	y	
-2	$\|0\rangle\|\text{-}2\rangle, \|\text{-}1\rangle\|\text{-}1\rangle, \|\text{-}2\rangle\|0\rangle$	3	y	y	y		
-3	$\|\text{-}1\rangle\|\text{-}2\rangle, \|\text{-}2\rangle\|\text{-}1\rangle$	2	y	y			
-4	$\|\text{-}2\rangle\|\text{-}2\rangle$	1	y				
		$\sum d = 25$	9	7	5	3	1

It would appear that we could make two-quadrupole phonon states with $I^\pi = 4^+, 3^-, 2^+, 1^-, 0^+$. However, phonons are unit spin excitations, and follow Bose-Einstein statistics, Therefore, only symmetric combinations can occur. Accounting for this, as we have done following, leads us to conclude that the only possibilities are: $I^\pi = 4^+, 2^+, 0^+$.

$\mu = \mu_1 + \mu_2$	Symmetric combinations	d	$\mu_{\lambda=4}$	$\mu_{\lambda=2}$	$\mu_{\lambda=0}$
4	$\|2\rangle\|2\rangle$	1	y		
3	$(\|2\rangle\|1\rangle+\|1\rangle\|2\rangle)$	1	y		
2	$(\|2\rangle\|0\rangle+\|0\rangle\|2\rangle)$, $\|1\rangle\|1\rangle$	2	y	y	
1	$(\|2\rangle\|\text{-}1\rangle+\|\text{-}1\rangle\|2\rangle)$, $(\|1\rangle\|0\rangle+\|0\rangle\|1\rangle)$	2	y	y	
0	$(\|2\rangle\|\text{-}2\rangle+\|\text{-}2\rangle\|2\rangle)$, $(\|1\rangle\|\text{-}1\rangle+\|\text{-}1\rangle\|1\rangle)$, $\|0\rangle\|0\rangle$	3	y	y	y
-1	$(\|1\rangle\|\text{-}2\rangle+\|\text{-}2\rangle\|1\rangle)$, $(\|0\rangle\|\ 1\rangle+\|\text{-}1\rangle\|0\rangle)$	2	y	y	
-2	$(\|0\rangle\|\text{-}2\rangle+\|\text{-}2\rangle\|0\rangle)$, $\|\text{-}1\rangle\|\text{-}1\rangle$	2	y	y	
-3	$(\|\text{-}1\rangle\|\text{-}2\rangle+\|\text{-}2\rangle\|\text{-}1\rangle)$	1	y		
-4	$\|\text{-}2\rangle\|\text{-}2\rangle$	1	y		
		$\sum d = 15$	9	5	1

Three-quadrulpole phonon excitations

Applying the same methods, one can easily (hah!) show, that the combinations give $I^\pi = 6^+, 4^+, 3^+, 2^+, 0^+$.

She Krane's Figure 5.19, p. 141, for evidence of phonon excitation.

Nuclear Rotations (Rotons)

Nuclei in the mass range $150 < A < 190$ and $A > 200$ have permanent non-spherical deformations. The quadrupole moments of these nuclei are larger by about an order of magnitude over their non-deformed counterparts.

This permanent deformation is usually modeled as follows:

$$R_N(\theta) = R_{\text{avg}}[1 + \beta Y_{20}(\theta)] \ . \tag{12.17}$$

β is called the deformation parameter. β is called the deformation parameter, (12.17) describes (approximately) an ellipse. (This is truly only valid if β is small. β is related to the eccentricity of an ellipse as follows,

$$\beta = \frac{4}{3}\sqrt{\frac{\pi}{5}}\frac{\Delta R}{R_{\text{avg}}} \ , \tag{12.18}$$

where ΔR is the difference between the semimajor and semiminor axes of the ellipse. When $\beta > 0$, the nucleus is a *prolate* ellipsoid (cigar shaped). When $\beta < 0$, the nucleus is an *oblate* ellipsoid (shaped like a curling stone). Or, if you like, if you start with a spherical blob of putty and roll it between your hands, it becomes prolate. If instead, you press it between your hands, it becomes oblate.

The relationship between β and the quadrupole moment[2] of the nucleus is:

$$Q = \frac{3}{\sqrt{5\pi}} R_{\text{avg}}^2 Z\beta \left[1 + \frac{2}{7}\left(\frac{5}{\pi}\right)^{1/2}\beta + \frac{9}{28\pi}\beta^2\right] \ . \tag{12.19}$$

Energy of rotation

Classically, the energy of rotation, E_{rot} is given by:

$$E_{\text{rot}} = \frac{1}{2}\mathcal{I}\omega^2 \ , \tag{12.20}$$

where $\mathcal{I}$ is the *moment of inertia* and ω is the rotational frequency. The transition to Quantum Mechanics is done as follows:

$$E_{\text{rot}}^{\text{QM}} = \frac{1}{2}\frac{\vec{\mathcal{I}}\cdot\vec{\mathcal{I}}}{\mathcal{I}}\omega^2 = \frac{1}{2}\frac{(\vec{\mathcal{I}}\omega)\cdot(\vec{\mathcal{I}}\omega)}{\mathcal{I}} = \frac{1}{2}\frac{\langle(\vec{I}\hbar)\cdot(\vec{I}\hbar)\rangle}{\mathcal{I}} = \frac{\hbar^2}{2\mathcal{I}}\langle\vec{I}\cdot\vec{I}\rangle = \frac{\hbar^2}{2\mathcal{I}}I(I+1) \tag{12.21}$$

Technical aside:

Moment of Inertia?

Imagine that an object is spinning around the z-axis, which cuts through its center of mass, as shown in Figure 12.15. We place the origin of our coordinate system at the object's center of mass. The angular frequency of rotation is ω.

The element of mass, $\mathrm{d}m$ at $\vec{x}$ is $\rho(\vec{x})\mathrm{d}\vec{x}$, where $\rho(\vec{x})$ is the mass density. $[M = \int \mathrm{d}\vec{x}\,\rho(\vec{x})]$. The speed of that mass element, $|v(\vec{x})|$ is $\omega r\sin\theta$. Hence, the energy of rotation, of that element of mass is:

$$\mathrm{d}E_{\text{rot}} = \frac{1}{2}\mathrm{d}m\,|v(\vec{x})|^2 = \frac{1}{2}\mathrm{d}\vec{x}\,[\rho(\vec{x})r^2\sin^2\theta]\omega^2 \ . \tag{12.22}$$

Integrating over the entire body gives:

[2]Krane's (5.16) is incorrect. The β-term has a coefficient of 0.16, rather than 0.36 as implied by (12.19). Typically, this correction is about 10%. The additional term provided in (12.19) provides about another 1% correction.

Figure 12.15: A rigid body in rotation. (Figure needs to be created.)

$$E_{\rm rot} = \frac{1}{2}\mathcal{I}\omega^2 \ , \tag{12.23}$$

which defines the moment of inertia *to be:*

$$\mathcal{I} = \int {\rm d}\vec{x}\, \rho(\vec{x}) r^2 \sin^2\theta \ . \tag{12.24}$$

The moment of inertia is an intrinsic property of the object in question.

Example 1: Moment of inertia for a spherical nucleus

Here,

$$\rho(\vec{x}) = M\frac{3}{4\pi R_N^3}\Theta(R_N - r) \ .$$

Hence,

$$\begin{aligned}
\mathcal{I}_{\rm sph} &= M\frac{3}{4\pi R_N^3}\int_{|\vec{x}|\leq R_N} {\rm d}\vec{x}\, r^2 \sin^2\theta \\
&= \frac{3M}{2R_N^3}\int_0^{R_N} {\rm d}r\, r^4 \int_0^{\pi} \sin\theta {\rm d}\theta\ \sin^2\theta \\
&= \frac{3MR_N^2}{10}\int_{-1}^{1} {\rm d}\mu\, (1-\mu^2) \\
\mathcal{I}_{\rm sph} &= \frac{2}{5}MR_N^2
\end{aligned} \tag{12.25}$$

Example 2: Moment of inertia for an elliptical nucleus

Here, the mass density is a constant, but within a varying radius given by (12.17), namely

$$R_N(\theta) = R_{\rm avg}[1 + \beta Y_{20}(\theta)] \ .$$

The volume of this nucleus is given by:

$$\begin{aligned}
V &= \int_{|\vec{x}|\leq R_{\rm avg}[1+\beta Y_{20}(\mu)]} {\rm d}\vec{x} \\
&= 2\pi\int_{-1}^{1} {\rm d}\mu \int_0^{R_{\rm avg}[1+\beta Y_{20}(\mu)]} r^2 {\rm d}r \\
&= \frac{2\pi R_{\rm avg}^3}{3}\int_{-1}^{1} {\rm d}\mu\, [1 + \beta Y_{20}(\mu)]^3
\end{aligned} \tag{12.26}$$

$$\begin{aligned}
\mathcal{I}_\ell &= \int \mathrm{d}\vec{x}\,\rho(\vec{x}) r^2 \sin^2\theta \\
&= \frac{M}{V}(2\pi)\int_{-1}^{1}\mathrm{d}\mu\,(1-\mu^2)\int_0^{R_{\rm avg}[1+\beta Y_{20}(\mu)]}\mathrm{d}r\,r^4 \\
&= \frac{MR_{\rm avg}^5}{V}\frac{2\pi}{5}\int_{-1}^{1}\mathrm{d}\mu\,(1-\mu^2)[1+\beta Y_{20}(\mu)]^5 \\
\mathcal{I}_\ell &= MR_{\rm avg}^2\left(\frac{3}{5}\right)\left[\int_{-1}^{1}\mathrm{d}\mu\,(1-\mu^2)[1+\beta Y_{20}(\mu)]^5\right]\Bigg/\left[\int_{-1}^{1}\mathrm{d}\mu\,[1+\beta Y_{20}(\mu)]^3\right] \quad (12.27)
\end{aligned}$$

(12.27) is a ratio a $5^{\rm th}$-order polynomial in β, to a $3^{\rm rd}$-order polynomial in β. However, it can be shown that it is sufficient to keep only $O(\beta^2)$. With,

$$Y_{20}(\mu) = \sqrt{\frac{5}{16\pi}}(3\mu^2-1)$$

(12.27) becomes:

$$\begin{aligned}
\mathcal{I}_\ell &= \left(\frac{2}{5}\right)MR_{\rm avg}^2\left[1-\frac{1}{2}\sqrt{\frac{5}{\pi}}\beta+\frac{71}{28\pi}\beta^2+O(\beta^3)\right] \\
&= \left(\frac{2}{5}\right)MR_{\rm avg}^2\left[1-0.63\beta+0.81\beta^2+(<1\%)\right]\ . \quad (12.28)
\end{aligned}$$

Rotational bands

$E_{\rm rot}(I^\pi)$	Value	Interpretation
$E(0^+)$	0	ground state
$E(2^+)$	$6(\hbar^2/2\mathcal{I})$	1st rotational state
$E(4^+)$	$20(\hbar^2/2\mathcal{I})$	2nd rotational state
$E(6^+)$	$42(\hbar^2/2\mathcal{I})$	3rd rotational state
$E(8^+)$	$72(\hbar^2/2\mathcal{I})$	4th rotational state
$\vdots$	$\vdots$	$\vdots$

Using $\mathcal{I}_{\rm rigid}$, assuming a rigid body, gives a spacing that is low by a factor of about off by about 2–3. Using

$$\mathcal{I}_{\rm fluid} = \frac{9}{8\pi} M_N R_{\rm avg}^2 \beta$$

for a fluid body in rotation[3], gives a spacing that is high by a factor of about off by about 2–3. Thus the truth for a nucleus, is somewhere in between:

$$\mathcal{I}_{\rm fluid} < \mathcal{I}_N < \mathcal{I}_{\rm rigid}$$

[3]Actually, the moment of inertia of a fluid body is an ill-defined concept. There are two ways I can think of, whereby the moment of inertia may be reduced. One model could be that of a "static non-rotating core". From (12.29), this would imply that:

$$\mathcal{I}_\ell = -\left(\frac{2}{5}\right) M R_{\rm avg}^2 \left[\frac{1}{2}\sqrt{\frac{5}{\pi}}\beta - \frac{71}{28\pi}\beta^2\right] \approx -\left(\frac{2}{5}\right) M R_{\rm avg}^2 \left[\beta - 0.81\beta^2\right] \ .$$

Another model would be that of viscous drag, whereby the angular frequency becomes a function of r and θ. For example, $\omega = \omega_0(r\sin\theta/R_{\rm avg})^n$. One can show that the reduction, R_n in $\mathcal{I}$ is of the form $R_{n+1} = \frac{2(n+2)}{7+2n} R_n$, where $R_0 \equiv 1$. A "parabolic value", $n = 2$, gives the correct amount of reduction, about a factor of 3. This also makes some sense, since rotating liquids obtain a parabolic shape.

Chapter 13

Radioactive Decay

Note to students and other readers: This Chapter is intended to supplement Chapter 6 of Krane's excellent book, "Introductory Nuclear Physics". Kindly read the relevant sections in Krane's book first. This reading is supplementary to that, and the subsection ordering will mirror that of Krane's, at least until further notice.

13.1 The Radioactive Decay Law

Exponential decay law

Consider a system of particles, N_0 in number at time, $t = 0$. Each of these particles has an independent, but equal probability of decay per unit time, λ. How many particles are observed at a later time? The traditional way of answering this question is to assume that N is large enough, that we may use calculus. Since particles are integral quantities, we recognize that this is, somewhat, a leap of faith!

Thus, the change in N us given by:

$$\begin{aligned} \mathrm{d}N &= -\lambda N \mathrm{d}t; \quad N(0) = N_0 \\ \frac{\mathrm{d}N}{N} &= -\lambda \mathrm{d}t \\ \mathrm{d}[\log N] &= -\lambda \mathrm{d}t \\ \log N - \log N_0 &= -\lambda t \\ \log N &= \log N_0 - \lambda t \\ N &= N_0 \exp(-\lambda t) \end{aligned} \tag{13.1}$$

Thus we have derived the well-known *exponential decay law*, $N(t) = N_0 e^{-\lambda t}$.

Half-life

The *half-life*, $t_{1/2}$, is defined as follows:

$$\frac{N(t+t_{1/2})}{N(t)} \equiv \frac{1}{2} = \frac{N_0 \exp(-\lambda t - \lambda t_{1/2})}{N_0 \exp(-\lambda t)} = \exp(-\lambda t_{1/2}) \ ,$$

or,

$$t_{1/2} = \frac{\log 2}{\lambda} \approx \frac{0.693}{\lambda} \ . \tag{13.2}$$

Thus we see, a population of N radioactive particles at t would be reduced by half (on average) at time $t + t_{1/2}$.

Lifetime, or mean lifetime

The exponential law can also be interpreted as the *decay probability* for a single radioactive particle to decay in the interval $\mathrm{d}t$, about t.. This probability, $p(t)$, properly normalized, is given by:

$$p(t)\mathrm{d}t = \lambda e^{-\lambda t}\mathrm{d}t \quad ; \quad \int_0^\infty p(t)\mathrm{d}t = 1 \ . \tag{13.3}$$

The we see that the probability a particle decays within time t, $P(t)$ is given by,

$$P(t) = \int_0^t p(t')\mathrm{d}t' = 1 - e^{-\lambda t}. \tag{13.4}$$

The *mean lifetime* or *lifetime* of a particle, τ, is evaluated by calculating $\langle t \rangle$, using the probability distribution (13.3):

$$\tau = \lambda \int_0^\infty t e^{-\lambda t}\mathrm{d}t \ = \frac{1}{\lambda} \ . \tag{13.5}$$

Activity

The number of decays, ΔN, observed from t and $t + \Delta t$, obtained from (13.1) is:

$$\Delta N = N(t) - N(t+\Delta t) = N_0 e^{-\lambda t}(1 - e^{-\lambda \Delta t}) \ .$$

If $\Delta t \ll \tau$, then, in the limit as $\Delta t \to 0$, we may rewrite the above as:

$$\left|\frac{\mathrm{d}N}{\mathrm{d}t}\right| = \lambda N_0 e^{-\lambda t} = \lambda N(t) \equiv \mathcal{A}(t) = \mathcal{A}_0 e^{-\lambda t} \ , \tag{13.6}$$

defining the *activity*, $\mathcal{A}(t)$, and its initial value, $\mathcal{A}_0$. Activity is usually what is measured, since N_0 and $N(t)$ are usually unknown, nor of particular interest in many applications. What is generally of real interest is the activity of a source, and, consequently, the ability of the radiation from a source, to interact.

It must be emphasized that (13.6) is an approximate relationship, based on $\Delta t \ll \tau$. Consequently, using (13.6) in any other expression, is subject to the same constraint.

The previous considerations only apply to the decay of a single isotope, N_1, to another (presumably stable) nucleus, N_2.

The differential equations describing the decline of N_1 and the growth of N_2 are given as follows:

$$\begin{aligned} \mathrm{d}N_1 &= -N_1 \lambda \mathrm{d}t \\ \mathrm{d}N_2 &= N_1 \lambda \mathrm{d}t \\ \mathrm{d}(N_1 + N_2) &= 0 \ , \end{aligned} \tag{13.7}$$

with solutions:

$$\begin{aligned} N_1 &= N_1(0) e^{-\lambda t} \\ N_2 &= N_2(0) + N_1(0)(1 - e^{-\lambda t}) \\ N_1 + N_2 &= N_1(0) + N_2(0) \end{aligned} \tag{13.8}$$

One isotope, two decay channels

Now imagine that N can decay, with λ_a into N_a, or into N_b with λ_b. The total decay rate is $\lambda_t = \lambda_a + \lambda_b$.

The differential equations are:

$$\begin{aligned} \mathrm{d}N &= -N \lambda_t \mathrm{d}t \\ \mathrm{d}N_a &= N \lambda_a \mathrm{d}t \\ \mathrm{d}N_b &= N \lambda_b \mathrm{d}t \\ \mathrm{d}(N + N_a + N_b) &= 0 \ , \end{aligned} \tag{13.9}$$

with solutions:

$$\begin{aligned} N &= N(0)e^{-\lambda_t t} \\ N_a &= N_a(0) + (\lambda_a/\lambda_t)N(0)(1-e^{-\lambda t}) \\ N_b &= N_b(0) + (\lambda_b/\lambda_t)N(0)(1-e^{-\lambda t}) \\ N + N_a + N_b &= N(0) + N_a(0) + N_b(0)\ . \end{aligned} \tag{13.10}$$

One parent, many stable daughters

The results of the one parent (nuclear isotope $\longrightarrow$ 2 stable daughters), can easily be generalized to many daughters. The differential equations are:

$$\begin{aligned} \mathrm{d}N &= -N\lambda_t \mathrm{d}t \\ \mathrm{d}N_1 &= N\lambda_1 \mathrm{d}t \\ \mathrm{d}N_2 &= N\lambda_2 \mathrm{d}t \\ \vdots &= \vdots \\ \mathrm{d}N_n &= N\lambda_n \mathrm{d}t \\ \mathrm{d}\left(N + \sum_{i=1}^{n} N_i\right) &= 0\ , \end{aligned} \tag{13.11}$$

where $\lambda_t = \sum_{i=1}^{n} \lambda_i$. The solutions are given by:

$$\begin{aligned} N &= N(0)e^{-\lambda_t t} \\ N_i &= N_i(0) + (\lambda_i/\lambda_t)N_0(1-e^{-\lambda t}) \\ N + \sum_{i=1}^{n} N_i &= N(0) + \sum_{i=1}^{n} N_i(0)\ . \end{aligned} \tag{13.12}$$

The quantity λ_i/λ_t is called the *branching ratio* for decay into channel i.

Two isotopes, independent decay channels

In this case, the total activity measured is:

$$\mathcal{A}(t) = \mathcal{A}_0^a e^{-\lambda_a t} + \mathcal{A}_0^b e^{-\lambda_b t}\ , \tag{13.13}$$

where a and b label the two different isotopes.

The question arises: How to determine $\mathcal{A}_0^a$, $\mathcal{A}_0^b$, λ_a and λ_b? Krane outlines a strategy portrayed in his Figure 6.2. If, for example, isotope a has a considerably longer half-life, the linear tail of the log-linear plot of $\mathcal{A}$ can be extrapolated backward to isolate $\mathcal{A}_0^a$. The slope of this line also yields λ_a. The one plots $\log(\mathcal{A}(t) - \mathcal{A}_0^a e^{-\lambda_a t})$ that should give a straight line log-linear plot. The values of $\mathcal{A}_0^b$ and λ_b can then be determined.

13.2 Quantum Theory of Radioactive Decay

The Quantum Theory of Radioactive Decay starts with a statement of Fermi's Golden Rule[1] #2, the equation from which decays rates, and cross sections are obtained. It is one of the central equations in Quantum Mechanics. Fermi's Golden Rule #2 for the transition rate (probability of transition per unit time), λ, is given by:

$$\lambda = \frac{2\pi}{\hbar} \left|\langle \psi_f | V_{\rm p} | \psi_i \rangle\right|^2 \frac{{\rm d}n_f}{{\rm d}E_f} \ , \tag{13.14}$$

where ψ_i is the initial quantum state, operated on by a perturbation (transition) potential, $V_{\rm p}$, resulting in the final quantum state, ψ_f. The factor ${\rm d}n_f/{\rm d}E_f$ is called the *density of final states* [sometimes given the notation $\rho(E_f)$]. The density of final states factor enumerates the number of possible final states (degeneracy) that can acquire the final energy E_f. It is not possible to express a less generic form of this factor, without a specific application in mind. It must be derived on a case-by-case basis, for a given application. We shall have opportunity to do this several times before the conclusion of this course.

Application to nuclear γ decay

In this case, we have the following situation:

$$\begin{aligned} N_i^* &\longrightarrow N_f + \gamma \\ \psi^{N_i^*} &\longrightarrow \psi^{N_f} \psi^{\gamma} \\ E_i &= E_f + E_\gamma + E_{\rm R} \ . \end{aligned} \tag{13.15}$$

That is, a nucleus in an initial excited state, N_i^*, has a γ-transition to a final state N_f. The final state may be an intermediate (but lower in energy) excited state. (It is conventional to use an asterisk to represent an excited state.) Without loss of generality, we can assume, for

[1] A derivation of Fermi's Golden Rule #2 is given at the end of this section.

the remaining discussion, that N_f represents the ground state. In (13.15) we see that the energy of the γ is given by the difference in energies of the two nuclear states, less the recoil energy, E_f imparted to the daughter (resultant) nucleus.

If the energy of the excited state is uncertain, we know that its lifetime and its energy are connected through the Heisenberg Uncertainly relationship:

$$\Delta E \Delta t \geq \hbar/2 \ .$$

This is a consequence of the wave description of matter. So, $\Delta E \uparrow \Rightarrow \Delta t \downarrow$, if the uncertainty in energy increases, the uncertainty in the lifetime decreases. Conversely, $\Delta E \downarrow \Rightarrow \Delta t \uparrow$, if the uncertainty in energy decreases, the uncertainty in the lifetime increases.

It remains to discover, therefore, what is the exact relationship between a state's lifetime, and the distribution of energies that are observed? The derivation is sketched below and the results presented. The details of the derivation are left to the optional section at the end of this section.

We start by assuming that the final nuclear state is given by:

$$\begin{aligned} \psi^{N_f}(\vec{x},t) &= \psi^{N_f}(\vec{x}) e^{iE_f t/\hbar} e^{-t/(2\tau)} \\ |\psi^{N_f}(\vec{x},t)|^2 &= |\psi^{N_f}(\vec{x})|^2 e^{-t/\tau} \ , \end{aligned} \tag{13.16}$$

to agree with our discussion, in the last section, of the probability of decay of a single particle. Recall that τ is the "lifetime".

The derivation in the next section reveals that the probability of observing decay energy E, $p(E)$, is given by:

$$p(E) = \frac{\Gamma}{2\pi} \frac{1}{(E-E_f)^2 + (\Gamma/2)^2} \ , \tag{13.17}$$

where $\Gamma \equiv \hbar/\tau$. This probability distribution is normalized:

$$\int_{-\infty}^{\infty} \mathrm{d}E \, p(E) = 1 \ .$$

The peak of this distribution is $p(E_f)$ and Γ width of the distribution at half-maximum. That is, $p(E_f \pm \Gamma/2) = \frac{1}{2} p(E_f)$. Also, $\langle E \rangle = E_f$.

This distribution is called the *Lorentz distribution*, or simply, the *Lorentzian* function. It is also known as *Cauchy-Lorentz distribution*, the *Cauchy distribution*, or the *Breit-Wigner*

distribution. Seems that everyone wants to crash this party! Wikipedia has a useful page on this topic.

The unnormalized Lorentzian is plotted in Figure 13.1, while the normalized Lorentzian is plotted in Figure 13.2.

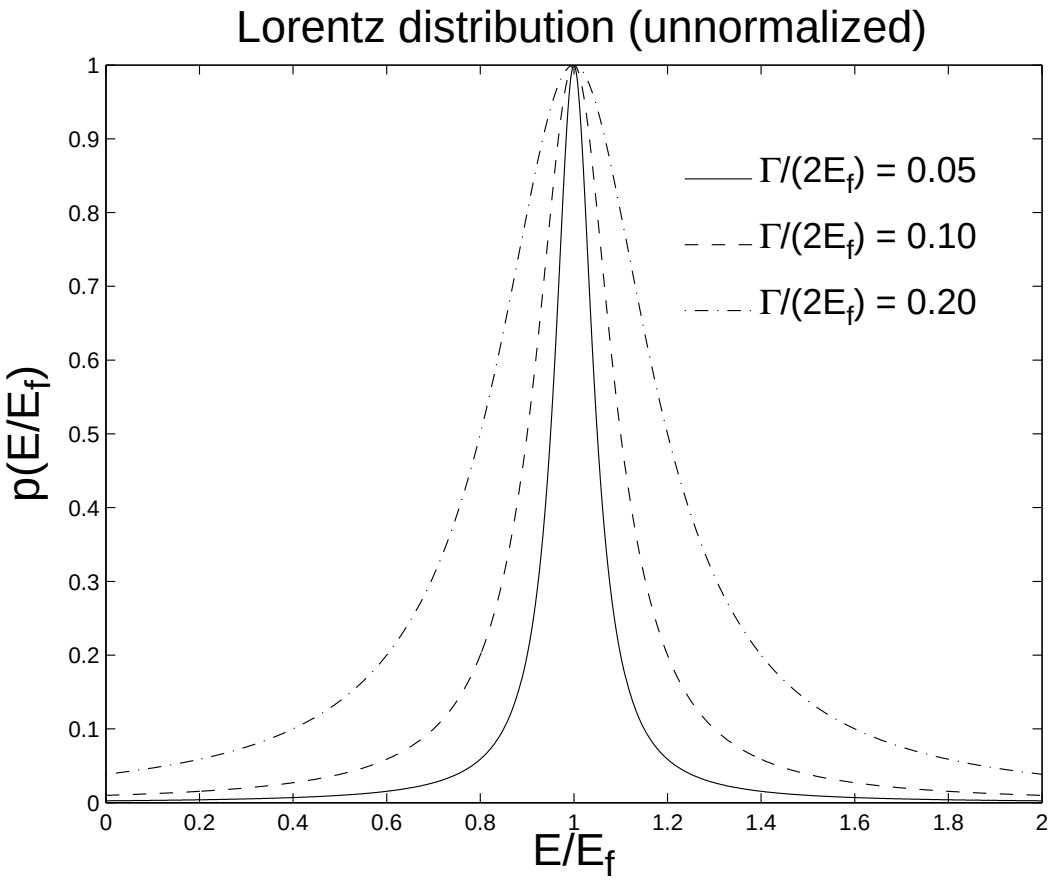

Figure 13.1: The unnormalized Lorentzian.

We note that this spread of energies is intrinsic; it has nothing to do with measurement uncertainties. Even with a perfect detector, we would observe this spread of detected energies.

Finally, we investigate, for typical γ-transition lifetimes, what is the expected range of energy-spreads that is likely to be observed? For 10^{-12} s $< \tau < \infty$, typical for γ decays, we find that 0.00066 eV $> \Gamma > 0$. That is, γ spectroscopy can exquisitely isolate the individual energy levels. The situation is drastically difference for high-energy physics, where intrinsic widths can be of the order of 1 GeV or so. Nearby excitation can overlap with each other, and the identification of excited states (of hadrons) can be very difficult.

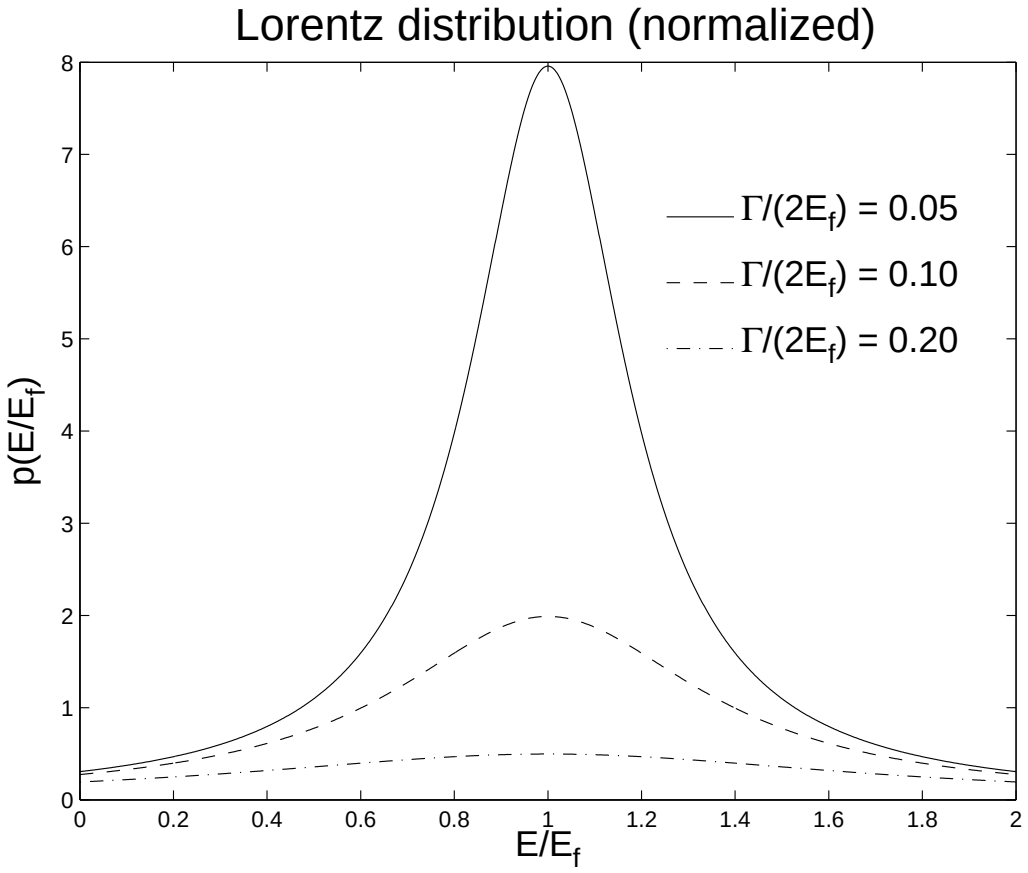

Figure 13.2: The normalized Lorentzian.

Density of final states

Given a final energy of a quantum system, how many states, $\mathrm{d}n_f$ fall in the range, $E_f \longrightarrow E_f + \mathrm{d}E_f$? If we can calculate this, then we can form the ratio $\mathrm{d}n_f/E_f$, the *density of final states*. We proceed with the derivation, assuming that there is just one free particle in the final state. This will cover most situations of interest in this course.

We start by expressing the free particle wave function, as it would exist in a cubical box ($V = 0$ inside, $V \to \infty$ outside, one corner at the origin of the coordinate system)) with side L, and take the limit $L \to \infty$ at the end. As we discovered in NERS311, the wavefunction is given by:

$$\psi_{n_x,n_y,n_z}(x,y,z) = \left(\frac{2}{L}\right)^{3/2} \sin\left(\frac{n_x \pi x}{L}\right) \sin\left(\frac{n_y \pi y}{L}\right) \sin\left(\frac{n_z \pi z}{L}\right) \ , \tag{13.18}$$

where $1 \leq n_i < \infty$ are the 3 quantum numbers ($i = 1, 2, 3$) in the 3D system. The 3

momentum components are given by:

$$p_i = \frac{n_i \pi \hbar}{L} \ . \tag{13.19}$$

We can imagine a 3D lattice of (n_x, n_y, n_z) points occupying the $(+,+,+)$ octant in space (since the n_i's are positive). L is very big, and so, we can treat the n_i as continuous. Let $\vec{n} \equiv n_x\hat{x} + n_y\hat{y} + n_z\hat{z}$ and $n^2 = \vec{n} \cdot \vec{n}$. The number of states, $\mathrm{d}n_f$ in a shell of thickness $\mathrm{d}n$ (all with the same momentum and energy) is given by:

$$\begin{aligned} \mathrm{d}n_f &= \frac{1}{8}\frac{4\pi}{3}[(n+\mathrm{d}n)^3 - n^3] \\ &= \frac{\pi}{6}[n^3 + 3n^2\mathrm{d}n + 3n(\mathrm{d}n)^2 + (\mathrm{d}n)^3 - n^3] \\ &= \frac{\pi}{6}[3n^2\mathrm{d}n + 3n(\mathrm{d}n)^2 + (\mathrm{d}n)^3] \\ &\to \frac{\pi}{2}n^2\mathrm{d}n \ . \end{aligned} \tag{13.20}$$

Thus

$$\frac{\mathrm{d}n_f}{\mathrm{d}E_f} = \frac{\pi}{2}n^2\frac{\mathrm{d}n}{\mathrm{d}E_f} \ . \tag{13.21}$$

Now, it is a simple matter of relating E_f to the magnitude of the quantum number vector n and we are done!

γ-decay

For one photon in the final state, from (13.19)

$$E_\gamma = cp_\gamma = n\pi\hbar c/L \ . \tag{13.22}$$

Thus,

$$\begin{aligned} n &= \frac{E_\gamma L}{\pi\hbar c} \\ \frac{\mathrm{d}n}{\mathrm{d}E_\gamma} &= \frac{L}{\pi\hbar c} \ . \end{aligned} \tag{13.23}$$

Recognizing that $E_f = E_\gamma$, the results of (13.23) used in (13.21) gives:

$$\frac{\mathrm{d}n_f}{\mathrm{d}E_\gamma} = \frac{1}{2\pi^2}\frac{L^3}{(\hbar c)^3}E_\gamma^2 \ . \tag{13.24}$$

Specializing to γ decay, we adapt (13.14) using the notation of (13.15) along with result of (13.24):

$$\lambda_\gamma = \frac{1}{\pi\hbar(\hbar c)^3}\left|\langle\psi^{N_f}[L^{3/2}\psi^\gamma]|V_\mathrm{p}|\psi^{N_i}\rangle\right|^2 E_\gamma^2 \ . \tag{13.25}$$

Note that the $L^{3/2}$ denormalizes the photon wavefunction. Let us call this denormalized wavefunction $L^{3/2}\psi^\gamma \equiv \tilde{\psi}^\gamma$. It has no units associated with it. Hence the expression, $|\langle\psi^{N_f}\tilde{\psi}^\gamma|V_\mathrm{p}|\psi^{N_i}\rangle|^2$ has units (energy)^2(length)^3, and has a scale proportional to the volume of the nucleus. Hence, λ_γ has units s^{-1}, and is correctly dimensioned.

Derivation of Fermi's Golden Rule #2

Here is the theoretical background for the earlier parts of this section. It's optional material, but may be of interest to some readers.

Fermi's Golden Rule #2 is one of the central equations in radiation physics, as it is employed to obtain decay rates and cross sections. Thus, a clear derivation is called for.

Consider the Schrödinger equation for a single particle in a static binding potential:

$$\mathcal{H}_0\Psi(\vec{x},t) = \frac{i}{\hbar}\Psi(\vec{x},t) \tag{13.26}$$

where

$$\begin{aligned} \mathcal{H}_0 &= \mathcal{T} + V(\vec{x}) \\ \mathcal{T} &= -\frac{\hbar^2}{2m}\nabla^2 \end{aligned} \tag{13.27}$$

We know that such a potential has a set of orthonormal eigenstates:

$$|j\rangle = \Psi_j(\vec{x},t) = \Psi_j(\vec{x})e^{-E_jt/\hbar} \ , \tag{13.28}$$

with eigenenergies, E_j. These eigenstates are orthonormal, that is,

$$\langle i|j\rangle = \delta_{ij} \ . \tag{13.29}$$

We know that the E_j's are constants, and fixed. By Heisenberg's Uncertainly Principle, we also know that all eigenstates are stable, as there is no mechanism for decay. In Nature, we know that excited states eventually decay to the ground state, and the purpose of this derivation is to obtain an expression for that decay rate.

We start by assuming that there is a perturbation potential that is time dependent, $V_{\rm p}(\vec{x},t)$.

Now we solve:

$$(\mathcal{H}_0 + V_{\rm p})\Psi = \frac{i}{\hbar}\frac{\partial\Psi}{\partial t} \ , \tag{13.30}$$

where Ψ is the general solution to the entire problem, with both static and perturbation potentials included.

To start, we write $\Psi(\vec{x},t)$ as a superposition of the eigenstates of the $\mathcal{H}_0$ operator, that is:

$$\Psi(\vec{x},t) = \sum_j a_j(t)\Psi_j(\vec{x},t) \tag{13.31}$$

Taking the partial derivative (13.31) with respect to t gives: (Henceforth, for brevity, obvious functional dependences on space and time will usually be suppressed.)

$$\frac{\partial\Psi}{\partial t} = \sum_j \left(\dot{a}_j - i\frac{E_j}{\hbar}\right)\Psi_j \ . \tag{13.32}$$

(13.32) + (13.31) $\longrightarrow$ *(13.30)* $\Rightarrow$

$$\sum_j a_j(\mathcal{H}_0 - E_j)\Psi_j + \sum_j (a_j V_\mathrm{p} - i\hbar\dot{a}_j)\Psi_j = 0 \ . \tag{13.33}$$

The first summation is zero, because each Ψ_j *is a eigenfunction of the unperturbed* $\mathcal{H}_0$ *with eigenenergy* E_j*. Thus,*

$$\sum_j (a_j V_\mathrm{p} - i\hbar\dot{a}_j)\Psi_j = 0 \ , \tag{13.34}$$

or,

$$\sum_j (a_j V_\mathrm{p} - i\hbar\dot{a}_j)|j\rangle = 0 \ . \tag{13.35}$$

Let $|f\rangle$ *be the state that the excited states* $|j\rangle$ *transitions to. You can think of* $|f\rangle$ *as the ground state, or at least a lower excited state.*

$\langle f| \bigotimes$ *(13.35)* $\Rightarrow$

$$\sum_j (a_j \langle f|V_\mathrm{p}|j\rangle e^{i(E_j - E_f)/\hbar} - i\hbar\dot{a}_j)\delta_{jf} = 0 \ . \tag{13.36}$$

Using the shorthand notation $V_{jf} \equiv \langle f|V_\mathrm{p}|j\rangle$ *and* $\omega_{jf} \equiv (E_j - E_f)/\hbar$*, we have:*

$$i\hbar\dot{a}_f = \sum_j a_j V_{jf} e^{i(E_j - E_f)/\hbar} \ . \tag{13.37}$$

(13.37) represents, at least in principle, an exact solution the problem. All one needs to do is to set an initial condition, say, $a_n(0) = 1$ *(the excited state) and then al the other a's, potentially an infinite number (!) to zero, and then let the solution evolve. Note that every single eigenstate can be involved in the eventual de-excitation of* $|n\rangle$*. This approach is more amenable to numerical solution. So, to proceed with the analysis, we make the ...*

Small perturbation approximation

In this approximation, we only have two states, the initial excited and final states, $|i\rangle$ and $|f\rangle$. None of the other states are are assumed to be involved. In the spirit of this approximation, we treat the a's on the right hand side of (13.37) as constants. (This is how the system would evolve for small t for any perturbation, large or small.)

Hence we set $a_i(t) = 1 \ \forall \ t$, $a_f(0) = 0$, we allow these to change with time, and all the other a's are set to zero for all time. This allows us to integrate the equation, resulting in:

$$a_f = V_{if} \frac{1 - e^{i\omega_{if}}}{\hbar\omega_{if}} \ . \tag{13.38}$$

Now, we evaluate the occupation probability of the state to which the transition is made,

$$P = |a_f|^2 = |V_{if}|^2 \frac{(1 - e^{i\omega_{if}})(1 - e^{-i\omega_{if}})}{(\hbar\omega_{if})^2} \ . \tag{13.39}$$

Using some trigonometric identities, this can be recast into the following form:

$$P = |a_f|^2 = \frac{|V_{if}|^2}{\hbar^2} \frac{\sin^2(\omega_{if}t/2)}{(\omega_{if}/2)^2} \ . \tag{13.40}$$

The derivation of (13.40) assumed that the energy of the initial state $|i\rangle$ is precisely known. However, we know from the Heisenberg's Uncertainly Principle, $\Delta E \Delta t \geq \hbar/2$, that the energy of an excited state can not be known precisely, but distributed in some way. So, assume that the energy of the excited state is distributed according to some distribution $\rho(\omega)$. We must integrate over all of these to obtain the occupation probability:

$$P = \int_{-\infty}^{\infty} \mathrm{d}\omega \ \frac{|V_{if}|^2}{\hbar^2} \rho(\omega) \frac{\sin^2((\omega_{if} - \omega)t/2)}{((\omega_{if} - \omega)/2)^2} \ . \tag{13.41}$$

The

$$\frac{\sin^2((\omega_{if} - \omega)t/2)}{((\omega_{if} - \omega)/2)^2}$$

term in the above equation acts as a delta function for large t, narrowing as t increases. We eventually want to consider the decay of the excited state to the final state, so we take the large t limit to obtain, after a change of variables:

$$P = \frac{|V_{if}|^2}{\hbar^2} \rho(\omega_{if}) 2t \int_{-\infty}^{\infty} \mathrm{d}x \ \frac{\sin^2 x}{x^2} \ . \tag{13.42}$$

The integral evaluates numerically to π, thus

$$P = \frac{2\pi}{\hbar^2}|V_{if}|^2\rho(\omega_{if})t \tag{13.43}$$

We can also rewrite $\rho(\omega_{if})$ in terms of E_{if}. Since $E_{if} = \hbar\omega_{if}$,

$$P = \frac{2\pi}{\hbar}|V_{if}|^2\rho(E_{if})t \ . \tag{13.44}$$

Finally, the rate of decay, $\lambda = \mathrm{d}P/\mathrm{d}t$. Hence,

$$\lambda = \frac{2\pi}{\hbar}|V_{if}|^2\rho(E_{if}) \ , \tag{13.45}$$

and we have derived Fermi's Golden Rule #2.

A few comments are in order.

The "blurring" function $\rho(E_{if})$ is sometimes referred to as the "density of final states". We had to introduce it, in a somewhat ad hoc *fashion to recognize that excited states are, indeed, "blurred". However, it is fascinating to note, that this blurring is directly connected to the existence of final states for the system to accept the decay. For example, a typical nuclear decay involves the release of a γ. Unless this γ has a quantum state to occupy it, there can be no quantum mechanical transition. Hence, our interpretation of the 'blurring" of excited states depends on our ability to measure its decay. If there is no decay mode, then this density of states function drops to zero, the decay does not occur, and hence, the energy of the excited state is precise! (But not measurable!)*

What is the nature of this "blurring"?

The Lorentz distribution

If an excited state can decay, we may write its wavefunction in the following form:

$$\Psi(\vec{x},t) = \Psi(\vec{x})e^{iE_it/\hbar}\frac{e^{-t/(2\tau)}}{\sqrt{\tau}} \ , \tag{13.46}$$

where τ is its mean life. This interpretation follows directly from the probability density of the excited state:

$$|\Psi(\vec{x},t)|^2 = |\Psi(\vec{x})|^2 \frac{e^{-t/\tau}}{\tau} \ , \tag{13.47}$$

giving the well-known exponential decay law, properly normalized over the domain $0 \leq t < \infty$. *Here we are adopting the normalization convention that*

$$\int_0^\infty \mathrm{d}t \, |\Psi(\vec{x},t)|^2 = |\Psi(\vec{x})|^2 \ .$$

Just as the dynamic variables k *and* x *are related by Fourier transforms in the operational sense, this is true as well for* ω *and* t. *Hence the above distribution in time, namely* $e^{-t/\tau}$, *is converted to a distribution in frequency by its Fourier transform, namely,*

$$\Psi_i(\vec{x},\omega) = \Psi_i(\vec{x}) \frac{1}{\sqrt{2\pi\tau}} \int_0^\infty \mathrm{d}t \, e^{i(\omega_i - \omega)t} e^{-t/(2\tau)} \ , \tag{13.48}$$

where $\omega_i = E_i$ *and* $\omega = E$.

After performing the integral

$$\Psi_i(\vec{x},\omega) = \Psi_i(\vec{x}) \frac{1}{\sqrt{2\pi\tau}} \frac{1}{i(\omega_i - \omega) + 1/(2\tau)} \ , \tag{13.49}$$

Therefore,

$$|\Psi_i(\vec{x},\omega)|^2 = |\Psi_i(\vec{x})|^2 \frac{1}{2\pi\tau} \left(\frac{1}{(\omega_i - \omega)^2 + (1/(2\tau))^2} \right) \ . \tag{13.50}$$

In terms of E *rather than* ω,

$$|\Psi_i(\vec{x},E)|^2 = |\Psi_i(\vec{x})|^2 \frac{\Gamma}{2\pi} \left(\frac{1}{(E_i - E)^2 + (\Gamma/2)^2} \right) \ , \tag{13.51}$$

where $\Gamma \equiv \hbar/\tau$.

Thus we have found the form of the Lorentz distribution:

$$|\Psi_i(\vec{x},E)|^2 = |\Psi_i(\vec{x})|^2 \frac{\Gamma}{2\pi} \left(\frac{1}{(E_i - E)^2 + (\Gamma/2)^2} \right) \ . \tag{13.52}$$

One may easily verify that:

$$\int_{-\infty}^{\infty} \mathrm{d}E \, |\Psi_i(\vec{x}, E)|^2 = |\Psi(\vec{x})|^2 \ . \tag{13.53}$$

13.3 Production and Decay of Radioactivity

Secular equilibrium

Consider a beam of radiation, with intensity I, that impinges upon a block of material containing nuclei of type "0". There are N_0 nuclei in the target to start, and the external radiation activates the material, producing nuclear species "1". We make two assumptions:

1. The target is "thin enough", so that the external radiation is not attenuated.
2. The irradiation is weak enough so that N_0 does not decline.

With these assumptions, R, the rate of production of N_1 is given by:

$$R = I\sigma N_0 \ , \tag{13.54}$$

where σ is the radioactivity production cross section.

The differential equation describing the production of N_1 is given by:

$$\mathrm{d}N_1 = R\mathrm{d}t - \lambda_1 N_1 \mathrm{d}t \ , \tag{13.55}$$

where λ_1 is the decay rate of nucleus "1". Solving (13.55):

$$\begin{aligned}
\dot{N}_1 + \lambda_1 N_1 &= R \\
(\dot{N}_1 + \lambda_1 N_1) e^{\lambda_1 t} &= R e^{\lambda_1 t} \\
\frac{\mathrm{d}}{\mathrm{d}t}(N_1 e^{\lambda_1 t}) &= R e^{\lambda_1 t} \\
N_1 e^{\lambda_1 t} - N_1(0) &= \frac{R}{\lambda_1}(e^{\lambda_1 t} - 1) \\
N_1 - N_1(0) e^{-\lambda_1 t} &= \frac{R}{\lambda_1}(1 - e^{-\lambda_1 t}) \\
N_1 &= N_1(0) e^{-\lambda_1 t} + \frac{R}{\lambda_1}(1 - e^{-\lambda_1 t}) \ .
\end{aligned} \tag{13.56}$$

Usually the target contains no activity at $t = 0$. If $N_1(0) = 0$:

$$\begin{aligned} N_1 &= \frac{R}{\lambda_1}(1 - e^{-\lambda_1 t}) \\ \mathcal{A}_1 &= R(1 - e^{-\lambda_1 t}) \ . \end{aligned} \tag{13.57}$$

Condition	Beam	$\mathcal{A}_1(t)$	Description
$\lambda_1 t \ll 1$ *i.e.* $t \ll \tau$	ON	$R\lambda_1 t$	initial production
$\lambda_1 t \gg 1$ *i.e.* $t \gg \tau$	ON	R	secular equilibrium
$t \geq t_0$, t_0 is arbitrary	OFF (at $t = t_0$)	$N_1(t_0)\lambda_1 e^{-\lambda_1(t-t_0)}$	decay of activity
$t \geq t_0 \gg \tau$	OFF (at $t = t_0$)	$Re^{-\lambda_1(t-t_0)}$	decay of activity (from secular equilibrium)

During the condition of *secular equilibrium*, the rate of production is the same as the rate of decay, producing an unchanging number of radioactive daughter nuclei. (There will be some statistic fluctuation of this number.)

A depiction of a nuclide reaching secular equilibrium is shown in Figure 13.3.

A real-life engineering application

A typical engineering challenge, in the area of creating radioactive sources, is to minimize the cost of producing a given amount of activity. We model this as follows:

The cost, C, per unit activity, factoring start-up costs, S_0, (manufacture of the inactive source, delivery costs, operator start-up and take-down), and the cost of running the accelerator or reactor, per unit meanlife, R_0, is given as follows:

$$C = \frac{S_0 + R_0 x_0}{1 - e^{-x_0}} \ , \tag{13.58}$$

where x_0 is the number of meanlifes that the target is irradiated.

The optimization condition is given by:

$$S_0/R_0 = e^{x_0} - (1 + x_0) \ . \tag{13.59}$$

For small S_0/R_0, the optimum $x_0 \approx \sqrt{2S_0/R_0}$. For large S_0/R_0, the optimum $x_0 \approx \log(S_0/R_0)$.

The solutions for the optimum value of x_0 can be obtained from Figure 13.4.

The figure has been split into two parts, $x_0 < 1$ for which S_0/R_0 is shown, and $x_0 > 1$ for which $\log(S_0/R_0)$ is shown. The approximations discussed above, are plotted as dotted lines.

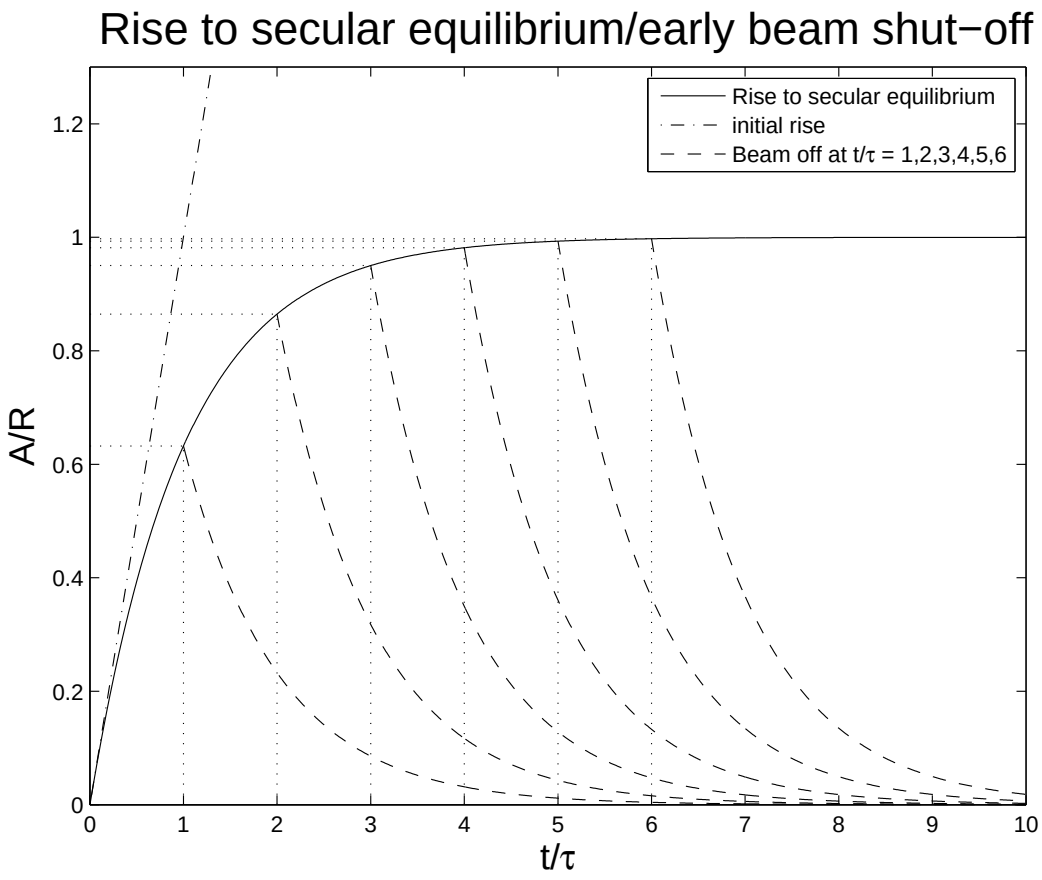

Figure 13.3: A nuclide reaching secular equilibrium is depicted. Also depicted are the decays of the source once the beam is shot off at $t/\tau = 1, 2, 3, 4, 5$.

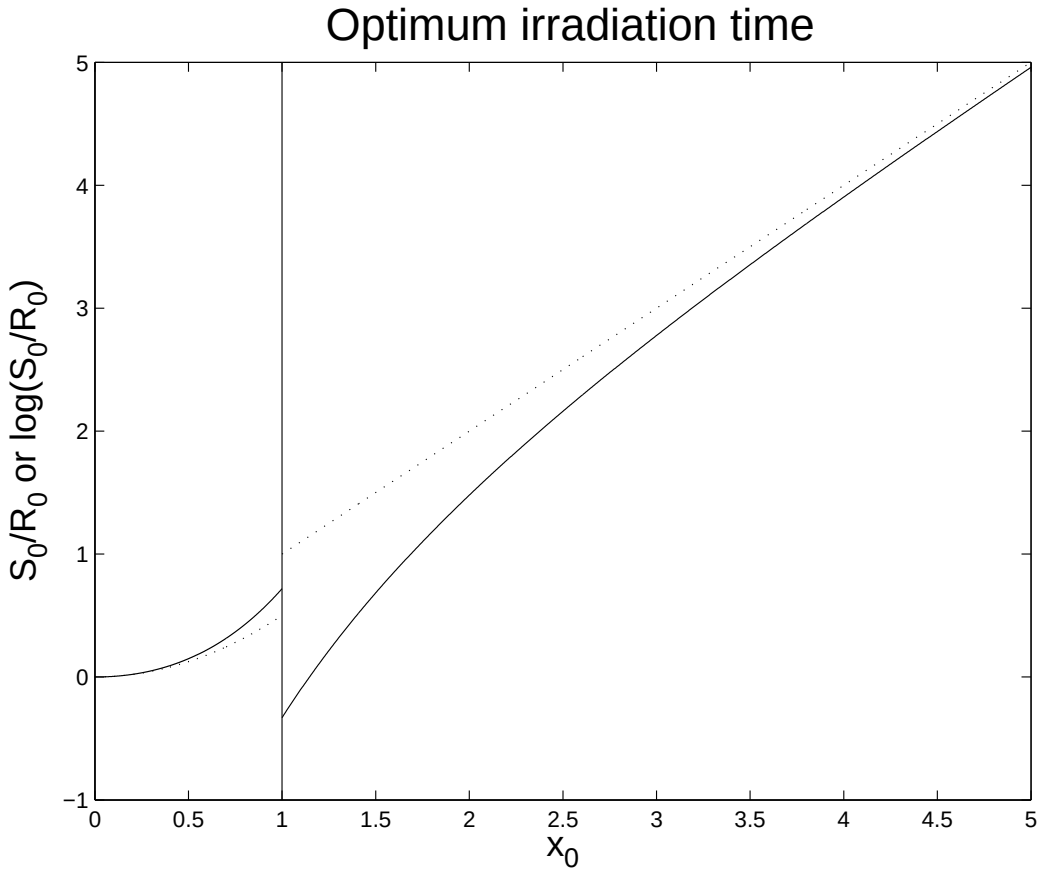

Figure 13.4: Optimization curves for determining x_0, as a function of $\alpha = S_0/R_0$.

13.4 Growth of Daughter Activities

Parent ⇒ Daughter ⇒ Granddaughter (stable)

We now describe the simplest decay *chain*, whereby a parent decays to an unstable daughter, that decay to a stable granddaughter. We'll use Krane's notation:

Differential equation	At $t = 0$	Description
$\dot{N}_1 = -\lambda_1 N_1$	$N_1(0) = N_0$	N_1: Parent–rate constant λ_1 (decay only)
$\dot{N}_2 = \lambda_1 N_1 - \lambda_2 N_2$	$N_2(0) = 0$	N_2: Daughter–growth, decay rate constant λ_2
$\dot{N}_3 = \lambda_2 N_2$	$N_3(0) = 0$	N_3: Granddaughter–growth only
$\dot{N}_1 + \dot{N}_1 + \dot{N}_3 = 0$		"Conservation of particles"

The integrals are elementary, giving, for the N_i's:

$$\begin{aligned} N_1 &= N_0 e^{-\lambda_1 t} \\ N_2 &= N_0 \frac{\lambda_1}{\lambda_2 - \lambda_1}(e^{-\lambda_1 t} - e^{-\lambda_2 t}) \\ N_3 &= N_0 - N_1 - N_2 \end{aligned} \tag{13.60}$$

In this discussion, we concern ourselves mostly with the activity of the daughter, in relation to the parent, namely:

$$\mathcal{A}_2 = \mathcal{A}_1 \frac{\lambda_2}{\lambda_2 - \lambda_1}(1 - e^{-(\lambda_2 - \lambda_1)t}) \ , \tag{13.61}$$

and consider some special cases.

Very long-lived parent: $\lambda_1 \lll \lambda_2$

In this case, the parent's meanlife is considered to be much longer than that of the daughter, essentially infinite within the time span of any measurement of interest. In other words, the activity of the parent is constant. In this case, (13.61) becomes:

$$\mathcal{A}_2 = \mathcal{A}_1(0)(1 - e^{-\lambda_2 t}) \ . \tag{13.62}$$

Comparing with (13.57), we see that (13.62) describes $\mathcal{A}_2$'s rise to secular equilibrium, with effective rate constant, $\mathcal{A}_1(0)$.

Long-lived parent: $\lambda_1 \ll \lambda_2$

In this case, the parent lives much longer than the daughter, but the parent does have a measurable decline, within the time span of the measurement.

We rewrite (13.61) slightly as:

$$\mathcal{A}_2(t) = \mathcal{A}_1(t) \left(\frac{\lambda_2}{\lambda_2 - \lambda_1} (1 - e^{-(\lambda_2 - \lambda_1)t}) \right) \ . \tag{13.63}$$

(13.63) describes $\mathcal{A}_2(t)$ a modulation of $\mathcal{A}_1(t)$. An example is shown in figure 13.5.

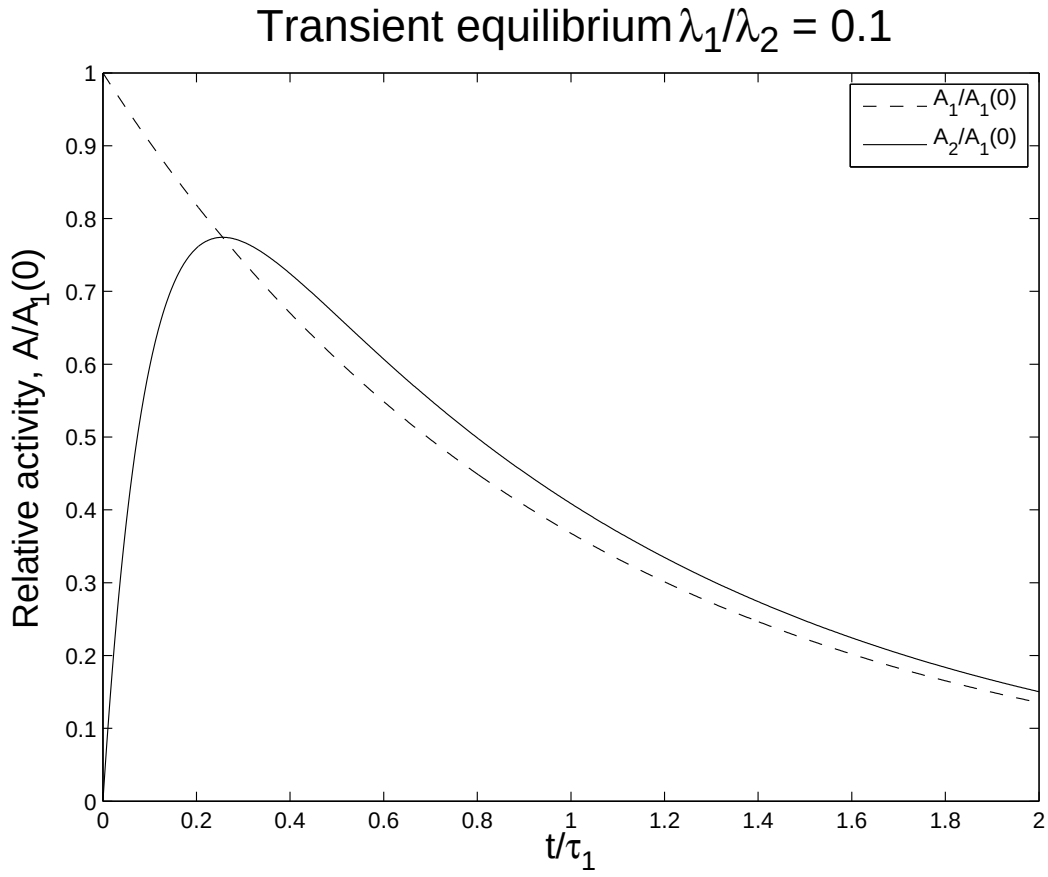

Figure 13.5: The relative activity of the daughter, $\mathcal{A}_2$ and the parent, $\mathcal{A}_2$, for $\lambda_2 = 10\lambda_1$.

We see, from the figure, that the activity of the daughter, $\mathcal{A}_2$, rises quickly to match the parent, and then follows the parent activity closely. This latter condition, beyond a few meanlifes of the daughter, is called the region of *transient secular equilibrium*, or more commonly, *transient equilibrium*. In the region of transient equilibrium, the activity of the

daughter is always slightly greater than that of the parent, with a temporal offset of about τ_2.

Special case: $\lambda = \lambda_1 = \lambda_2$

In this case, parent and daughter decay with the same meanlife. This is more of a mathematical curiosity, but should it occur, the result can be derived from (13.63) by assuming $\lambda_1 = \lambda$, $\lambda_1 = \lambda + \epsilon$, performing a series expansion in ϵ, and taking the $\epsilon \to 0$ at the end. The result is:

$$\mathcal{A}_2(t) = \mathcal{A}_1(t)\lambda t \ . \tag{13.64}$$

Series of Decays

In this case, we consider a series of descendents, $N_1 \Rightarrow N_2 \Rightarrow N_2 \cdots \Rightarrow N_n$, with rate constants, $\lambda_1, \lambda_2 \cdots \lambda_n$. That is, there are n generations, starting with the parent, N_1, and ending with a final stable (grand)$^{n-2}$daughter, for $n \geq 2$.

The result of the solution of the differential equations:

Differential equation	At $t = 0$	Description
$\dot{N}_1 = -\lambda_1 N_1$	$N_1(0) = N_0$	N_1: Parent–rate constant λ_1 (decay only)
$\dot{N}_i = \lambda_{i-1}N_{i-1} - \lambda_i N_i$	$N_i(0) = 0$	N_i: (grand)$^{n-2}$, decay rate constant λ_i
$\dot{N}_n = \lambda_n N_n$	$N_n(0) = 0$	N_n: Stable end of chain (growth only)
$\sum_{i=1}^{n} \dot{N}_i = 0$		"Conservation of particles"

The result is given by the *Bateman equations*:

$$\begin{aligned} N_1 &= N_0 e^{-\lambda_i t} \\ N_{1<i<n} &= N_0 \sum_{j=1}^{i} \left(\frac{\prod_{k=1;k\neq i}^{i} \lambda_k}{\prod_{k=1;k\neq j}^{i} (\lambda_k - \lambda_j)} \right) e^{-\lambda_j t} \\ N_n &= N_0 - \sum_{i=2}^{n-1} N_i \ . \end{aligned} \tag{13.65}$$

Note the exclusions in the product terms.

13.5 Types of Decays

Details are covered elsewhere in this course. Here we just give a list.

α decay

This is the form employed when an accurate mass calculation is to be performed. Electron masses cancel, and the small differences in electron binding energy are ignored.

$$ {}^{A}_{Z}X_{N} \longrightarrow {}^{A-4}_{Z-2}X'_{N-2} + {}^{4}_{2}\mathrm{He}_{2} \ . $$

Usually the following shorthand is employed:

$$ {}^{A}X \longrightarrow {}^{A-4}X' + \alpha \ . $$

To come, more details on ...
Applications of α-emitters:

- "Gadget" initiators (α-decay followed by n-emission.)
- Search for superheavy elements. See
  `http://t2.lanl.gov/tour/shn.html`
- Smoke detectors.
- Power generation in space probes and artificial hearts.
- Unsealed source radiotherapy.
- Can be used to reduce static cling. (Really! I'm not kidding! The real question is "How?")

β decay

$$
\begin{array}{rcll}
n & \longrightarrow & p + e^{-} + \overline{\nu}_{e} & \beta^{-} \text{ decay} \\
{}^{A}_{Z}X_{N} & \longrightarrow & {}^{A}_{Z+1}X'_{N-1} + e^{-} + \overline{\nu}_{e} & \\
p & \longrightarrow & n + e^{+} + \nu_{e} & \beta^{+} \text{ decay} \\
{}^{A}_{Z}X_{N} & \longrightarrow & {}^{A}_{Z-1}X'_{N+1} + e^{+} + \nu_{e} & \\
p + e^{-} & \longrightarrow & n + \nu_{e} & \text{electron capture } (\varepsilon) \\
{}^{A}_{Z}X_{N} & \longrightarrow & {}^{A}_{Z-1}X'_{N+1} + \nu_{e} &
\end{array}
$$

A free neutron will β^- decay with a meanlife of 886.7(8) s. A neutron in a nucleus will β^- decay, but only when that process is favorable energetically.

Free protons do not decay, that is, it has never been observed. Proton decay is predicted by Grand Unified Theories (GUTs). However, the predicted probability of decay is exceedingly small. A lower bound for proton decay has been established experimentally, setting the half-life at greater than 6.6×10^{33} years. This is interesting, but of little consequence for Nuclear Engineering. Protons in a nucleus, if favored energetically, do β^+ decay.

Finally, there is a process called *electron capture*, (ε), or *K-capture*, whereby a proton in a nucleus captures an orbital electron (usually from a $1s$ atomic orbital, and converts itself to a neutron.

All these process result in a *electron neutrino*, ν_e, or an *electron antineutrino*, $\overline{\nu}_e$. By convention, antiparticles, like the antiproton, $\overline{p}$, and the antineutron, $\overline{n}$, are written with an overline $\bar{}$ or an "overtilde" $\tilde{}$. There are exceptions to this rule. The positron, e^+ is the e^-'s antiparticle. However, it is never written as $\overline{e^-}$.

To come, more details on ...
Applications of β-emitters:

- Betavoltaics (non-thermal) (long-life, low-power batteries).
- Radiotherapy (brachytherapy).
- PET (Positron Emission Tomography.)
- Radiopharmaceuticals.
- Quality assurance in large-scale paper production.
- Irradiation of domestic ruminant (cattle, goats, sheep, bison, deer, camels, alpacas, llamas) behinds to cure the effects of "fly strike". (I'm not kidding about this one either.) (And I'd really rather not delve into the details of "fly strike". Kindly google this one on your own.)

γ decay

$$ {}^{A}X^{*} \longrightarrow {}^{A}X + \gamma $$

Here, a nucleus in an excited state, denoted by the asterisk, decays via the γ process, to a lower excited state, or the ground state. All nuclei that are observed to have excited states, ($A > 5$), have γ transitions.

To come, more details on ...
Applications of γ-emitters:

- Basic physics: Nuclear structure, astrophysics.
- Radiotherapy, ^{60}Co, ^{137}Cs, brachytherapy..
- Sterilization of pharmaceutical products, food.
- Imaging vehicles for National Security Administration purposes.
- Industrial quality assurance.
- Discovery of oil. (Oil-well logging.)

Internal conversion

$$ {}^{A}_{Z}X^{*}_{N} \longrightarrow {}^{A}_{Z}X_{N} + e^{-} $$

Here, a nucleus in an excited state, de-excites by exchanging a virtual photon with a K-shell electron in a "close encounter" with the nucleus. The electron acquires the de-excitation energy and exits the nucleus.

Nucleon emission

$$ \begin{aligned} {}^{A}_{Z}X_{N} &\longrightarrow {}^{A-1}_{Z-1}X_{N} + p \\ {}^{A}_{Z}X_{N} &\longrightarrow {}^{A-1}_{Z}X_{N-1} + n \end{aligned} $$

To come, more details on ...
Applications of nucleon emitters:

- Fission.

Spontaneous fission

$$ {}^{A}_{Z}X_N \longrightarrow \sum_{i,j} c_{i,j}[{}^{i+j}_{i}X_j + {}^{A-i-j}_{Z-i}X_{N-j}] $$

Here a nucleus fractures into 2 (equation shown) or more (equation not shown) nuclei. This is similar to "normal" fission, except that it occurs spontaneously. Generally a spectrum of nuclei result, with the probabilities given by the c coefficients.

Cluster decay

$$ {}^{A}_{Z}X_N \longrightarrow {}^{i+j}_{i}X_j + {}^{A-i-j}_{Z-i}X_{N-j} $$

where $i, j > 2$.

From:

`http://en.wikipedia.org/wiki/Cluster_decay`!...

Cluster decay is a type of nuclear decay in which a radioactive atom emits a cluster of neutrons and protons heavier than an alpha particle. This type of decay happens only in nuclides which decay predominantly by alpha decay, and occurs only a small percentage of the time in all cases. Cluster decay is limited to heavy atoms which have enough nuclear energy to expel a portion of its nucleus.

13.6 Natural Radioactivity

Not covered in 312

13.7 Radioactive Dating

Not covered in 312

13.8 Units for Measuring Radiation

Some useful radiometric quantities are listed in Table 13.1, along their traditional (outdated but still in some use), along with their new, almost universally adopted, SI[2].

Quantity	Measures...	Old Units	New (SI) Units
Activity ($\mathcal{A}$)	decay rate	curie (Ci)	bequerel (Bq)
Exposure (X)	ionization in air	röntgen (R)	C/kg
Absorbed Dose (D)	Energy absorption	rad	gray (Gy = J/kg)
Dose Equivalent (DE)	Radiological effectiveness	rem	sievert (Sv = J/kg)

Table 13.1: Units for the measurement of radiation

SI units	Definition	Notes:
Bq	1 "decay"/s	derived
Gy	1 J/kg	derived
Sv	1 J/kg	derived
Traditional units	**Conversion**	**Notes:**
Ci	3.7×10^{10} Bq (exactly)	
R	1 esu/(0.001293 g) $= 2.58 \times 10^{-4}$ C/kg	Charge/(1g) of dry, STP air
rad	1 ergs/g $= 10^{-2}$ Gy	
rem	1 rem $= 10^{-2}$ Sv	

Table 13.2: Conversion factors

A derived unit is one that is based upon the sever base units in SI, namely: m, kg, s, A, K, mol (mole), cd (candela, luminosity).

Activity

Activity ($\mathcal{A}$) has been covered already. However, the units of measurement were not discussed. The traditional unit, the *curie*, (Ci),was named in honor of Marie Curie, and the modern unit in honor of Henri Bequerel.

[2]SI stands for *le* **S***ystème* **I***nternational d'unitś*, that was adopted universally (almost) in 1960. For more information, see: `http://en.wikipedia.org/wiki/SI` units. SI is an abbreviation of a French-language phrase. France also houses the international metrology, the BIPM (*le* **B***ureau* **I***nternational des* **P***oids et* **M***esures.*) See, as well, `http://en.wikipedia.org/wiki/BIPM` .

Exposure

Exposure, given the symbol X, is defined as

$$X = \lim_{\Delta m \to 0} \frac{\Delta Q}{\Delta m} \ , \tag{13.66}$$

where ΔQ is the amount of charge of one sign produced in, dry, STP air. (NIST definition: STP at STP: 20°C (293.15 K, 68°F, and an absolute pressure of 101.325 kPa (14.696 psi, 1 atm).) There are no accepted derived SI unit for exposure. Exposure measurements are probably the most accurately measured radiometric quantity.

Absorbed Dose

Absorbed dose measures the energy absorbed in matter, due to radiation. The traditional unit, the rad, has been supplanted by the Gy.

Dose Equivalent

The tradition unit, the rem (for röntgen equivalent man) and its modern counterpart, the Sv, attempts to accounts for the radiological damage from different "qualities" (species of particle imparting the dose) of radiation. Quality factors dependent on the energy of the radiation and are given in Table 13.2. The conversion from D to DE is given by:

$$\mathrm{DE} = \sum_i \int \mathrm{d}E \, D_i(E) \times \mathrm{QF}_i(E) \ , \tag{13.67}$$

where we sum over radiation types, and integrate over the energy of the radiation that imparts dose.

Radiation	Energy	QF
X-rays, γ, $e^{\pm}$, $\mu^{\pm}$	all	1
p (non-recoil)	> 1 MeV	5
n	< 10 keV	5
	10–100 keV	10
	10 keV – 2 MeV	20
	2–20 MeV	10
	>20 MeV	5
α, fission fragments, heavy nuclei	all	20

Table 13.3: Units for the measurement of radiation

Chapter 14

α Decay

Note to students and other readers: This Chapter is intended to supplement Chapter 8 of Krane's excellent book, "Introductory Nuclear Physics". Kindly read the relevant sections in Krane's book first. This reading is supplementary to that, and the subsection ordering will mirror that of Krane's, at least until further notice.

14.1 Why α Decay Occurs

See Krane's 8.1.

14.2 Basic α Decay Processes

An α decay is a nuclear transformation in which a nucleus reduces its energy by emitting an α-particle.

$$ {}^{A}_{Z}X_{N} \longrightarrow {}^{A-4}_{Z-2}X'_{N-2} + {}^{4}_{2}\mathrm{He}_{2} \ , $$

or, more compactly :

$$ {}^{A}X \longrightarrow X' + \alpha \ . $$

The resultant nucleus, X' is usually left in an excited state, followed, possibly, by another α decay, or by any other form of radiation, eventually returning the system to the ground state.

The energetics of α decay

The α-decay process is "fueled" by the rest mass energy difference of the initial state and final state. That is, using a relativistic formalism:

$$\begin{aligned} E_{\rm i} &= E_{\rm f} \\ m_{_X}c^2 &= m_{_{X'}}c^2 + T_{X'} + m_\alpha c^2 + T_\alpha \\ Q &= T_{X'} + T_\alpha \quad \text{where} \\ Q &\equiv m_{_X}c^2 - m_{_{X'}}c^2 - m_\alpha c^2 \\ Q/c^2 &\approx m(^A X) - m(^{A-4}X') - m(^4\text{He}) \ , \end{aligned} \tag{14.1}$$

where $T_{X'}$ and T_α are the kinetic energies of the nucleus and the α-particle following the decay. Note that atomic masses may be substituted for the nuclear masses, as shown in the last line above. The electron masses balance in the equations, and there is negligible error in ignoring the small differences in electron binding energies.

The line of flight of the decay products are in equal and opposite directions, assuming that X was at rest. Conservation of energy and momentum apply. Thus we may solve for T_α in terms of Q (usually known). X' is usually not observed directly. Solving for T_α by eliminating X':

$$\begin{aligned} Q &= T_\alpha + T_{X'} \qquad (14.2) \\ |\vec{p}_\alpha| &= |\vec{p}_{_{X'}}| \\ p_\alpha^2 &= p_{_{X'}}^2 \\ 2m_\alpha T_\alpha &= 2m_{_{X'}}T_{X'} \\ (m_\alpha/m_{_{X'}})T_\alpha &= T_{X'} \ . \qquad (14.3) \end{aligned}$$

Using (14.3) and (14.2) to eliminate $T_{X'}$ results in:

$$\begin{aligned} Q &= T_\alpha(1 + m_\alpha/m_{_{X'}}) \quad \text{or} \qquad (14.4) \\ T_\alpha &= \frac{Q}{(1 + m_\alpha/m_{_{X'}})} \qquad (14.5) \\ T_\alpha &\approx \frac{Q}{(1 + 4/A')} \quad \text{or} \qquad (14.6) \\ T_\alpha &\approx \frac{Q}{(1 + 4/A)} \quad \text{or} \qquad (14.7) \\ T_\alpha &\approx Q(1 - 4/A) \qquad (14.8) \end{aligned}$$

Equations (14.4) and (14.5) are exact within a non-relativistic formalism. Equation (14.6) is an approximation, but a good one that is suitable for all α-decay's, including ^{8}Be$\rightarrow 2\alpha$. Equation (14.7) is suitable for all the other α-emitters, while (14.8) is only suitable for the heavy emitters, since it assumes $A \gg 4$.

We see from (14.8) that the typical recoil energy, for heavy emitters is:

$$T_{X'} = Q - T_\alpha \approx (4/A)Q \ . \tag{14.9}$$

For a typical α-emitter, this recoil energy ($Q = 5$ MeV, $A = 200$) is 100 keV. This is not insignificant. α-emitters are usually found in crystalline form, and that recoil energy is more than sufficient to break atomic bonds, and cause a microfracture along the track of the recoil nucleus.

Relativistic effects?

One may do a fully relativistic calculation, from which it is found that:

$$T_\alpha = \frac{Q\left(1+\frac{1}{2}\frac{Q}{m_{X'}c^2}\right)}{\left(1+\frac{m_\alpha}{m_{X'}}+\frac{Q}{m_{X'}c^2}\right)} \ , \tag{14.10}$$

$$T_{X'} = \frac{\left(\frac{m_\alpha}{m_{X'}}\right)Q\left(1+\frac{1}{2}\frac{Q}{m_\alpha c^2}\right)}{\left(1+\frac{m_\alpha}{m_{X'}}+\frac{Q}{m_{X'}c^2}\right)} \ . \tag{14.11}$$

Even in the worst-case scenario (low-A) this relativistic correction is about 2.5×10^{-4}. Thus the non-relativistic approximation is adequate for determining T_α or $T_{X'}$.

14.3 α Decay Systematics

As Q increases, $t_{1/2}$ decreases

This is, more or less, self-evident. More "fuel" implies faster decay.

The "smoothest" example of this "law" is seen in the α decay of the even-even nuclei. Shell model variation is minimized in this case, since no pair bonds are being broken. See Figure 14.1, where $\log_{10}(t_{1/2})$ is plotted *vs.* Q. Geiger and Nuttal proposed the following phenomenological fit for $\log_{10}(t_{1/2}(Q))$:

$$\log_{10}\lambda = C - DQ^{-1/2} \quad \text{or} \tag{14.12}$$
$$\log_{10} t_{1/2} = -C' + DQ^{-1/2}\ , \tag{14.13}$$

where C and D are fitting constants, and $C' = C - \log_{10}(\ln 2)$. Odd-odd, even-odd and odd-even nuclei follow the same general systematic trend, but the data are much more scattered, and their half-lives are 2–1000 times that of their even-even counterparts.

Figure 14.1: Paste in Krane's Figure 8.1.

Prediction of Q from the semiempirical mass formula

The semiempirical mass formula can be employed to estimate Q_α, as a function of Z and A.

$$\begin{aligned} Q &= B(Z-2,A-4) + B(^e\mathrm{He}) - B(Z,A) \\ &\approx 28.3 - 4a_{\mathrm{v}} + \frac{8}{3}a_{\mathrm{s}}A^{-1/3} + 4a_{\mathrm{c}}ZA^{-1/3}(1-Z/3A) - 4a_{\mathrm{sym}}(1-2Z/A)^2 + 3a_{\mathrm{p}}A^{-7/4}\ . \end{aligned} \tag{14.14}$$

A plot of $Q(Z,A)$ using (14.14) is given in Figure 14.2.

These trends, from experimental data, are seen in Figure 14.3. However, there is also evidence of the impact of the shell closing at $N = 126$, that is not seen in Figure 14.3.

14.4 Theory of α Emission

Figure 14.4 shows 3 potentials that are used in the estimation of barrier penetration probabilities, for determining the halflife of an α-emitter. The simplest potential, the rectilinear box potential, shown by the dashed line, although crude, maybe used to explain the phenomenon of α decay.

The simplest theory of α emission

In this section we solve for the decay probability using the simplest rectilinear box potential.

This potential is characterized by:

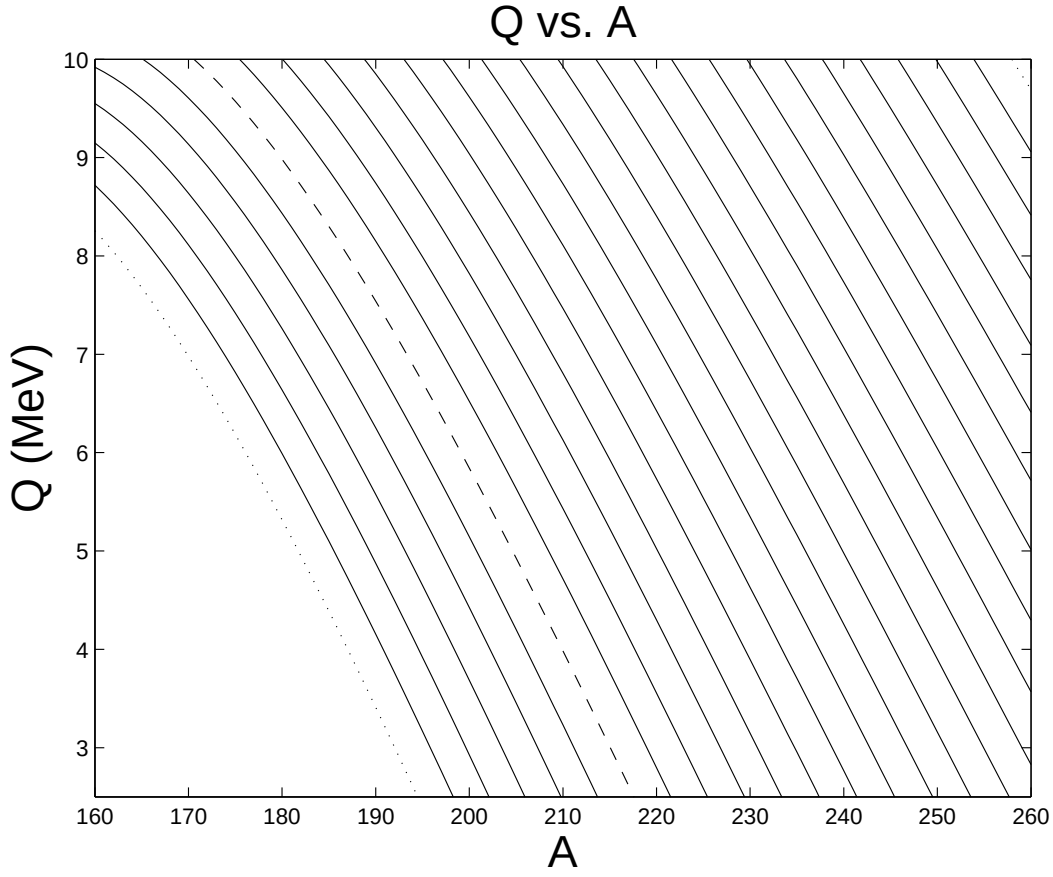

Figure 14.2: $Q(Z, A)$ using (14.14). The dashed line is for Pb ($Z = 82$), while the lower dotted is for Os ($Z = 76$). The upper dotted line is for Lr ($Z = 103$). Each separate Z has its own line with higher Z's oriented to the right.

$$\begin{aligned} V_1(r < R_{\rm N}) &= -V_0 \\ V_2(R_{\rm N} < r < b) &= V_{\rm C} \\ V_3(r > b) &= 0 \ , \end{aligned} \tag{14.15}$$

where V_0 and $V_{\rm C}$ are constants.

The 3-D radial wavefunctions (assuming that the α is in an s-state), are of the form, $R_i(r) = u_i(r)/r$ take the form:

Figure 14.3: Paste in Krane's Figure 8.2.

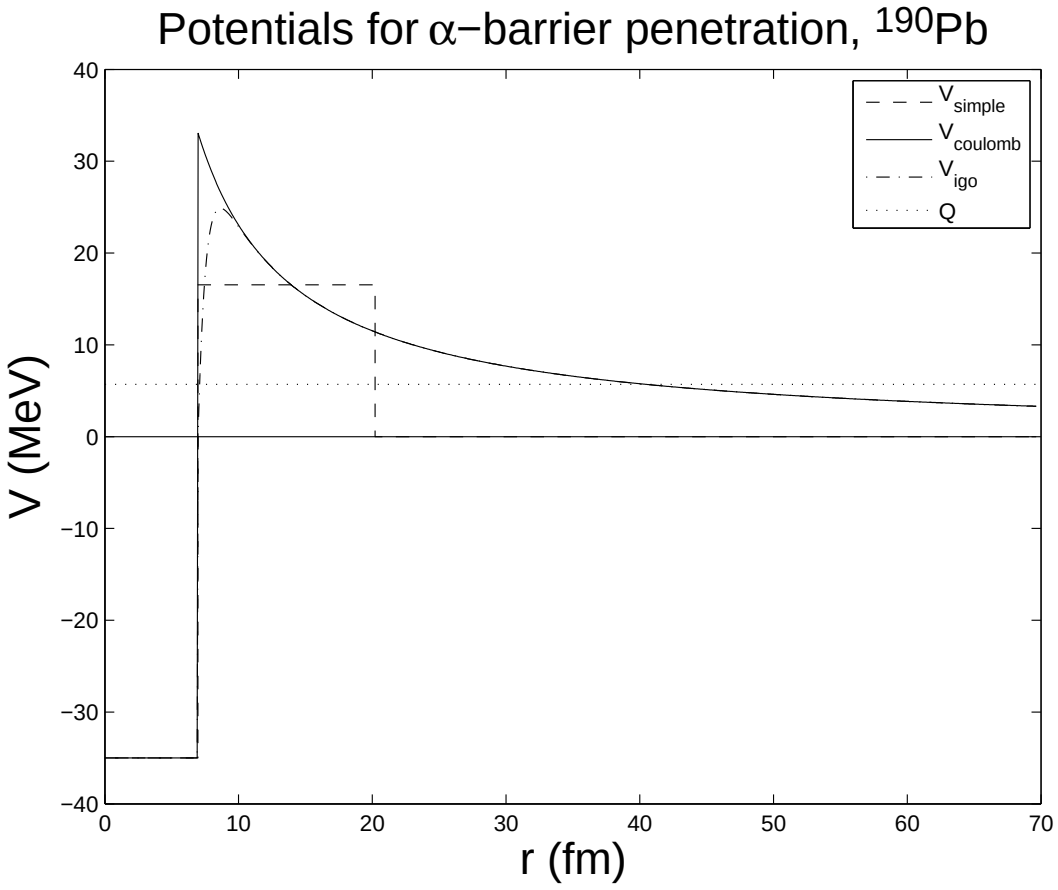

Figure 14.4: Potentials for α decay.

$$\begin{aligned} u_1(r) &= Ae^{ik_1 r} + Be^{-ik_1 r} \\ u_2(r) &= Ce^{k_2 r} + De^{-k_2 r} \\ u_3(r) &= Fe^{ik_3 r} \ , \end{aligned} \tag{14.16}$$

where

$$\begin{aligned} k_1 &= \sqrt{2m(V_0 + Q)}/\hbar \\ k_2 &= \sqrt{2m(V_{\rm C} - Q)}/\hbar \\ k_3 &= \sqrt{2mQ}/\hbar \ . \end{aligned} \tag{14.17}$$

Turning the mathematical crank, we arrive at the transmission coefficient:

$$T = \left[\frac{1}{4}\left(2 + \frac{k_1}{k_3} + \frac{k_3}{k_1}\right) + \frac{\sinh^2[2k_2(b - R_\mathrm{N})]}{4}\left(\frac{k_1 k_3}{k_2^2} + \frac{k_2^2}{k_1 k_3} + \frac{k_1}{k_3} + \frac{k_3}{k_1}\right)\right]^{-1} \tag{14.18}$$

Note: We solved a similar problem in NERS 311, but with $V_0 = 0$, that is, $k_1 = k_3$.

The factor $k_2(b - R_\mathrm{N}) \approx 35$ for typical α emitters. Thus, we can simplify to:

$$T = \frac{16 e^{-2k_2(b-R_\mathrm{N})}}{\left(\frac{k_1 k_3}{k_2^2} + \frac{k_2^2}{k_1 k_3} + \frac{k_1}{k_3} + \frac{k_3}{k_1}\right)} \tag{14.19}$$

Recall that the transmission coefficient is the probability of escape by a single α-particle. To calculate the transmission rate, we estimate a "frequency factor", f, that counts the number of instances, per unit time, that a α, with velocity v_α presents itself at the barrier as an escape candidate. There are several estimates for f:

f	Source	Estimate (s^{-1})	Remarks
v_α/R_N	Krane	$\approx 10^{21}$	Too low, by 10^1–10^2
$v_\alpha/(2R_\mathrm{N})$	Others	$\approx 5 \times 10^{20}$	Too low, by 10^1–10^2
	Fermi's Golden Rule # 2	$\approx 10^{24}$	Too high, by 10^1–10^2

The correct answer, determined by experiment, lies in between these two extremes. However approximate our result it, it does show an extreme sensitivity to the shape of the Coulomb barrier, through the exponential factor in (14.19).

Gamow's theory of α decay

Gamow's theory of α decayis based on an approximate solution[1] to the Schrödinger equation. Gamow's theory gives:

$$T = \exp\left[-2\left(\frac{2m}{\hbar^2}\right)^{1/2}\int_{R_\mathrm{N}}^{b} \mathrm{d}r\,\sqrt{V(r) - Q}\right] \ , \tag{14.20}$$

where b is that value of that defines the r where $V(r) = Q$, on the far side of the barrier.

If we apply Gamow's theory to the potential of the previous section, we obtain:

[1]The approximation Gamow used, is a semi-classical approximation to the Schrödinger equation, called the WKB (Wentzel-Kramers-Brillouin) method. The WKB method works best when the potential changes slowly with position, and hence the frequency of the wavefunction, $k(x)$, also changes slowly. This is not the case for the nucleus, due to its sharp nuclear edge. Consequently, it it thought that Gamow's solution can only get to within a factor or 2 or 3 of the truth. In nuclear physics, a factor of 2 or 3 is often thought of as "good agreement"!

$$T_{\rm exact} = \frac{16}{\left(\frac{k_1 k_3}{k_2^2} + \frac{k_2^2}{k_1 k_3} + \frac{k_1}{k_3} + \frac{k_3}{k_1}\right)} T_{\rm Gamow} \ . \tag{14.21}$$

That factor in front is about 2–3 for most α emitters. This discrepancy is usually ignored, considering the large uncertainly in the f factor.

Krane's treatment of α-decay

Krane starts out with (14.20), namely:

$$T = \exp\left[-2\left(\frac{2m}{\hbar^2}\right)^{1/2} \int_a^b {\rm d}r\, \sqrt{V(r) - Q}\right] \ ,$$

where

$$\begin{aligned} V(x) &= \frac{2(Z-2)e^2}{4\pi\epsilon_0 x} \\ V(a) \equiv B &= \frac{2(Z-2)e^2}{4\pi\epsilon_0 a} \\ a &= R_0(A-4)^{1/3} \\ V(b) \equiv Q &= \frac{2(Z-2)e^2}{4\pi\epsilon_0 b} \ . \end{aligned} \tag{14.22}$$

That is, the α moves in the potential of the *daughter* nucleus, B is the height of the potential at the radius of the daughter nucleus, and b is the radius where that potential is equal to Q. (See Krane's Figure 8.3 on page 251.)

We note that $a/b = Q/B$.

Substituting the potential in (14.22) into (14.20) results in:

$$T = \exp\left\{-2\left(\frac{2m'_\alpha c^2}{Q(\hbar c)^2}\right)^{1/2} \frac{zZ'e^2}{4\pi\epsilon_0}\left[\arccos(\sqrt{x}) - \sqrt{x(1-x)}\right]\right\} \ , \tag{14.23}$$

where $x \equiv a/b = Q/B$. Note that the reduced mass has been used:

$$m'_\alpha = \frac{m_\alpha m_{X'}}{m_\alpha + m_{X'}} \approx m_\alpha(1 - 4/A) \ . \tag{14.24}$$

This "small" difference can result in a change in T by a factor of 2–3, even for heavy nuclei!

Krane also discusses the approximation to (14.23) that results in his equation (8.18). This comes from the Taylor expansion:

$$\arccos(\sqrt{x}) - \sqrt{x(1-x)} \longrightarrow \frac{\pi}{2} - 2\sqrt{x} + \mathcal{O}(x^{3/2}) \ .$$

This is only valid for small x. Typically $x \approx 0.3$, and use of Krane's (8.18) involves too much error. So, stick with the equation given below.

Factoring in the frequency factor, one can show that:

$$\begin{aligned} t_{1/2} &= \ln(2)\frac{a}{c}\sqrt{\frac{m_\alpha c^2}{2(V_0+Q)}} \times \\ &\quad \exp\left\{2\left(\frac{2m'_\alpha c^2}{Q(\hbar c)^2}\right)^{1/2}\frac{zZ'e^2}{4\pi\epsilon_0}\left[\arccos(\sqrt{x}) - \sqrt{x(1-x)}\right]\right\} \ . \end{aligned} \tag{14.25}$$

14.4.1 Comparison with Measurements

In this section we employ the simplest form of f and compute the half-life for α-decay as follows:

$$t_{1/2} = \ln(2)\frac{a}{c}\sqrt{\frac{m_\alpha c^2}{2(V_0+Q)}}\exp\left\{2\left(\frac{2m'_\alpha c^2}{Q(\hbar c)^2}\right)^{1/2}\frac{zZ'e^2}{4\pi\epsilon_0}\left[\arccos(\sqrt{x}) - \sqrt{x(1-x)}\right]\right\} \tag{14.26}$$

The data are shown in the following table, where the half-lives of the even-even isotopes of Th ($Z = 90$) are shown. The calculations were performed using a nuclear radius of $a = 1.25A^{1/3}$ (fm), and $V_0 = 35$ (MeV). The absolute comparison exhibits the same trends for both experiment and calculations, with the calculations being overestimated by 2–3 orders of magnitude. This is most likely due to a gross underestimate of f. the relative comparisons are in much better shape, showing discrepancies of about a factor of 2–3, quite a success for such a crude theory. We note that small changes in Q result in enormous differences in the results. In this table Q changes by about a factor of 2, while the half-lives span about 23 orders of magnitude. The probability of escape is greatly influenced by the height and width of the Coulomb barrier. Besides this dependence, the only other variation in the comparison relates to the nuclear radius. This also affects the barrier since the nuclear radius is proportional to $A^{1/3}$. This hints that the remaining discrepancy, at least for the relative comparison, is related to the fine details of the shape of the barrier, perhaps mostly in the vicinity of the inner turning point. A more refined shape of the Coulomb barrier would likely yield better results, as well would a higher-order WKB analysis that would account more

precisely, for that shape variation. Additionally, the α-particle was treated as if it were a point charge in this analysis. A refined calculation should certainly take this effect into account.

A	Q (MeV)	$t_{1/2}$ (s) abs. meas.	$t_{1/2}$ (s) abs. calc.	$t_{1/2}$ (s) rel. meas.	$t_{1/2}$ (s) rel. calc.
220	8.95	10^{-5}	10^{-3}	5.4×10^{-9}	3.6×10^{-9}
222	8.13	2.8×10^{-3}	2.1×10^{-1}	1.5×10^{-6}	7.3×10^{-7}
224	7.31	1.04	1.1×10^{2}	5.6×10^{-4}	3.8×10^{-4}
226	6.45	1854	2.9×10^{5}	$\equiv 1$	$\equiv 1$
228	5.52	6.0×10^{7}	1.2×10^{10}	3.2×10^{4}	4.2×10^{4}
230	4.77	2.5×10^{12}	6.0×10^{14}	1.3×10^{9}	2.1×10^{9}
232	4.08	4.4×10^{17}	1.8×10^{20}	2.4×10^{14}	6.2×10^{14}

Table 14.1: Half-lives of Th isotopes, absolute and relative comparisons of measurement and theory.

Cluster decay probabilities

If α decay can occur, surely ^{8}Be and ^{12}C decay can occur as well. It is just a matter of relative probability. For these decays, the escape probabilities are given approximately by:

$$\begin{aligned} T_{^{8}\mathrm{Be}} &= T_{\alpha}^{2} \\ T_{^{12}\mathrm{C}} &= T_{\alpha}^{3} \\ T_{^{a}\mathrm{x}} &= T_{\alpha}^{z/2} \ . \end{aligned} \tag{14.27}$$

The last estimate is for a ^{a}x cluster, with z protons and an atomic mass of a.

14.5 Angular momentum and parity in α decay

Angular momentum

If the α-particle carries off angular momentum, we must add the repulsive potential associated with the centrifugal barrier to the Coulomb potential, $V_{\mathrm{C}}(r)$:

$$V(r) = V_{\mathrm{C}}(r) + \frac{l(l+1)\hbar^{2}}{2m'_{\alpha}r^{2}} \ , \tag{14.28}$$

represented by the second term on the right-hand side of (14.28).

The effect on ^{90}Th, with $Q = 4.5$ MeV is:

l	0	1	2	3	4	5	6
T_l/T_0	1	0.84	0.60	0.36	0.18	0.078	0.028

So, as $l \uparrow$, $T \downarrow$.

Conservation of angular momentum and parity

α decay's must satisfy the constraints given by the conservation of total angular momentum:

$$\begin{aligned} \vec{I_i} &= \vec{I_f} + \vec{I_\alpha} \\ \Pi_i &= \Pi_f \times \Pi_\alpha \ , \end{aligned} \tag{14.29}$$

where i represents the parent nucleus, and f represents the daughter nucleus. Since the α-particle is a 0^+ nucleus, (14.29) simplifies to:

$$\begin{aligned} \vec{I_i} &= \vec{I_f} + \vec{l_\alpha} \\ \Pi_i &= \Pi_f \times (-1)^{l_\alpha} \ , \end{aligned} \tag{14.30}$$

where l_α is the orbital angular momentum carried off by the α-particle. If I_i is non-zero, the α decay is able to populate any excited state of the daughter, or go directly to the ground state.

If the initial state has total spin 0, with few exceptions it is a 0^+. In this case, (14.30) becomes.

$$\begin{aligned} \vec{0} &= \vec{I_f} + \vec{l_\alpha} \\ +1 &= \Pi_f \times (-1)^{l_\alpha} \ , \end{aligned} \tag{14.31}$$

or.

$$\begin{aligned} \vec{I_f} &= \vec{l_\alpha} \\ \Pi_f + &= (-1)^{l_\alpha} \ , \end{aligned} \tag{14.32}$$

Thus the only allowed daughter configurations are: $0^+, 1^-, 2^+, 3^-, 4^+, 5^-, 6^+, 7^-, 8^+, 9^- \cdots$ All other combinations are absolutely disallowed.

The α decay can show these allowed transitions quite nicely. A particularly nice example is the case where the transition is $0^+ \longrightarrow 0^+$, where the low-lying rotational band, and higher energy phonon structure are explicitly revealed through α decay. (See Figure 8.7 in Krane.)

Angular intensity of α decays for elliptic nuclei

This is well described in Krane, pages 260–261.

14.6 α-decay spectroscopy

Not covered in NERS312.

Chapter 15

β Decay

Note to students and other readers: This Chapter is intended to supplement Chapter 9 of Krane's excellent book, "Introductory Nuclear Physics". Kindly read the relevant sections in Krane's book first. This reading is supplementary to that, and the subsection ordering will mirror that of Krane's, at least until further notice.

β-particle's are either electrons[1] or positrons that are emitted through a certain class of nuclear decay associated with the "weak interaction". The discoverer of electrons was Henri Becquerel, who noticed that photographic plates, covered in black paper, stored near radioactive sources, became fogged. The black paper (meant to keep the plates unexposed) was thick enough to stop α-particles, and Becquerel concluded that fogging was caused by a new form of radiation, one more penetrating than α-particles. The name "β", followed naturally as the next letter in the Greek alphabet after α, α-particles having already been discovered and named by Rutherford.

Since that discovery, we have learned that β-particles are about 100 times more penetrating than α-particles, and are spin-$\frac{1}{2}$ fermions. Associated with the electrons is a conserved quantity, expressed as the quantum number known as the *lepton number*. The lepton number of the negatron is, by convention +1. The lepton number of the positron, also the anti-particle of the negatron, is -1. Thus, in a negatron-positron annihilation event, the next lepton number is zero. Only leptons can carry lepton number. (More on this soon.) Recall, from Chapter 13 (Chapter 6 in Krane), our discussion of the various decay modes that are associated with β decay:

[1]Technically, the word "electron" can represent either a negatron (a fancy word for e^-) or a positron (e^+). I'll use "electron" interchangeably with this meaning, and also e^-. Usually the context determines the meaning.

$$\begin{array}{lcll} {}^{A}_{Z}X_N & \longrightarrow & {}^{A}_{Z+1}X'_{N-1} + e^- + \overline{\nu}_e & \beta^- \text{ decay} \\ {}^{A}_{Z}X_N & \longrightarrow & {}^{A}_{Z-1}X'_{N+1} + e^+ + \nu_e & \beta^+ \text{ decay} \\ {}^{A}_{Z}X_N & \longrightarrow & {}^{A}_{Z-1}X'_{N+1} + \nu_e & \text{electron capture } (\varepsilon) \end{array} \tag{15.1}$$

We see from the above processes that there are other particles called *neutrinos*. Neutrinos are also spin-$\frac{1}{2}$ leptons (part of the larger fermion family). They are very nearly massless (but proven to have mass[2]). The electron neutrino is given the symbol ν_e, and has lepton number +1. The antineutrino, the $\overline{\nu}_e$, has lepton number -1. A sketch of the organization of fundamental particles is given in Figure 15.1.

Figure 15.1: The particle physics classification of bosons and fermions, with the sub-classifications of baryons and fermions shown.

Three views of β decay

There are three ways of viewing β decay. The first is the "radiological physics view" expressed by (15.1). The next is the "nuclear physics view", where we recognize that the decays of the nuclei are actually caused by transformations of the nucleon constituents, as expressed in (15.2).

$$\begin{array}{rcll} n & \longrightarrow & p + e^- + \overline{\nu}_e & \beta^- \text{ decay} \\ p & \longrightarrow & n + e^+ + \nu_e & \beta^+ \text{ decay} \\ p + e^- & \longrightarrow & n + \nu_e & \text{electron capture } (\varepsilon) \end{array} \tag{15.2}$$

A free neutron will decay with a meanlife, $\tau = 885.7(8)$s, about 11 minutes. A free proton is basically stable. Once these nucleons are bound in a nucleus, however, conservation of energy, with the availability of lower energy states, dictates whether or not these processes are free to proceed.

Then, there is the more microscopic view, the "particle physics view" expressed in (15.3),

$$\begin{array}{rcll} d & \longrightarrow & u + e^- + \overline{\nu}_e & \beta^- \text{ decay} \\ u & \longrightarrow & d + e^+ + \nu_e & \beta^+ \text{ decay} \\ u + e^- & \longrightarrow & d + \nu_e & \text{electron capture } (\varepsilon) \end{array} \tag{15.3}$$

[2]A direct measurement of neutrino mass suggests that its upper limit is $m_{\nu_e} < 2.2$eV. Indirect measurement of the neutrino mass suggest that $0.04\text{eV} < m_{\nu_e} < 0.3\text{eV}$. For the more massive lepton family groups, $m_{\nu_\mu} < 180$keV, and $m_{\nu_\tau} < 15.5$MeV.

that represents the transitions of nucleons, as really transitions between the up (u) and down (d) quarks. A particle physics picture of β^--decay is given in Figure 15.2.

Figure 15.2: The particle physics view of β^--decay. In this case, the weak force is carried by the intermediate vector boson, the W^-. In the case of β^--decay, the weak force is carried by the intermediate vector boson, the W^+, the antiparticle to the W^-. There is also a neutral intermediate vector boson, Z^0, that is responsible for such things as $\nu\nu$ scattering.

Consequences of β-decay's 3-body final state

$\beta^\pm$-decay has 3 "bodies" in the final state: the recoil daughter nucleus, the $e^\pm$, and a neutrino. Typically, the daughter nucleus (even in the case of free neutron decay, is much more massive than the leptons, therefore, the leptons carry off most of the energy. (Even in the worst possible case, that of free neutron decay, the recoil proton can at most about 0.4 keV, or about 0.05% of the reaction Q-value.) Consequently, if one measures the kinetic energy of the resultant electron, one measures a distribution of energies, that (generally) peaks at small energies, and reaches an "end-point" energy, the so-called *β-endpoint*. This β-endpoint represents the case where the ν's energy approaches zero. See Figure 15.3.

Figure 15.3: A typical electron energy spectrum that is measured in a β decay. The endpoint energy is the maximum energy that can be given to the electron, and that is closely related to the reaction Q-value (small recoil correction). At lesser energies, the ν carries off some of the available kinetic energy that Q provides.

This leads naturally to a discussion of ...

15.1 Energy release in β decay

Neutron decay

$$\begin{aligned} n &\longrightarrow p + e^- + \overline{\nu}_e \\ m_n c^2 &= m_p c^2 + m_{e^-} c^2 + m_{\overline{\nu}_e} c^2 + Q_n \\ Q_n &= m_n c^2 - m_p c^2 - m_{e^-} c^2 - m_{\overline{\nu}_e} c^2 \\ Q_n &= (939.565580(81) - 938.272013(23) - 0.5110999(0))[\text{MeV}] - m_{\overline{\nu}_e} c^2 \\ Q_n &= 0.782568(84)[\text{MeV}] - m_{\overline{\nu}_e} c^2 \end{aligned} \tag{15.4}$$

Since $4 \times 10^{-8} < m_{\overline{\nu}_e} c^2 < 2.2 \times 10^{-6}$[MeV], we can safely ignore the neutrino rest mass energy, within the experimental uncertain of the reaction Q,

$$Q_n = 0.782568(84)[\text{MeV}] \tag{15.5}$$

Accounting for proton recoil, the exact relationship between the electron endpoint energy and Q, is given by:

$$\begin{aligned} T_e^{\max} &= (m_p + m_e)c^2 \left[-1 + \sqrt{1 + \frac{2Q_n m_p c^2}{[(m_p + m_e)c^2]^2}} \right] \\ T_e^{\max} &\approx \frac{Q_n}{1 + m_e/m_p} \ . \end{aligned} \tag{15.6}$$

Putting in numerical values, was calculate $T_e^{\max} = 0.782142(84)[\text{MeV}]$, which agrees with the direct measurement of $T_e^{\max} = 0.782(13)[\text{MeV}]$.

We can calculate the proton's recoil energy by using Conservation of Energy:

$$\begin{aligned} T_p^{\max} &= Q_n - T_e^{\max} \\ T_e^{\max} &\approx Q_n \left(1 - \frac{1}{1 + m_e/m_p} \right) \\ T_e^{\max} &\approx Q_n (m_e/m_p) \ . \end{aligned} \tag{15.7}$$

This evaluates numerically to $T_p^{\max} \approx 0.426(84)[\text{keV}]$.

Q for β^--decay

For β^--decay

$${}^{A}_{Z}X_N \longrightarrow {}^{A}_{Z+1}X'_{N-1} + e^- + \overline{\nu}_e \tag{15.8}$$

Going back to the definition of Q in terms of nuclear masses, and ignoring, henceforth, the mass of the neutrino:

$$Q_{\beta^-} = \left[m_{\text{N}}({}^{A}_{Z}X_N) - m_{\text{N}}({}^{A}_{Z+1}X'_{N-1}) - m_e \right] c^2 \ , \tag{15.9}$$

where the subscript "N" connotes nuclear (not atomic) masses.

The relationship between the nuclear (no subscript "N") and atomic mass is:

$$m(^A_Z X_N)c^2 = m_{\rm N}(^A_Z X_N)c^2 + Zm_e c^2 - \sum_{i=1}^{Z} B_i \ , \tag{15.10}$$

where B_i is the binding energy of the i'th atomic electron.

Substituting (15.10) in (15.9), to eliminate the (less well known) nuclear masses results in:

$$\begin{aligned} Q_{\beta^-} &= \left[m(^A_Z X_N) - Zm_e\right]c^2 - \left[m(^A_{Z+1}X'_{N-1}) - (Z+1)m_e\right]c^2 - m_e c^2 + \left[\sum_{i=1}^{Z} B_i - \sum_{i=1}^{Z+1} B'_i\right] \\ &= \left[m(^A_Z X_N) - m(^A_{Z+1}X'_{N-1})\right]c^2 + \left[\sum_{i=1}^{Z} B_i - \sum_{i=1}^{Z+1} B'_i\right] \ , \\ &= \left[m(^A_Z X_N) - m(^A_{Z+1}X'_{N-1})\right]c^2 + \left[\sum_{i=1}^{Z} (B_i - B'_i) - B'_{Z+1}\right] \ , \end{aligned} \tag{15.11}$$

noting that the electron masses have canceled in this case. The factor

$$\sum_{i=1}^{Z} B_i - \sum_{i=1}^{Z+1} B'_i = \sum_{i=1}^{Z} (B_i - B'_i) - B'_{Z+1}$$

is the difference in the energy of the electronic orbital configuration of the parent and daughter nuclei. Generally, this difference can be ignored. However, in the case of large Z nuclei, it can amount to about 10 keV. For accurate determinations of Q, the difference in atomic electron binding energy must be accounted for.

Q for β^+-decay

Similar considerations for β^+ decay lead to:

$$Q_{\beta^+} = \left[m(^A_Z X_N) - m(^A_{Z-1}X'_{N+1}) - 2m_e\right]c^2 + \left[\sum_{i=1}^{Z} B_i - \sum_{i=1}^{Z-1} B'_i\right] \ . \tag{15.12}$$

Here we note that the electron rest-mass energies do not completely cancel. However, the discussion regarding the electron binding energy remains the same.

Q for electron capture

For electron capture:

$$Q_\varepsilon = \left[m(^A_Z X_N) - m(^A_{Z-1} X'_{N+1})\right] c^2 - B_n + \left[\sum_{i=1}^{Z} B_i - \sum_{i=1}^{Z-1} B'_i\right] \ . \tag{15.13}$$

The latter term related to electron binding energy,

$$\sum_{i=1}^{Z} B_i - \sum_{i=1}^{Z-1} B'_i$$

is generally ignored, for the reasons cited above. However, the the binding energy of the captured electron, B_n can approach 100 keV for large-Z nuclei, and can *not* be ignored.

Discussion point: Free neutron decay, revisited

From our current understanding of the weak interaction, the electron is created when a down quark changes into an up quark. The Q value for this reaction is 0.782 MeV. Let us see if we can apply some reasoning from classical physics to say something about the observation of such a decay.

If the electron were a "point" particle, and it was created somewhere inside the neutron at radius r, is would feel an attraction:

$$V(r) = -\frac{e^2}{4\pi\epsilon_0}\left\{\frac{\Theta(R_p - r)}{R_p}\left[\frac{3}{2} - \frac{1}{2}\left(\frac{r}{R_p}\right)^2\right] + \frac{\Theta(r - R_p)}{r}\right\} \ ,$$

where R_p is the radius of the proton. We are assuming that the quarks are moving so fast inside the proton, that all the electron sees is a continuous blur of charge adding up to one unit of charge. So, if $R_p \approx 1.2$fm (from $R_{\rm N} = 1.22 - 1.25[{\rm fm}]A^{1/3}$), we can conclude that the kinetic energy that the electron is required to have to escaped the nucleus falls in the range:

$$\begin{aligned} \frac{e^2}{4\pi\epsilon_0 R_p} &\leq T_e \leq \frac{3}{2}\frac{e^2}{4\pi\epsilon_0 R_p} \\ 1.2[{\rm MeV}] &\leq T_e \leq 1.8[{\rm MeV}] \end{aligned}$$

in other words, it can not happen. This is in contradiction with the observation that it does decay, with a meanlife of about 11 minutes.

Class discussion: Can you explain this?

15.2 Fermi's theory of β decay

Fermi's theory of β decay starts with a statement of Fermi's Golden Rule #2 for transition rate, λ:

$$\lambda = \frac{2\pi}{\hbar}|V_{if}|^2\rho(E_{if}) \ , \tag{15.14}$$

where V is a potential that causes the transition from an initial quantum state Ψ_i (the parent nucleus in the this case) to a final one, Ψ_f, that includes wavefunctions of the daughter nucleus, the electron and its neutrino. $V_{if} \equiv \langle\Psi_f|V|\Psi_i\rangle$ is the transition amplitude.

The derivation of Fermi's Golden Rule #2 is generally reserved for graduate courses in Quantum Mechanics, but a version of the derivation is available in Chapter 13, for your interest.

What concerns us now, is to calculate the density of final states, $\rho(E_{if})$, for the β-transition. This derivation figures so prominently in the β-spectrum, and the endpoint energy.

Starting in Chapter 13, the density of states is derived for non-relativistic particles with mass, relativistic particles with mass (the electron in this case), and massless particles (the neutrino in this case).

We start with (13.21). The number of states, N, of a particle in the final state with energy E is given by:

$$\mathrm{d}N = \frac{\pi}{2}n^2\mathrm{d}n \ . \tag{15.15}$$

where $n = \sqrt{n_x^2 + n_y^2 + n_z^2}$, and (n_x, n_y, n_z) are the quantum numbers of a free particle in n infinite box potential, with side L. the momentum and the n's are related by:

$$p_i = n_i\pi\hbar/L \ . \tag{15.16}$$

Putting (15.16) into (15.15) gives:

$$\mathrm{d}N = \frac{1}{2\pi^2}\frac{L^3}{\hbar^3}p^2\mathrm{d}p \ . \tag{15.17}$$

Or, dividing by $\mathrm{d}E$,

$$\frac{\mathrm{d}N}{\mathrm{d}E} = \frac{1}{2\pi^2}\frac{L^3}{\hbar^3}p^2\frac{\mathrm{d}p}{\mathrm{d}E} \ . \tag{15.18}$$

We should point out that (15.18) is valid for all particles, massless, relativistic and non-relativistic, since (15.16) is universal.

All we need do now is relate momentum to energy to compute the density factors. For the neutrino, which we are now treating as massless,

$$\begin{aligned} p_\nu &= E_\nu/c \\ \mathrm{d}p_\nu &= \mathrm{d}E_\nu/c \\ \frac{\mathrm{d}N_\nu}{\mathrm{d}E_\nu} &= \frac{1}{2\pi^2}\frac{L^3}{\hbar^3 c^3}E_\nu^2 \end{aligned} \tag{15.19}$$

For the electron, that must be treated relativistically,

$$\begin{aligned} p_e &= \sqrt{E_e^2 - (m_e c^2)^2}/c \\ \mathrm{d}p_e &= [E_e/(c\sqrt{E_e^2 - (m_e c^2)^2})]\mathrm{d}E_e \\ \frac{\mathrm{d}N_e}{\mathrm{d}E_e} &= \frac{1}{2\pi^2}\frac{L^3}{\hbar^3 c^3}\sqrt{E_e^2 - (m_e c^2)^2}E_e \\ \frac{\mathrm{d}N_e}{\mathrm{d}T_e} &= \frac{1}{2\pi^2}\frac{L^3}{\hbar^3 c^3}\sqrt{T_e(T_e + 2m_e c^2)}(T_e + m_e c^2) \end{aligned} \tag{15.20}$$

For β decay we have two particles in the final state, so we can express the rate of decay to produce an electron with momentum p as:

$$\frac{\mathrm{d}\lambda_\beta}{\mathrm{d}p} = \frac{2\pi}{\hbar}|V_{if}|^2\frac{\mathrm{d}N_e}{\mathrm{d}p}\frac{\mathrm{d}N_\nu}{\mathrm{d}E_{if}} \ , \tag{15.21}$$

If q is the momentum of the neutrino,

$$\begin{aligned} E_{if} &= T_e + cq \\ \mathrm{d}E_{if} &= c(\mathrm{d}q) \quad (T_e \text{ fixed}) \ . \end{aligned} \tag{15.22}$$

Thus,

$$\frac{\mathrm{d}\lambda_\beta}{\mathrm{d}p} = \frac{2\pi}{\hbar c}|V_{if}|^2\frac{1}{2\pi^2}\frac{L^3}{\hbar^3}p^2\frac{1}{2\pi^2}\frac{L^3}{\hbar^3}q^2\delta(E_{if} - [T_e + T_\nu]) \ . \tag{15.23}$$

Where the δ-function accounts specifically for the conservation of energy.

Recall that the free electron and neutrino wavefunctions have the form $L^{-3/2}\exp(i\vec{p}\cdot x/\hbar)$ and $L^{-3/2}\exp(i\vec{q}\cdot x/\hbar)$, respectively. Thus, the L for the side of the box disappears from the calculation. We also replace $q = (Q - T_e)/c$, ignoring the recoil of the daughter nucleus. Finally, integrating over all possible neutrino energies, we obtain:

$$\begin{aligned} \frac{\mathrm{d}\lambda_\beta}{\mathrm{d}p} &= \frac{|\mathcal{M}_{if}|^2}{2\pi^3\hbar^7c^3}p^2(Q-T_e)^2 \text{ or} \\ \frac{\mathrm{d}\lambda_\beta}{\mathrm{d}p} &= \frac{|\mathcal{M}_{if}|^2}{2\pi^3\hbar^7c}p^2q^2 \end{aligned} \tag{15.24}$$

where $\mathcal{M}_{if} = L^3V_{if}$.

Thus we have derived Fermi's celebrated equation.

Just a brief note on dimensions: $|V_{if}|^2$ has units $[E^2]$ because all the wavefunctions inside are normalized. Getting rid of all the L's results in $\mathcal{M}_{if}$ having units [length$^3\times$ energy]. (15.24) *is* correct dimensionally.

Allowed transitions

Now we examine the form of the "matrix element" $\mathcal{M}_{if}$. This has changed form several times during the derivation, and will again, to conform with Krane's book.

We now rewrite

$$\begin{aligned} \mathcal{M}_{if} &= gM_{if} \\ M_{if} &= \langle (e^{i\vec{p}\cdot x/\hbar})(e^{i\vec{q}\cdot x/\hbar})\psi_{x'}|\mathcal{O}_\beta|\psi_x\rangle \ , \end{aligned} \tag{15.25}$$

where g is the "strength" of the β transition. This is a scalar quantity that plays the role of e, the electric charge, for electromagnetic transitions. The unnormalized electron wavefunction is $\exp(i\vec{p}\cdot x/\hbar)$, and the unnormalized neutrino wavefunction is $\exp(i\vec{q}\cdot x/\hbar)$. $\psi_{x'}$ is the wavefunction of the daughter nucleus, while ψ_x is the wavefunction of the parent nucleus. Finally, $\mathcal{O}_\beta$ is the weak interaction operator, the cause of the transition.

We recall from the class discussions, that the electron and neutrino wavefunctions have wavelengths that are many times the size of the nucleus. So, it seems reasonable to expand these wavefunctions in a Taylor series expansion, to see how far we get. Namely,

$$\begin{aligned} \exp(i\vec{p}\cdot x/\hbar) &= 1 + \frac{i\vec{p}\cdot x}{\hbar} - \left(\frac{\vec{p}\cdot x}{\hbar}\right)^2 + \cdots \\ \exp(i\vec{q}\cdot x/\hbar) &= 1 + \frac{i\vec{q}\cdot x}{\hbar} - \left(\frac{\vec{q}\cdot x}{\hbar}\right)^2 + \cdots \end{aligned} \tag{15.26}$$

Thus the leading-order term of (15.25) is:

$$M^0_{if} = \langle \psi_{x'} | \mathcal{O}_\beta | \psi_x \rangle \ . \tag{15.27}$$

If $M^0_{if} \neq 0$, the β decay is called an "allowed" transition, and the rate is relatively prompt. If $M^0_{if} = 0$, then we must go to higher order terms in (15.26). These are called "forbidden" transitions, and occur, but at much slower rates. (More on this topic later.)

Krane likes to adopt the following shorthand. For allowed transitions, we see that:

$$\frac{\mathrm{d}\lambda^0_\beta}{\mathrm{d}p} = g^2 \frac{|M^0_{if}|^2}{2\pi^3\hbar^7 c} p^2 q^2 \ . \tag{15.28}$$

If we have $N(t)$ β-emitters in a sample, the momentum spectrum of electrons that may be measured is:

$$N^0(p)\mathrm{d}p = N(t)\mathrm{d}\lambda^0_\beta = \left(g^2 N(t) \frac{|M^0_{if}|^2}{2\pi^3\hbar^7 c^5} \right) p^2 q^2 \mathrm{d}p \ . \tag{15.29}$$

If $N(t)$ changes little over the course of the measurement of the spectrum (the usual case):

$$N^0(p)\mathrm{d}p = C^{(0)} p^2 q^2 \mathrm{d}p \ , \tag{15.30}$$

where we have gathered all constants with inside the large parentheses in (15.29) into a global constant $C^{(0)}$, that is determined experimentally. It can be determined through the a normalization condition,

$$\int \mathrm{d}p \, N^0(p) \equiv 1 \ .$$

Conventional forms: $N^0(p)$, $N^0(T_e)$

$N^0(p)$ expressed in (15.30) contains p and q, that are related by conservation of energy. In terms of single momentum variable,

$$N^0(p)\mathrm{d}p = \frac{C^{(0)}}{c^2}p^2\left[Q - \sqrt{(cp)^2 + (m_e c^2)^2} + m_e c^2\right]^2 \mathrm{d}p \ , \tag{15.31}$$

using relativistic kinematic relationships. The maximum possible p occurs when the neutrino component drops to zero. This is easily found to be:

$$p_{\max} = \frac{1}{c}\sqrt{Q^2 + 2Qm_c c^2} \ . \tag{15.32}$$

An even more common expression is to show N^0 in terms of T_e.

We find this by saying:

$$N^0(T_e)\mathrm{d}T_e = N^0(p)\mathrm{d}p = N^0(p)\left(\frac{\mathrm{d}p}{\mathrm{d}T_e}\right)\mathrm{d}T_e \ , \tag{15.33}$$

Applying relativistic kinematic relationships, we find:

$$N^0(T_e)\mathrm{d}T_e = \frac{C^{(0)}}{c^5}\sqrt{T_e^2 + 2T_e m_e c^2}(T_e + m_e c^2)(Q - T_e)^2\mathrm{d}T_e \ . \tag{15.34}$$

Here the β-endpoint at $Q = T_e$ is evident.

Accounting of "forbiddeness" and nuclear Coulomb effect.

There are two other attributes of β-spectra we must take account of, before we start using the theoretical spectral shape to assist in analyzing data.

The first of these has to do with the interaction of the daughter's Coulomb charge with the resultant electron or positron in the final state. This nuclear charge has no effect, of course, on the neutral neutrino. Going back to (15.25), we wrote the electron wavefunction as a free plane wave. In actual fact, that was a fairly crude approximation. These plane waves are distorted significantly by the attraction the β^- would feel, and the repulsion that the positron would feel. Incidentally, there is no effect on our conclusions regarding "allowed" or "forbidden".

Accounting for this is quite involved, but not beyond our capabilities. We would have to go back to (15.25) and write the electron wave functions in terms of free particle solutions to the Coulomb potential. (In NERS 311 we learn a lot about bound states of the Coulomb potential.) I have never seen detailed discussion of this in even graduate-level texts, and interested students are usually told to seek out the papers in the literature. The result is, however, that the β-spectra are multiplied by a correction factor, the *Fermi function*, that depends on the charge of the daughter nucleus, Z', and the electron momentum and sign,

$F^{\pm}(Z', p)$. The effect it has could have been anticipated from classical considerations. The electron spectra is dragged back toward lesser values, while the positron spectra are pushed toward higher values. See Figure (9.3) in Krane.

The "forbiddeness" of the decay also affects the shape of the spectrum. This is also a multiplicative correction to the β-spectrum. There are difference shapes depending on the level of "forbiddeness", and that is determined by the amount of orbital angular momentum, L, carried away by the electron-neutrino pair, as well as their momenta. Examples of these shape factors are given in Table 15.2, for the "unique forbidden transitions"[3].

L	$S^L(p,q)$	
0	1	Allowed
1	$(p^2+q^2)/(m_ec)^2$	Unique first forbidden
2	$(p^4+\frac{10}{3}p^2q^2+q^4)/(m_ec)^4$	Unique second forbidden
3	$(p^6+7p^4q^2+7p^2q^4+q^6)/(m_ec)^6$	Unique third forbidden
$\vdots$	$\vdots$	$\vdots$

Table 15.1: Shape factors for the first three unique forbidden transitions.

The β-spectrum revealed

With all these various factors affecting the spectral shape and decay rates for β decay, we write down the final form that is employed for data analysis:

$$N(p) \propto |M_{if}^L|^2 p^2 (Q - T_e)^2 S^L(p,q) F^{\pm}(Z', p) \ , \tag{15.35}$$

where,

1. M_{if}^L is the nuclear matrix element associate with the transition. It can depend on p and q, as well as the alignment of spin and angular momentum vectors. It exhibits a very strong dependence on the angular momentum, L, carried off by the lepton pair. M_{if}^L also depends strongly on the "closeness" of the initial and final nuclear quantum wavefunctions. The closer the initial and final nuclear quantum states are, the larger their overlap, resulting in a larger M_{if}^L.

2. $p^2(Q - T_e)^2$ is the "statistical factor" associated with the density of final states.

[3]Relativistic quantum mechanics allows us to calculate these in the special case of unique transitions. These transitions are ones in which the angular momentum vector and the two lepton spins are all aligned.

3. $F^{\pm}(Z', p)$, the Fermi function. It accounts for the distortion of the spectral shape due to attraction/repulsion of the electron/positron.

4. $S^L(p, q)$ accounts for spectral shape differences. It depends on the total orbital angular momentum carried off by the electron-neutrino pair, $\vec{L}$, their total spin value, $\vec{S}$, and their orientation with respect to each other.

15.3 Experimental tests of Fermi's theory

Kurie plots: Shape of the β spectrum

To employ (15.35) to analyze β spectra, one plots:

$$\sqrt{\frac{N(p)}{S^L(p,q)F^{\pm}(Z',p)}} \quad vs. \quad T_e, \tag{15.36}$$

using the initial assumption that $L = 0$, so that $S^L(p, q) = 1$. If the data points fall an a straight line (statistical tests may be necessary), once can easily obtain the Q-value from the x-intercept. This type of plot is called a Kurie plot (named after Franz Kurie.) one has also identified, from the shape, that this is an allowed transition.

If the Kurie plot is not straight, one must successively test shape factors until a straight line match is obtained. Once the shape factor is determined, the level of forbiddeness is determined, and the Q-value may be extrapolated from the data unambiguously.

Total decay rate: The $ft_{1/2}$, $\log_{10} ft$ values

Putting in the Coulomb and shape factors into (15.28) allows us to determine the total decay rate for a β-decay process,

$$\begin{aligned}
\lambda_\beta &= g^2 \frac{|M_{if}^L|^2}{2\pi^3\hbar^7 c} \int_0^{p_{\max}} \mathrm{d}p\, S^L(p,q) F^{\pm}(Z',p) p^2 q^2 \\
&= g^2 \frac{m_e^5 c^4 |M_{if}^L|^2}{2\pi^3\hbar^7} \left[\frac{1}{(m_e c)^5} \int_0^{p_{\max}} \mathrm{d}p\, S^L(p,q) F^{\pm}(Z',p) p^2 q^2 \right] \\
&\equiv g^2 \frac{m_e^5 c^4 |M_{if}^L|^2}{2\pi^3\hbar^7} f_L(Z', Q) \ ,
\end{aligned} \tag{15.37}$$

where the dimensionless integral in large square brackets, is a theoretical factor that may be pre-computed and employed in the data analysis. This is conventionally written in terms of halflife, $t_{1/2} = \log(2)/\lambda_\beta$.

Thus,

$$f_L(Z', Q)t_{1/2} \equiv ft_{1/2} = \frac{\log_e(2)2\pi^3\hbar^7}{g^2 m_e^5 c^4 |M_{if}^L|^2} \ . \tag{15.38}$$

This is known colloquially as the ft value. (Pronounced *eff tee*.) The ft's can be quite large, and sometimes the "log ft" value is quoted. (Pronounced *log eff tee*.) The precise definition is $\log_{10}(ft_{1/2})$.

Mass of the neutrino

Our applications of β-decay ignore the neutrino mass, but they turn out to be critically important for cosmology.

There is one important fact: they **do** have mass, but it is very small.

The table below shows the current state of the mass determinations of the three generations of leptons, e, μ, and τ.

lepton flavor	neutrino symbol	mass (eV)
e	ν_e	$0.04 \longrightarrow 2.2$
μ	ν_μ	$< 1.70 \times 10^5$
τ	ν_τ	$< 1.55 \times 10^7$

15.4 Angular momentum and parity selection rules

Classification of transitions in β decay

The e and the ν in the final states of a β decay each have intrinsic spin-$\frac{1}{2}$. Conservation of total angular momentum requires that:

$$\vec{I}_X = \vec{I}_{X'} + \vec{L} + \vec{S} \ , \tag{15.39}$$

where $\vec{I}_X$, $\vec{I}_{X'}$ are the total angular momenta of the parent and daughter, respectively, and $\vec{L}$, $\vec{S}$ are the total orbital and total spin angular momentum, respectively, of the $e\nu$ pair.

Therefore, the ΔI can be $\pm L.$ or $\pm|L \pm 1|$. If $L = 0$, then $\Delta I = \pm 1$. There are only two cases for lepton spin alignment. $S = 0$, when the $e\nu$ intrinsic spins anti-align, is called a Fermi transition. $S = 1$, when the $e\nu$ intrinsic spins align, is called a Gamow-Teller transition. Generally, as $L \uparrow$, $\lambda \downarrow$, $t_{1/2} \uparrow$, because there is much less overlap of the $e\nu$ wavefunctions with the nucleus.

The entire characterization scheme is given in Table 15.4 .

Type of Transition	Selection Rules	$L_{e\nu}$	$\Delta\pi$?	ft
superallowed	$\Delta I = 0, \pm 1^*$	0	no	1×10^3–1×10^4
allowed	$\Delta I = 0, \pm 1$	0	no	2×10^3–10^6
1^{st} forbidden	$\Delta I = 0, \pm 1$	1	yes	10^6–10^8
unique$^{**}1^{\text{st}}$ forbidden	$\Delta I = \pm 2$	1	yes	10^8–10^9
2^{nd} forbidden	$\Delta I = \pm 1^{***}, \pm 2$	2	no	2×10^{10}–2×10^{13}
unique 2^{nd} forbidden	$\Delta I = \pm 3$	2	no	10^{12}
3^{rd} forbidden	$\Delta I = \pm 2^{***}, \pm 3$	3	yes	10^{18}
unique 3^{rd} forbidden	$\Delta I = \pm 4$	3	yes	4×10^{15}
4^{th} forbidden	$\Delta I = \pm 3^{***}, \pm 4$	4	no	10^{23}
unique 4^{th} forbidden	$\Delta I = \pm 5$	4	no	10^{19}

Table 15.2: Classification of transitions in β decay. Notes: (*) $0^+ \to 0^+$ can only occur via Fermi decay. (**) Unique transitions are Gamow-Teller transitions where $\vec{L}$ and $\vec{S}$ are aligned. The shape factors have very simple forms in this case. (***) For the $n \geq 2$ forbidden transitions, the $\Delta I = \pm(n-1)$ transition is often associated with the $n-2$ forbidden transition, being indistinguishable in the measurements of these processes.

Nomenclature alert!

Nomenclature	Meaning
$\vec{L}, L$	Total orbital angular momentum of the $e\nu$ pair
$\vec{S}, S$	Total spin angular momentum of the $e\nu$ pair
Fermi (F) transition	$e\nu$ intrinsic spins anti-align, $S = 0$
Gamow-Teller (GT) transition	$e\nu$ intrinsic spins align, $S = 1$
Superallowed	The nucleon that changed form, did not change shell-model orbital.
Allowed	$L = 0$ transition. $M^0_{if} \neq 0$. See (15.27).
n^{th} forbidden	The $e\nu$ pair carry off n units of orbital angular momentum
Unique	$\vec{L}$ and $\vec{S}$ are aligned.

Examples of allowed β decays

This is straight out of Krane.

$^{14}O(0^+) \rightarrow {}^{14}N^*(0^+)$ must be a pure Fermi decay since it is $0^+ \rightarrow 0^+$. Other examples are ^{34}Cl$\rightarrow^{34}$S, and ^{10}C$\rightarrow^{10}$B*.

$^{6}He(0^+) \rightarrow {}^{6}Li(1^+)$, a $0^+ \rightarrow 1^+$ transition. This must be a pure Gamow-Teller decay. Other similar examples are ^{13}B$(\frac{3}{2}^-)\rightarrow^{13}C(\frac{1}{2}^-)$, and ^{230}Pa$(2^-)\rightarrow^{230}Th^*(3^-)$.

$n(\frac{1}{2}^+) \rightarrow p(\frac{1}{2}^+)$ This is a mixed transition. The F transition preserves the nucleon spin direction, the GT transition flips the nucleon spin. (Show drawing.)

β decay can either be of the F type, the GT type or a mixture of both. We may generalize the matrix element and coupling constant as follows, for allowed decays:

$$gM^0 = g_{\rm F} M^0_{\rm F} + g_{\rm GT} M^0_{\rm GT} = g_{\rm F} \langle \psi_{X'} | \mathbf{1} | \psi_X \rangle + g_{\rm GT} \langle \psi_{X'} | \mathcal{O}_{\uparrow\downarrow} | \psi_X \rangle \ , \tag{15.40}$$

where $\mathcal{O}_{\uparrow\downarrow}$ symbolizes an operator that flips the nucleon spin for the GT transition. The operator for the F transition is simply $\mathbf{1}$, (*i.e.* unity), and just measures the overlap between the initial and final nuclear states.

The fraction of F transitions is:

$$f_{\rm F} = \frac{g^2_{\rm F} |M^0_{\rm F}|^2}{g^2_{\rm F} |M^0_{\rm F}|^2 + g^2_{\rm GT} |M^0_{\rm GT}|^2} = \frac{y^2}{1+y^2} \ , \tag{15.41}$$

where,

$$y \equiv \frac{g_{\rm F} M^0_{\rm F}}{g_{\rm GT} M^0_{\rm GT}} \ . \tag{15.42}$$

Tables of y values are given in Krane on page 290.

15.4.1 *Matrix elements for certain special cases*

This section is meant to explain several things given without explanation in Krane's Chapter 9.

$M_{if} = \sqrt{2}$, for superallowed $0^+ \to 0^+$ transitions

This was stated near the top of the text on Krane's p. 284.

We know that a $0^+ \to 0^+$ allowed transition (super or regular), must be an F transition. In the case that it is also a superallowed transition, we can write explicitly:

$$M_{if} = \left\langle \psi_{X'}(0^+) \left(\frac{1}{\sqrt{2}}[e(\uparrow)\nu(\downarrow) + e(\downarrow)\nu(\uparrow)] \right) \middle| \mathbf{1} \middle| \psi_X(0^+) \right\rangle \ , \tag{15.43}$$

where the intrinsic spins of the $e\nu$ pair are shown explicitly. This spin wavefunction is properly normalized with the $\sqrt{2}$ as shown.

Separating the spins part, and the space part,

$$M_{if} = \frac{1}{\sqrt{2}} \langle \psi_{X'} | \psi_X \rangle \langle (e(\uparrow)\nu(\downarrow) + e(\downarrow)\nu(\uparrow)) | \vec{0} \rangle \ = \sqrt{2} \ , \tag{15.44}$$

since $\langle \psi_{X'} | \psi_X \rangle = 1$ for superallowed transitions, and $\langle e(\uparrow)\nu(\downarrow) | \vec{0} \rangle = \langle e(\downarrow)\nu(\uparrow)) | \vec{0} \rangle = 1$.

Using this knowledge, one can measure directly, g_{F} from $0^+ \to 0^+$ superallowed transitions. Adapting (15.38) for superallowed transitions,

$$g_{\text{F}}^2 = \frac{\log_e(2)\pi^3\hbar^7}{m_e^5 c^4} \left(\frac{1}{f t_{1/2}} \right)_{\text{meas}} \ , \tag{15.45}$$

giving a direct measurement of g_{F} via measuring ft. Table 9.2 in Krane (page 285) shows how remarkable constant ft is for $0^+ \to 0^+$ superallowed transitions. This permits us to establish the value for g_{F} to be:

$$g_{\text{F}} = 0.88 \times 10^{-4} \text{ MeV} \cdot \text{fm}^3 \ . \tag{15.46}$$

15.5 Comparative half-lives and forbidden decays

Not covered in NERS312.

15.6 Neutrino physics

Not covered in NERS312.

15.7 Double-β Decay

Not covered in NERS312.

15.8 β-delayed electron emission

Not covered in NERS312.

15.9 Non-conservation of parity

Not covered in NERS312.

15.10 β spectroscopy

Not covered in NERS312.

$M_{if} = 1$, **for neutron** β **decay,** $n \rightarrow p + e^- + \tilde{\nu}_e$

This was stated near the top of the text on Krane's p. 290.

In this case, for an F transition:

$$M_{if} = \left\langle \psi_{x'}(0^+) \left(\frac{1}{\sqrt{2}} [e(\uparrow)\nu(\downarrow) + e(\downarrow)\nu(\uparrow)] \right) \middle| \mathbf{1} \middle| \psi_x(0^+) \right\rangle , \tag{15.47}$$

Chapter 16

γ Decay

Note to students and other readers: This Chapter is intended to supplement Chapter 10 of Krane's excellent book, "Introductory Nuclear Physics". Kindly read the relevant sections in Krane's book first. This reading is supplementary to that, and the subsection ordering will mirror that of Krane's, at least until further notice.

So far we have discussed α decay and β decay modes of de-excitation of a nucleus.

Figure 16.1: Generic decay schemes for α decay and β decay

As seen in Figure 16.2, we have indicated explicitly, that the daughter nucleus may be in an excited state. This is, in fact, the usual case. The most common form of nuclear de-excitation is via γ decay, the subject of this chapter.

$$\begin{aligned} {}^{A}_{Z}X_N &\longrightarrow {}^{A-4}_{Z-2}X^*_{N-2} + \alpha && [\alpha - \text{decay}] \\ {}^{A}_{Z}X_N &\longrightarrow {}^{A}_{Z\pm1}X^*_{N\mp1} + e^{\mp} + (\overline{\nu}_e/\nu_e) && [\beta^{\mp} \text{ decay}] \end{aligned} \tag{16.1}$$

A comparison of α decay, β decay, and γ decay

Now that we are discussing that last decay mode process, it makes sense to compare them. Most naturally radioactive nuclei de-excite via an α decay. The typical α-decay energy is 5 MeV, and the common range between 4 and 10 MeV. The "reduced" de Broglie wavelength is:

$$\lambda\!\!\!^{-} = \frac{\hbar}{p} = \frac{\hbar c}{pc} = \frac{\hbar c}{\sqrt{T(T+2mc^2)}} \tag{16.2}$$

Figure 16.2: Generic decay schemes for α decay and β decay

Thus, for the α-particle, the typical $\lambda\!\!\!^{-}$ is about 1.02 fm, with a range of about 0.72–1.14 fm. This dimension is small in comparison, and this is why a semi-classical treatment of α decay is successful. One can reasonably talk about α-particle formation at the edge of the nucleus, and then apply quantum tunneling predictions to estimate theoretically, the escape probability, and the halflife.

β decay, on the other hand, involves any energy up to the reaction Q, typically 1 MeV, but ranging from a few keV to tens of MeV. Thus, the typical $\lambda\!\!\!^{-}$ is about 140 fm, and ranges from 10 fm up. Thus, the typical β-particle has a large $\lambda\!\!\!^{-}$ in comparison to the nuclear size, and a quantum mechanical approach is dictated, and the result of the previous chapter are testament to that.

γ decay is now under our microscope. the typical γ decay is 1 MeV and ranges from about 0.1 – 10 MeV. The typical $\lambda\!\!\!^{-}$ is about 40 fm, and ranges from about 20 – 2000 fm. Clearly, only a quantum mechanical approach has a chance of success. Fortunately, the development of Classical Electrodynamics was very mature by the time Quantum Mechanics was discovered. The "wave mechanics" of photons, meshed very easily with the wave mechanics of particles.

Non-relativistic and relativistic Quantum Electrodynamics started from a very solid classical wave-friendly basis.

The foundations of Quantum Electrodynamics

γ spectroscopy yields some of the most precise knowledge of nuclear structure, as spin, parity, and ΔE are all measurable.

Borrowing from our knowledge of atomic physics and working within the shell-model of the nucleus, we can write (in a formal fashion, at least) the nuclear wave function as a composite of single-particle nucleon wavefunctions, as follows:

$$\Psi_{\rm N} = \prod_{a=1}^{A} C(l_a, s_a, t_a)\psi_a(l_a, s_a, t_a) \ , \tag{16.3}$$

where the composite wavefunction, $\Psi_{\rm N}$, is the product of a combinatorial factor C, that combines the states as a collection of fermions. C combines the individual orbital (l) and spin (s) angular momenta, and isospin (t) quantum numbers. Isospin is a quantum number analogous to intrinsic spin. Recognizing that the strong force is almost independent of nucleon type, the two nucleon states are "degenerate" much like spin states in atomic physics. So, we can assign a conserved quantum number, called isospin. By convention, a proton has $t_p = \frac{1}{2}$, while a neutron has $t_n = -\frac{1}{2}$.

Transition rates between initial, $\Psi^*_{\rm N}$ and final, $\Psi'_{\rm N}$, nuclear states, resulting from an electromagnetic decay producing a photon with energy, E_γ, can be described by Fermi's Golden Rule #2:

$$\lambda = \frac{2\pi}{\hbar} \left|\langle \Psi'_{\rm N}\psi_\gamma|\mathcal{O}_{\rm em}|\Psi^*_{\rm N}\rangle\right|^2 \frac{{\rm d}n_\gamma}{{\rm d}E_\gamma} \ , \tag{16.4}$$

where $\mathcal{O}_{\rm em}$ is the electromagnetic transition operator, and $({\rm d}n_\gamma/{\rm d}E_\gamma)$ is the density of final states factor. The photon wavefunction, ψ_γ and $\mathcal{O}_{\rm em}$ are well known, therefore, measurements of λ provide detailed knowledge of nuclear structure. Theorists attempt to model $\Psi_{\rm N}$. The degree to which their predictions agree with experiments, indicates how good the models are, and this leads us to believe we understand something about nuclear structure.

A γ-decay lifetime is typically 10^{-12} seconds or so, and sometimes even as short as 10^{-19} seconds. However, this time span is an *eternity* in the life of an excited nucleon. It takes about 4×10^{-22} seconds for a nucleon to cross the nucleus.

Why does γ decay take so long?

There are several reasons:

1. We have already seen that the photon wavelength, from a nuclear transition, is many times the size of the nucleus. Therefore there is little overlap between the photon's wavefunction and the nucleon wavefunctions, the nucleon that is responsible for the emission of the photon. The reduction factor is approximately $(\lambda\!\!\!^{-}/R_{\rm N})^3$.

2. The photon carries off at least one unit of angular momentum. Therefore, the transition involves some degree of nucleon re-orientation. That is, $\Psi'_{\rm N}$ does not closely resemble $\Psi^*_{\rm N}$, the disparity growing with increased j_γ. (The γ has one integral unit of intrinsic spin.)

3. The electromagnetic force is relatively weak compared to the strong force, about a factor of 100.

16.1 Energetics of γ decay

A typical γ decay is depicted in Figure 16.3, the decay scheme and its associated energetics are described in (16.2). X^* represents the initial excited states, while X' is the final state of the transition, though usually, it is a lower energy excited state, that also decays by one of the known modes.

$$\begin{aligned} {}^{A}_{Z}X^*_N &\longrightarrow {}^{A}_{Z}X'_N + \gamma \\ [m_{X^*} - m_{X'}]c^2 &= T_{X'} + E_\gamma \\ Q &= T_{X'} + E_\gamma \end{aligned} \tag{16.5}$$

Thus we see that the reaction Q is distributed between the recoil energy of the daughter nucleus and the energy of the photon. Note that m_{X^*} and $m_{X'}$, are *nuclear* masses.

It turns out to be easier to use a relativistic formalism to determine the share of kinetic energy between the photon and the daughter nucleus, so we proceed that way. It can be shown that:

$$\begin{aligned} E_\gamma &= Q\left[\frac{1 + Q/2m_{X'}c^2}{1 + Q/m_{X'}c^2}\right] \\ T_{X'} &= \frac{Q}{2}\left[\frac{Q/m_{X'}c^2}{(1 + Q/m_{X'}c^2)}\right] . \end{aligned} \tag{16.6}$$

Since $Q \lll m_{X'}c^2$, or $(10^{-4}/A) < (Q/m_{X'}c^2) < (10^{-2}/A)$, we can approximate

Figure 16.3: Generic decay schemes for α decay and β decay

$$\begin{aligned} E_\gamma &\approx Q - \frac{Q^2}{2m_{_{X'}}c^2} \\ T_{X'} &\approx \frac{Q^2}{2m_{_{X'}}c^2} \end{aligned} \tag{16.7}$$

.

Although these recoil energies are small, they are in the range $(5 \rightarrow 50000 \text{ eV})/A$. Except in the lower range, these recoil energies are strong enough to overwhelm atomic bonds and cause crystal structure fissures.

Finally, Krane uses a non-relativistic formalism to obtain the recoil energy. It can be shown that

$$\frac{E_\gamma^{\text{rel}} - E_\gamma^{\text{non-rel}}}{Q} \approx 1.5 \times (10^{-13} \rightarrow 10^{-7})/A^3 \ . \tag{16.8}$$

The relativistic correction can be ignored, but it is interesting that the relativistic calculation is easier! This is one place where correct intuition at the outset, would have caused you more work!

Obtaining Q from atomic mass tables

Finally, let us deal with a small subtlety regarding the reaction Q. The Q employed in (16.5) is different than what one would obtain from a different of atomic masses from the mass tables.

The two are:

$$\begin{aligned} Q &= [m_{X^*} - m_{X'}]c^2 \\ Q' &= [m({}^A_Z X^*_N) - m({}^A_Z X'_N)]c^2 \ . \end{aligned} \tag{16.9}$$

Going back to the definition of atomic mass, we obtain:

$$Q = Q' + \sum_{i=1}^{Z} (B_i^* - B_i') \ , \tag{16.10}$$

where the B_i's are the atomic binding energies of the i'th atomic electron. About the only difference, insofar as the atomic electrons are concerned, is the different nuclear spin that these electrons see. This effect the hyperfine splitting energies of the atomic states, and can probably be ignored in (16.10). (Makes one wonder, though. Someone care to attempt some library research on this topic?)

16.2 Classical Electromagnetic Radiation

The structure (and many of the conclusions) of the Quantum Mechanical description of electromagnetic radiation follows from the classical formulation. Most important of these is the classical limit, through the correspondence principle. Therefore, a detailed review of Classical Electromagnetic Radiation is well motivated.

Multipole expansions

Electric multipoles

The electric multipole expansion starts by considering the potential due to a static charge distribution:

$$V(\vec{x}) = \frac{1}{4\pi\epsilon_0}\int \mathrm{d}\vec{x}'\ \frac{\rho(\vec{x}')}{|\vec{x}-\vec{x}'|}\ . \tag{16.11}$$

We have encountered such an object before, in Chapter 10, but now we attempt to be a little more general than simply (!) describing the nuclear charge distribution. Generally, we shall only consider charge conserving systems, where the time dependency may arise through a vibration or rotation of the charges in the distribution, but not through loss or gain of charge. Assuming the charges to be localized, we expand (16.11) in $\vec{x}$. That is, we are considering $\vec{x}$ to be outside of the charge distribution. The result is:

$$\begin{aligned} V(\vec{x}) &= \frac{1}{4\pi\epsilon_0}\left[\frac{Q_0}{|\vec{x}|}+\frac{Q_1}{|\vec{x}|^2}+\frac{Q_2}{|\vec{x}|^3}\cdots\right] && (16.12)\\ Q_0 &= \int \mathrm{d}\vec{x}'\,\rho(\vec{x}',t) && (16.13)\\ Q_1 &= \int \mathrm{d}\vec{x}'\,z'\rho(\vec{x}') && (16.14)\\ Q_2 &= \frac{1}{2}\int \mathrm{d}\vec{x}'\,(3z'^2-r'^2)\rho(\vec{x}') && (16.15) \end{aligned}$$

where Q_0 is the total charge (*aka* the monopole term), Q_1 is the dipole moment, and Q_2 is the quadrupole moment. Higher moments would include the octupole moment, and the hexadecapole moment, and more.

In general,

$$V(\vec{x},t) = \frac{1}{4\pi\epsilon_0}\frac{1}{|\vec{x}|}\sum_n \frac{Q_n}{|\vec{x}|^n} \tag{16.16}$$

Q_0 could be zero, for neutral charge distributions. If the charge distribution contains charge of only one sign, the dipole moment could be made to disappear by choosing the coordinate system to be at the center of charge.

In classical E&M theory, the higher n's diminish in influence as $|\vec{x}|$ grows. In Quantum E&M theory, the higher n's are associated with transitions that become weaker with increased n.

Electric dipoles and quadrupoles

To illustrate some features of electric dipoles, consider the situation described in Figure 16.4. Here, a charge q (assumed, without loss of generality, to be positive), is located on the z-axis at $z = l$. A charge of the opposite sign is on the z-axis, at $z = -l$. This is a pure electric dipole:

Figure 16.4: A simple example of an electric dipole

$$\begin{aligned} \rho(\vec{x}) &= q[\delta(x)\delta(y)\delta(z-l) - \delta(x)\delta(y)\delta(z+l)] \\ Q_0 &= 0 \\ Q_1 &= ql + (-q)(-l) = 2ql \\ Q_{n\geq 2}(t) &= 0 \end{aligned} \tag{16.17}$$

Under a parity operation, $\vec{x} \to -\vec{x}$, the configuration in Figure 16.4, is opposite to its original configuration. Thus the parity of the electric dipole radiation is $\Pi(E^1) = -1$.

A similar argument for an electric quadrupole would lead us to conclude that $\Pi(E^2) = +1$. In general, the parity of an electric multipole is:

$$\Pi(EL) = (-1)^L \ . \tag{16.18}$$

Magnetic dipoles

Considerations for static magnetic multipole expansions are much more involved. Instead, we focus on the magnetic dipole moment:

$$\vec{B}(\vec{x}) = \frac{\mu_0}{4\pi}\left[\frac{3\vec{n}(\vec{n}\cdot\vec{m}) - \vec{m}}{|\vec{x}|^3}\right] , \tag{16.19}$$

where $\vec{n}$ is a unit vector in the direction of $\vec{x}$, $\vec{m}$ is the magnetic moment,

$$\vec{m} = \frac{1}{2}\int \mathrm{d}\vec{x}' \, [\vec{x}' \times \vec{J}(\vec{x}')] \, . \tag{16.20}$$

Here, $\vec{J}$ is the current density.

To illustrate some features of magnetic dipoles, consider the situation described in Figure 16.5.

Figure 16.5: A simple example of a magnetic dipole

Under a parity change, the magnetic dipole is unchanged. So, in this case, $\Pi(B^1) = +1$. A magnetic quadrupole, on the other hand, changes its sign. In general,

$$\Pi(ML) = -(-1)^L \ . \tag{16.21}$$

Characteristics of multipolarity

L	multipolarity	$\Pi(EL)$	$\Pi(ML)$	angular distribution
1	dipole	-1 / +1	Unique angular distribution, given later	
2	quadrupole	+1 / -1	”	
3	octupole	-1 / +1	”	
4	hexadecapole	+1 / -1	”	
⋮	⋮	⋮	⋮	⋮

Parity

For electric multipoles

$$\Pi(EL) = (-1)^L \ ,$$

while for magnetic multipoles

$$\Pi(EL) = (-1)^{L+1} \ .$$

Power radiated

The power radiated is proportional to:

$$P(\sigma L) = \propto \frac{2(L+1)c}{\varepsilon_0 L[(2L+1)!!]^2} \left(\frac{\omega}{c}\right)^{2L+2} [m(\sigma L)]^2 \ , \tag{16.22}$$

where, σ means either E or M, and $m(\sigma L)$ is the E or M multipole moment of the appropriate kind.

16.2.1 A general and more sophisticated treatment of classical multipole fields

In order to make the transition to Quantum Mechanics a little more transparent, our jumping-off point from Classical Electrodynamics has to be a somewhat more advanced. From advanced $E\&M$ (for example, J D Jackson's *Classical Electrodynamics*)...

If

$$\rho(\vec{x},t) = \rho(\vec{x})e^{i\omega t} \tag{16.23}$$
$$\vec{J}(\vec{x},t) = \vec{J}(\vec{x})e^{i\omega t} \tag{16.24}$$
$$\vec{m}(\vec{x},t) = \vec{m}(\vec{x})e^{i\omega t}\ , \tag{16.25}$$

are the time-dependent charge density (protons density), current density (protons with orbital angular momentum), and magnetic moment density (proton and neutron intrinsic spins), the radiation fields are characterized by the electric, Q_{lm}, and magnetic, M_{lm}, multipoles:

$$Q_{lm} = \int \mathrm{d}\vec{x}\,|\vec{x}|^l Y^*_{lm}(\theta,\phi)\left[\rho(\vec{x}) - \frac{i\omega}{(l+1)c^2}\vec{\nabla}\cdot[\vec{x}\times\vec{m}(\vec{x})]\right]\ , \tag{16.26}$$
$$M_{lm} = -\int \mathrm{d}\vec{x}\,|\vec{x}|^l Y^*_{lm}(\theta,\phi)\left[\nabla\cdot\vec{m}(\vec{x}) + \frac{1}{(l+1)}\vec{\nabla}\cdot[\vec{x}\times\vec{J}(\vec{x})]\right]\ . \tag{16.27}$$

The power, $\mathrm{d}P$, radiated into solid angle $\mathrm{d}\Omega$, by mode (l,m) is:

$$\frac{\mathrm{d}P}{\mathrm{d}\Omega}\left(l,m,\begin{bmatrix}E\\M\end{bmatrix}\right) = \frac{2(l+1)c}{\varepsilon_0 l(2l+1)[(2l+1)!!]^2}\left(\frac{\omega}{c}\right)^{2l+2}\left|\begin{matrix}Q_{lm}\\M_{lm}\end{matrix}\right|^2 |X_{lm}(\theta,\phi)|^2\ , \tag{16.28}$$

where (suppressing explicit dependence on θ and ϕ),

$$|X_{lm}|^2 = \frac{\frac{1}{2}(l-m)(l+m+1)|Y_{l,m+1}|^2 + \frac{1}{2}(l+m)(l-m+1)|Y_{l,m-1}|^2 + m^2|Y_{l,m}|^2}{l(l+1)}\ . \tag{16.29}$$

If all the m's contribute equally,

$$\sum_{m=-l}^{l}|X_{lm}(\theta,\phi)|^2 = \frac{2l+1}{4\pi}\ . \tag{16.30}$$

In this case, the radiation is isotropic. You will also need (16.30) to get Krane's (10.8).

For the non-isotropic distributions, first we recall the spherical harmonics

l (2^l-pole)	$\lvert Y_{l,0}\rvert^2$	$\lvert Y_{l,\pm1}\rvert^2$	$\lvert Y_{l,\pm2}\rvert^2$	$\lvert Y_{l,\pm3}\rvert^2$
1 (dipole)	$\frac{3}{4\pi}\cos^2\theta$	$\frac{3}{8\pi}\sin^2\theta$	(n/a)	(n/a)
2 (quadrupole)	$\frac{5}{16\pi}(\cos^2\theta-1)^2$	$\frac{1}{8\pi}\sin^2\theta\cos^2\theta$	$\frac{15}{32\pi}\sin^4\theta$	(n/a)
3 (octopole)	$\frac{49}{16\pi}(5\cos^3\theta-3\cos\theta)^2$	$\frac{21}{64\pi}\sin^2\theta(5\cos^2\theta-1)^2$	$\frac{105}{32\pi}\sin^4\theta\cos^2\theta$	$\frac{35}{64\pi}\sin^6\theta$

l (2^l-pole)	$\lvert X_{l,0}\rvert^2$	$\lvert X_{l,\pm1}\rvert^2$	$\lvert X_{l,\pm2}\rvert^2$	$\lvert X_{l,\pm3}\rvert^2$
1 (dipole)	$\frac{3}{8\pi}\sin^2\theta$	$\frac{3}{16\pi}(1+\cos^2\theta)$	(n/a)	(n/a)
2 (quadrupole)	$\frac{15}{8\pi}\sin^2\theta\cos^2\theta$	$\frac{5}{16\pi}(1-3\cos^2\theta+4\cos^4\theta)$	$\frac{5}{16\pi}(1-\cos^4\theta)$	(n/a)
3 (octopole)	?	?	?	?

These distributions are shown in Figure 16.6.

Figure 16.6: Angular distributions for $X_{1,m}$ and $X_{2,m}$

The angular distributions indicate how a measurement of the angular distribution map of the radiation field can identify the multipolarity of the radiation. Measurement of the parity is accomplished by performing a secondary scattering experiment that is sensitive to the direction of, for example, the electric field vector. The Compton interaction often used for this purpose.

16.3 Transition to Quantum Mechanics

The transition to Quantum Mechanics is remarkably simple! Most of the hard work has been done in the classical analysis.

In Quantum Mechanics, the transition rate is given by:

$$\frac{\mathrm{d}\lambda}{\mathrm{d}\Omega}\left(l,m,\begin{bmatrix}E\\M\end{bmatrix}\right)=\frac{1}{\hbar\omega}\frac{\mathrm{d}P}{\mathrm{d}\Omega}\left(l,m,\begin{bmatrix}E\\M\end{bmatrix}\right)\ . \tag{16.31}$$

that is, the transition rate (per photon) is taken from the expression for the power radiated, divided by the energy per photon, $\hbar\omega$. The structure of the right hand side is identical to the classical expression, except that the charge density, current density and intrinsic magnetization density are replaced by the probability density, the probability current density, and the magnetic moment density.

$$Q_{lm}^{i\to f} = e\int \mathrm{d}\vec{x}\,|\vec{x}|^l Y_{lm}^*(\theta,\phi)\left[\sum_{i=1}^{Z}(\psi_i^*)_f(\psi_i)_i\right] , \tag{16.32}$$

$$M_{lm}^{i\to f} = -\frac{1}{(l+1)}\frac{e\hbar}{m_p}\int \mathrm{d}\vec{x}\,|\vec{x}|^l Y_{lm}^*(\theta,\phi)\left[\vec{\nabla}\cdot[\sum_{i=1}^{Z}(\psi_i^*)_f|\vec{L}|(\psi_i)_i]\right] . \tag{16.33}$$

The Weisskopf Estimates

A detailed investigation of (16.32) and (16.33) requires detailed knowledge of the nuclear wavefunctions, in order to pin down the absolute decay rates of the various transition types. he angular distributions, however, and parities have been established already.

Detailed knowledge of the wavefunctions is not known. However, it would be nice to have a "ballpark" estimate, to get relative transition rates. Such an approximation has been done by Weisskopf, using the following strategy.

Let the radial part of both the initial and final wavefunctions be:

$$R(r) = \theta(R_N - r)\Big/\sqrt{\int_0^{R_N}\mathrm{d}r\,r^2},$$

where R_N is the nuclear edge, given by $R_N = R_0 A^{1/3}$. We note that these radial wavefunctions are properly normalized, since,

$$\int_0^\infty \mathrm{d}r\,r^2 R(r) = 1.$$

The radial part of (16.32) is thus given by:

$$Q_{lm}^{i\to f} = e\int_0^\infty \mathrm{d}r\,r^2 r^l |R(r)|^2 = eR_N^l\frac{3}{l+3} . \tag{16.34}$$

Substituting (16.34) and (16.33) results in:

$$\lambda(El) = \frac{8\pi(l+1)}{l[(2l+1)!!]^2}\left\{\frac{e^2}{4\pi\varepsilon_0\hbar c}\right\}\left(\frac{E_\gamma R_N}{\hbar c}\right)^{2l+1}\left(\frac{3}{l+3}\right)^2\frac{c}{R_N} , \tag{16.35}$$

for electric l-pole transitions. All quantities enclosed in parentheses (of all kinds) are unitless. Moreover, the quantity inside the {}'s is recognized as the fine structure constant, $\alpha = 1/137.036...$. The factor c/R is 1/(the time for a photon to cross a nuclear diameter).

Similar considerations (I'm still looking for the source of this calculation) gives:

$$\lambda(Ml) = \frac{8\pi(l+1)}{l[(2l+1)!!]^2}\left(\mu_p - \frac{1}{l+1}\right)^2\left(\frac{\hbar c}{m_p c^2 R_N}\right)^2\left\{\frac{e^2}{4\pi\varepsilon_0\hbar c}\right\}\left(\frac{E_\gamma R_N}{\hbar c}\right)^{2l+1}\left(\frac{3}{l+2}\right)^2\frac{c}{R_N}\ , \tag{16.36}$$

where the second term in parentheses comes from the nuclear magnetron, rendered unitless by additional factors of c and R_N. Krane never defines the factor μ_p, but according to my search (so far) is related to the gyromagnetic ration of the proton, divided by 2. Krane also goes on to say that the factor $[\mu_p - 1/(l+1)]^2$ is often simply replaced by 10. (!)

Evaluating (16.35) and (16.36) leads to (according to Krane):

$$\begin{aligned}
\lambda(E1) &= 1.0\times10^{14}A^{2/3}E_\gamma^3 \\
\lambda(E2) &= 7.3\times10^{7}A^{4/3}E_\gamma^5 \\
\lambda(E3) &= 3.3\times10^{1}A^{2}E_\gamma^7 \\
\lambda(E4) &= 1.1\times10^{-5}A^{8/3}E_\gamma^9
\end{aligned} \tag{16.37}$$

$$\begin{aligned}
\lambda(M1) &= 5.6\times10^{13}E_\gamma^3 \\
\lambda(M2) &= 3.5\times10^{7}A^{2/3}E_\gamma^5 \\
\lambda(M3) &= 1.6\times10^{1}A^{4/3}E_\gamma^7 \\
\lambda(M4) &= 4.5\times10^{-6}A^{2}E_\gamma^9
\end{aligned} \tag{16.38}$$

Some conclusions about these:

Same order, different type

$$\frac{\lambda(El)}{\lambda(Ml)} \approx 2A^{2/3}\ .$$

Thus, for a given l, electric transition always dominates, with the difference getting large with increases A.

Nearby order, same parity

$$\frac{\lambda(E(l+1))}{\lambda(Ml)} \approx 10^{-6}A^{4/3}E^2\ .$$

Thus, for large A and E, $E2$ can compete with $M1$, $E3$ can compete with $M2$ and so on.

Same type, different order

$$\frac{\lambda(\sigma(l+1))}{\lambda(\sigma l)} \approx 10^{-8} A^{2/3} E^2 \ ,$$

where σ is ether E or M. The factor $A^{2/3}E^2 \leq 10^4$, so, as $l \uparrow$, $\lambda \downarrow$, dramatically!

16.4 Angular momentum and parity selection rules

Conservation of total angular momentum require and parity dictates that:

$$\begin{aligned} \vec{I_f} &= \vec{I_i} + \vec{l} \\ \pi_f &= (-1)^l \pi_i \qquad (E-\text{type}) \\ \pi_f &= (-1)^{l+1} \pi_i \qquad (M-\text{type}) \end{aligned} \tag{16.39}$$

Recalling the rules of quantized angular momentum addition, $|I_f - l| \leq I_i + l$, or $\Delta I = |I_f - I_i| \leq l \leq I_f + I_i$. Note that the emission of an electromagnetic decay photon can not be associated with a $0 \rightarrow 0$ transition. (The can occur via internal conversion, discussed later.) The above parity selection rules can also be stated as follows:

$$\begin{aligned} \Delta\pi = \text{no} &\Rightarrow \text{even } E/\text{odd } M \\ \Delta\pi = \text{yes} &\Rightarrow \text{odd } E/\text{even } M \end{aligned}$$

Some examples

$\underline{\frac{3}{2}^\pi \rightarrow \frac{5}{2}^\pi, \Delta\pi = \text{no}}$

$\Delta I = 1$. Therefore, $M1$, $E2$, $M3$, $E4$...

$\underline{\frac{3}{2}^\pi \rightarrow \frac{5}{2}^\pi, \Delta\pi = \text{yes}}$

$\Delta I = 1$. Therefore, $E1$, $M2$, $E3$, $M4$...

$\underline{0^\pi \rightarrow 0^\pi, \Delta\pi = \text{unknown}}$

$\Delta I = 4$. Therefore, $E4$ if $\Delta\pi = \text{yes}$, $M4$ otherwise.

$\underline{2^+ \rightarrow 0^+}$

This is an $E2$ transition.

Real-life example

One of the most important, and useful γ decays is the decay of ^{60}Co. It has been used extensively for radiotherapy purposes, and used today for industrial radiation processes, sterilization, food processing, material transformation, and other applications.

^{60}Co does not occur naturally, as it has a half-life of 5.27y. it is produced by neutron activation of stable ^{59}Co. The entire activation and decay sequences are given as follows, with a decay chart given in Figure 16.7. The decay chart also has information about spin and parity assignments that are needed to decipher the following table.

$$^{59}_{27}\mathrm{Co}_{32} + n \longrightarrow ^{60}_{27}\mathrm{Co}_{33} \longrightarrow ^{60}_{28}\mathrm{Ni}^{*}_{32} + \beta^{-} + \overline{\nu}_e \text{ (5.271y)} \longrightarrow ^{60}_{28}\mathrm{Ni}_{32} + n\gamma \text{ (prompt)}$$

Figure 16.7: ^{60}Co decay scheme.

I_i^π	I_f^π	E_N (keV)	E_{γ_n} (keV)	exp	modes	τ (ps)	frac
4^+		2505.766				3.3	
	2_1^+		1173.237 (γ_4)	E2+M3	**E2**,M3,E4,M5,E6		$\equiv 1$
	2_2^+		346.93 (γ_5)	unk	**E2**,M3,E4,M5,E6		7.6×10^{-5}
	0_1^+		2505.766 (γ_6)	E4	**E4** (pure)		2.0×10^{-8}
0_2^+		2284.87				> 1.5	
2_2^+		2158.64				0.59	
	2_1^+		826.06 (γ_2)	M1+E2	**M1**,E2,M3,E4		$\equiv 1$
	0_1^+		2158.57 (γ_3)	E2	**E2** (pure)		0.176
2_1^+		1332.518				0.77	
	0_1^+		1332.518 (γ_1)	E2	**E2** (pure)		

Table 16.1: The decay scheme of ^{60}Ni that is generated from the most probable β decay of ^{60}Co.

The likely explanation of the nuclear structure of ^{60}Ni is that the levels shown are a single quadrupole phonon excitation at 1.333 MeV with a two quadrupole phone triplet at about 2.5 MeV. The 0^+ state is not fed by this β decay.

Comparing	Details	theory	exp	ratio	Comments
γ_4, γ_1	E2(1173)/E2(1333)	0.53	0.23	2.3	
γ_4 modes	M3/E2			2.6×10^{-5}	
	E4/E2			5.1×10^{-13}	Mostly E2
γ_4, γ_5	E2(347)/E2(1173)	2.3×10^{-3}	7.6×10^{-5}	30	ψ_i/ψ_f mismatch?
γ_6, γ_4	E4(2505)/E2(1173)	6.2×10^{-8}	2.0×10^{-8}	3.1	
γ_6, γ_5	E4(2505)/E2(347)	2.7×10^{-5}	2.6×10^{-4}	0.10	Collective effect?
γ_2 modes	E2/M1			2.1×10^{-4}	Mostly M1
γ_2, γ_3	E2(2159)/M1(826)	0.026	0.176	0.15	

Table 16.2: Comparison of measurements of the decay rates for the γ transition rates for the decay photons of ^{60}Ni that are generated from the most probable β decay of ^{60}Co.

Comparison with Weisskopf estimates

16.5 Angular Distribution and Polarization Measurements

Not covered in NERS312. Parts were covered earlier.

16.6 Internal Conversion

We discussed previously, that $0^+ \rightarrow 0^+$ transitions can not occur via electromagnetic γ transitions. This is because the electromagnetic operator does not have an $l = 0$ component, since the photon's intrinsic spin is $s = 1$. However, there is an electromagnetic process that can cause a $0^+ \rightarrow 0^+$ transition, a process called *internal conversion*.

The classical visualization is that an electron (predominantly a K-shell electron) enters the nucleus, feels the electromagnetic force from a nucleon in an excited states, or a collection of nucleons in an excited states, and acquires enough energy to liberate the electron from the nucleus cause the nucleus to transition to a lower energy level. The nucleus, as a whole, recoils to conserve momentum.

The quantum mechanical picture is similar, and is depicted graphically in Figure 16.8.

We've learned that, whether we're adapting classical electrodynamics to quantum electrodynamics, or if we are starting with a more rigorous Fermi Golden Rule #2 approach, that the most important part, and the least known part, is the calculation of the transition matrix element, $\mathcal{M}^{i \rightarrow f}$.

Figure 16.8: The Quantum Mechanical description of internal conversion.

For internal conversion, the matrix element is:

$$\mathcal{M}_{ic}^{i\to f} = \langle \psi_N^f \psi_e^{\text{free}} | \mathcal{O}_{em} | \psi_e^{\text{bound}} \psi_N^i \rangle \ . \tag{16.40}$$

This is to be compared with the matrix element for γ transitions:

$$\mathcal{M}_{\gamma}^{i\to f} = \langle \psi_N^f \psi_\gamma^{\text{free}} | \mathcal{O}_{em} | \psi_N^i \rangle \ . \tag{16.41}$$

Note the similarity between the matrix elements. They contain many physical similarities, that are accompanied by mathematical similarity. In fact, *every* γ decay is in competition with internal conversion (more on this later). The only one that stands alone is a $0^+ \to 0^+$ internal conversion, that has no γ counterpart.

Internal conversion, β decay and internal conversion energetics

When a nucleus in an excited state decays, it does so via α decay, β decay, or γ decay. Often a decay can proceed via more than one decay channel, and the daughter, and her progeny, can decay as well. A particular interesting case, from the standpoint of measurement, is when β decay and internal conversion happen in close temporal proximity. For example:

$$^{203}_{80}\mathrm{Hg}_{123} \longrightarrow ^{203}_{81}\mathrm{Tl}^{*}_{122} + e^{-} + \overline{\nu} \longrightarrow ^{203}_{81}\mathrm{Tl}_{122} + e^{-}\ (\mathrm{IC})\ .$$

Thus, a measurement of the electrons being emitted y radioactive $^{203}_{80}\mathrm{Hg}_{123}$, sees both β decay electrons, as well as IC electrons. However, the signatures of both of these processes are very distinct. The β decay electrons give a continuous energy spectrum, while the IC electrons are seen as sharp lines on the β spectrum, at the energies of the nuclear transition (less recoil).

Generally, the energy of the kinetic electron is given by:

$$T_e = \frac{Q - B}{1 + m_e/m_{x'}}\ . \tag{16.42}$$

The denominator term is usually ignored. (It is about a $1/(2000 * A)$ correction.) The B term is the binding energy of the converted electron. This can not be ignored, and depends upon the atomic shell from which the electron was converted.

For our specific example, $Q = 279.910$, and:

X-ray notation	spectroscopic notation	B (keV)	T_e (keV)
K	$1s_{1/2}$	85.529	193.661
$\mathrm{L_I}$	$2s_{1/2}$	15.347	263.843
$\mathrm{L_{II}}$	$2p_{1/2}$	14.698	264.492
$\mathrm{L_{III}}$	$2p_{3/2}$	12.657	266.533
$\mathrm{M_I}$	$3s_{1/2}$	3.704	275.486

Internal conversion contribution to decay rate

As mentioned previously, since γ decay and internal conversion both contribute to the electromagnetic decay rate, we can write the total decay rate as a sum of the processes, in increasing specificity:

$$\lambda_{em} = \lambda_\gamma + \lambda_e\ , \tag{16.43}$$

where λ_γ is the γ transition rate, and λ_e is the internal conversion transition rate.
In terms of the ratio, $\alpha \equiv \lambda_e/\lambda_\gamma$,

$$\begin{aligned}
\lambda_{em} &= \lambda_\gamma(1+\alpha) \\
\lambda_{em} &= \lambda_\gamma + \lambda_{e_{\rm K}} + \lambda_{e_{\rm L}} + \lambda_{e_{\rm M}} \cdots \\
\text{or} \quad & \lambda_\gamma(1+\alpha_{\rm K} + \alpha_{\rm L} + \alpha_{\rm M} \cdots) \\
\lambda_{em} &= \lambda_\gamma + \lambda_{e_{\rm K}} + \lambda_{e_{\rm L_I}} + \lambda_{e_{\rm L_{II}}} + \lambda_{e_{\rm L_{III}}} + \lambda_{e_{\rm M_I}} \cdots \\
\text{or} \quad & \lambda_\gamma(1+\alpha_{\rm K} + \alpha_{\rm L_I} + \alpha_{\rm L_{II}} + \alpha_{\rm L_{III}} + \alpha_{\rm M_I} \cdots)
\end{aligned} \tag{16.44}$$

Using hydrogenic wavefunctions, we may estimate:

$$\begin{aligned}
\alpha({\rm E}l) &\cong \frac{Z^3}{n^3}\left(\frac{l}{l+1}\right)\alpha^4\left(\frac{2m_ec^2}{E_\gamma}\right)^{l+5/2} \\
\alpha({\rm M}l) &\cong \frac{Z^3}{n^3}\alpha^4\left(\frac{2m_ec^2}{E_\gamma}\right)^{l+3/2}
\end{aligned} \tag{16.45}$$

The trends that are predicted, all verified by experiment, are:

$\alpha(\sigma l)$	$\propto Z^3$
$E_\gamma \uparrow$	$\alpha(\sigma l) \downarrow$
$l \uparrow$	$\alpha(\sigma l) \uparrow$
$n \uparrow$	$\alpha(\sigma l) \downarrow$

Problems and Projects

Review-type questions

1. Derive (16.6) and (16.7).

2. Show (16.8).

3. Find an expression for the classical, static quadruple moment. Using a simple example, show that it has the expected parity.

4. Derive (16.42).

Exam-type questions

1. Nucleus A decays to its ground state with a known Q-value.

   (a) Show that, if one accounts for nuclear recoil non-relativistically, that E_γ and Q are related by:

   $$E_\gamma = \frac{2Q}{1+\sqrt{1+\frac{2Q}{m_A c^2}}} \ . \tag{16.46}$$

   (b) For typical gamma decay energies, (16.46) is often approximated by:

   $$E_\gamma = Q\left(1-\frac{Q}{2m_A c^2}\right) \ . \tag{16.47}$$

   Discuss how this approximation is obtained and derive (16.47).

   (c) Show that the fully relativistic expression for (16.46) is:

   $$E_\gamma = \frac{Q\left(1+\frac{Q}{2m_A c^2}\right)}{1+\frac{Q}{m_A c^2}} \ .$$

2. The energy-level scheme drawn below, represents some of the low-lying levels of ^{120}Te. The number to the left of each line represents the level of the excited state, with (0) being the ground state. The number to the right is the known I^π for that level. For example, the level labeled '(3)' has $I^\pi = 4^+$.

   (a) In the energy-level scheme below, use vertical lines to connect all the possible electromagnetic transitions.

   (5) ——————————————————————— 3^-

   (4) ——————————————————————— 2^+

   (3) ——————————————————————— 4^+

   (2) ——————————————————————— 0^+

   (1) ——————————————————————— 2^+

   (0) ——————————————————————— 0^+

   (b) Refer to the chart on the previous page. Then, in the table below, fill in all the empty boxes. Please follow the example given for the (1) $\rightarrow$ (0) transition.

   Column 1 The level transition,

   Column 2 The starting I_i^π,

   Column 3 The ending I_f^π,

   Column 4 Whether or not a parity change occurs,

   Column 5 All possible EL, ML or IC transitions. Using square brackets, [ ], indicate which is the most probable γ-transition. If two γ-transitions can compete for most probable, indicate so by bracketing them both.

Transition	I_i^π	I_f^π	$\Delta\pi$?	M-poles
$(1) \rightarrow (0)$	2^+	0^+	no	[E2] IC

3. (a) Explain the importance of observing and measuring γ-decay transitions with respect to understanding nuclear structure. Be sure to mention multipolarity, parity, orbital angular momentum, electric and magnetic transitions. In your discussion, describe how the multipolarity and parity change of a γ-decay transition is determined experimentally.

   (b) Sort, in order of decreasing electromagnetic decay probabilities, the electric and magnetic multipole transitions for the $\Delta\pi = yes$ transitions. Then, do the same for the $\Delta\pi = no$ transitions. Under what circumstances will a higher order multiple compete with the decay rate of a lower order multipole?

   (c) A $0^+ \longrightarrow 0^+$ transition can not decay through the release of a single gamma. Why not? If there are no intermediate states between the two 0^+ levels, how can this nucleus de-excite electromagnetically? Make a drawing that illustrates this process.

   (d) ^{60}Co decays via the following scheme:
   Figure to be supplied...

      i. What is the probable nature (order of multipolarity, electric or magnetic) of the $4^+ \rightarrow 2^+$ and the $2^+ \rightarrow 0^+$ transitions?

      ii. Is the $4^+ \rightarrow 0^+$ transition possible? Why?

4. A nucleus with atomic mass M_X has two excited levels, E_1 and E_2, where $E_2 > E_1$. It can de-excite to the ground state via a single γ decay with energy E_a, or via a pair of gammas, with energies E_b and E_c. You have made measurements of the 3 gammas.

   (a) Draw the decay scheme.

   (b) You observe that $E_a \neq E_b + E_c$. Why?

   (c) Develop, from first principles, an expression for $E_b + E_c - E_a$.

Chapter 17

Nuclear Reactions

Note to students and other readers: This Chapter is intended to supplement Chapter 11 of Krane's excellent book, "Introductory Nuclear Physics". Kindly read the relevant sections in Krane's book first. This reading is supplementary to that, and the subsection ordering will mirror that of Krane's, at least until further notice.

17.1 Types of Reactions and Conservation Laws

A typical nuclear reaction is depicted in Figure 17.1. The following two ways of describing that reaction are equivalent:

$$\mathrm{a} + \mathrm{X} \rightarrow \mathrm{Y} + \mathrm{b} \ ,$$

or

$$\mathrm{X(a,b)Y} \ .$$

From now on, we shall usually use the latter because it is more compact (and easier to type!).

The above reaction is the kind we shall focus on because they represent most of the important reactions in Nuclear Physics and Engineering and the Radiological Sciences. There are only two bodies in the final state: a and Y. The particle labelled "a" is the projectile. We will generally restrict ourselves to considering light projectiles, with $A \leq 4$, and projectile energies, $T_{\mathrm{a}} \lesssim 10$ MeV. The particle labelled "X" is to be thought of as the "target". The particle labelled "b" is generally the lighter reaction product, and is often the particle that is observed by the measurement apparatus. The remaining reaction product, is "Y". The is generally the heavier of the two reaction products, and is usually unobserved, as it stays within the target "foil".

Figure 17.1: A typical nuclear reaction.

Some nomenclature

reaction	name	example
X(a,γ)Y	*radiative capture*	${}^{A}_{Z}\mathrm{X}_{N}(n,\gamma)^{A+1}_{Z}\mathrm{X}_{N+1}$
X(γ,b)Y	*nuclear photoeffect*	${}^{A}_{Z}\mathrm{X}_{N}(\gamma,p)^{A-1}_{Z-1}\mathrm{X}_{N}$
X(a,a)X	*nuclear scattering*	${}^{A}_{Z}\mathrm{X}_{N}(\alpha,\alpha)^{A}_{Z}\mathrm{X}_{N}$, Rutherford scattering
X(a,a)X*	*inelastic scattering*	${}^{A}\mathrm{X}(n,n)^{A}\mathrm{X}^{*}$
	knock out reaction	${}^{A}_{Z}\mathrm{X}_{N}(n,nn)^{A}_{Z}\mathrm{X}_{N-1}$, ${}^{A}_{Z}\mathrm{X}_{N}(n,np)^{A}_{Z-1}\mathrm{X}_{N}$
	transfer reaction	${}^{A}_{Z}\mathrm{X}_{N}(n,p)^{A}_{Z-1}\mathrm{X}_{N+1}$
	direct reactions	"a" interacts with only one or a few nucleons in X
	compound reactions	a + X $\rightarrow \mathrm{Y}^{\mathrm{m}}_{t_{1/2}\gg\sim 10^{-23}\mathrm{s}} \rightarrow$ fragments
	resonance reaction	n or p + X $\rightarrow \mathrm{Y}^{\mathrm{m}} \rightarrow$ decay products

17.1.1 Observables

Returning back to an X(a,b)Y reaction, the most comprehensive experiment one can perform is to determine the b-particle type, and map out its angular distribution pattern, a so-called 4π experiment. At each different angle, we also measure $T_{\rm b}$, because that can change with direction as well. Refer to Figure 17.2.

Figure 17.2: A typical set-up for a 4π experiment.

By knowing the intensity of the beam, we can thus compute the differential cross section, differential in $T_{\rm b}$, $\theta_{\rm b}$, and $\phi_{\rm b}$, presented here in the 3 different forms that one encounters in the literature.

$$\frac{{\rm d}\sigma(T_{\rm b},\theta_{\rm b},\phi_{\rm b})}{{\rm d}\Omega_{\rm b}{\rm d}T_{\rm b}} = \frac{{\rm d}\sigma}{{\rm d}\Omega_{\rm b}{\rm d}T_{\rm b}} = \sigma(T_{\rm b},\theta_{\rm b},\phi_{\rm b}) \ , \tag{17.1}$$

where ${\rm d}\Omega_{\rm b}$ is the differential solid angle associated with the direction of the b-particle, namely:

$$\mathrm{d}\Omega_\mathrm{b} = \sin\theta_\mathrm{b}\mathrm{d}\theta_\mathrm{b}\mathrm{d}\phi_\mathrm{b} \ .$$

The third form is favored by some authors (not me) because of its brevity. However, its use is common, and I wanted to familiarize you with it.

From this differential cross section, alternative, integrated forms my be found:

the cross section differential in angles only,

$$\sigma(\theta_\mathrm{b},\phi_\mathrm{b}) = \frac{\mathrm{d}\sigma}{\mathrm{d}\Omega_\mathrm{b}} = \frac{\mathrm{d}\sigma(\theta_\mathrm{b},\phi_\mathrm{b})}{\mathrm{d}\Omega_\mathrm{b}} = \int \mathrm{d}T_\mathrm{b}\left(\frac{\mathrm{d}\sigma(T_\mathrm{b},\theta_\mathrm{b},\phi_\mathrm{b})}{\mathrm{d}\Omega_\mathrm{b}\mathrm{d}T_\mathrm{b}}\right) \ , \tag{17.2}$$

the cross section differential in energy only,

$$\sigma(T_\mathrm{b}) = \frac{\mathrm{d}\sigma}{\mathrm{d}T_\mathrm{b}} \ = \frac{\mathrm{d}\sigma(T_\mathrm{b})}{\mathrm{d}T_\mathrm{b}} \ = \int \mathrm{d}\Omega_\mathrm{b}\left(\frac{\mathrm{d}\sigma(T_\mathrm{b},\theta_\mathrm{b},\phi_\mathrm{b})}{\mathrm{d}\Omega_\mathrm{b}\mathrm{d}T_\mathrm{b}}\right) \ , \tag{17.3}$$

and the total cross section,

$$\sigma = \int \mathrm{d}T_\mathrm{b}\int \mathrm{d}\Omega_\mathrm{b}\left(\frac{\mathrm{d}\sigma(T_\mathrm{b},\theta_\mathrm{b},\phi_\mathrm{b})}{\mathrm{d}\Omega_\mathrm{b}\mathrm{d}T_\mathrm{b}}\right) \ . \tag{17.4}$$

If one normalize (17.1) as follows:

$$p(T_\mathrm{b},\theta_\mathrm{b},\phi_\mathrm{b}) = \frac{1}{\sigma}\frac{\mathrm{d}\sigma(T_\mathrm{b},\theta_\mathrm{b},\phi_\mathrm{b})}{\mathrm{d}\Omega_\mathrm{b}\mathrm{d}T_\mathrm{b}} \ , \tag{17.5}$$

$p(T_\mathrm{b},\theta_\mathrm{b},\phi_\mathrm{b})$ is a "joint" probability distribution, properly normalized, over the variables, T_b, θ_b, and ϕ_b. From this probability distribution, we can determine quantities like, $\overline{T_\mathrm{b}}$, the average energy, or $\overline{1-\cos\theta_\mathrm{b}}$, the so-called *scattering power*.

17.1.2 Conservation laws

The conservation laws are essential tools in scattering analysis. Conservation of energy and linear momentum allow us to deduce the properties of X and Y. Conservation of neutron and proton number also helps us deduce the properties of X and Y. Conservation of angular momentum and parity, allow us to deduce spins and parities.

17.2 Energetics of Nuclear Reactions

General Considerations in a Relativistic Formalism

For the X(a,b)Y reaction, conservation of Total Energy means:

$$m_{\rm a}c^2 + m_{\rm X}c^2 + T_{\rm a} + T_{\rm X} = m_{\rm b}c^2 + m_{\rm Y}c^2 + T_{\rm b} + T_{\rm Y} \ , \tag{17.6}$$

or,

$$Q + T_{\rm a} + T_{\rm X} = T_{\rm b} + T_{\rm Y} \ , \tag{17.7}$$

where,

$$Q \equiv (m_{\rm a} + m_{\rm X} - [m_{\rm b} + m_{\rm Y}])c^2 \ . \tag{17.8}$$

Q is the *reaction Q-value*. When $Q > 0$, the reaction is exothermic (or exoergic). Energy is released by the transformation. When $Q < 0$, the reaction is endothermic (or endoergic). Energy is required, by the kinetic energies of the initial reactants, to make the transformation "go".

Recall that (17.7) is a relativistic expression. Therefore, we should use relativistic expressions for the kinetic energies. Doing so,

$$T_{\rm rel} = mc^2(\gamma - 1) \ . \tag{17.9}$$

Since the maximum energy projectile we deal with is about 10 MeV, we have the situation where $T \ll mc^2$. Thus we can find a relationship that relates $T_{\rm rel}$, to its non-relativistic counterpart, $T_{\rm NR}$:

$$T_{\rm rel} = T_{\rm NR}[1 + \frac{3}{4}\beta^2 + \mathcal{O}(\beta^4)] \ . \tag{17.10}$$

In the worst possible case ($T = 10$ MeV, $m_i = m_p$, the relativistic correction amounts to:

$$\frac{3}{4}\beta^2 \cong \frac{3T}{2m_pc^2} \cong 0.015 \ . \tag{17.11}$$

Therefore, in the worst possible $Q = 0$ case, there is a 1.5% correction, and up to double that in the large Q case. This can be an important correction, depending on the accuracy of the measurement. It represents a systematic error that may be swamped by other experimental

errors. However, from now on we shall ignore it, but keep in mind that large T and/or large Q analyses, with small masses, may be problematic, unless we adopt a relativistic correction.

Photons are always relativistic. So, if they are involved, we use $T_\gamma = E_\gamma$, and T_γ/c for its momentum.

Laboratory frame, non-relativistic analysis

In the laboratory frame, in a non-relativistic analysis, we make the following approximations:

1)	$T_{\rm a} < 10$ MeV	kinetic energy of the projectile
2)	$\vec{p}_{\rm a} = p_{\rm a}\hat{z}$	projectile's direction is along the positive z-axis
3)	$T_{\rm X} = 0$	target is at rest
4)	$1 \leq m_{\rm a}, m_{\rm b} \leq 4u$	small mass projectile, observed particle
5)	$m_{\rm X}, m_{\rm Y} \geq 4u$	large mass target, unobserved particles
6)	$\gamma_i = 1$	no relativistic corrections

With these approximations, Conservation of Energy and Conservation of Linear Momentum can be expressed in the following equations:

$$Q + T_{\rm a} = T_{\rm b} + T_{\rm Y} \ , \tag{17.12}$$

$$\vec{p}_{\rm a} = \vec{p}_{\rm b} + \vec{p}_{\rm Y} \ . \tag{17.13}$$

Since the Y-particle is unobserved, we choose to eliminate it from the (17.12) and (17.13), with the result:

$$T_{\rm b}(m_{\rm Y} + m_{\rm b}) - 2\sqrt{m_{\rm a} m_{\rm b} T_{\rm a}}\cos\theta_{\rm b}\sqrt{T_{\rm b}} - [m_{\rm Y}(Q + T_{\rm a}) - m_{\rm a} T_{\rm a}] = 0 \ . \tag{17.14}$$

This is a quadratic equation in $\sqrt{T_{\rm b}}$, in terms of the (presumably) known quantities, $T_{\rm a}$, Q, and the masses. Solving the quadratic equation yields:

$$T_{\rm b} = \frac{\sqrt{m_{\rm a} m_{\rm b} T_{\rm a}}\cos\theta_{\rm b} \pm \sqrt{m_{\rm a} m_{\rm b} T_{\rm a}\cos^2\theta_{\rm b} + (m_{\rm Y} + m_{\rm b})[m_{\rm Y} Q + (m_{\rm Y} - m_{\rm a})T_{\rm a}]}}{(m_{\rm Y} + m_{\rm b})} \ . \tag{17.15}$$

Thus, we see through (17.14), that 2-body reactions involve a direct correlation of the scattering angle, $\theta_{\rm b}$ and the b-particle's energy, $T_{\rm b}$. Consequently, if one measures, $T_{\rm b}$, and $\cos\theta_{\rm b}$ is also determined. The relationship between the two differential cross sections is:

$$\frac{{\rm d}\sigma}{{\rm d}\Omega_{\rm b}} = \frac{{\rm d}\sigma}{{\rm d}\phi_{\rm b}{\rm d}T_{\rm b}}\left(\frac{{\rm d}T_{\rm b}}{{\rm d}(\cos\theta_{\rm b})}\right) \ , \tag{17.16}$$

or

$$\frac{\mathrm{d}\sigma}{\mathrm{d}\phi_{\mathrm{b}}\mathrm{d}T_{\mathrm{b}}} = \frac{\mathrm{d}\sigma}{\mathrm{d}\Omega_{\mathrm{b}}} \left(\frac{\mathrm{d}(\cos\theta_{\mathrm{b}})}{\mathrm{d}T_{\mathrm{b}}}\right) . \tag{17.17}$$

The derivatives inside the large parentheses in (17.16) and (17.17) may be worked out from (17.14) and (17.15).

(17.15) may be complicated, but is is also very rich in physical content. Several interesting features should be noted:

1. If $Q > 0$, then

$$\sqrt{m_{\mathrm{a}} m_{\mathrm{b}} T_{\mathrm{a}}}\cos\theta_{\mathrm{b}} < \sqrt{m_{\mathrm{a}} m_{\mathrm{b}} T_{\mathrm{a}}\cos^2\theta_{\mathrm{b}} + (m_{\mathrm{Y}} + m_{\mathrm{b}})[m_{\mathrm{Y}} Q + (m_{\mathrm{Y}} - m_{\mathrm{a}})T_{\mathrm{a}}]} ,$$

   and, therefore, we must always choose the positive sign in (17.15).

2. If $Q < 0$, then there exists the possibility that, given a a certain value of T_{a}, at e angle $\theta_{\mathrm{b}} < \pi/2$, there can be two possible values of T_{b}. There is an energy threshold on T_{a} for this to occur. At threshold, $\theta_{\mathrm{b}} = 0$, as demonstrated in Figure 17.3.

   At this threshold, the $\sqrt{()}$ term vanishes. This implies that, at $T_{\mathrm{a}} = T_{\mathrm{th}}$, we have the condition:

$$0 = m_{\mathrm{a}} m_{\mathrm{b}} T_{\mathrm{th}}\cos^2\theta_{\mathrm{b}} + (m_{\mathrm{Y}} + m_{\mathrm{b}})[m_{\mathrm{Y}} Q + (m_{\mathrm{Y}} - m_{\mathrm{a}})T_{\mathrm{th}}] .$$

   Solving for T_{th} gives:

$$T_{\mathrm{th}} = \frac{-Q(m_{\mathrm{Y}} + m_{\mathrm{b}})}{m_{\mathrm{Y}} + m_{\mathrm{b}} - m_{\mathrm{a}}} . \tag{17.18}$$

3. Once $T_{\mathrm{a}} > T_{\mathrm{th}}$, there is an upper limit on T_{a}, called T'_{a} for this double-valued behavior on T_{b}. When $T_{\mathrm{a}} = T'_{\mathrm{a}}$, the smaller T_{b} falls to zero. This requires that:

$$\sqrt{m_{\mathrm{a}} m_{\mathrm{b}} T_{\mathrm{a}}}\cos\theta_{\mathrm{b}} = \sqrt{m_{\mathrm{a}} m_{\mathrm{b}} T_{\mathrm{a}}\cos^2\theta_{\mathrm{b}} + (m_{\mathrm{Y}} + m_{\mathrm{b}})[m_{\mathrm{Y}} Q + (m_{\mathrm{Y}} - m_{\mathrm{a}})T_{\mathrm{a}}]} ,$$

   from which we conclude that:

$$T'_{\mathrm{a}} = \frac{-Q m_{\mathrm{Y}}}{m_{\mathrm{Y}} - m_{\mathrm{a}}} . \tag{17.19}$$

Figure 17.3: Laboratory and center of momentum pictures of the X(a,b)Y interaction process.

4. For double-valued behavior on $T_{\rm b}$, combining the results of (17.18) (17.19), we see that $T_{\rm a}$ must fall in the range:

$$\frac{m_{\rm Y}+m_{\rm b}}{m_{\rm Y}+m_{\rm b}-m_{\rm a}} \leq \frac{T_{\rm a}}{|Q|} \leq \frac{m_{\rm Y}}{m_{\rm Y}-m_{\rm a}} \ . \tag{17.20}$$

5. If $T_{\rm th} < T_{\rm a} < T'_{\rm a}$, there are also scattering angles for which double-valued behavior can not exist. This happens when the argument of the $\sqrt{()}$ falls to zero. This defines a maximum scattering angle for double-valued observation. From (17.15), we see that this maximum angle is given by:

$$\cos^2\theta_{\rm b}^{\rm max} = \frac{m_{\rm Y}+m_{\rm m}}{m_{\rm a}m_{\rm b}T_{\rm a}}[-m_{\rm Y}Q-(m_{\rm Y}-m_{\rm a})T_{\rm a}] \tag{17.21}$$

These concepts are illustrated in Krane's Figures 11.2(a) and 11.2(b) on pages 382–384, as well (eventually) in Figure 17.4.f

Figure 17.4: Demonstration of the double-valued nature of $T_{\rm b}$.

Determining Q from scattering experiments

Up to now, we have assumed that Q was known. In some cases it is not, but, we can determine it from a scattering experiment. Reorganizing (17.14) as follows,

$$Q = T_{\rm b}\left(1+\frac{m_{\rm b}}{m_{\rm Y}}\right) - T_{\rm a}\left(1+\frac{m_{\rm a}}{m_{\rm Y}}\right) - 2\cos\theta_{\rm b}\left(\frac{m_{\rm a}m_{\rm b}}{m_{\rm Y}^2}T_{\rm a}T_{\rm b}\right)^{1/2} , \tag{17.22}$$

appears that we have isolated Q. However, recalling the definition of Q,

$$Q \equiv (m_{\rm a} + m_{\rm X} - [m_{\rm b} + m_{\rm Y}])c^2 , \tag{17.23}$$

our lack of knowledge of Q is tantamount to not knowing, at least with sufficient accuracy, one (or more) of the masses. For this type of experiment, it is usually the case, that $m_{\rm Y}$ is the unknown factor. "X" is usually in the ground state, and hence, well characterized. "a"

and "b" are light particles with $A \leq 4$, and therefore, extremely well known. "Y" is often left in an excited state, and is not known. Its ground state mass may be well known, but not its excited state. So, to recover this situation, we solve for $m_{\rm Y}$ in terms of Q, and substitute for $m_{\rm Y}$ in (17.23). We also perform the analysis at $\theta_{\rm b} = \pi/2$ so simplify the arithmetic. (This is not a necessary step, but it does save brain cells for more useful activities.)

The result is:

$$Q = T_{\rm b} - T_{\rm a} + \frac{(T_{\rm a} m_{\rm a} c^2 + T_{\rm b} m_{\rm b} c^2)}{[m_{\rm X} c^2 + m_{\rm a} c^2 - m_{\rm b} c^2] - Q} \ . \tag{17.24}$$

The most common approach to solving (17.24) is to form a common denominator, and then solve the resulting quadratic equation for Q. An alternative is presented below, treating (17.24) as an iterative or recursive equation.

It goes as follows:

1. Define a time-saving shorthand:

$$Q = \delta + \frac{()}{[] - Q} \ , \tag{17.25}$$

   where $\delta \equiv T_{\rm b} - T_{\rm a}$, and we have simply left the contents of the brackets empty. By using different types of brackets, we keep the symbols from getting mixed up. A clash of symbols is to be avoided.

2. Form the lowest order solution:

$$Q_0 = \delta + \frac{()}{[]} \ , \tag{17.26}$$

3. The $n^{\rm th}$ correction to Q is found from

$$\sum_{i=0}^{n} Q_i = \delta + \frac{()}{[] - \sum_{i=0}^{n-1} Q_i} \ , \tag{17.27}$$

4. The final answer is

$$Q = \sum_{i=0}^{n} Q_i \ . \tag{17.28}$$

   The iteration is stopped when the answer is "good enough".

Illustration:

$$\begin{aligned} Q_0 &= \delta + \frac{()}{[]} \\ Q_0 + Q_1 &= \delta + \frac{()}{[] - Q_0} \\ Q_0 + Q_1 &= \delta + \frac{()}{[]}\left(\frac{1}{1 - Q_0/[]}\right) \\ Q_0 + Q_1 &\equiv \delta + \frac{()}{[]}\left(1 + Q_0/[]\right) \\ Q_0 + Q_1 &= Q_0 + Q_0()/[]^2 \\ Q_1 &= Q_0()/[]^2 \end{aligned} \tag{17.29}$$

Thus, the fractional correction is:

$$\frac{Q_1}{Q_0} = \frac{(T_{\rm a} m_{\rm a} c^2 + T_{\rm b} m_{\rm b} c^2)}{[m_{\rm X} c^2 + m_{\rm a} c^2 - m_{\rm b} c^2]^2} \ . \tag{17.30}$$

In the worst possible case, $m_{\rm X} = m_{\rm a} = m_{\rm b} \cong 4u$, and $T_{\rm a} = T_{\rm b} \cong 10$ MeV, giving $Q_1/Q_0 \cong 5 \times 10^{-3}$. Since Q-values are known typically to $\approx 1 \times 10^{-4}$, this can be an important correction, especially for small-A target nuclei.

17.3 Isospin

We know that the strong force does not distinguish between protons and neutrons (mostly). Therefore, one can consider this to be another kind "of symmetry", and symmetries have quantum numbers associated with them. Consider neutrons and protons to be two states of a more general particle, called the nucleon, a name we have used throughout our discussions. However, now associate a new quantum number called "isospin", with the symbol T_3, and the following numerical assignments.

particle	T_3
p	$+\frac{1}{2}$
n	$-\frac{1}{2}$
${}^{A}_{Z}\mathrm{X}_{N}$	$\frac{1}{2}(Z-N)$

Table 17.1: Isospin assignments

The assignment of the plus sign to the proton is completely arbitrary, but now part of convention.

Historically, isospin has been called *isotopic spin*, where a given Z, T_3 combination identifies a specific isotope associated with Z, or *isobaric spin*, where a given A, T_3 combination identifies a specific isobar associated with A. Today, "isospin" appears to be the preferred name.

As long as the strong force does not distinguish between isobars associated with a given A, we expect to see some similarity in the excitation levels associated with nuclei with the same A. There is evidence for this, as seen in Figure 11.5 in Krane.

Isospins combine just as regular spins do. This is seen in the following example:

The dinucleon

Let us now consider the possible ways of combining two nucleons. We form the composite wavefunctions for two nucleons, one with spatial wavefunction $\psi(\vec{x}_1)$ and one with spatial wavefunction $\psi(\vec{x}_2)$. We label these as nucleon "1" and "2". We also in include there isospin as either up. $\uparrow$, or down, $\downarrow$. Finally, since they are intrinsic spin-$\frac{1}{2}$ particles, they must obey the Pauli Exclusion Principle, and form composite wavefunctions that are antisymmetric under the exchange of quantum numbers. Doing so, results in:

Note that the parity is associated with the space part of the wavefunction only. Also note, that the difference between the observed deuteron and its odd parity counterpart (unobserved) is how the antisymmetry is achieved. In the unobserved case, it is the spatial part that is antisymmetrized, while the observed deuteron has a positive parity spatial wavefunction and an antisymmetrized isopin wavefunction. In order to make full use of the attractive strong force, the nucleons must come into close proximity. All of the members of the isobaric

T	T_3	composite wavefunction	π	
1	1	$2^{-1/2}[\psi_1(\vec{x}_1)\psi_2(\vec{x}_2) - \psi_1(\vec{x}_2)\psi_2(\vec{x}_1)](\uparrow_1\uparrow_2)$	-1	diproton
1	0	$2^{-1}[\psi_1(\vec{x}_1)\psi_2(\vec{x}_2) - \psi_1(\vec{x}_2)\psi_2(\vec{x}_1)](\uparrow_1\downarrow_2 + \downarrow_1\uparrow_2)$	-1	odd parity deuteron?
1	-1	$2^{-1/2}[\psi_1(\vec{x}_1)\psi_2(\vec{x}_2) - \psi_1(\vec{x}_2)\psi_2(\vec{x}_1)](\downarrow_1\downarrow_2)$	-1	dineutron
0	0	$2^{-1}[\psi_1(\vec{x}_1)\psi_2(\vec{x}_2) + \psi_1(\vec{x}_2)\psi_2(\vec{x}_1)](\uparrow_1\downarrow_2 - \downarrow_1\uparrow_2)$	+1	Deuteron

Table 17.2: The dinucleon quantum states

triplet have antisymmetric spatial wavefunctions. That is why none are bound.

17.4 Reaction Cross Sections

Covered elsewhere, and partly in 311.

17.5 Experimental Techniques

Not covered in 312.

17.6 Coulomb Scattering

Covered in 311.

17.7 Nuclear Scattering

Covered in Chapter 10.

17.8 Scattering and Reaction Cross Sections

Consider a $\hat{z}$-direction plane wave incident on a nucleus, as depicted in Figure 17.5.

The wavefunction for the incident plane wave:

$$\psi_{\text{inc}} = Ae^{ikz} \ . \tag{17.31}$$

Figure 17.5: Scattering of a plane wave from a nucleus.

We have seen elsewhere, that (17.31) is a solution to the Schrödinger equation in a region of space where there is no potential (or a constant potential). Since no potential is also a central potential (in the sense that it does not depend on orientation), we should be able to recast the solution in spherical-polar coordinates, and identify the angular momentum components of the incident wave. If we did this, we could show:

$$\psi_{\rm inc} = Ae^{ikz} = A\sum_{l=0}^{\infty} i^l(2l+1)j_l(kr)P_l(\cos\theta)\ . \tag{17.32}$$

The j_l's are the "spherical Bessel functions, and the P_l's are the regular Legendre polynomials, that we have encountered before.

The properties of the j_l's are:

$$\begin{aligned}
j_0(z) &= \frac{\sin z}{z} \\
j_1(z) &= \frac{\sin z}{z^2} - \frac{\cos z}{z} \\
j_2(z) &= \frac{3\sin z}{z^3} - \frac{3\cos z}{z^2} - \frac{\sin z}{z} \\
j_l(z) &= (-z)^l \left(\frac{1}{z}\frac{\mathrm{d}}{\mathrm{d}z}\right)^l j_0(z) \\
\lim_{z\to 0} j_l(z) &= \frac{z^l}{(2l+1)!!} + \mathcal{O}(z^{l+1}) \\
\lim_{z\to\infty} j_l(z) &= \frac{\sin(z - l\pi/2)}{z} + \mathcal{O}(z^{-2})
\end{aligned} \tag{17.33}$$

Thus, we have identified the angular momentum components of the incoming wave, with angular momentum components $l\hbar$. The magnetic quantum number associated with l, namely, m_l does not appear in (17.32) because (17.31) has azimuthal symmetry. This is not a requirement, and is easy to account for, but is not required for our discussions. (17.33) is called the "partial wave expansion", and exploiting it to extract physical results is called "partial wave analysis".

17.8.1 Partial wave analysis

Semi-classical introduction

As an introduction to this section, first let's estimate the cross section of a nucleus, using semi-classical physics. We know, from classical scattering analysis, that the impact parameter, b, is associated with the angular momentum of the projectile about the target, centered at the origin. Equating the quantum mechanical angular momentum of the wave component with its classical counterpart, we get:

$$pb = l\hbar \ , \tag{17.34}$$

or

$$b = \frac{l\hbar}{p} = \frac{l}{2\pi}\frac{h}{p} = l\frac{\lambda}{2\pi} = l\lambda \ , \tag{17.35}$$

in terms of the reduced wavelength, λ.

So, continuing with this semiclassical train of thought:

$l = 0 \rightarrow 1$ covers the area $\pi\lambda^2$
$l = 1 \rightarrow 2$ covers the area $(4-1)\pi\lambda^2$
$l \rightarrow l+1$ covers the area $[(l+1)^2 - l^2]\pi\lambda^2 = (2l+1)\pi\lambda^2$

Summing up all these contributions:

$$\sigma = \sum_{l=0}^{[R/\lambda]} (2l+1)\pi\lambda^2 = \pi(R+\lambda)^2 \ , \tag{17.36}$$

where R is the nuclear radius. Thus, we see that λ factors into the computation of the cross section as an effective size of the projectile.

The quantum approach

We start by recognizing that we wish to consider the mathematic representation of the wave at locations far from the scattering center. Thus, for $kr \gg 1$, we use the asymptotic result of (17.33),

$$\lim_{kr\to\infty} j_l(kr) = \frac{\sin(kr - l\pi/2)}{kr} = i\frac{\left[e^{-i(kr-l\pi/2)} - e^{i(kr-l\pi/2)}\right]}{2kr} \ . \tag{17.37}$$

Combining (17.36) with (17.32) gives,

$$\psi_{\rm inc} = Ae^{ikz} = \frac{A}{2kr}\sum_{l=0}^{\infty} i^{l+1}(2l+1)\left[e^{-i(kr-l\pi/2)} - e^{i(kr-l\pi/2)}\right] P_l(\cos\theta) \ . \tag{17.38}$$

This is an interesting result! The $e^{-ikr}/(kr)$ part represents a spherical wave converging on the nucleus, while the $e^{ikr}/(kr)$ part represents a spherical wave moving away from the nucleus. The nucleus can only modify the outgoing part. One way of representing this is via a modification of the outgoing part. Thus, the total solution, with incoming and scattered parts, is written:

$$\psi = Ae^{ikz} = \frac{A}{2kr}\sum_{l=0}^{\infty} i^{l+1}(2l+1)\left[e^{-i(kr-l\pi/2)} - \eta_l e^{i(kr-l\pi/2)}\right] P_l(\cos\theta) \ , \tag{17.39}$$

where η_l is a complex coefficient that represents the mixing the two parts of the outgoing wave, part of which is associated with the initial plane wave, as well as the scattered part. Thus, the total wave is a combination of both,

$$\psi = \psi_{\rm inc} + \psi_{\rm sc} \ , \tag{17.40}$$

allowing us to express the scattered part by itself,

$$\psi_{\rm sc} = \frac{Aie^{ikr}}{2kr}\sum_{l=0}^{\infty}(2l+1)(1-\eta_l)P_l(\cos\theta)\ . \tag{17.41}$$

As in 1D, we use the probability current density to evaluate the effectiveness of the scatterer. The scattered probability current is:

$$j_{\rm sc} = \frac{\hbar}{2im}\left[\psi^*_{\rm sc}\left(\frac{\partial\psi_{\rm sc}}{\partial r}\right) - \left(\frac{\partial\psi^*_{\rm sc}}{\partial r}\right)\psi_{\rm sc}\right]\ . \tag{17.42}$$

Putting (17.41) into (17.42) results in:

$$j_{\rm sc} = |A|^2\left(\frac{\hbar}{4kr^2}\right)\left|\left[\sum_{l=0}^{\infty}(2l+1)(1-\eta_l)P_l(\cos\theta)\right]\right|^2\ . \tag{17.43}$$

Since the incoming wave has probability current

$$j_{\rm inc} = \frac{\hbar k}{m}\ , \tag{17.44}$$

the differential cross section is expressed as follows:

$$\frac{{\rm d}\sigma}{{\rm d}\Omega} = \frac{j_{\rm sc}}{j_{\rm inc}}r^2\ , \tag{17.45}$$

in analogy with the 1D transmission and reflection coefficients.

Then, we can show that

$$\frac{{\rm d}\sigma_{\rm sc}}{{\rm d}\Omega} = \frac{1}{4k^2}\left|\sum_{l=0}^{\infty}(2l+1)(1-\eta_l)P_l(\cos\theta)\right|^2\ , \tag{17.46}$$

and

$$\sigma_{\rm sc} = \frac{\pi}{k^2}\sum_{l=0}^{\infty}(2l+1)|1-\eta_l|^2\ . \tag{17.47}$$

Since both the incident and outgoing waves have wavenumber k, the cross sections discussed above model "elastic" scattering. Elastic scattering is characterized by no loss of probability of the incoming particle. Mathematically, this expressed by,

$$|\eta_l| = 1 \ ,$$

for all l. Thus, the only thing that the target does is to redirect the wave and shift its phase. Hence we, define a *phase shift*, δ_l, for each l-component, using the following convention,

$$\eta_l = e^{2i\delta_l} \ ,$$

from which we can derive:

$$\sigma_{\rm sc}^{\rm elas} = 4\pi\lambda\!\!\!^{-2} \sum_{l=0}^{\infty} (2l+1) \sin^2 \delta_l \ . \tag{17.48}$$

From now on, we'll reserve the name, $\sigma_{\rm sc}$ for elastic scattering only. Note that $1/k = \lambda/(2\pi) \equiv \lambda\!\!\!^{-}$.

Reaction cross sections

Generally, however, $|\eta_l| < 1$, as the incoming beam can be absorbed, and part of it unabsorbed. We will identify:

$$\frac{{\rm d}\sigma_{\rm r}}{{\rm d}\Omega} = \frac{j_{\rm in} - j_{\rm out}}{j_{\rm inc}} r^2 \ , \tag{17.49}$$

as the *reaction* cross section, involving the difference between the currents of the incoming and outgoing spherical waves.

From (17.38) we see that:

$$\begin{aligned}
\psi_{\rm in} &= \frac{A}{2kr} \sum_{l=0}^{\infty} i^{2l+1} (2l+1) \left[e^{-i(kr - l\pi/2)} \right] P_l(\cos\theta) \\
&= \frac{Aie^{-ikr}}{2kr} \sum_{l=0}^{\infty} i^{2l} (2l+1) P_l(\cos\theta) \qquad (17.50) \\
\psi_{\rm out} &= -\frac{A}{2kr} \sum_{l=0}^{\infty} i^{2l} (2l+1) \eta_l \left[e^{i(kr - l\pi/2)} \right] P_l(\cos\theta) \\
&= \frac{-Aie^{ikr}}{2kr} \sum_{l=0}^{\infty} (2l+1) \eta_l P_l(\cos\theta) \ . \qquad (17.51)
\end{aligned}$$

Adapting (17.42) we obtain the incoming and outgoing probability currents:

$$j_{\rm in} = |A|^2 \left(\frac{\hbar}{4kr^2}\right) \left| \left[\sum_{l=0}^{\infty} i^{2l}(2l+1)P_l(\cos\theta) \right] \right|^2 \tag{17.52}$$

$$j_{\rm out} = |A|^2 \left(\frac{\hbar}{4kr^2}\right) \left| \left[\sum_{l=0}^{\infty} (2l+1)\eta_l P_l(\cos\theta) \right] \right|^2 \tag{17.53}$$

Combining (17.49) with (17.44), (17.52) and (17.53), and then integrating over all angles, results in:

$$\sigma_{\rm r} = \pi\lambda\!\!\!^{-2} \sum_{l=0}^{\infty} (2l+1)(1-|\eta_l|^2) \ . \tag{17.54}$$

Note that for elastic scattering, $\sigma_{\rm r} = 0$.

Total cross section

The total cross section is the sum of the inelastic and reaction cross sections. Adding (17.47) and (17.54) result in:

$$\sigma_{\rm t} = \sigma_{\rm sc} + \sigma_{\rm r} = 2\pi\lambda\!\!\!^{-2} \sum_{l=0}^{\infty} (2l+1)[1-\Re(\eta_l)] \ , \tag{17.55}$$

where $\Re()$ is some typesetting software's idea of "real part".

Our results are summarized in the following table, for the contribution to the cross sections from the l'th partial wave.

Process	η_l	$\sigma^l_{\rm sc}/(\pi\lambda\!\!\!^{-2}(2l+1))$	$\sigma^l_{\rm r}/(\pi\lambda\!\!\!^{-2}(2l+1))$	
elastic only	$\lvert\eta_l\rvert = 1$	$\lvert 1-\eta_l\rvert^2$	0	no loss of probability
absorption only	$\eta_l = 0$	1	1	equal!
Mixed	η_l =?	$\lvert 1-\eta_l\rvert^2$	$1-\lvert\eta_l\rvert^2$	work to do!

The most interesting feature is, that even with total absorption of the l'th partial wave, elastic scattering is predicted. This is because waves will always (eventually) fill in the shadow region behind an absorber. A good way to demonstrate this for yourself, is to hold a pencil near the ground, on one of those rare sunny days in Michigan. Near the ground, the shadow is sharp, well-defined. As you raise the pencil the edges become fuzzy. Eventually, if you hold it high enough, its shadow disappears entirely.

How are the partial wave amplitudes are computed?

Although the foregoing analysis is elegant, we still have considerable work to do for the general case. For the theoreticians amongst us, we have to solve the radial Schrödinger equation for the potential that causes the scattering (assuming it's a central potential) and guarantee slope and value continuity everywhere. The η_l's are then determined the asymptotic forms of the solutions. Typically a numerical procedure is followed. For the experimentalists among us, the differential cross sections have to be mapped out, and the η_l's are inferred by inverting equations (17.46) as well as its reaction counterpart. Fortunately, for nuclear scattering, only the first few partial waves are important. Interested readers should consult Krane's book, Section 4.2 for more details.

17.9 The Optical Model

The optical model of the nucleus employs a model of the nucleus that that has a complex part to it's potential. Calling this generalized potential, $U(r)$, we have the definition:

$$U(r) = V(r) - iW(r) \ , \tag{17.56}$$

where $V(r)$ is the usual attractive potential (treated as a central potential in the optical model), and it's imaginary part, $W(r)$, where $W(r)$ is real and positive. The real part is responsible for elastic scattering, while the imaginary part is responsible for absorption. (With a plus sign, in (17.56), this can even be employed to model probability increase (particle creation), but I have never seen it employed in this fashion.)

The theoretical motivation for this approach comes from the continuity relationship for Quantum Mechanics (derived in NERS311):

$$\frac{\partial P}{\partial t} + \vec{\nabla} \cdot \vec{S} = \frac{2}{\hbar} \Psi^* \Im(U\Psi) \ , \tag{17.57}$$

where P is the probability density, $\vec{S}$ is the probability current density, and $\Im()$ is some typesetting software's idea of "imaginary part". When the potential is real, probability is conserved, the left-hand side of (17.57) expressing the balance between probability and where it's moving. (This is really the transport equation for probability.) When the imaginary part is negative, loss of probability is described. When the imaginary part is positive, (17.57) describes probability growth.

The potentials that are used for optical modeling are:

$$\begin{aligned} V(r) &= \frac{-V_0}{1 + e^{(r-R_{\rm N})/a}} \ , \\ W(r) &= \mathrm{d}V/\mathrm{dr} \ , \end{aligned} \tag{17.58}$$

where R_N is the nuclear radius, a is the skin depth, and $-V_0$ is the potential at the center of the nucleus (almost). These are plotted in Figure 17.6

Figure 17.6: The optical model potentials

This is a clever choice for the absorptive part. The absorption can only happen at the edges of the nucleus where there are vacancies in the shells (at higher angular momentum).

See Figures 11.17 and 11.18 in Krane.

17.10 Compound-Nucleus Reactions

See Figure 17.7.

In this reaction, projectile "a" , enters the nucleus with a small impact parameter (small value of l). It interacts many times inside the nucleus, boosting individual nucleons into excited states, until it comes to rest inside the nucleus. This" compound nucleus" has too much energy to stay bound, and one method it may employ is to "boil off" nucleons, to

Figure 17.7: Schematic of a compound nucleus reaction

reach stability. One, two, or more nucleons can be shed. The nucleons that are boiled off, are usually neutrons, because protons are reflected back inside, by the Coulomb barrier. Symbolically, the reaction is:

$$a + X \rightarrow C^* \rightarrow Y_i + b_i$$

The resultant light particle b_i can represent one or more particles.

In this model, the reaction products lose track of how the compound nucleus was formed. The consequences and restrictions of this model are:

1. Different initial reactants, $a + X$ can form the same C^* with the same set of decays. Once the projectile enters the nucleus it loses identity and shares its nucleons with C^*. It should not matter how C^* is formed. Figure 11.19 in Krane shows how different ways of creating ${}^{64}_{30}\mathrm{Zn}^*$ leads (mostly) to the same cross sections for each decay channel.

2. The b_i are emitted isotropically (since the compound nucleus loses sense of the ini-

tial direction of a, since it scatters many times within the compound nucleus and "isotropises". This is especially important when the projectile is light, and the angular momentum not too high. See Figure 11.20 in Krane for experimental evidence of this.

3. Initial projectile energies are generally in the range 10–20 MeV, and X is usually a medium or heavy nucleus. This is so that the projectile can not exit the nucleus with its identity, and some of its initial kinetic energy, intact.

4. In order for the compound nucleus to form, it needs substantial time to do so, typically, 10^{-18}–10^{-16} s.

As an example:

$$\begin{array}{lcl} p + {}^{63}_{29}\mathrm{Cu} & \searrow & \nearrow \quad {}^{63}_{30}\mathrm{Zn} + n \\ \alpha + {}^{60}_{28}\mathrm{Ni} \implies {}^{64}_{30}\mathrm{Zn}^* & \implies & {}^{62}_{29}\mathrm{Cu} + n + p \\ & \searrow & {}^{62}_{30}\mathrm{Zn} + 2n \end{array}$$

Heavy projectile (such as α-particle's) with large l exhibit compound nucleus decays that have a completely different signature. The b_i's are generally emitted in the forward and backward direction, as both the angular momentum and angular momentum must be conserved. As the projectiles energy increases, once can see more neutrons being emitted in proportion. Krane's Figure 11.21 illustrates this very well.

17.11 Direct Reactions

A "direct reaction" involves a projectile that is energetic enough to have a reduced wavelength, $\lambda\!\!\!^{-}$, of the order of 1 fm (a 20 MeV nucleon, for example), that interacts in the periphery of the nucleus (where the nuclear density starts to fall off), and interacts with single valence nucleon. That single nucleon interacts with the projectile leaving them both in bound, but unstable orbits. This state typically lives for about 10^{-21} s, which is long enough for the valence nucleon and projectile to (in classical terms) make several round trips around the nucleus, before one of them finds a way to escape, possibly encountering the Coulomb barrier along the way. Since angular and linear momentum must be conserved, the ejected particle is generally ejected into the forward direction.

Krane shows some interesting data in his Figure 11.19, where both the compound nucleus cross section and direct reaction cross section for $^{25}\mathrm{Mg}(p,p)\mathrm{Mg}^{25}$ are plotted, having been obtained from measurements. The compound nucleus interaction is seen to be nearly isotropic,

while the direct reaction is peaked prominently in the forward direction. The measurement makes use of the different lifetimes for these reactions, to sort out the different decay modes.

A (p,p) direct reaction, if the nucleus is left in its ground state, is an elastic collision. The same may be said for (n,n) collisions. If the nucleus is left in an excited state, it is an inelastic collision. (p,p) and (n,n) direct reactions are sometimes called "knock-out" collisions. Other examples of inelastic direct reaction collisions are (n,p) and (p,n) knock-out collisions. Yet other examples are "deuteron stripping" reactions, (d,p) or (d,n), and "α-stripping" reactions, (α,n) and (α,p). The inverse reactions are also possible, (p,d), (n,d), (n,α), (p,α), and so on. These are called "pick-up" reactions. Measurements of inelastic direct reaction with light projectiles are very useful for determining the nuclear structure of excited states.

17.12 Resonance Reactions

We learned most of what we need to know intuitively about resonance reactions, from our discussion, in NERS311, regarding the scattering of waves from finite-size, finite-depth barriers. Recalling those results, for a particle wave with particle mass, m, energy, E incident on a potential well, $V=-V_0$ between $-R\le z\le R$, and zero everywhere else, the transmission coefficient turns out to be:

$$T=\frac{1}{1+\frac{V_0^2}{4E(E+V_0)}\sin^2(2KR)}\ , \tag{17.59}$$

where $K=\sqrt{2m(E+V_0)/\hbar^2}$. We note that the transmission coefficient is unity, when $2KR$ is a multiple of π. This is called a resonance. Resonances are depicted in Figure 17.8 for neutrons incident on a potential with depth, $V=40$ MeV, and nuclear radius, $R=3.5$ fm. Note the dense population of resonant lines. Figure 17.9 isolates only one of these resonances.

In 3 dimensions the analogous thing happens. In fact, it resonances are common everyday occurrence. All it requires is a bound state that has a given frequency, that can be matched by an external identical, or nearby frequency. All radios work this way. Unbounded radio waves are received by antennae that have bound-state frequencies that match. That's a good resonance. Good resonances are responsible for a piano's rich tone. If you look "underneath the hood" of a piano, you may have wondered why some hammers hit 3 strings simultaneously (upper registers), two strings in the middle registers, and one in the bass registers. These nearby strings, grouped at the same pitch, when struck together, cause sympathetic vibrations and overtones that add to the rich sound. Strings of different pitches can interact as well. For example, try the following (on an acoustic piano): Strike A4 (440 Hz the A above middle C) quite hard, and then hold down the damper pedal, if your hearing acuity is quite good, you may start to hear E5 ($659.26 = 1.4983\times 440$ Hz, a fifth above A4) start to

ring, and then, possibly, C#6 (an octave plus a third above A4, 1108.73 = 2.5198×440 Hz). Both are near half-integral multiples of 440, and are close enough to resonate. You may have wondered why old-school piano technicians can tune an entire piano, with one tuning fork (A4). A4 is tuned against the fork, then E5, and so on, in increments of fifths and octaves, until the job is complete.

Returning now, to nuclei, it is the same effect, except that the bound-state frequencies are defined by the quantum mechanical solutions to the Schrödinger equation. It does not matter that a level is unoccupied. If a passing free neutron has the right energy (frequency), that level will ring, and cause a sharp spike in the cross section.

Shape of a resonance

We can use our partial wave analysis to analyze this. Starting with (17.55):

$$\sigma_{\rm t} = \sigma_{\rm sc} + \sigma_{\rm r} = 2\pi\lambda\!\!\!^{-2} \sum_{l=0}^{\infty} (2l+1)[1 - \Re(\eta_l)] \ . \tag{17.60}$$

For illustrative purposes we shall consider the resonance

$$n + {}^{60}\mathrm{Co} \rightarrow {}^{60}\mathrm{Co} + n$$

that has a known resonance in the vicinity of $E_n = 130$ keV.

In this case,

$$\lambda\!\!\!^{-} = \frac{\hbar c}{\sqrt{2 m_n c^2 T}} \approx 400\mathrm{fm} \ ,$$

a reduced wavelength that is considerably larger than the nucleus.

Let us imagine that just one of the η_l's is causing the resonance. From (17.60), we see that $\sigma_{\rm t}$ maximizes when $\Re(\eta_l) = -1$. Also, considering that this resonance we'll model as an elastic process, we set

$$\eta_l = -1 = e^{2i\delta_l} \Rightarrow \delta_l = \pi/2 \ .$$

To determine the shape of the resonance, we shall expand the phase shift in the vicinity of E_n, where $\delta_l(E_n = E_{\rm res}) = \pi/2$.

Doing so,

$$\cot\delta_l(E_n) \rightarrow \cot\delta_l(E_n)\Big|_{\delta_l(E_{\rm res})=\pi/2} + (E_n - E_{\rm res}) \frac{\partial \cot\delta_l(E_n)}{\partial E_n}\Big|_{E_n=E_{\rm res}} + \cdots$$

$$\frac{\partial \cot \delta_l(E_n)}{\partial E_n} = -\frac{\partial \delta_l(E_n)}{\partial E_n} - \frac{\cos^2 \delta_l(E_n)}{\sin \delta_l(E_n)} \frac{\partial \delta_l(E_n)}{\partial E_n}$$

The second term vanishes above. Defining

$$\Gamma = 2 \left(\frac{\partial \delta_l(E_n)}{\partial E_n} \right)^{-1} \Big|_{E_n = E_{\rm res}} ,$$

we have, from the above,

$$\cot \delta_l(E_n) = -\frac{E_n - E_{\rm res}}{\Gamma/2} , \tag{17.61}$$

Since,

$$\sin() = \frac{1}{\sqrt{1 + \cot^2() \ ,}}$$

we have

$$\sin \delta_l = \frac{\Gamma/2}{[(E_n - E_{\rm res})^2 + \Gamma^2/4]^{1/2}} . \tag{17.62}$$

Finally, combining (17.62) with (17.48)

$$\sigma_{\rm sc}^{\rm el}(E_n) = \pi \lambda\!\!\!^{-2} (2l+1) \frac{\Gamma^2}{[(E_n - E_{\rm res})^2 + \Gamma^2/4]} . \tag{17.63}$$

At resonance,

$$\sigma_{\rm sc}^{\rm elas}(E_n) = 4\pi \lambda\!\!\!^{-2} (2l+1) . \tag{17.64}$$

In this example, $\lambda\!\!\!^{-} \approx 200$ fm, giving a resonant cross section of about $200(2l+1)$ barns. Recalling that the cross section area of a typical nucleus is about 1 b, this is enormous!

What we have calculated so far is only for the case where there is one exit mode for the

$$a + X \longrightarrow X + a$$

resonance.

Gregory Breit and Eugene Wigner generalized (17.63) as follows:

$$\sigma_{\rm sc}^{\rm el}(E_n;[X(a,a)X]) = \pi\lambda\!\!\!^{-2}\frac{2I+1}{(2s_a+1)(2s_{_X}+1)}\frac{\Gamma_{aX}^2}{[(E_n-E_{\rm res})^2+\Gamma^2/4]} \quad (17.65)$$

$$\sigma_{\rm sc}^{\rm in}(E_n;[X(a,b_i)Y_i]) = \pi\lambda\!\!\!^{-2}\frac{2I+1}{(2s_a+1)(2s_{_X}+1)}\frac{\Gamma_{aX}\Gamma_{b_iY_i}}{[(E_n-E_{\rm res})^2+\Gamma^2/4]} \quad (17.66)$$

The I in the above equations comes from the coupling of the intrinsic spins of the reactants with the orbital angular momentum of the outgoing wave component,

$$\vec{I} = \vec{s}_{_X} + \vec{s}_a + \vec{l}\,.$$

Γ in the denominator of both expressions above, pertains to the sum of all the partial widths of all the decay modes:

$$\Gamma = \sum_i \Gamma_i\ .$$

The factors Γ_{aX} and $\Gamma_{b_iY_i}$ in the above equations, pertain to the partial interaction probabilities for resonance formation, Γ_{aX} and decay, Γ_{aX}, in the case of one of the elastic channels, or $\Gamma_{b_iY_i}$.

Shape-elastic scattering

Resonant scattering rarely takes place in isolation, but in addition to other continuous elastic scattering, such as Rutherford scattering from a potential. If we call the potential scattering phase-shift, $\delta_l^{\rm P}$, one can show, from (17.47), that:

$$\sigma_{\rm sc} = \pi\lambda\!\!\!^{-2}(2l+1)\left|e^{-2\delta_l^{\rm P}} - 1 + i\frac{i\Gamma}{(E_n-E_{\rm res})+i\Gamma/2}\right|^2\ . \quad (17.67)$$

Far from the resonance, the resonance dies out, and the cross section has the form:

$$\sigma_{\rm sc} \longrightarrow 4\pi\lambda\!\!\!^{-2}(2l+1)\sin^2\delta_l^{\rm P}\ ,$$

while at the resonance, the resonance dominates and we have:

$$\sigma_{\rm sc} \approx 4\pi\lambda\!\!\!^{-2}(2l+1)\ .$$

In the vicinity of the resonance, the Lorentzian shape is skewed, with a "dip" for $E < E_{\rm res}$, that arises from destructive interference between the potential and resonance phases. See Krane's Figures 11.27 and 11.28 for examples of these.

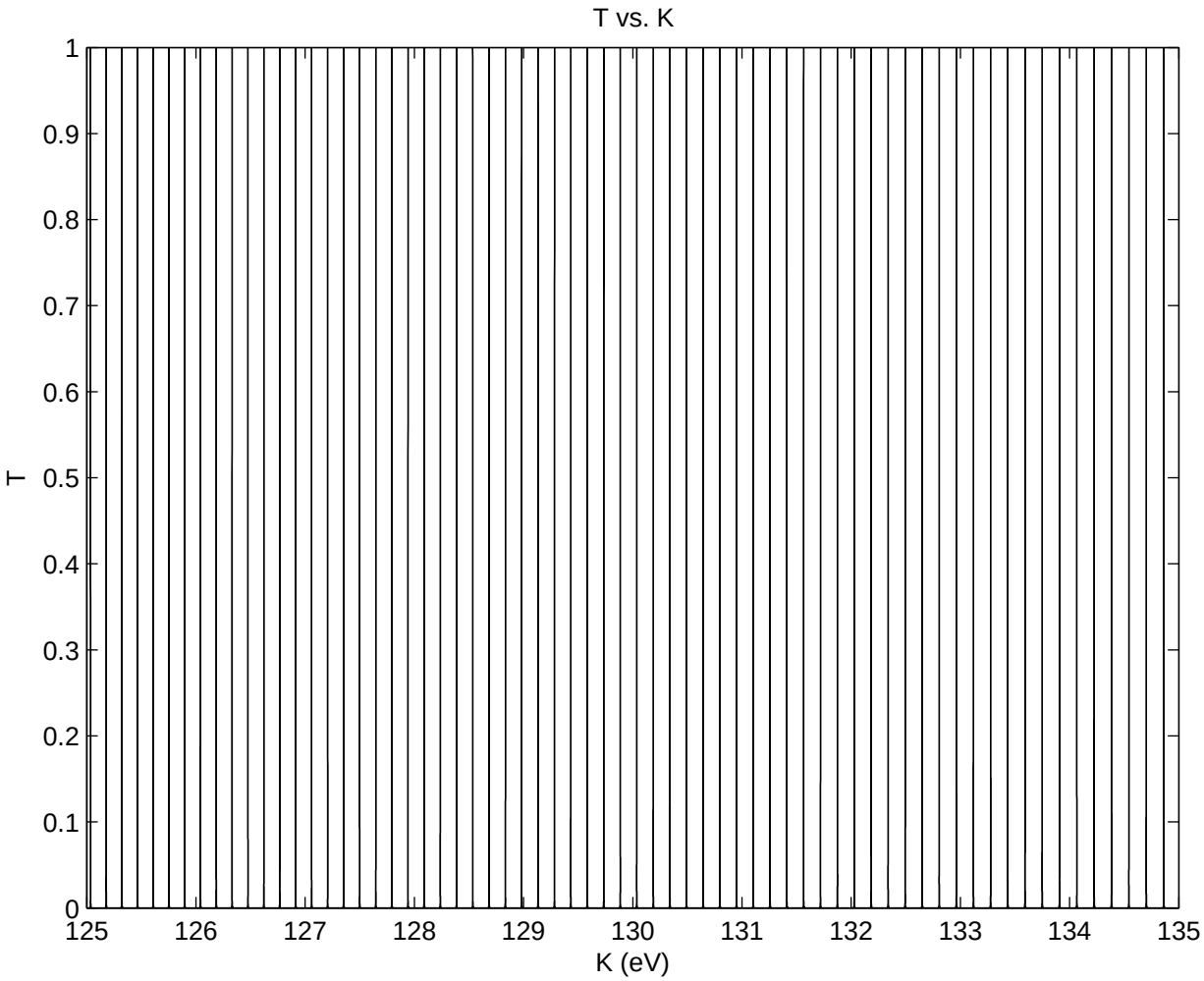

Figure 17.8: Resonant structure for an incident neutron. In this case, $V_0 = 40$ MeV, $R = 3.5$ fm.

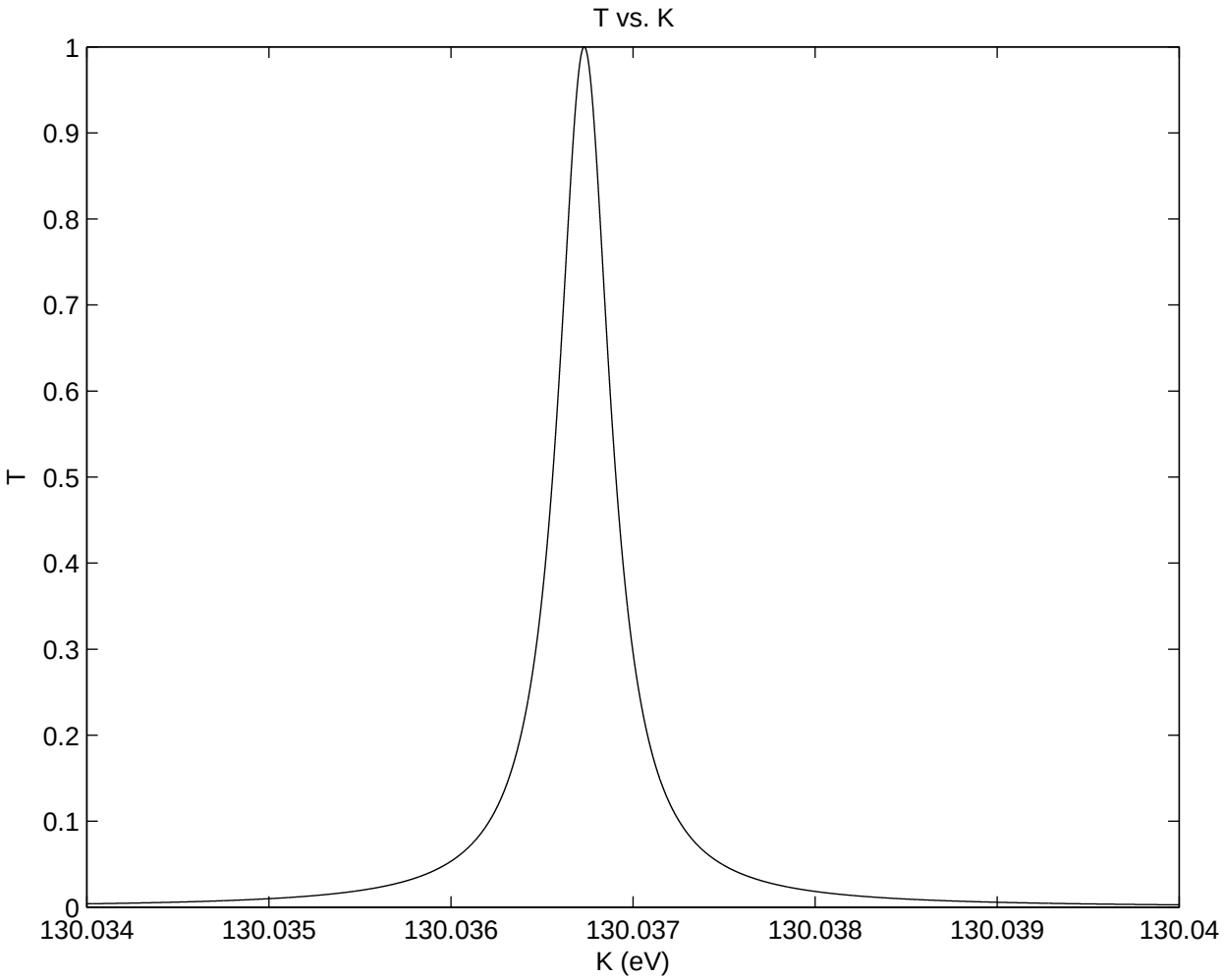

Figure 17.9: Resonant structure near one of the peaks.

Problems

1. Derive (17.10).
2. Derive (17.11).
3. Derive (17.14) and (17.15).
4. Work out the derivatives inside the large parentheses in (17.16) and (17.17).
5. Solve the quadratic equation implied by (17.24).
6. Work out Q_2 in (17.27).
7. Derive (17.47).
8. Derive (17.48).
9. The screened Rutherford cross section, differential in solid angle, is often used to describe the angular distribution of light charged particles scattering elastically from heavy nuclei. It has the following form:

$$\frac{\mathrm{d}\sigma}{\mathrm{d}\Omega} = \frac{A}{(1-\cos\theta+a)^2} \ ,$$

where A and a are constants for any nucleus-projectile combination. The total cross section is known to be σ_0.

   (a) Show that:

$$A = \sigma_0 \frac{a(2+a)}{4\pi} \ .$$

   (b) If the forward ($\theta = 0$) intensity is 10^6 times greater than that in the backward direction ($\theta = \pi$), show that:

$$a = \frac{2}{999} \ .$$

   (c) If the forward ($\theta = 0$) intensity is 4 times greater than that in the backward direction ($\theta = \pi$), Show that:

$$a = 2 \ .$$

   (d) In the limit that $a \longrightarrow \infty$, show that the cross section is isotropic.

10. In the $X(a,b)Y$ reaction with known Q and X at rest, it was shown that:

$$T_b^{1/2} = \frac{(m_a m_b T_a)^{1/2}\cos\theta \pm \{m_a m_b T_a \cos^2\theta + (m_Y + m_b)[m_Y Q + (m_Y - m_a)T_a]\}^{1/2}}{m_Y + m_b} \ .$$

Show that:

(a) When $Q < 0$, there is a minimum value of T_a for which the reaction is not possible. Show that this threshold energy is given by:

$$T_{\text{th}} = (-Q)\frac{m_Y + m_b}{m_Y + m_b - m_a} \ .$$

(b) When $Q < 0$, and $T_a > T_{\text{th}}$, T_b can take on two values. The maximum T_a that this can occur is called T'_a. Show that:

$$T'_a = (-Q)\frac{m_Y}{m_Y - m_a} \ .$$

11. Projectile A, that has mass M_A, scatters elastically off of target nucleus X, that has mass M_X. $Q = 0$, and there is no exchange of matter.

(a) Find a relationship between A's magnitude of momentum, and its angle of deflection.

(b) Show that there is a maximum scattering angle only when $m_A > m_X$.

(c) Find the expression for this maximum angle, when $m_A > m_X$.

Chapter 18

†Mathematical Techniques and Notation Used in this Book

18.1 Vectors and Operators in 3D

For some vector $\vec{a}$, written explicitly in terms of its three components in a geometry with 3 orthonormal basis vectors $(\hat{\alpha}, \hat{\beta}, \hat{\gamma})$:

$$\vec{a} = a_\alpha \hat{\alpha} + a_\beta \hat{\beta} + a_\gamma \hat{\gamma} \ ,$$

where $\hat{\alpha}$, $\hat{\beta}$ and $\hat{\gamma}$, are unit vectors along the α-, β-, and γ- directions.

Its magnitude squared is written several ways:

$$a^2 = |\vec{a}|^2 = \vec{a} \cdot \vec{a} \ ,$$

and is given by:

$$a^2 = (a_\alpha \hat{\alpha} + a_\beta \hat{\beta} + a_\gamma \hat{\gamma}) \cdot (a_\alpha \hat{\alpha} + a_\beta \hat{\beta} + a_\gamma \hat{\gamma}) = (a_\alpha^2 + a_\beta^2 + a_\gamma^2)$$

This is often a form of confusion since, without context, a^2 could stand for a times a or $\vec{a} \cdot \vec{a}$. It should be clear from the context in which it is used.

The magnitude of a vector is:

$$a = |\vec{a}| = +\sqrt{a_\alpha^2 + a_\beta^2 + a_\gamma^2} \ .$$

Note that the positive square root is taken.

Some other useful identities:

$$\begin{aligned} \vec{a}\cdot\vec{b} &= a_\alpha b_\alpha + a_\beta b_\beta + a_\gamma b_\gamma = |\vec{a}||\vec{b}|\cos\theta_{\vec{a},\vec{b}} \\ |\vec{a}+\vec{b}|^2 &= a^2 + 2\vec{a}\cdot\vec{b} + b^2 \end{aligned} \tag{18.1}$$

where $\theta_{\vec{a},\vec{b}}$ is the angle between the vectors $\vec{a}$ and $\vec{b}$.

18.1.1 Some common coordinate system representations

The common realizations of 3D coordinate ststems are:

coordinate system	variable names	domain	unit vectors
rectilinear	(x, y, z)	$-\infty < x < \infty$ $-\infty < y < \infty$ $-\infty < z < \infty$	$(\hat{x}, \hat{y}, \hat{z})$, or $(\hat{\imath}, \hat{\jmath}, \hat{k})$, or $(\hat{n}_x, \hat{n}_y, \hat{n}_z)$
cylindrical	(ρ, ϕ, z)	$0 \le \rho < \infty$ $-\infty < z < \infty$ $0 \le \phi < 2\pi$	$(\hat{\rho}, \hat{\phi}, \hat{z})$, or $(\hat{n}_\rho, \hat{n}_\phi, \hat{n}_z)$
spherical-polar	(r, θ, ϕ)	$0 \le r < \infty$ $0 \le \theta \le \pi$ $0 \le \phi < 2\pi$	$(\hat{r}, \hat{\theta}, \hat{\phi})$, or $(\hat{n}_r, \hat{n}_\theta, \hat{n}_\phi)$

The 3D rectilinear coordinate system

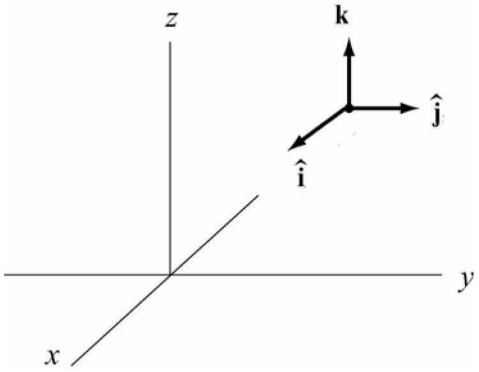

The vector for position in this coordinate system is:

$$\vec{x} = x\hat{x} + y\hat{y} + z\hat{z} \tag{18.2}$$

with the properties:

$$x = \hat{x} \cdot \vec{x} \quad ; \quad y = \hat{y} \cdot \vec{x} \quad ; \quad z = \hat{z} \cdot \vec{x} \tag{18.3}$$

An elemental volume, $\mathrm{d}V = \mathrm{d}x\,\mathrm{d}y\,\mathrm{d}z$ in this coordinate system is shown below.

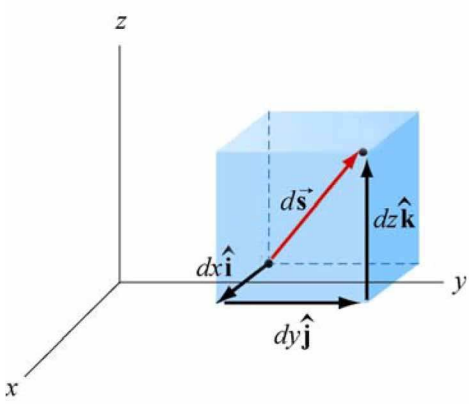

A 3D integral in this coordinate system is represented by:

$$\int \mathrm{d}\vec{x}\, f(x,y,z) \quad \text{or} \quad \int \mathrm{d}x \int \mathrm{d}y \int \mathrm{d}z\, f(x,y,z) \quad \text{or} \quad \iiint \mathrm{d}x\,\mathrm{d}y\,\mathrm{d}z\, f(x,y,z) \tag{18.4}$$

All forms of (18.4) are employed in this book.

The 3D cylindrical-planar coordinate system

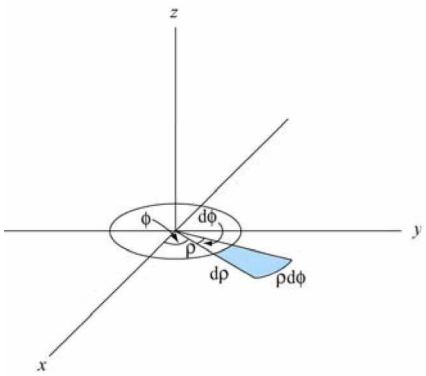

The vector for position in this coordinate system is:

$$\vec{x} = \rho\hat{\rho} + \rho\hat{\phi} + z\hat{z} \tag{18.5}$$

An elemental volume, $\mathrm{d}V = r\mathrm{d}\rho\,\mathrm{d}\phi\,\mathrm{d}z$ in this coordinate system is shown below.

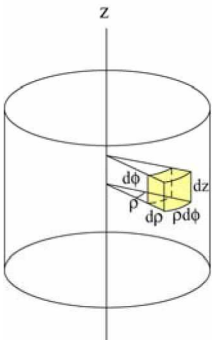

A 3D integral in this coordinate system is represented by:

$$\int \mathrm{d}\vec{x}\, f(\rho,\phi,z) \quad \text{or} \quad \int \mathrm{d}\rho \int \rho\, \mathrm{d}\phi \int \mathrm{d}z\, f(\rho,\phi,z) \quad \text{or} \quad \iiint \rho\, \mathrm{d}\rho\, \mathrm{d}\phi\, \mathrm{d}z\, f(\rho,\phi,z) \tag{18.6}$$

The 3D spherical-polar coordinate system

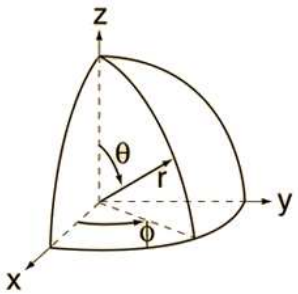

The vector for position in this coordinate system is:

$$\vec{x} = r\hat{r} + r\hat{\theta} + r\sin\theta\hat{\phi} \tag{18.7}$$

An elemental volume, $\mathrm{d}V = r^2 \mathrm{d}r\, \mathrm{d}\theta\, \mathrm{d}\phi$ in this coordinate system is shown below.

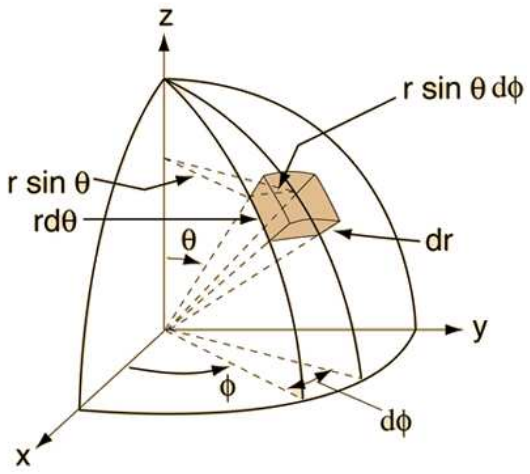

A 3D integral in this coordinate system is represented by:

$$\int \mathrm{d}\vec{x}\, f(r,\theta,\phi) \quad \text{or} \quad \int \mathrm{d}r \int r\mathrm{d}\theta \int r\sin\theta \mathrm{d}\phi\, f(r,\theta,\phi) \quad \text{or} \quad \iiint r^2 \sin\theta\, \mathrm{d}r\mathrm{d}\theta\mathrm{d}\phi\, f(r,\theta,\phi) \tag{18.8}$$

Yet another form used in this book is

$$\int r^2 \mathrm{d}r\mathrm{d}\Omega\, f(r,\theta,\phi) \tag{18.9}$$

where $\mathrm{d}\Omega$ is the differential element of solid angle.

Transformations between coordinate systems

Here are the two most common transformations:

$$\begin{aligned} \vec{x} &= \rho\cos\phi\hat{x} + \rho\sin\phi\hat{x} + z\hat{z} \\ &= r\sin\theta\cos\phi\hat{x} + r\sin\theta\sin\phi\hat{y} + r\cos\theta \end{aligned} \tag{18.10}$$

18.2 Common Trigonometric Relations

$$\begin{aligned}
\cos(a \pm b) &= \cos a \cos b \mp \sin a \sin b \\
\sin(a \pm b) &= \sin a \cos b \pm \cos a \sin b \\
\cos^2 a &= \frac{1 + \cos(2a)}{2} \\
\sin^2 a &= \frac{1 - \cos(2a)}{2} \\
\sin^2 a + \cos^2 a &= 1 \\
1 + \cos a &= 2\cos^2(a/2) \\
1 - \cos a &= 2\sin^2(a/2)
\end{aligned} \tag{18.11}$$

18.3 Common Hyperbolic Functions

$$\begin{aligned}
\cosh a &= \frac{e^a + e^{-a}}{2} \\
\sinh a &= \frac{e^a - e^{-a}}{2} \\
\cosh(a \pm b) &= \cosh a \cosh b \pm \sinh a \sinh b \\
\sinh(a \pm b) &= \sinh a \cosh b \pm \cosh a \sinh b \\
\cosh^2 a &= \frac{\cosh(2a) + 1}{2} \\
\sinh^2 a &= \frac{\cosh(2a) - 1}{2} \\
\cosh^2 a - \sinh^2 a &= 1 \\
\cosh a + 1 &= 2\cosh^2(a/2) \\
\cosh a - 1 &= 2\sinh^2(a/2)
\end{aligned} \tag{18.12}$$

18.4 Complex Numbers or Functions

$$
\begin{aligned}
i &= \sqrt{-1} \\
z &= x + iy \\
z^* &= x - iy \\
x &= \mathrm{Re}(z) \\
y &= \mathrm{Im}(z) \\
e^{iy} &= \cos y + i \sin y \\
\cos x &= \frac{e^{ix} + e^{-ix}}{2} \\
\sin x &= \frac{e^{ix} - e^{-ix}}{2i} \\
\cos ix &= \cosh x \\
\sin ix &= i \sinh x \\
\cosh ix &= \cos x \\
\sinh ix &= i \sin x \\
\cos z &= \cos x \cosh y - i \sin x \sinh y \\
\sin z &= \sin x \cosh y + i \cos x \sinh y \\
\cos^2 z + \sin^2 z &= 1 \\
\cosh z &= \cosh x \cos y + i \sinh x \sin y \\
\sinh z &= \sinh x \cos y + i \cosh x \sin y \\
\cosh^2 z - \sinh^2 z &= 1
\end{aligned}
\tag{18.13}
$$

where x and y are real.

18.5 3D Differential Operators in a Cartesian Coordinate System

$$\begin{aligned}
(\hat{\alpha},\hat{\beta},\hat{\gamma}) &= (\hat{x},\hat{y},\hat{z}) \\
\vec{\nabla}\psi &= \hat{x}\frac{\partial\psi}{\partial x}+\hat{y}\frac{\partial\psi}{\partial y}+\hat{z}\frac{\partial\psi}{\partial z} \\
\vec{\nabla}\cdot\vec{F} &= \frac{\partial F_x}{\partial x}+\frac{\partial F_y}{\partial y}+\frac{\partial F_z}{\partial z} \\
\vec{\nabla}\times\vec{F} &= \hat{x}\left(\frac{\partial F_z}{\partial y}-\frac{\partial F_y}{\partial z}\right)+\hat{y}\left(\frac{\partial F_x}{\partial z}-\frac{\partial F_z}{\partial x}\right)+\hat{z}\left(\frac{\partial F_y}{\partial x}-\frac{\partial F_x}{\partial y}\right) \\
\vec{\nabla}\cdot\vec{\nabla}\psi=\nabla^2\psi &= \frac{\partial^2\psi}{\partial x^2}+\frac{\partial^2\psi}{\partial y^2}+\frac{\partial^2\psi}{\partial z^2}
\end{aligned} \tag{18.14}$$

where ψ is an arbitrary scalar function, and $\vec{F}$ is an arbitrary vector function of (x,y,z).

18.6 3D Differential Operators in a Cylindrical Coordinate System

$$\begin{aligned}
(\hat{\alpha},\hat{\beta},\hat{\gamma}) &= (\hat{\rho},\hat{\phi},\hat{z}) \\
\vec{\nabla}\psi &= \hat{\rho}\frac{\partial\psi}{\partial\rho}+\hat{\phi}\frac{1}{\rho}\frac{\partial\psi}{\partial\phi}+\hat{z}\frac{\partial\psi}{\partial z} \\
\vec{\nabla}\cdot\vec{F} &= \frac{1}{\rho}\frac{\partial(\rho F_\rho)}{\partial\rho}+\frac{1}{\rho}\frac{\partial F_\phi}{\partial\phi}+\frac{\partial F_z}{\partial z} \\
\vec{\nabla}\times\vec{F} &= \hat{\rho}\left(\frac{1}{\rho}\frac{\partial F_z}{\partial\phi}-\frac{\partial F_\phi}{\partial z}\right)+\hat{\phi}\left(\frac{\partial F_\rho}{\partial z}-\frac{\partial F_z}{\partial\rho}\right)+\hat{z}\frac{1}{\rho}\left(\frac{\partial(\rho F_\phi)}{\partial\rho}-\frac{\partial F_\rho}{\partial\phi}\right) \\
\nabla^2\psi &= \frac{1}{\rho}\frac{\partial}{\partial\rho}\left(\rho\frac{\partial\psi}{\partial\rho}\right)+\frac{1}{\rho^2}\frac{\partial^2\psi}{\partial\phi^2}+\frac{\partial^2\psi}{\partial z^2}
\end{aligned} \tag{18.15}$$

18.7 3D Differential Operators in a Spherical Coordinate System

$$
\begin{aligned}
(\hat{\alpha},\hat{\beta},\hat{\gamma}) &= (\hat{r},\hat{\theta},\hat{\phi}) \\
\vec{\nabla}\psi &= \hat{r}\frac{\partial\psi}{\partial r}+\hat{\theta}\frac{1}{r}\frac{\partial\psi}{\partial\theta}+\hat{\phi}\frac{1}{r\sin\theta}\frac{\partial\psi}{\partial\phi} \\
\vec{\nabla}\cdot\vec{F} &= \frac{1}{r^2}\frac{\partial(r^2F_r)}{\partial r}+\frac{1}{r\sin\theta}\frac{\partial(\sin\theta F_\theta)}{\partial\theta}+\frac{1}{r\sin\theta}\frac{\partial F_\phi}{\partial\phi} \\
\vec{\nabla}\times\vec{F} &= \hat{r}\frac{1}{r\sin\theta}\left(\frac{\partial(\sin\theta F_\phi)}{\partial\theta}-\frac{\partial F_\theta}{\partial\phi}\right)+\hat{\theta}\left(\frac{1}{r\sin\theta}\frac{\partial F_r}{\partial\phi}-\frac{1}{r}\frac{\partial(rF_\phi)}{\partial r}\right)+\hat{\phi}\frac{1}{r}\left(\frac{\partial(rF_\theta)}{\partial r}-\frac{\partial F_r}{\partial\theta}\right) \\
\nabla^2\psi &= \frac{1}{r^2}\frac{\partial}{\partial r}\left(r^2\frac{\partial\psi}{\partial r}\right)+\frac{\mathcal{L}^2(\theta,\phi)\psi}{r^2} \\
\nabla^2\psi &= \frac{1}{r}\frac{\partial^2(r\psi)}{\partial r^2}+\frac{\mathcal{L}^2(\theta,\phi)\psi}{r^2} \quad \text{(alternative form)} \\
\mathcal{L}^2(\theta,\phi)\psi &\equiv \frac{1}{\sin\theta}\frac{\partial}{\partial\theta}\left(\sin\theta\frac{\partial\psi}{\partial\theta}\right)+\frac{1}{\sin^2\theta}\frac{\partial^2\psi}{\partial\phi^2}
\end{aligned}
\tag{18.16}
$$

18.8 Dirac, Kronecker Deltas, Heaviside Step-Function

$$
\begin{aligned}
\int_{x_1}^{x_2} \mathrm{d}x\,\delta(x)f(x) &= f(x_0),\ \text{if } x_1\le x_0\le x_2 \text{ (Dirac}'\text{s delta function)} \\
&= 0,\ \text{if } x_0<x_1,\ \text{or, } x_0>x_2 \\
\delta_{mn} &= 1,\ \text{if } m=n \text{ (Kronecker}'\text{s delta)} \\
&= 0,\ \text{if } m\neq n \\
\theta(x) &= 1,\ \text{if } x\ge 0 \text{ (Heaviside}'\text{s step function)} \\
&= 0,\ \text{if } x<0
\end{aligned}
\tag{18.17}
$$

18.9 Taylor/MacLaurin Series

Let $f(x)$ be a function of a single variable that is infinitely differentiable. We define $f^{(k)}(a)$ to be the k^{th} derivative of $f(x)$, evaluated at $x=a$. That is,

$$\begin{aligned} f^{(k)}(a) &= \left(\frac{\mathrm{d}^k f(x)}{\mathrm{d}x^k}\right)_{x=a} \\ f^{(0)}(a) &= f(a) \\ f^{(1)}(a) &= f'(a) \\ f^{(2)}(a) &= f''(a) \\ &\vdots \\ etc. \end{aligned} \tag{18.18}$$

The *Taylor Series* of $f(x)$ in the vicinity of $x = a$ is

$$f(x) = \sum_{k=0}^{\infty} \frac{f^{(k)}(a)}{k!}(x-a)^k \ . \tag{18.19}$$

When $a = 0$, the series is known at the *MacLaurin Series*:

$$f(x) = \sum_{k=0}^{\infty} \frac{f^{(k)}(0)}{k!}x^k \ . \tag{18.20}$$

Examples:

$$\begin{aligned} \log(1+x) &= x - \frac{x^2}{2} + \frac{x^3}{3} - \frac{x^4}{4}\cdots \\ e^x &= 1 + x + \frac{x^2}{2} + \frac{x^3}{6} + \frac{x^4}{24}\cdots \\ A + Bx + Cx^2 &= A + Ba + Ca^2 + (B + 2Ca)(x-a) + C(x-a)^2 \\ (1-\beta^2)^{-1/2} &= 1 + \frac{\beta^2}{2} + \frac{3}{8}\beta^4\cdots \end{aligned} \tag{18.21}$$